esoc
European Space Operations Centre
Robert-Bosch-Strasse 5
D-64293 Darmstadt
Germany
T +49 (0)6151 900
F +49 (0)6151 90495
www.esa.int

DOCUMENT

JUICE - Jupiter Icy moons Explorer Consolidated Report on Mission Analysis (CReMA)

Prepared by **Arnaud Boutonnet and Gabor Varga**
Reference **JUI-ESOC-MOC-RP-001**
Issue **3**
Revision **2**
Date of Issue **25/04/2017**
Status **Approved**
Document Type **TN**
Distribution

European Space Agency
Agence spatiale européenne

APPROVAL

Title JUICE - Jupiter Icy moons Explorer Consolidated Report on Mission Analysis (CReMA)	
Issue 3	**Revision** 2
Author A. Boutonnet	**Date** 25/04/2017 Arnaud Boutonnet Digitally signed by Arnaud Boutonnet DN: cn=Arnaud Boutonnet, o=ESA/ESOC, ou=HSO-GFA, email=arnaud.boutonnet@esa.int, c=DE Date: 2017.04.25 14:33:30 +02'00'
Approved by J. Schoenmaekers	**Date** Johannes Schoenmaekers Digitally signed by Johannes Schoenmaekers Date: 2017.04.25 16:57:20 +02'00'

CHANGE LOG

Reason for change	Issue	Revision	Date
First version based on the MAG	1	0	29/05/2012
New launch options. Update of various chapters	1	1	15/07/2013
New launch options	1	2	02/10/2013
Compliance with the latest MRD	1	3	02/12/2013
Input for the SRR	2	0	18/07/2014
Typo on the launcher performance	2	1	13/08/2014
Input for Phase B2: new Jupiter tour connecting with 141a	3	0	12/10/2015
Input for PDR: retrograde option connecting with 141a	3	1	23/09/2016
Version for PDR board meeting: decrease radiation dose, reduce number of eclipses, better shadowing of Jupiter during EGA	3	2	25/04/2017

CHANGE RECORD

Issue 3	Revision 2		
Reason for change	**Date**	**Pages**	**Paragraph(s)**
Summary table		8	Summary
New tour		70-126 and 155-161	5-6-7-8-9-10-11-15
Jupiter shadowing		80	6
Effect of higher GCO		101	9.3
Maximum rates		127	11.4

Distribution List:

Recipient	Organisation
OPS/GFA, all staff	ESOC
Andrea Accomazzo	ESOC
Frank Budnik	ESOC
Vicente Companys	ESOC
Ruaraidh Mackenzie	ESOC
Michael Mueller	ESOC
Ignacio Tanco	ESOC
Christian Erd	ESTEC
Robert Furnell	ESTEC
Daniele Gherardi	ESTEC
Giuseppe Sarri	ESTEC
Olivier Witasse	ESTEC
Nicolas Altobelli	ESAC
Cyril Cavel	ADS
Eric Ecale	ADS
Frédéric Faye	ADS
Stephen Kemble	ADS
Vincent Poinsignon	ADS
Pascal Régnier	ADS

Document Summary:

This document presents the mission analysis work performed for the JUICE mission. The scientific objectives are to study Jupiter, its environment and its Galilean moons. Close fly-bys will be performed with three of the moons: Europa, Ganymede and Callisto. At the end of the mission, the spacecraft is put into orbit around Ganymede.

The mission is based on a launch from Kourou with Ariane 5 ECA with direct escape. The baseline launch is in 2022. The most promising options for a launch between 2022 to 2025 are reported (3 in 2022, 3 in 2023, 3 in 2024 in 2 in 2025).

The interplanetary transfer sequence is case dependent and relies on gravity assist with Venus, the Earth and Mars. The innovative option based on Lunar-Earth gravity assist are also included. The spacecraft on-board propulsion is chemical with high thrust to mass ratio.

All interplanetary transfer are based on an initial Earth to Earth arc, which is justified by the strong dependence of the launcher performance on the escape declination. It is also necessary to benefit from the abovementioned Lunar-Earth gravity assist.

After a variable time of flight (7.4 to 8.9 year in 2022, 7.9 to 9.7 in 2023, 8.0 to 9.0 in 2024 and 8.0 in 2025), the spacecraft is injected around Jupiter via a capture manoeuvre. An initial Ganymede swing-by is performed before the capture manoeuvre in order to reduce the magnitude of the latter.

Following a series of Ganymede swing-bys that reduce the orbit energy, the inclination and the infinite velocity, the spacecraft is injected with the conditions necessary to initiate the Europa science phase. The initiation of the Europa science phase with Ganymede is a special case of the initiation with Callisto.

Later on, the spacecraft initiates the Europa science phase, which is composed of two fly-bys with closest approach at 400 km altitude and low infinite velocity. Because of the low distance between Europa and Jupiter, special care was attached to the radiation dose minimisation. The duration of this phase is about 39 days. The solar longitude (Sun-Jupiter-Europa) of the two fly-bys is 23 deg then 26 deg (in-line with the scientific objective to lie between -15 deg and 60 deg, but also power constraint to remain below 30 deg).

The Jupiter high latitudes phase follows the Europa science phase: it is based on a series of 1:1 resonant transfers with Callisto (a π-transfer from Ganymede to Callisto allows a preliminary crank of the orbit), which raise the inclination wr.t. Jupiter's equator to a maximum value of 29 deg. When the maximum inclination is reached, the spacecraft is injected into a 5:6 resonant transfer. The duration of this phase is around 6 months.

The spacecraft is then transferred from Callisto to Ganymede in two steps: the first step uses Callisto to reduce the infinite velocity w.r.t. Ganymede (Callisto-Ganymede ladder). Further infinite velocity leveraging is obtained in a second step via a low energy endgame with Ganymede: a series of 6 close encounters with Ganymede is followed by a

gravitational capture with the moon. A capture manoeuvre is nevertheless performed to reduce the apocentre to 10,000 km.

The science phase around Ganymede is decomposed into an elliptic subphase with a period close to 12 hours and a low altitude circular subphase. The elliptic subphase lasts 150 days during which the eccentricity quickly decreases, remain close to zero, before finally building up again under the influence of Jupiter. The circular subphase is performed at an altitude of 500 km for 130 days. The transfer between the elliptic and the circular subphases is done with 2 manoeuvres (to reduce the gravity losses and the navigation cost) separated by 2 days (to be operationally less risky). The gravity losses are ~1%. At the epoch of Ganymede orbit injection, the beta angle is 30 deg (in-line with the requirement of being between 20 deg and 30 deg).

At the end of this phase the eccentricity will naturally build up until the spacecraft impacts the surface in an uncontrolled manner. The total duration of the Jupiter tour is 3.7 year.

The stochastic DeltaV cost for navigation is on average of 15 m/s/GA for the interplanetary phase (except the Lunar-Earth gravity case) and 8 m/s/GA for the Jupiter tour. For the latter, the optical navigation is used for the first gravity assists of each moon, where there is a large uncertainty in the moon ephemeris. It also improves the navigation in general. The JOI cleanup was analysed and sums up to 30 m/s. The GOI cleanup analysis is on-going and will be released for the next update of the CReMA.

The overall DeltaV cost varies for each option. To summarize the deterministic DeltaV cost is around 1.8 km/s while the stochastic DeltaV cost is around 430 m/s.

The radiation level was kept as low as possible by avoiding low perijove/low period throughout the entire tour. The radiation dose behind 10 mm aluminium solid spheres shielding is about 235 krad. This assessment is based on several simplifications on the radiation dose flux computation. An accurate evaluation is out-of-scope of this document.

The longest eclipse of around 3.9 hours takes place shortly before the insertion around Ganymede. During the science around Ganymede there is very short decreasing eclipse by Ganymede right after the insertion (0.7 hour down to zero in 6 days). A preliminary analysis of the eclipse statistics for the 141a backups (Jupiter tour) shows that long eclipses (up to 6.7 hour) take place during the energy reduction phase. For some options they can be reduced to the battery upper limit, while it seems very challenging for others. Additional long eclipses during the rest of the tour also occur; it seems possible to reduce them to the upper limit by a redesign including additional fly-bys. A consolidated analysis of the backup transfer in 2023 is on-going.

For operations the mission will be affected by superior conjunctions (Earth occultation by the Sun): 3 during the interplanetary flight (maximum 19.5 days) and 4 during the tour (~13 days each). Following operational constraints, no DSM or gravity assist are applied around these events (including +/- 1 week around the conjunction). Moreover the minimum time constraint between consecutive flybys (8 days) is satisfied for all flybys (29).

The coverage analysis has shown that the maximum elevation is always greater than 60 deg. It corresponds to a daily pass of 10.5 hour. This performance is obtained by a proper selection of the ground station: until 2034 the southern groundtations (New Norcia and Malargue) give the best results. After 2034 Cebreros shall be used instead.

For the options with a launch in 2022 or 2023, the beginning of the Jupiter tour is performed at highest maximum elevation (around 80 deg, i.e. 12.5 hour daily pass) while the Ganymede in-orbit phase is done around the lowest maximum elevation (around 60 deg as written above). For the options with a launch in 2024 or 2025, the situation is reversed, the only difference being that the long daily passes (12.5 hour) are obtained with Cebreros instead of New Norcia or Malargue. During the Ganymede science phase, an average reduction of 0.3 hour of the daily pass shall be applied to take into account the regular occultations of the Earth by Jupiter.

In terms of planetary protection, the requirement related to Mars is satisfied by the introduction of a swing-by off-targeting strategy (when the interplanetary sequence includes a Mars swing-by). The DeltaV cost is small (several m/s) and can therefore be combined with a navigation trim manoeuvre. For Europa the total collision probability was decomposed into two terms: one related to short term (safe mode) and one related to long-term (total loss due to e.g. micro-meteoroid impact). The probability for the short term was tuned with via an off-targeting strategy. The selection of an a priori low probability led to a DeltaV cost of 8 m/s. The assessment of the other probabilities (S/C reliability, micro-meteoroid impact) are outside the scope of this document. A new analysis with updated/consolidated assumptions is on-going and due by Q4/2017.

The following table is a high level summary for the baseline of useful information pertaining to the spacecraft design and to science.

Phase	Subcategory	Event	Value	Unit
Interplanetary		Sequence	EVEME	
		Duration	7.4	[year]
JOI		JOI to CU	2	[day]
Europa Science	First EGA	rp latitude	-47	[deg]
		Ls	23	[deg]
		Jupiter hidden	0.0	[min]
	Second EGA	rp latitude	47	[deg]
		Ls	26	[deg]
		Jupiter hidden	1.2	[min]
High Latitudes		max inclination	29	[deg]
In-orbit Ganymede		Option	retrograde	
	GOI	Number of manoeuvres	1	
		β-angle	30	[deg]
	GCO	Number of manoeuvres	2	
		β-angle	62	[deg]
Tour		nb F/B	29	
		Duration	3.7	[year]
		Number of eclipse	93	
		TID*	235	[krad]
		DV deterministic	1800	[m/s]
		DV stochastic	427	[m/s]
	F/B max angular rate	Europa	0.12	[deg/s]
		Ganymede	0.13	[deg/s]
		Callisto	0.12	[deg/s]
	F/B max angular acc	Europa	0.16	[mdeg/s^2]
		Ganymede	0.19	[mdeg/s^2]
		Callisto	0.15	[mdeg/s^2]

* Computed with a simplified model, the quoted value is indicative (but usually shows a very good agreement with the refined analysis)

Table of contents:

List of Figures:

List of Tables:

List of Acronyms:

C/A	Closest Approach
DSM	Deep Space Manoeuvre
EME2000	Earth Mean Equator of 2000
F/B	Fly-By
FCT	Flight Control Team
FD	Flight Dynamics
FTA	Fixed Time of Arrival
GAM	Gravity Assist Manoeuvre
GCO	Ganymede Circular Orbit
GEO	Ganymede Elliptic Orbit
GOI	Ganymede Orbit Insertion
GTO	Geostationary Transfer Orbit
ITP	Interplanetary Transfer Phase
JGO	Jovian Ganymede Orbiter
JOI	Jupiter Orbit Insertion
JSE	Jupiter Solar Equatorial
JSO	Jupiter Solar Orbital
JUICE	JUpiter Icy moon Explorer
LEGA	Lunar Earth Gravity Assist
LS	Linear Sum
LTOF	Linear Time Of Flight
MC	Monte Carlo
OD	Orbit Determination
PP	Planetary Protection
PRM	Perijove Raising Manoeuvre

RAAN	Right Ascension of the Ascending Node
R_J	Jupiter Radius
RSS	Root Sum Square
SAA	Sun Aspect Angle
SADM	Solar Array Drive Mechanism
SRP	Solar Radiation Pressure
S/C	Spacecraft
TCM	Trim Correction Manoeuvre
VTA	Variable Time of Arrival
WOL	Wheel-Off-Loading

1 INTRODUCTION

The JUpiter ICy moon Explorer (JUICE) Consolidated Report on Mission Analysis (CReMA) summarizes the mission analysis tasks performed by OPS/GFA up to now, and presents relevant mission data for the design of the mission.

Data is presented for:

- Mission baseline description
- Launch with Ariane 5 ECA
- Interplanetary trajectory and associated data
- Transfer from Jupiter arrival to Europa fly-bys
- Europa fly-bys
- Jupiter high inclination phase and Callisto fly-bys
- Transfer to Ganymede
- Ganymede science phase
- Extended science phase
- Navigation
- Planetary protection
- Delta-V budget
- Eclipse and Earth occultation
- Ground stations coverage
- Trajectory computation and related files

2 DOCUMENTATION

2.1 Applicable Documents

AD1 JUICE - Jupiter Icy Moons Explorer Mission Requirements Document (MRD) Issue 8, Revision 1, JUI-EST-SYS-RS-001, September 2016

AD2 JUI-EST-SYS-RS-008 Planetary Protection Requirements

AD3 Laplace/JUICE Environmental Specification, JS-14-09, issue 5.1, October 2013

AD4 Amendment to JUICE Planetary Protection Categorization, G. Kminek, TEC-QI_14-117, March 2014

AD5 JUICE – Interface for exchange of mission data with Industry, F. Budnik, JUI-ESC-MOC-ICD-001, v1.0, September 2016

2.2 Reference Documents

RD1 Mission Analysis Guidelines, Issue 1, Revision 2, OPS-GFA-WP-532, June 2009

RD2 ExoMars mission on A5-ECA – Feasibility mission analysis – Trajectory & Performance study, S.Yevdochenko, Arianespace, A5-NT-1-H-018-AE, Issue 1, January 2007

RD3 JUICE: Options to increase the system margin, A. Boutonnet and J. Schoenmaekers, HSO-GFA TN-099, December 2013

RD4 Laplace Jupiter Phase Superior Conjunctions, R. Timm, OPS-HAS/2010/1001/RT-2, February 2010

RD5 Coordinate System Definitions for EJSM, Emma Bunce, Hauke Hussmann, Norbert Krupp, October 2009

RD6 CDF Study Report LAPLACE, Assessment of the Jupiter Ganymede Orbiter, CDF-77(A), July 2008

RD7 Navigation Analysis for Jupiter Tour, T. Yamaguchi, ESA-HSO-GFA-TN-092, June 2013

RD8 List of Top priority Target Sites for a Close Fly-by of Europa in the Trailing Hemisphere, JUICE Science Team Internal Memo, June 2011

RD9 Reference gravity fields for Ganymede, L. Iess, S. Finocchiaro, and M. Ducci, Internal Memo of Dipartimento di Ingegneria Meccanica e Aeronautica, La Sapienza, Rome, 2010

RD10 Stationkeeping Strategy for Laplace/JGO Science Phase around Ganymede, M. Boere and A. Boutonnet, AAS 11-526, August 2011, Girdwood, AK

RD11 Mission Analysis for the JUICE Mission, A. Boutonnet and J. Schoenmaekers, AAS 12-207, February 2012, Charleston, SC

RD12 JOREM per distance, C. Erd, email from 15/01/2012

RD13 Feasibility Mission Analysis – Trajectory and Performance Study. LAPLACE Mission on Ariane 5 ECA, A. Lux, Arianespace Report A5-NT-1-H-049-AE, March 2011

RD14 JGO: Consolidated Report on Mission Analysis (CReMA), A. Boutonnet, J. Schoenmaekers and D. Garcia, HSO/GFA WP 557, September 2010

RD15 JUpiter ICy moons Explorer (JUICE) Science Requirements Document (Sci-RD), ESA/SRE (2012)3, Issue 5.2, July 2014

RD16 JUICE : Mission Analysis for the Planetary Protection, A. Boutonnet and W. Martens, ESA-HSO-GFA-TN-091, Issue 1, Revision 0, April 2013

RD17 JUICE: Planetary Protection for Mars, A. Boutonnet, Memo, June 2013

RD18 JUICE Launcher performance evaluation, A. Schnork and A. Boutonnet, JUI-EST-LAU-SOW-001, Iss. 1.2, February 2015

RD19 JUICE: Updated Navigation Analysis for the Jupiter Moon Tour, T. Yamaguchi, HSO-GFA-TN-103, Issue 2, Revision 1, March 2015

RD20 Feasibility Mission Analysis on A5/ECA Launcher. Trajectory and Performance, JUICE, Single Launch, V. Boucher, NT-1/51920-H-01-AE, Issue 1, July 2015

RD21 Scientific constraints and possible scenarios for a tour meeting the core science goals of JUICE which can be achieved with any Jupiter arrival date and first orbit period, Y. Langevin, Memo, July 2014

RD22 Orbit Data Messages, CCSDS 502.0-B-2, Blue book, November 2009

RD23 JUICE: Management of the long Jupiter eclipses during the tour, A. Boutonnet, JUI-ESOC-MOC-TN-500_i1.0, February 2016

RD24 JUICE: Jupiter Orbit Insertion Cleanup Analysis, A. Rocchi, JUI-ESOC-MOC-TN-502 (OPS-GFA-TN-113), February 2017

3 REQUIREMENTS, DEFINITIONS AND ASSUMPTIONS

This document is compliant with all requirements given in the MRD (see AD1), which are applicable to mission analysis.

3.1 Background and Scientific Justification

The Jupiter Icy Moons Explorer is a mission chosen as the first L class mission in the framework of the Cosmic Vision 2015-2025 programme of the Science and Robotic Exploration Directorate of the European Space Agency. The JUICE mission will provide a thorough investigation of the Jupiter system in all its complexity with emphasis on the three ocean-bearing Galilean satellites Ganymede, Europa and Callisto, and their potential habitability. JUICE has been tailored to observe all the main components of the Jupiter system and untangle their complex interactions.

It will be the first spacecraft ever to orbit a Moon (Ganymede) of a Giant planet.

The JUICE mission will visit the Jupiter system concentrating on the characterization of Ganymede, Europa and Callisto as planetary objects and potential habitats and on the exploration of the Jupiter system considered as an archetype for gas giants in the solar system and elsewhere. The focus of JUICE is to characterize the conditions that may have led to the emergence of habitable environments among the Jovian icy satellites, with special emphasis on the three ocean-bearing worlds, Ganymede, Europa, and Callisto.

The mission will also focus on characterising the diversity of processes in the Jupiter system which may be required in order to provide a stable environment at Ganymede, Europa and Callisto on geologic time scales, including gravitational coupling between the Galilean satellites and their long term tidal influence on the system as a whole.

This includes focused studies of Jupiter's atmosphere (its structure, dynamics and composition), and magnetosphere (three-dimensional properties of the magnetodisc and coupling processes) and their interaction with the Galilean satellites.

In conclusion, by performing detailed investigations of Jupiter's system in all its complexity, JUICE will address in depth two of the themes of Cosmic Vision:

Theme 1: What are the conditions for planet formation and the emergence of life?

Theme 2: How does the Solar System work?

3.2 Science Objectives (MRD-JUI-0035)

The JUICE mission will perform detailed investigations of Jupiter and its system in all their inter-relations and complexity with particular emphasis on Ganymede as a planetary body and potential habitat. The investigations of the neighbouring moons, Europa and Callisto, will complete a comparative picture of the Galilean moons.

There are two overarching scientific objectives for JUICE which are split into three scientific sub-objectives each:

- Characterise Ganymede as a planetary object and possible habitat
- Explore Europa's recently active zones
- Study Callisto as a remnant of the early Jovian system
- Characterise the Jovian atmosphere
- Characterise the Jovian magnetosphere
- Characterise Jovian satellite and ring systems

3.3 Mission Requirements

3.3.1 Launch Vehicle, Site and Date

- The JUICE launch vehicle shall be an Arianespace Ariane 5 Evolved Cryogenic Upper Stage Type-A (ECA) (MRD-JUI-1685)
- The spacecraft development shall be compatible with the earliest launch from CSG (launch window opens) by 20th May 2022 (MRD-JUI-1700)
- The spacecraft development shall be compatible with annual alternative launch opportunities from CSG up to and including 2025 (MRD-JUI-1705)
- The mission shall be compatible with a launch period total duration of at least three weeks for each launch opportunity, from the beginning of the launch window (MRD-JUI-1710)

3.3.2 Mission Phases

3.3.2.1 Interplanetary Transfer Phase (ITP)

- The ITP shall be shorter than 10 years (MRD-JUI-1900)
- The ITP shall be optimized to maximize S/C mass after JOI (MRD-JUI-1905)
- The system design shall ensure that all fly-bys during the ITP are conducted at a safe closest approach distance under both, nominal and contingency operations (including Safe Mode) in line with the mission and planetary protection requirements [MRD-JUI-0040] (MRD-JUI-1920)
- The JOI shall be in Earth visibility (MRD-JUI-1945)

3.3.2.2 Nominal Science Phase (NSP)

- The NSP shall start upon completion of the ITP and end after completion of all sub-phases of the NSP, the last being 280 days in Ganymede orbit (MRD-JUI-1775)
- The duration between JOI and GOI shall be at least 2.5 years (MRD-JUI-1974)

- The spacecraft design shall allow for optimum instrument push-broom pointing during from at least –1 hour to +1 hour around the closest approach (MRD-JUI-2052)

3.3.2.2.1 Sampling of Europa

- The closest approach shall be less than 500 km for at least one fly-by (MRD-JUI-2100)
- During Europa flybys, the mission design shall provide near uniform lighting conditions at closest approach and solar phase angles < 60° (phase angle is the sun-target-aperture angle) (MRD-JUI-2106): still to be verified
- The spacecraft and mission design shall provide one Europa fly-by trajectory with a ground track passing over regions Thera and Thrace Macula (altitude w.r.t moon surface) in daylight (MRD-JUI-2115)

  Note: the second priority 1 target is Conamara Chaos.
- As a backup a second Europa flyby shall be implemented with a ground track passing over the region Lenticulae in daylight (MRD-JUI-2120)
- The infinite velocity shall be lower than 4 km/s (MRD-JUI-2150)
- The PP requirements shall be fulfilled (MRD-JUI-2495)
- Following RD21, the Sun-Jupiter-Europa angle at closest approach should be greater than -15 deg and lower than 30 deg (this is not a MRD requirement, but was used for the trajectory design)

3.3.2.2.2 Sampling of Callisto

- Minimum of 6 Fly-By (F/B) of less than 1000 km at C/A (MRD-JUI-2160)
- The spacecraft shall provide at least three (TBC) Callisto fly-bys with altitude at closest approach of 500 km or less (MRD-JUI-2170)
- During Callisto fly-bys, the mission design shall provide near uniform lighting conditions at closest approach and solar incidence angles 20° - 60° (incidence angle is the sun-target-target normal angle) at closest approach (MRD-JUI-2186)
- At least one F/B with equatorial inclination greater than 50 deg (MRD-JUI-2191)

3.3.2.2.3 Sampling of Ganymede (Ganymede in-orbit phase)

- The mission design shall provide for electric and magnetic field characterization over a range of distances to Ganymede, including observations inside and outside of Ganymede's magnetosphere with polar elliptical orbits around Ganymede with a minimum apocenter of 10,000 km and a maximum pericenter of 1000 km (MRD-JUI-2235)

- The beta angle at Ganymede Orbit Insertion (GOI) shall be lower than 30 deg (MRD-JUI-2240). Following RD21, it is scientifically desirable to have the beta angle at GOI greater than 20 deg (this is not a MRD requirement, but was used for the trajectory design)
- The beta angle shall increase in absolute value after GOI (MRD-JUI-2250)
- Circular near-polar orbit at 5000 km for at least 90 days (MRD-JUI-2255)
- Circular near-polar orbit at 500 km for at least 130 days (MRD-JUI-2260)
- [OPTIONAL] Circular near-polar orbit at less than 250 km for at least 30 days (MRD-JUI-2265)
- The 200 km circular orbit in MRD-JUI-2265 shall not be used for propellant sizing (corresponding tank volume shall be accounted for and provided) (MRD-JUI-2266)
- The mission design shall provide for orbits with inclination >80° while in orbit around Ganymede (MRD-JUI-2270)
- The mission design shall ensure that the angle between the spacecraft orbital plane and the s/c-Earth vector does not exceed 84° during the GCO500 phase (MRD-JUI-2271)
- There should not be any eclipse by Ganymede (MRD-JUI-2275), except right after the capture (due to large eccentricity together with low beta angle)

3.3.2.2.4 Sampling of Jupiter Atmosphere and Magnetosphere

- The mission trajectory shall allow for repeated imaging of the Jupiter atmosphere on timescales of 2 hours, few days, 1 month, 1 year from a distance between TBD and TBD (MRD-JUI-2315)
- The mission shall allow for repeated imaging of Jupiter from 15 RJ over a range from days to months (MRD-JUI-2320)
- The mission shall allow for continuous monitoring of Jupiter from TBD distance for at least 1 rotation (10.5 h) (MRD-JUI-2325)
- The S/C trajectory shall pass through the equatorial regions between Europa and Callisto (MRD-JUI-2370)
- The mission shall provide a series of consecutive orbits around Jupiter with increasing inclination up to an inclination of at least 22 deg with respect to the Jupiter equatorial plane (MRD-JUI-2375)
- In the case sufficient launch mass is available the inclination of the Jovian orbit should be raised up to 30° (MRD-JUI-2376)

  Note 1: There is significant scientific interest in the 30° inclination orbit in the optional/enhanced scenario and use of propellant margins/increased launcher capability may eventually allow reaching this orbit.

Note 2: Due to the inclination of Jupiter's magnetic dipole an equatorial latitude of 30° corresponds to a maximum of 40° in magnetic coordinates

3.3.2.3 Extended Science Phase

- The ESP shall start upon completion of the NSP and last for at least an additional 100 days in Ganymede Orbit (MRD-JUI-1780)

3.3.3 Planetary Protection

- The mission and spacecraft design shall respect the ESA Planetary Protection Requirements [MRD-JUI-0040] (MRD-JUI-2495)

3.4 Space Segment Requirements (Spacecraft Navigation and Guidance)

- The orbit of the spacecraft and the related model parameters shall be determined, and the orbit shall be corrected, by manoeuvres through all mission phases such that the predicted target point has the accuracy required by the subsequent mission phase within the allocated propellant budget and guaranteeing safety (MRD-JUI-2585)
- During the interplanetary cruise, conventional radio frequency tracking techniques (ranging and Doppler) from Ground using X/Ka band shall be used (MRD-JUI-2590)
- Before the JOI and Jovian moons fly-by radio frequency tracking shall be complemented with optical observables using the navigation camera system (MRD-JUI-2595)
- Guidance and navigation shall ensure the overall correction propellant cost to be below 8m/s on average per Gravity Assist (flyby) with at least 95% of confidence level (MRD-JUI-2625)

3.5 Ground Segment and Operations Requirements

3.5.1 Spacecraft Operations

- The mission and spacecraft design shall not require any ground communications (TM or TC) below SES angles of 3° during Superior Solar Conjunction and 0.35° during Inferior Solar Conjunction, for nominal as well as for contingency cases during all mission phases (MRD-JUI-0905)
- The spacecraft shall be capable of performing all manoeuvres without the need for real-time interaction with the ground (MRD-JUI-0910)
- The mission and spacecraft design shall not require any manoeuvres to be planned or commanded for SES angles lower than 5° in Superior Solar Conjunction, for nominal as well as for contingency cases during all mission phases (MRD-JUI-1801)

- There shall not be any critical mission events planned or performed (e.g. manoeuvres requiring ground contact) for SES angles below 5° (MRD-JUI-1795)

Following exchange with ESOC FD, the Jupiter tour is designed to avoid as much as possible manoeuvres and fly-bys one week before and one week after the 5° zone of a superior solar conjunction.

- The mission trajectory shall be designed with at least 8 days (TBC) between two successive flybys (MRD-JUI-2010)
- The spacecraft design shall allow for nadir pointing operations during any flyby from at least –12 hours to +12 hours around the closest approach in compliance with the payload instruments pointing requirements (MRD-JUI-2050)

3.5.2 Ground Stations

- The Ground Segment shall use ESTRACK ground stations for nominal operations (MRD-JUI-1655)
- After LEOP, the ESA station at Malargüe (35-m) shall be the primary station used for contact with the spacecraft, with Cebreros (35-m) and New Norcia (35-m) as backup (MRD-JUI-1660)

3.6 Definitions

The beta angle is used throughout the entire document: it corresponds to the unsigned angle between the orbital plane and the Sun direction. A 0 deg beta angle corresponds to a noon-midnight orbit, while a 90 deg beta angle corresponds to a 6:00h-18:00h orbit.

A detailed description of all frames can be found in RD5. The definition of the frames used in this report is recalled hereafter.

EME2000: The origin of the EME2000 coordinate system is the geocenter and the fundamental plane is the Earth's mean equator. The z-axis of this system is normal to the Earth's mean equator at epoch J2000, the x-axis is parallel to the vernal equinox of the Earth's mean orbit at epoch J2000, and the y-axis completes the right-handed coordinate system. The epoch J2000 is the Julian Ephemeris Date (JED) 2451545.0 (January 1, 2000, 12 hours ephemeris time).

Jupiter Equator of Date: The z-axis is along Jupiter North pole. The x-axis direction is the intersection of the mean Earth equator of 2000 with Jupiter mean equator of date. The positive x-direction is the ascending node of the Jupiter equator plane. The y-axis completes the right handed coordinate system. By definition this frame is non-rotating.

Jupiter Solar Orbital (JSO): The x-axis points towards the Sun, y lies in Jupiter's orbital plane, and z is the direction of Jupiter's orbit angular momentum. The system rotates once per Jovian year.

Jupiter Solar Equatorial (JSE): The z-axis is along the Jovian spin axis, positive in the direction of angular momentum (northward). The X-Z plane contains the Sun so that the x-

axis is the projection of the Sun direction into Jupiter's equatorial plane (positive towards the Sun). The y-axis completes the right handed coordinate system.

Jovimagnetic System III: It is derived from the Jovigraphic System III. System III (1965) The Jupiter system III is a *left-handed* Jupiter-centred system which rotates with the planet. The z-axis of the system is defined as the spin axis of Jupiter, with the positive direction oriented northward. The x-axis is fixed on the Jovian prime meridian, λIII = 0, as defined by the International Astronomical Union in 1976. In that frame the magnetic North pole is defined by its longitude (200.8 deg West) and its tilt (9.22 deg).

3.7 Models and Assumptions

3.7.1 Propagation

All trajectories are propagated using numerical integration, based on the following models:

- JPL ephemeris DE432 for the planets
- IMCCE L2 for the Jupiter's Galilean moons

The interplanetary cruise is integrated assuming the following forces: gravity of the Sun and the planets. The Jupiter tour is integrated assuming the following forces: gravity of the Sun, Jupiter and the Galilean moons. The J_2 term of the Jupiter's gravity field is also included. The Ganymede in-orbit phase is integrated assuming the following forces: gravity of Jupiter and the Sun, gravity potential of Ganymede as given in RD9. Other forces are considered to have a negligible effect on the trajectory design and DeltaV budget assessment. They will be included at a later stage.

The gravitational constant and the equatorial radius of the bodies involved in the trajectory design are given in Table 3-1.

Table 3-1: List of gravitational constants and equatorial radii

Body	Equatorial radius [km]	Gravitational constant [km^3/s^2]
Sun	696340.0	1.32712E+11
Venus	6052.3	3.24859E+05
Earth	6378.1	3.98600E+05
Mars	3397.5	4.28283E+04
Jupiter	71492.0	1.26687E+08
Moon	1737.4	4.90280E+03
Europa	1564.1	3.20273E+03
Ganymede	2632.4	9.88783E+03
Callisto	2409.4	7.17929E+03

The J_2 term of the Jupiter's gravity potential is equal to 0.014735.

The interplanetary trajectory plot is given with unit equal to an astronomical unit, i.e. roughly 149597870 km.

All trajectory plots around Jupiter are given with unit equal to the Jupiter radius.

3.7.2 Spacecraft Propulsion System

The spacecraft propulsion system is based on a typical bi-prop system: engine force of 424 N and specific impulse of 321 s (these assumptions are used to compute the gravity losses during the JOI and GOI)

3.7.3 Launcher Performance

This is currently the most powerful European launcher. It consists of the cryogenic (LH+LOX) core stage EPC, flanked by two large solid boosters EAP and uses the cryogenic upper stage ESC-A. In addition to the above constraints that apply to any launch from Kourou, the ESC-A is non-restartable and must be ignited immediately after EPC separation, which precludes an intermediate LEO.

For Laplace-JGO a generic mass performance was assumed (see RD2). In the meantime, a study has been conducted with Arianespace (see RD13) for the most promising interplanetary transfers identified over the launch period 2020-2024. This led to the detailed analysis for three cases in terms of escape infinite velocity: 3.05 km/s, 3.15 km/s and 3.38 km/s.

The recent need for lower escape velocities (options including a LEGA) led to conduct a new study with Arianespace. The launcher performance was optimised for all interplanetary options described in Chapter 4. These options were defined by the escape velocity and the right ascension, while the declination was free (optimally close to the equator), see RD18. It must be pointed that all options correspond to night launches. Another important assumption is that the maximum aerothermal flux (at 99%) for the second peak (after fairing jettisoning) is assumed to be 1135 W/m^2.

Under these assumptions, the launcher performance is given in Figure 3-1 (left) as a function of the escape velocity (this performance is taken from RD20). It includes the launcher adapter. The usable performance will therefore be obtained from this performance by subtracting the adapter mass (taken equal to 155 kg).

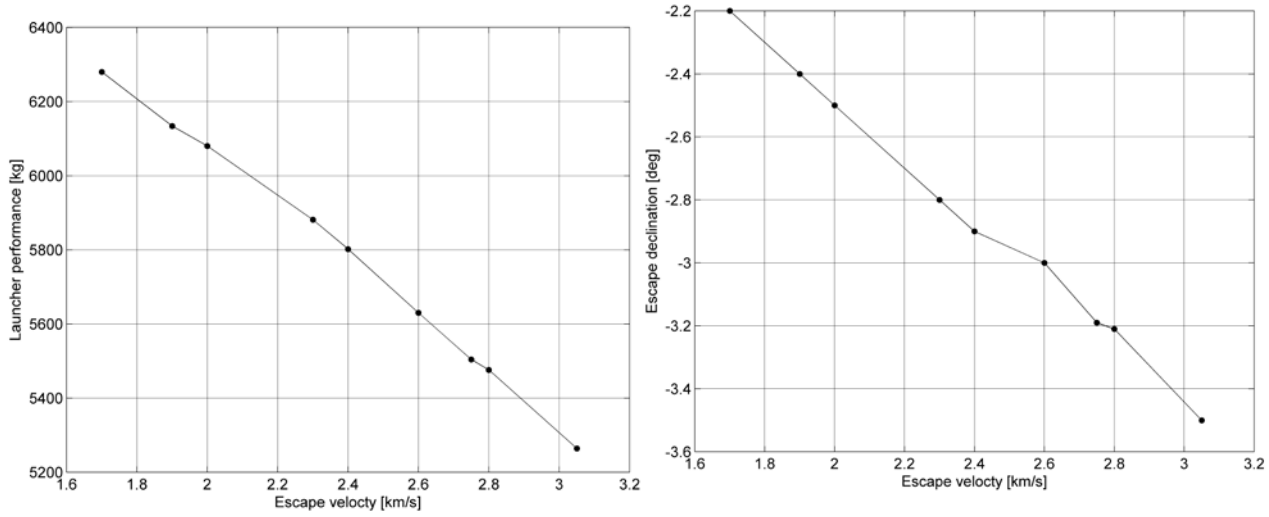

Figure 3-1: Ariane 5 ECA performance as a function of the escape velocity (left). Corresponding optimal escape asymptote declination (right)

A sensitivity analysis was conducted by Arianespace: if the maximum aerothermal flux second peak (constraint value of 1135 W/m²) is replaced by the maximum of the aerothermal flux integral after fairing jettisoning averaged by window of 300 s (constraint value of 600 W/m²), the performance penalty is around 50 kg for all cases.

The choice of the proper constraint and its value shall be an input given by the spacecraft prime contractor.

3.7.4 Ground Stations Location

The Ground Stations performing telemetry, TC and tracking operations are assumed to be one or two of the ESA 35 m network: Cebreros, New Norcia and Malargue. The coordinates of these stations are given in Table 3-2.

Table 3-2: Coordinates of the groundstations

Station	Cebreros	New Norcia	Malargue
Longitude [deg]	4.37 W	116.18 E	69.4 W
Latitude [deg]	40.45 N	31.03 S	35.8 S

It is assumed that a minimum elevation of 10 deg as seen from the ground station is necessary to establish a link with the spacecraft

3.7.5 Radiations Effects

The radiation environment and shielding effect are carefully defined in AD3. In this document an approximation of the model was used based on the planar case (see RD12): it gives the radiation dose as a function of the distance to Jupiter. Therefore the dose does depend neither on the longitude nor on the latitude. The radiation dose flux is given in Figure 3-2 and corresponds to the dose received behind 10 mm Aluminum solid spheres.

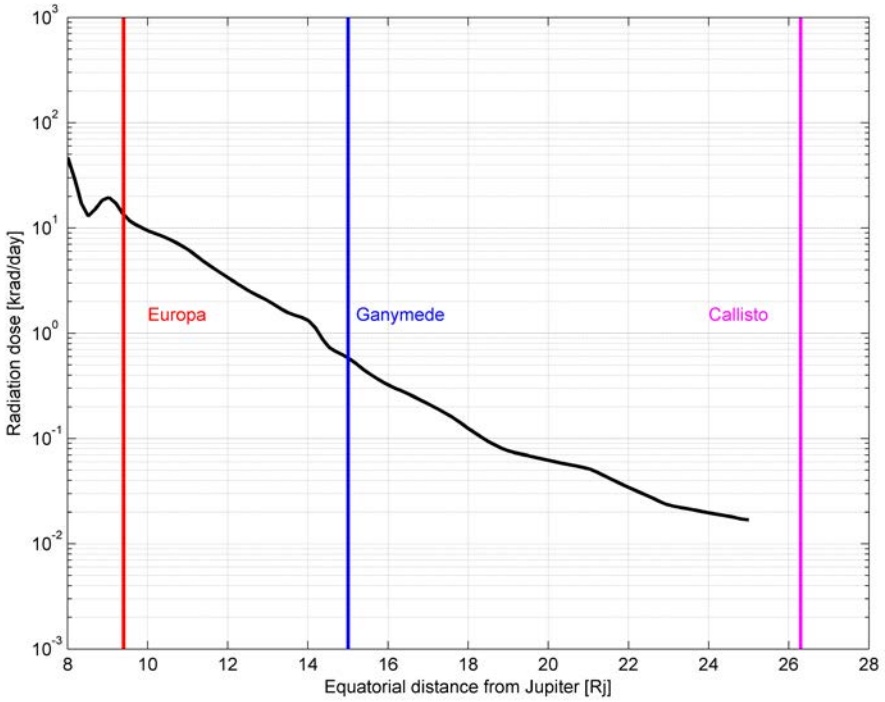

Figure 3-2: Radiation dose behind 10 mm Aluminium shielding as a function of range

A near exponential behavior can be observed.

Ganymede's magnetosphere protects to spacecraft from the harsh radiation environment around Jupiter (shielding effect): as a first guess, it is assumed that when in-orbit around Ganymede, the radiation flux that can be read on the above figure (0.6 krad/day) is reduced by 40% (0.36 krad/day).

The radiation model was used to perform trade-offs. A total radiation figure is quoted at the end of the document. However it is only a rough estimation. An accurate radiation dose estimation can be found in AD3.

3.7.6 Output Files

As an output of the CReMA, an 'oem' file is produced. These kind of files are compliant with CCSDS standard (see RD22). As a will to support the SWT and the industry, a Spice Kernel is also generated from the oem file. For this CReMA, both files are named (see AD5 for description):

- JUICE_CReMA3d2_Baseline_0001.oem
- JUICE_CReMA3d2_Baseline_0001.bsp

The regular step size for the numerical integration was chosen to keep the oem file size below 10 Mb.

The spacecraft ID is -28. The leap second file is #12.

4 INTERPLANETARY TRANSFER PHASE

4.1 Introduction

A selection of the most promising interplanetary transfers was analysed in RD3. Depending on the case, the transfer may involve fly-bys of Venus, the Earth and Mars. Recently it was found that the spacecraft maximum dry mass could be increased by using a special kind of Earth fly-by: the Lunar Earth Gravity Assist (LEGA).

Each option was optimised from launch until the end of the energy reduction phase after the Jupiter Orbit Insertion (JOI), see Chapter 5. It is assumed that the DeltaV cost of the Jupiter tour after that point is roughly the same for all options.

In the following paragraphs, a sub-selection of options is presented for the following launch years: 2022, 2023, 2024 and 2025. For each year at least one option without LEGA is given, then one or two options with LEGA.

For each option the spacecraft maximum wet mass is calculated as the launcher performance minus the launcher adapter (see RD20).

For each option the launch window was computed assuming a constant infinite velocity and declination, i.e. a constant launcher performance. This approach is near optimal whenever an Earth to Earth arc is used after launch, which is the case for all options hereafter.

In all tables a colour code is used: green for Venus, blue for the Earth, brown for the LEGA and red for Mars.

The launch date corresponds to the optimal solution; when taking into account the three weeks launch window, it roughly corresponds to the middle of the window, i.e. the first day where a launch is possible is about 10 days before the launch date mentioned in the tables.

4.2 Launch in 2022

The selection of options is presented in Table 4-1. The option 141a was used to design the Jupiter tour presented in the next chapters. The option 141a is the best candidate without LEGA. The LEGA options (150l0la and 150l0a) have higher system margin, but are longer (1.5 year) and fly closer to the Sun (0.64 AU vs 0.72 AU). The option 150l0la gives the highest system margin.

Table 4-1: Summary of transfer options for a launch in 2022

Case	141a	150l0a	150l0la
Launch date	22/06/01	22/09/04	22/09/05
Launch V-infinity max [km/s]	3.05	2.40	1.90
Launch mass [kg]	5109	5647	5979
Launch correction [m/s]	30	30	30
Launch window max [m/s]	57	80	59
DSM [m/s]	104	25	33
Swing-by date	23/05/31	23/09/02	23/09/02
DSM [m/s]	0	189	250
Swing-by date		24/08/23	24/08/21
Swing-by date	23/10/23	25/08/31	25/08/31
Swing-by date	24/09/02	26/09/29	26/09/29
Swing-by date	25/02/11		
DSM [m/s]	0	0	0
Swing-by date	26/11/26	29/01/18	29/01/18
Swing-by date			
Transfer navigation [m/s]	135	135	185
Arrival date	29/10/07	31/07/21	31/07/21
Arrival V-infinity [km/s]	5.49	5.75	5.75
Arrival right ascension [deg]	124.9	190.9	190.9
Arrival declination [deg]	-3.1	3.4	3.4
JOI [m/s]	792	903	903
Duration [year]	7.4	8.9	8.9
Closest distance to Sun [AU]	0.72	0.64	0.64
Closest DSM distance to Sun [AU]	0.91	0.89	0.89
Closest distance to Venus [km]	9123	5062	5082

4.2.1 Option 141a

The option 141a follows an EVEME-GA sequence. The inertial ecliptic projection is shown in Figure 4-1.

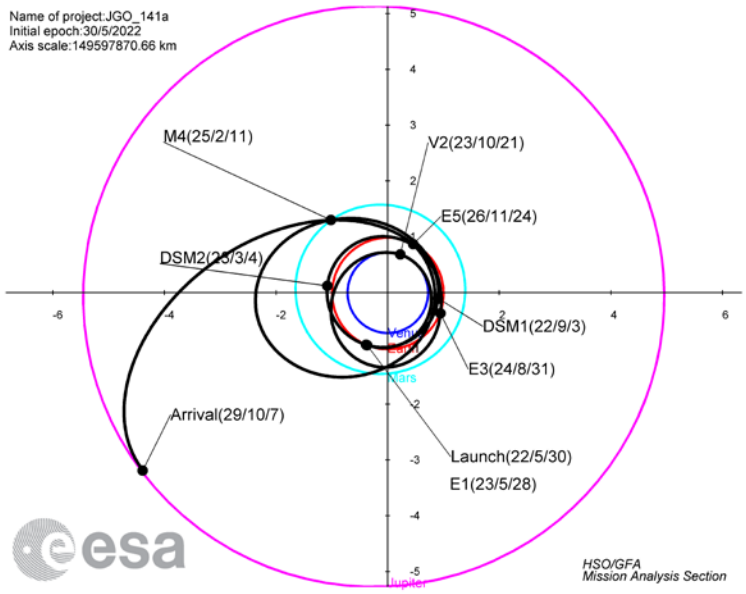

Figure 4-1: Interplanetary transfer in the ecliptic inertial frame (option 141a)

The projection in the Sun-Earth co-rotating frame is shown in Figure 4-2.

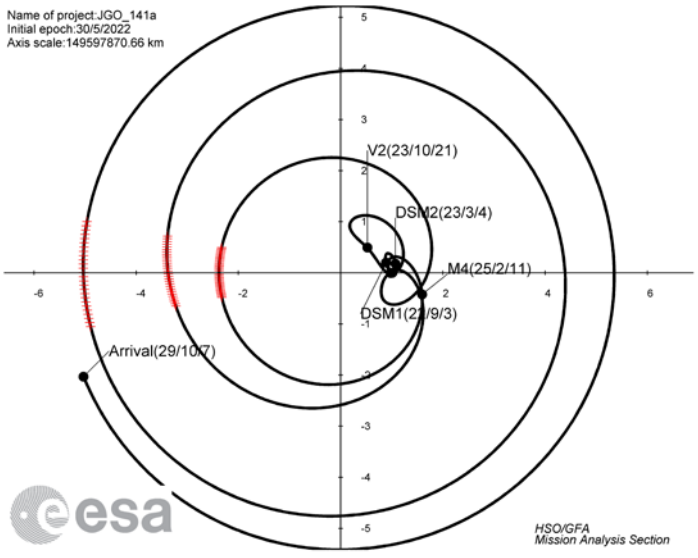

Figure 4-2: Interplanetary transfer in the Sun-Earth co-rotating frame. The superior conjunctions are shown with red '+' marker (option 141a)

It can be seen that most of the GA and DSM are far from the superior conjunctions. Jupiter arrival was chosen to be 35 days before entering the superior conjunction. This leaves plenty of time to perform the JOI and its clean-up.

Figure 4-3 shows the evolution of the Sun-s/c-Earth angle and the Sun-Earth-s/c angle. When both angles are close to zero there is a superior conjunction.

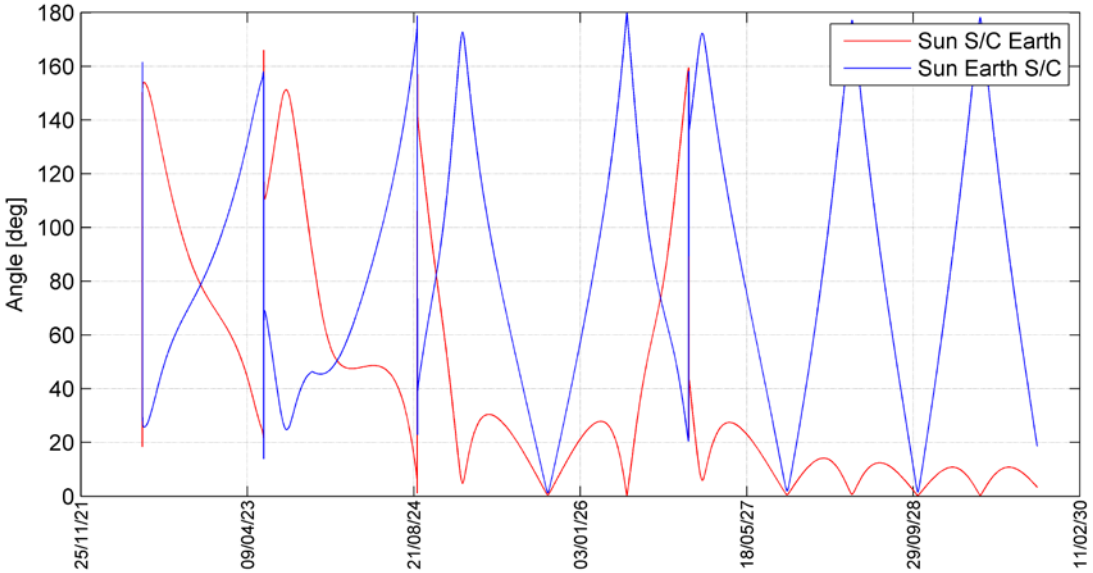

Figure 4-3: Evolution of Sun-S/C-Earth and Sun-Earth-S/C angles during the transfer (option 141a)

Figure 4-4 shows the evolution of the distance with respect to the Sun, Venus, Earth, Mars and Jupiter.

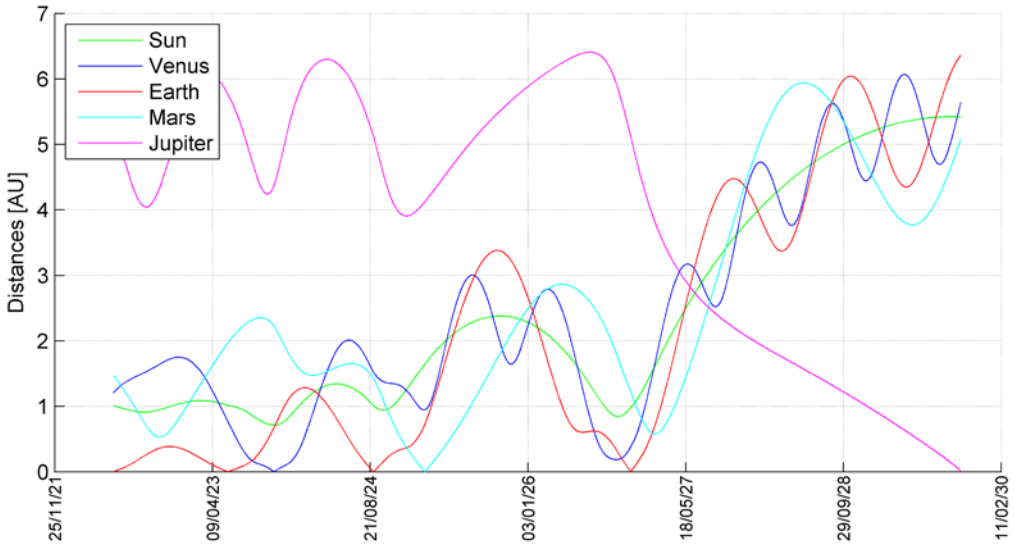

Figure 4-4: Evolution of distances during the interplanetary transfers (option 141a)

The groundtrack of the first EGA in 2023 is given in Figure 4-5.

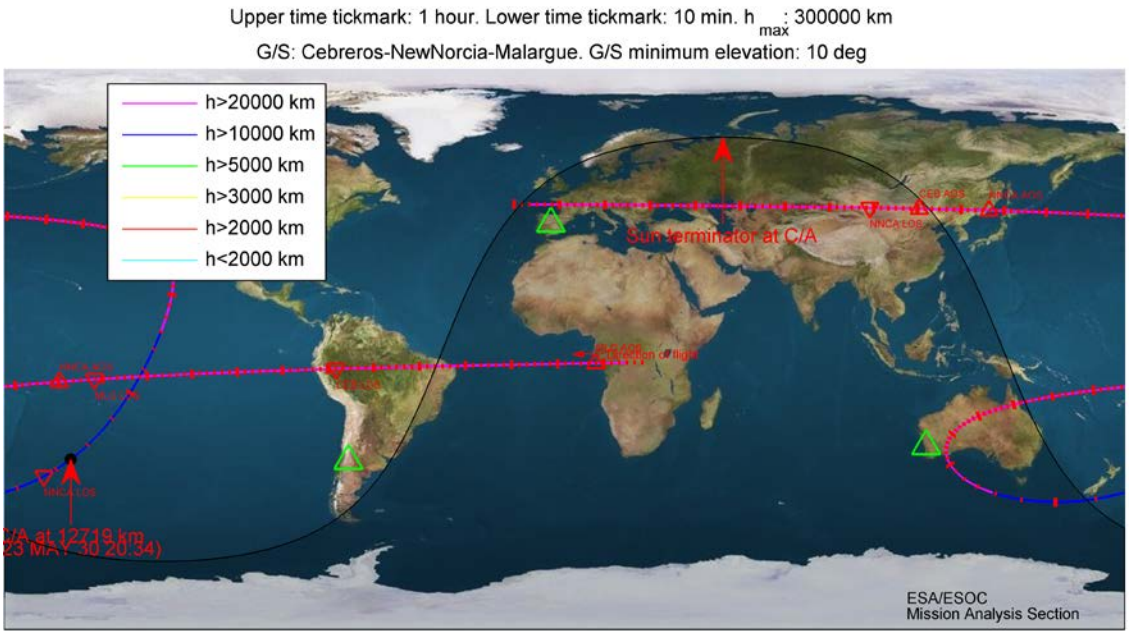

Figure 4-5: Groundtrack of the first EGA for Option 141a

The groundtrack of the second EGA in 2024 is given in Figure 4-6.

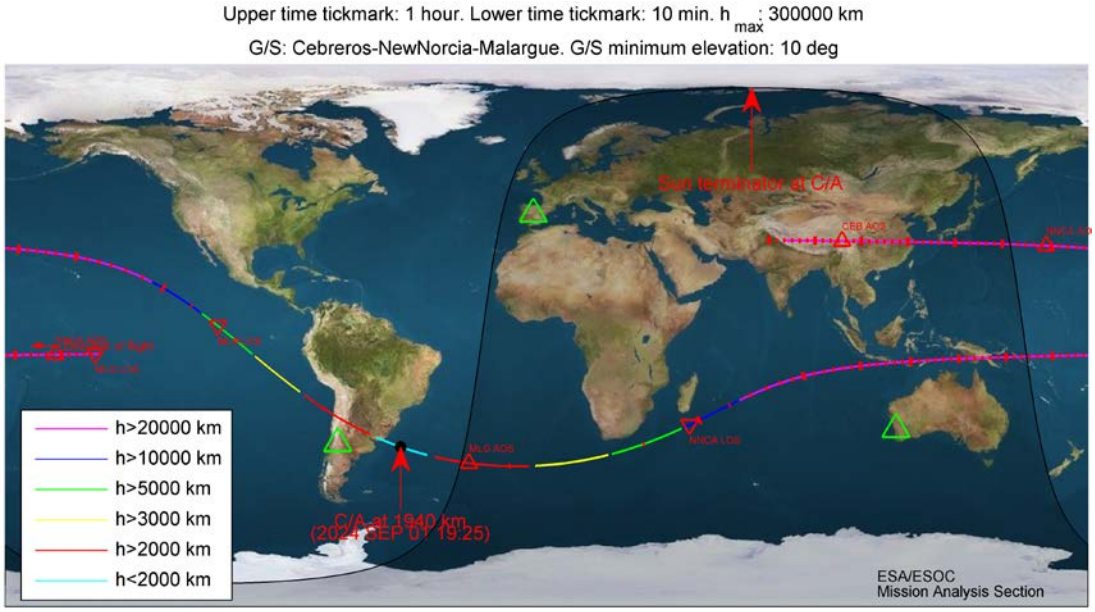

Figure 4-6: Groundtrack of the second EGA for Option 141a

The groundtrack of the third EGA in 2026 is given in Figure 4-7.

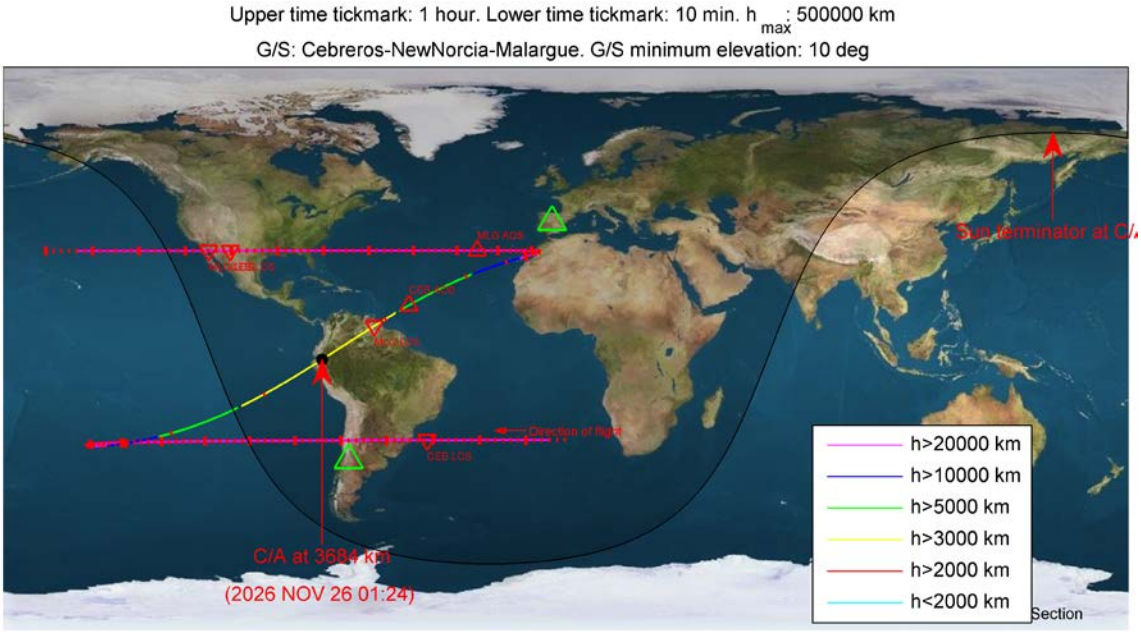

Figure 4-7: Groundtrack of the third EGA in 2026

4.2.2 Option 150l0a

The option 150l0a follows an EEVEE-GA sequence. All features are roughly identical to those presented in Paragraph 4.2.3 for the option 150l0la, except the second EGA, which is replaced by a LEGA for the 150l0la. Therefore all figures are not repeated here. The main features of the LEGA are slightly different though; they are summarised in Table 4-2.

Table 4-2: LEGA main features (option 150l0a)

	Moon fly-by	Earth fly-by
Date	01/09/2023	02/09/2023
Vinf [km/s]	2.92	2.99
Pericentre radius [km]	2037	186379
Pericentre altitude [km]	300	179751
Transfer duration [hour]	26	
LEGA Vinf leveraging [km/s]	0.5	

4.2.3 Option 150l0la

The option 150l0la follows an EEVEE-GA sequence. The inertial ecliptic projection is shown in Figure 4-8.

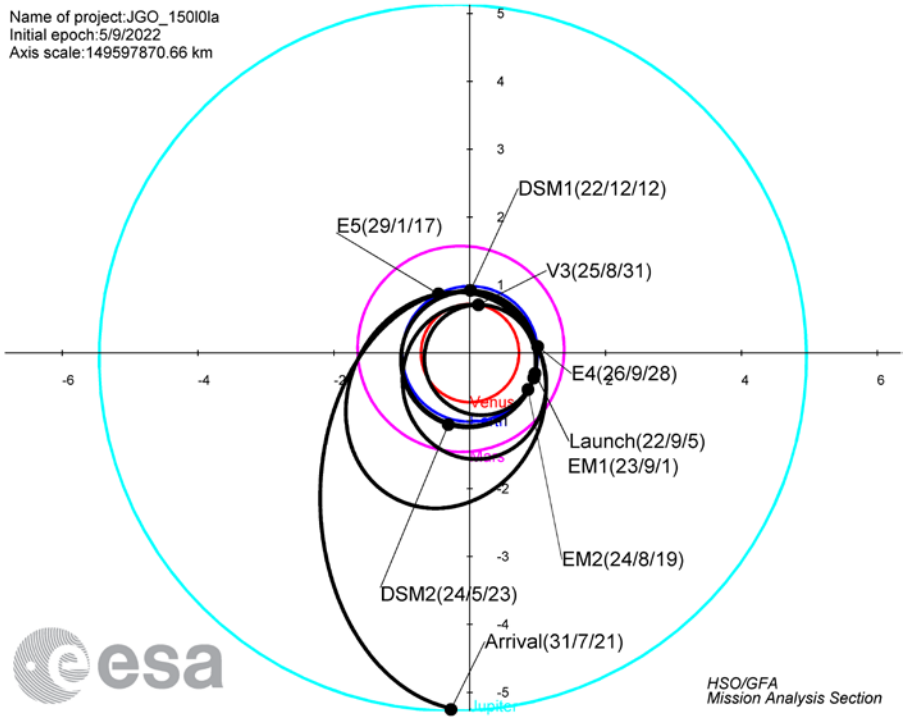

Figure 4-8: Interplanetary transfer in the ecliptic inertial frame (option 150l0la)

The projection in the Sun-Earth co-rotating frame is shown in Figure 4-9. It is visible that the Venus swing-by, the Jupiter arrival and the two DSM are far from the negative x-axis, meaning there is no risk of superior conjunction during or close to critical events of the interplanetary transfer.

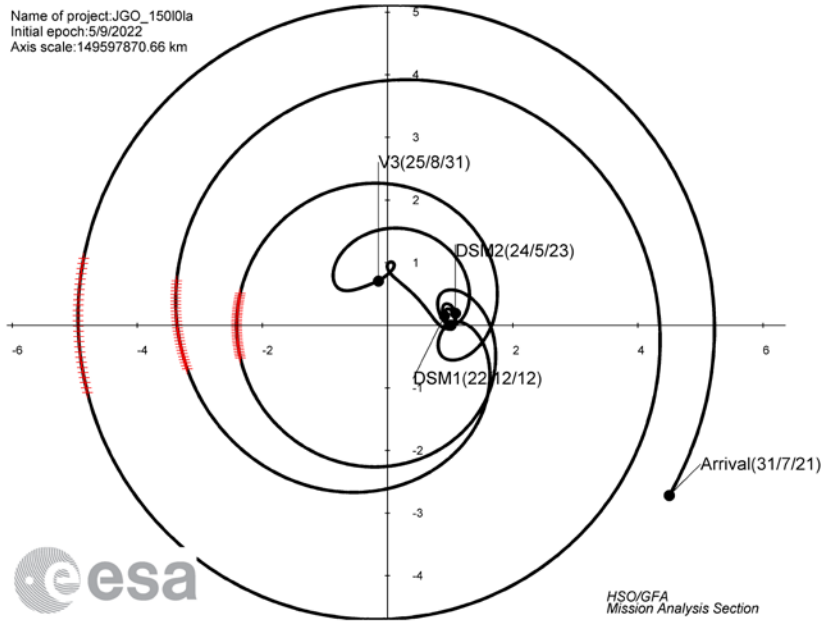

Figure 4-9: Interplanetary transfer in the Sun-Earth co-rotating frame. The superior conjunctions are shown with red '+' marker (Option 150l0la)

Figure 4-10 shows the evolution of the Sun-s/c-Earth angle and the Sun-Earth-s/c angle. When both angles are close to zero there is a superior conjunction.

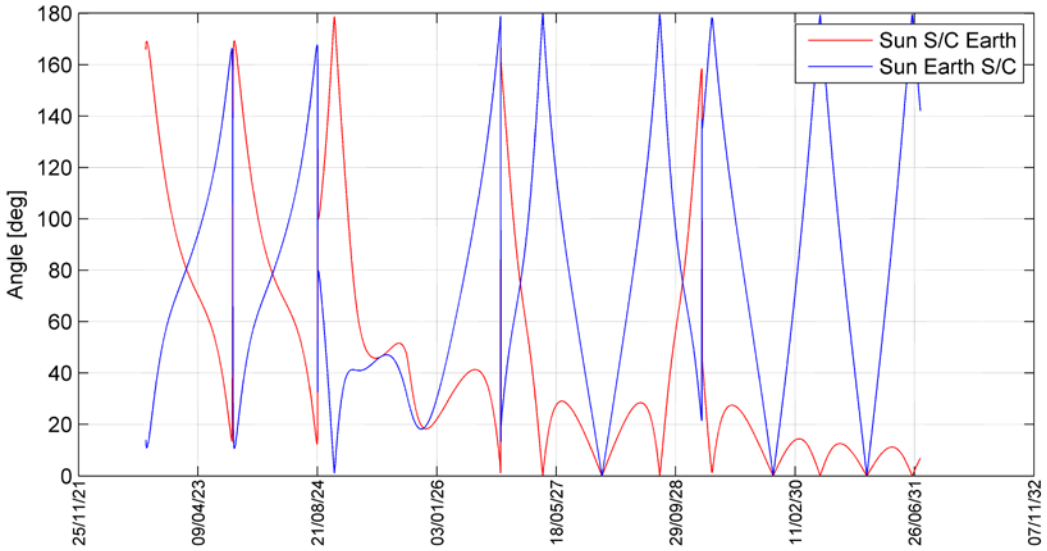

Figure 4-10: Evolution of Sun-S/C-Earth and Sun-Earth-S/C angles during the transfer (option 150l0la)

Figure 4-11 shows the evolution of the distance with respect to the Sun, Venus, Earth, Mars and Jupiter.

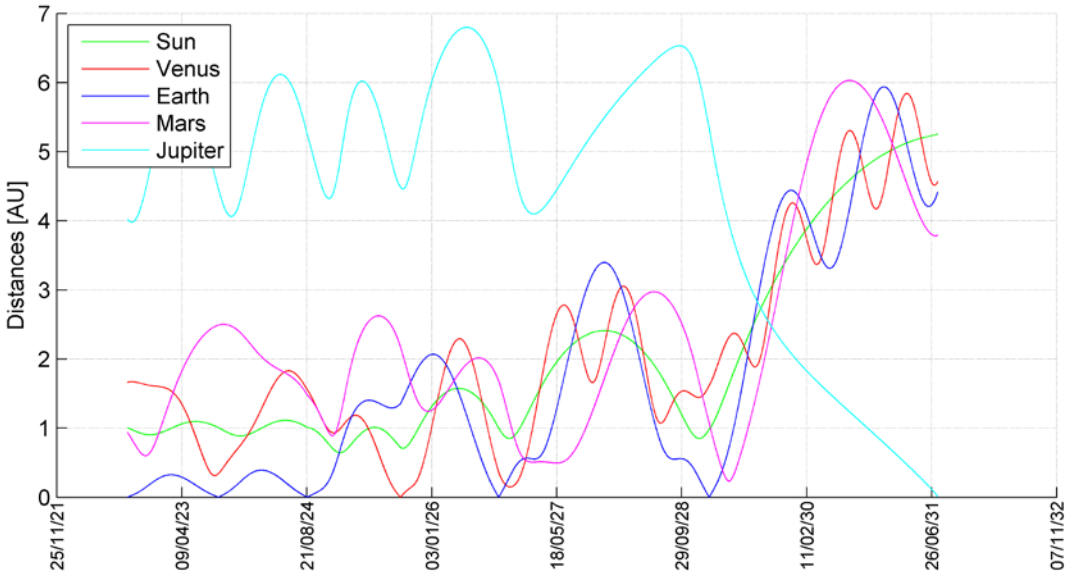

Figure 4-11: Evolution of distances during the interplanetary transfer (option 150lola)

The first LEGA takes place in September 2023 is shown in Figure 4-12 in the Sun-Earth co-rotating frame. It is an inbound radial/radial LEGA.

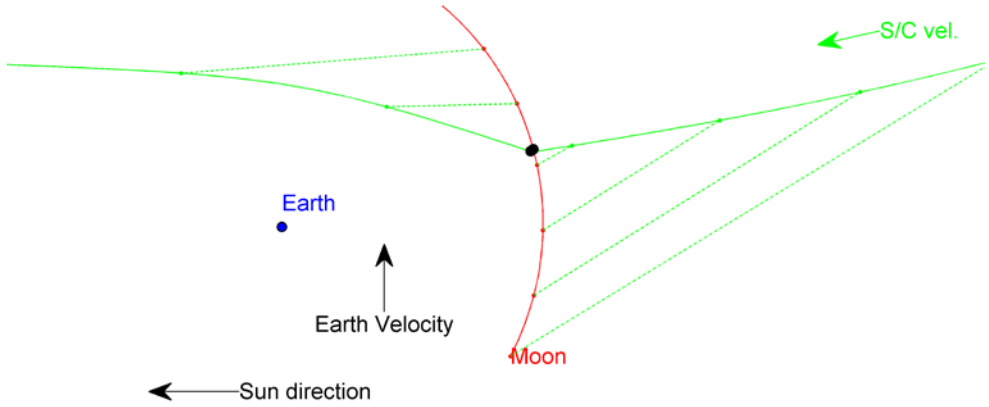

Figure 4-12: Ecliptic projection of the LEGA in the Sun-Earth co-rotating frame (first LEGA, option 150lola)

The first fly-by is performed with the Moon (periselenium altitude at 300 km) followed by a very high altitude EGA (perigee altitude at ~200000 km). The main features of the LEGA are summarized in Table 4-3. The infinite velocity leveraging of the LEGA is very good, about 600 m/s.

Table 4-3: LEGA main features (first LEGA, option 150lola)

	Moon fly-by	Earth fly-by
Date	01/09/2023	02/09/2023
Vinf [km/s]	2.57	2.64
Pericentre radius [km]	2037	196421
Pericentre altitude [km]	300	189793
Transfer duration [hour]	28	
LEGA Vinf leveraging [km/s]	0.6	

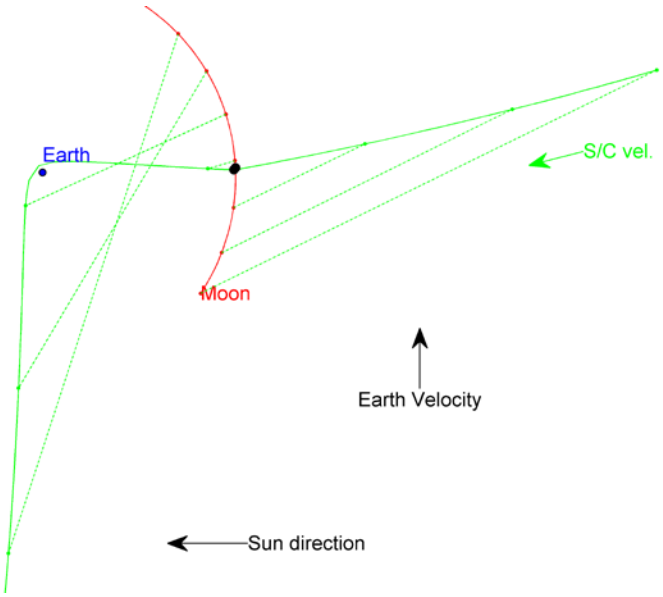

Figure 4-13: Ecliptic projection of the LEGA in the Sun-Earth co-rotating frame (second LEGA, option 150lola)

The second LEGA takes place in August 2024 is shown in Figure 4-13 in the Sun-Earth co-rotating frame. It is an inbound radial/tangential LEGA.

The first fly-by is performed with the Moon (periselenium altitude at 1000 km) followed by a "low" altitude EGA (perigee altitude of ~6500 km). The main features of the LEGA are summarized in

Table 4-4. The infinite velocity leveraging of the second LEGA is lower, about 300 m/s.

Table 4-4: LEGA main features (second LEGA, option 150lola)

	Moon fly-by	Earth fly-by
Date	19/08/2024	20/08/2024
Vinf [km/s]	3.65	3.30
Pericentre radius [km]	2811	13000
Pericentre altitude [km]	1074	6372
Transfer duration [hour]	25	
LEGA Vinf leveraging [km/s]	0.3	

4.3 Launch in 2023

The selection of options is presented in Table 4-5.

Table 4-5: Summary of transfer options for a launch in 2023

Case	160a	230la	150la
Launch date	23/04/03	23/08/09	23/08/22
Launch V-infinity max [km/s]	2.75	2.30	2.60
Launch mass [kg]	5349	5726	5475
Launch correction [m/s]	30	30	30
Launch window max [m/s]	44	42	36
DSM [m/s]	57	183	232
Swing-by date	24/04/02	24/08/08	
DSM [m/s]	66	0	0
Swing-by date		25/08/27	24/08/21
Swing-by date	26/07/04	26/12/06	25/08/31
Swing-by date	28/01/26	28/04/21	26/09/29
Swing-by date			
DSM [m/s]	2	0	0
Swing-by date	30/01/25	29/12/28	29/01/18
Swing-by date			
Transfer navigation (m/s)	110	160	160
Arrival date	32/12/25	32/08/12	31/07/21
Arrival V-infinity [km/s]	5.87	5.82	5.75
Arrival right ascension [deg]	214.6	218.4	190.9
Arrival declination [deg]	-2.0	3.3	3.4
JOI [m/s]	946	927	903
Duration [year]	9.7	9.0	7.9
Closest distance to Sun [AU]	0.78	0.66	0.64
Closest DSM distance to Sun [AU]	0.92	0.89	0.89
Closest distance to Venus [km]	N/A	3777	5080

4.3.1 Option 160a

The option 160a follows an EMEE-GA sequence. The inertial ecliptic projection is shown in Figure 4-14.

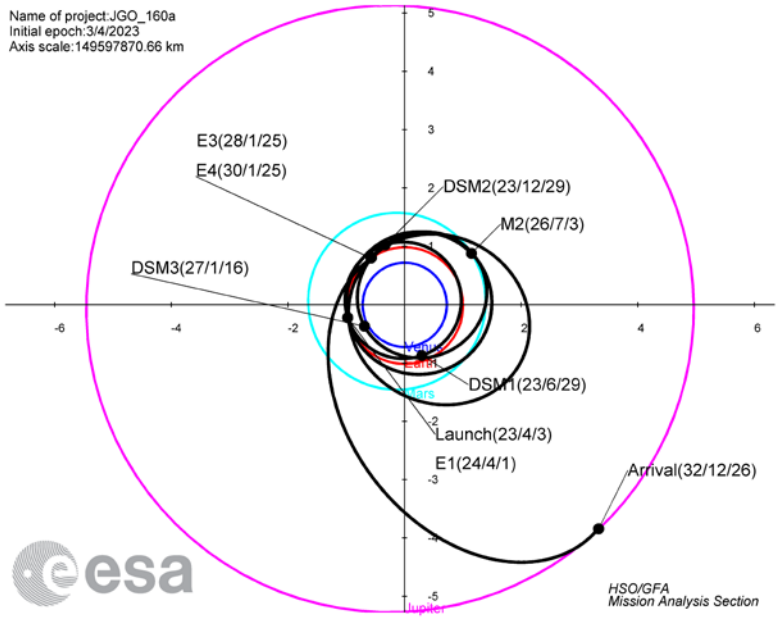

Figure 4-14: Interplanetary transfer in the ecliptic inertial frame (option 160a)

The projection in the Sun-Earth co-rotating frame is shown in Figure 4-15.

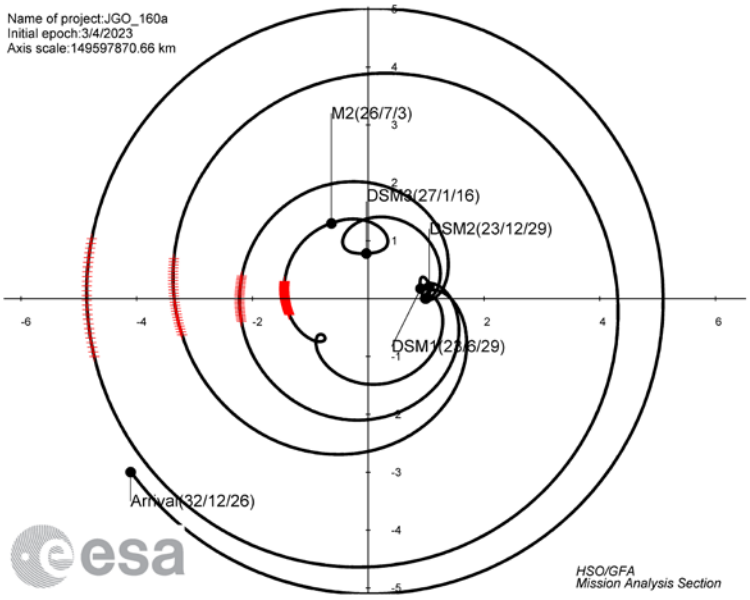

Figure 4-15: Interplanetary transfer in the Sun-Earth co-rotating frame. The superior conjunctions are shown with red '+' marker (option 160a)

It can be seen that the swing-bys and the DSM are far from a superior conjunction.

Figure 4-16 shows the evolution of the Sun-S/C-Earth angle and the Sun-Earth-s/c angle. When both angles are close to zero there is a superior conjunction.

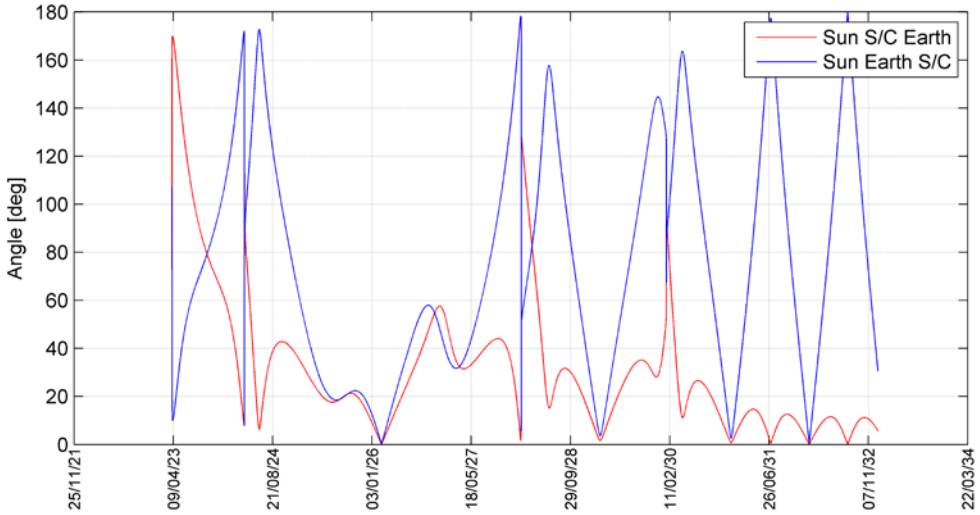

Figure 4-16: Evolution of Sun-S/C-Earth and Sun-Earth-S/C angles during the transfer (option 160a)

Figure 4-17 shows the evolution of the distance with respect to the Sun, Venus, Earth, Mars and Jupiter.

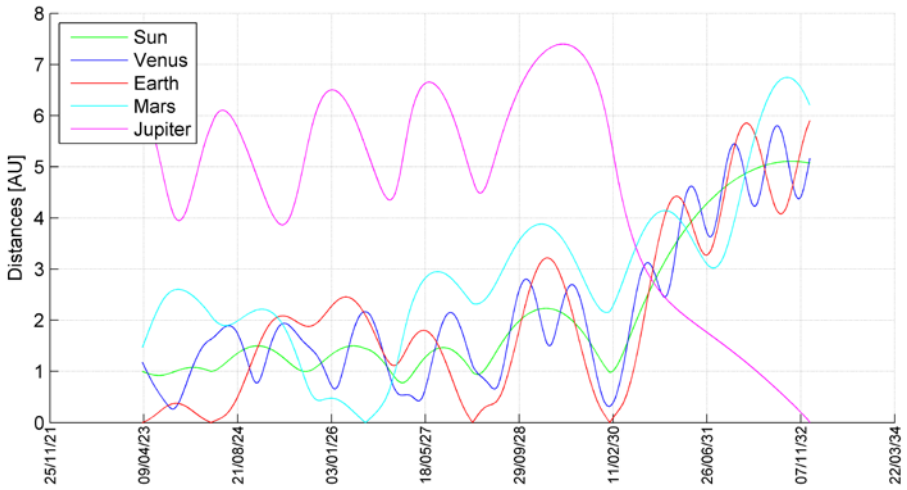

Figure 4-17: Evolution of distances during the interplanetary transfers (option 160a)

4.3.2 Option 230la

The transfer follows an EVVEE-GA sequence. The inertial ecliptic projection is shown in Figure 4-18.

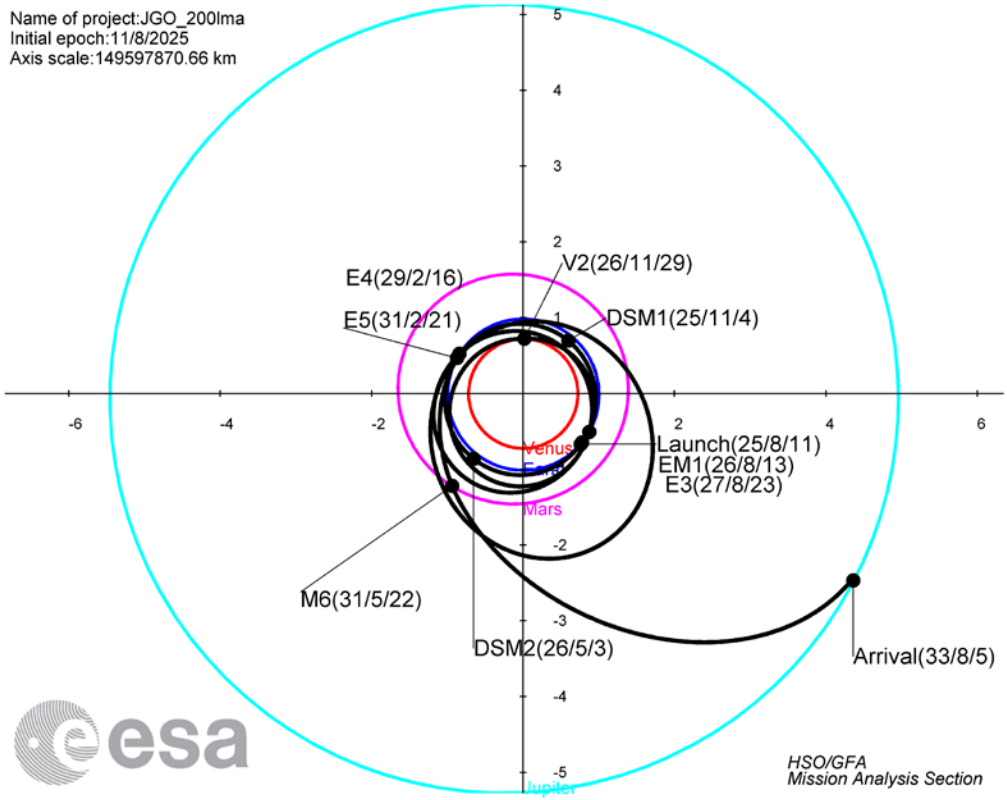

Figure 4-18: Interplanetary transfer in the ecliptic inertial frame (option 230la)

The projection in the Sun-Earth co-rotating frame is shown in Figure 4-19. It is visible that the Venus swing-by, the Jupiter arrival and the two DSM are far from the negative x-axis, meaning there is no risk of superior conjunction during or close to critical events of the interplanetary transfer.

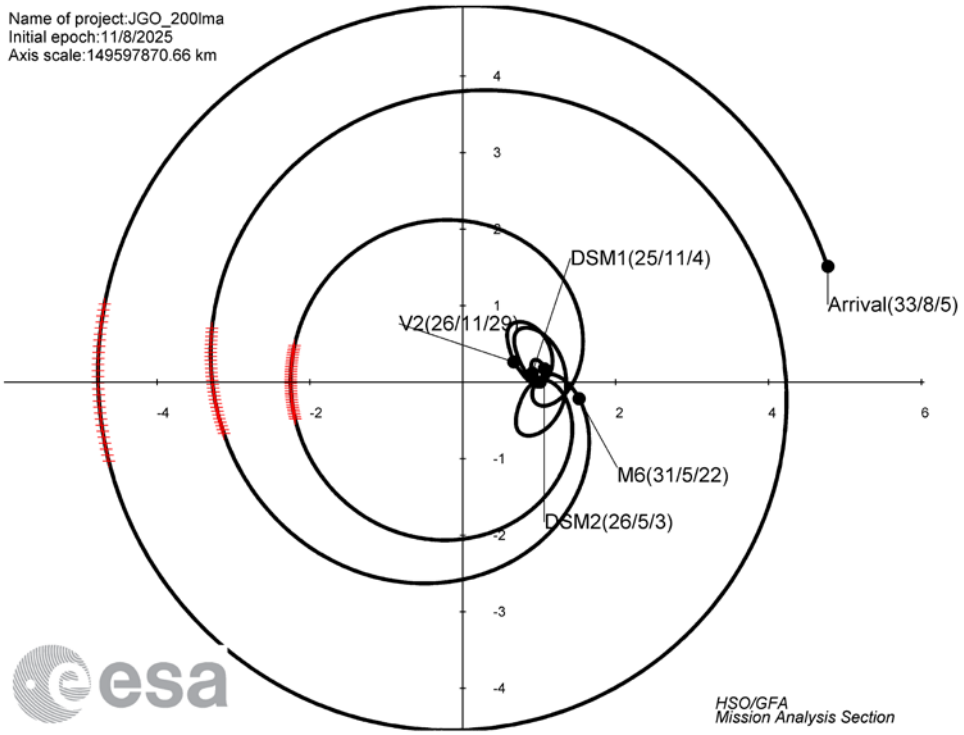

Figure 4-19: Interplanetary transfer in the Sun-Earth co-rotating frame. The superior conjunctions are shown with red '+' marker (option 230la)

Figure 4-20 shows the evolution of the Sun-s/c-Earth angle and the Sun-Earth-s/c angle. When both angles are close to zero there is a superior conjunction.

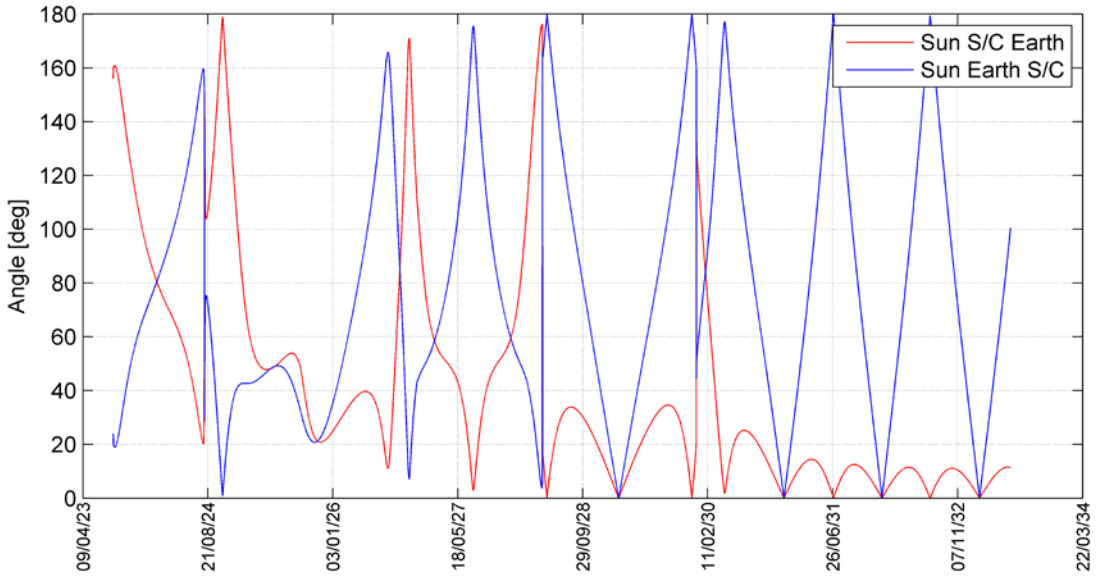

Figure 4-20: Evolution of Sun-S/C-Earth and Sun-Earth-S/C angles during the transfer (option 230la)

Figure 4-21 shows the evolution of the distance with respect to the Sun, Venus, Earth, Mars and Jupiter.

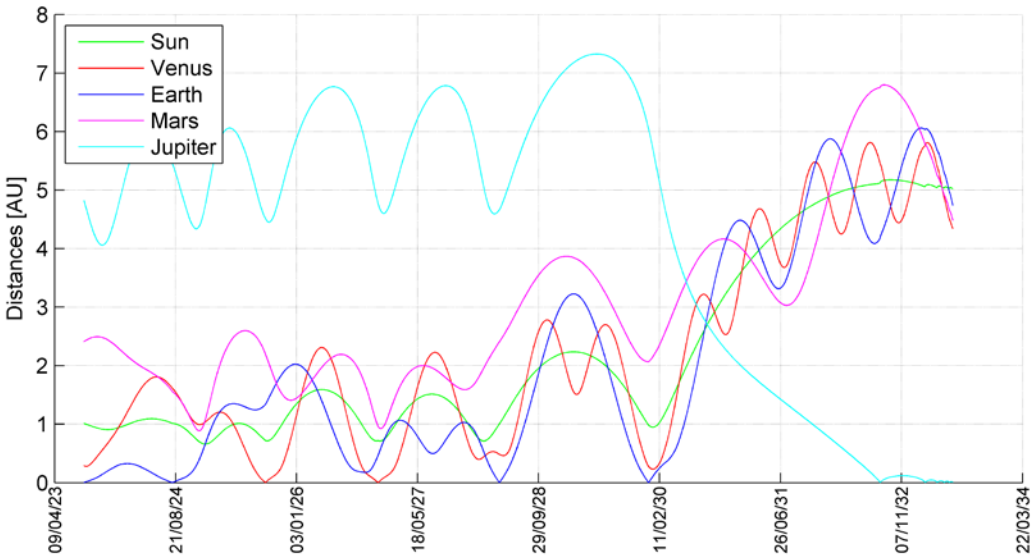

Figure 4-21: Evolution of distances during the interplanetary transfer (option 230la)

The LEGA takes place in August 2024 is shown in Figure 4-22 in the Sun-Earth co-rotating frame. It is inbound radial/tangential.

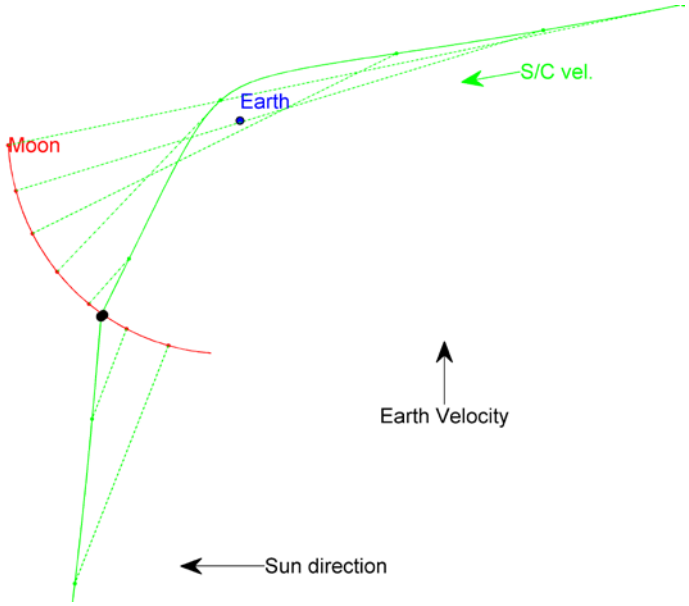

Figure 4-22: Ecliptic projection of the LEGA in the Sun-Earth co-rotating frame (option 230la)

The first fly-by is performed with the Earth (perigee altitude at 40,000 km) followed by the lunar fly-by (periselenium altitude of 300 km). The main features of the LEGA is summarized in Table 4 2. The leveraging of the LEGA is good, about 400 m/s. The time between both fly-bys (34 hours) is greater than the previous options (25 hours), for which the lunar fly-by takes place first.

Table 4-6: LEGA main features (option 230la)

	Earth fly-by	Moon fly-by
Date	07/08/2024	09/08/2024
Vinf [km/s]	2.65	2.98
Pericentre radius [km]	50231	2037
Pericentre altitude [km]	43603	300
Transfer duration [hour]	34	
LEGA Vinf leveraging [km/s]	0.4	

4.3.3 Option 150la

The transfer follows an EVEE-GA sequence. The inertial ecliptic projection is shown in Figure 4-23.

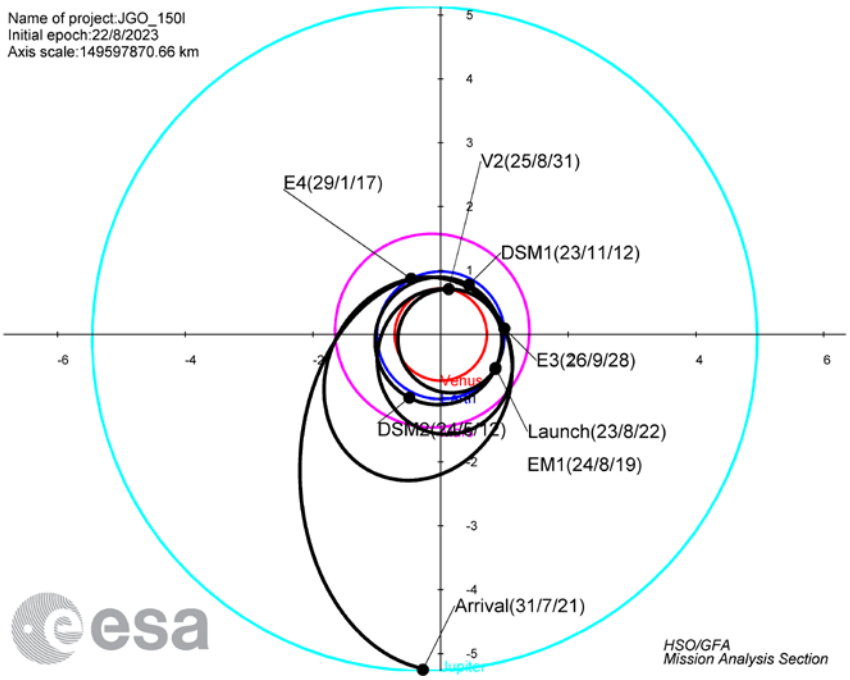

Figure 4-23: Interplanetary transfer in the ecliptic inertial frame (option 150la)

The projection in the Sun-Earth co-rotating frame is shown in Figure 4-24.

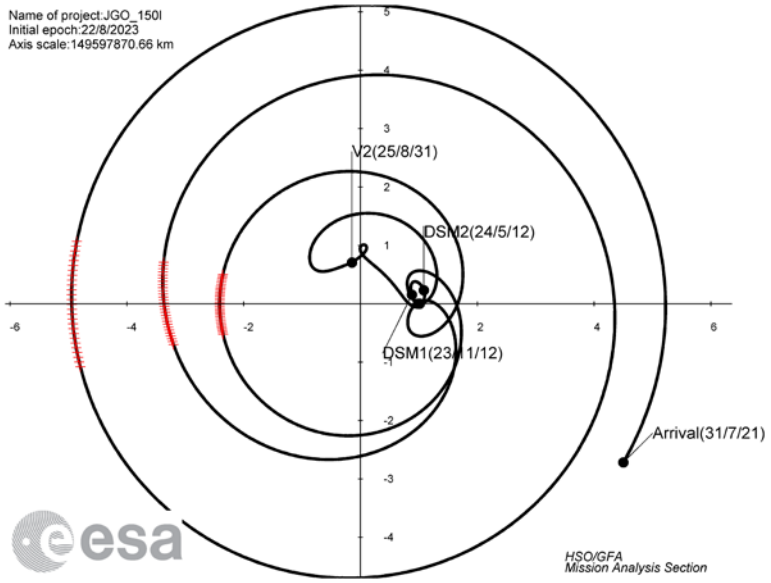

Figure 4-24: Interplanetary transfer in the Sun-Earth co-rotating frame. The superior conjunctions are shown with red '+' marker (option 150la)

It can be seen that the swing-bys and the DSM are far from a superior conjunction.

Figure 4-25 shows the evolution of the Sun-s/c-Earth angle and the Sun-Earth-s/c angle. When both angles are close to zero there is a superior conjunction.

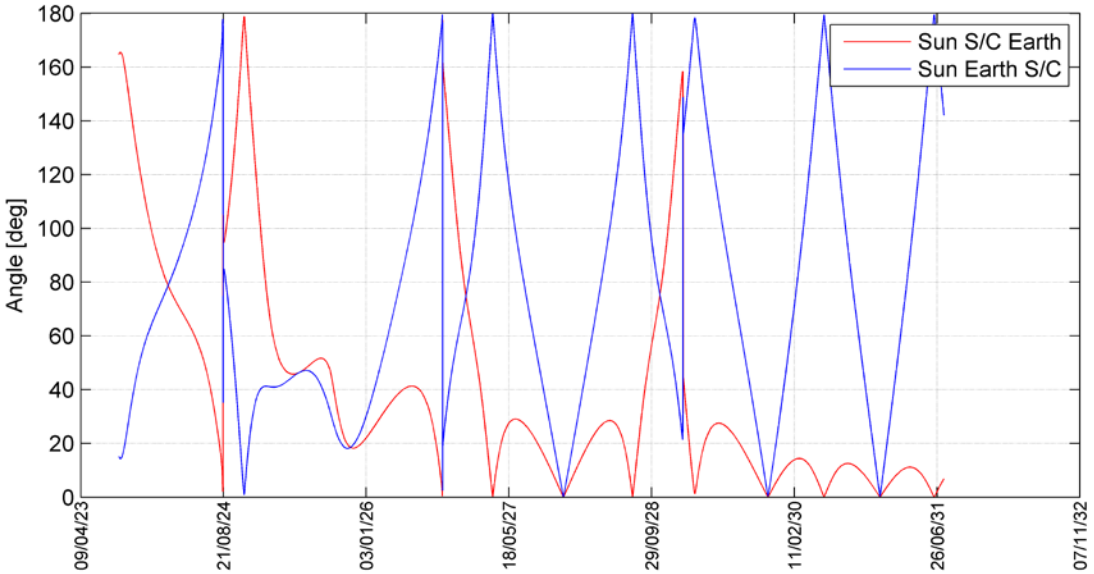

Figure 4-25: Evolution of Sun-S/C-Earth and Sun-Earth-S/C angles during the transfer (option 150la)

Figure 4-26 shows the evolution of the distance with respect to the Sun, Venus, Earth, Mars and Jupiter.

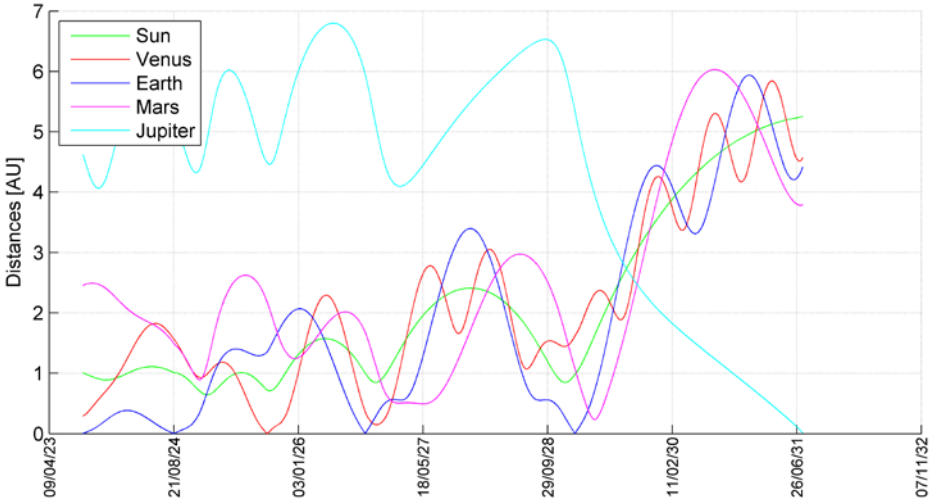

Figure 4-26: Evolution of distances during the interplanetary transfers (option 150la)

The LEGA is similar to the second LEGA of the option 150l0la, see Section 4.2.3.

4.4 Launch in 2024

The selection of options is presented in Table 4-7.

Table 4-7: Summary of transfer options for a launch in 2024

Case	1800ma	180lolma	17ImeIem
Launch date	24/08/04	24/08/15	24/09/12
Launch V-infinity max [km/s]	2.80	1.70	2.30
Launch mass [kg]	5321	6125	5726
Launch correction [m/s]	30	30	30
Launch window max [m/s]	63	103	90
DSM [m/s]	25	41	18
Swing-by date	25/08/03	25/08/12	25/09/10
DSM [m/s]	24	60	131
Swing-by date	26/08/03	26/08/13	26/09/14
Swing-by date	26/11/21	26/11/22	27/02/23
Swing-by date	28/03/13	28/03/13	27/12/30
Swing-by date			
DSM [m/s]	0	0	2
Swing-by date	31/03/13	31/03/13	29/12/29
Swing-by date	31/05/27	31/05/27	
Transfer navigation (m/s)	160	160	160
Arrival date	33/07/28	33/07/29	32/08/11
Arrival V-infinity [km/s]	5.78	5.78	5.81
Arrival right ascension [deg]	254.6	254.6	218.6
Arrival declination [deg]	4.3	4.3	3.3
JOI [m/s]	928	928	923
Duration [year]	9.0	9.0	7.9
Closest distance to Sun [AU]	0.72	0.72	0.65
Closest DSM distance to Sun [AU]	0.90	0.90	0.88
Closest distance to Venus [km]	3485	2240	12243

4.4.1 Option 1800ma

The option 1800ma transfer follows an EEVEE-GA sequence. The inertial ecliptic projection is shown in Figure 4-27.

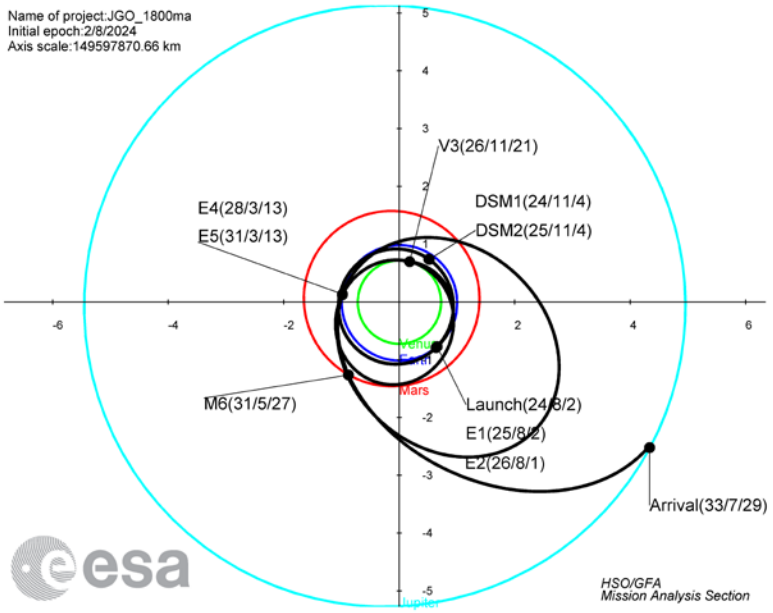

Figure 4-27: Interplanetary transfer in the ecliptic inertial frame (option 1800ma)

The projection in the Sun-Earth co-rotating frame is shown in Figure 4-28.

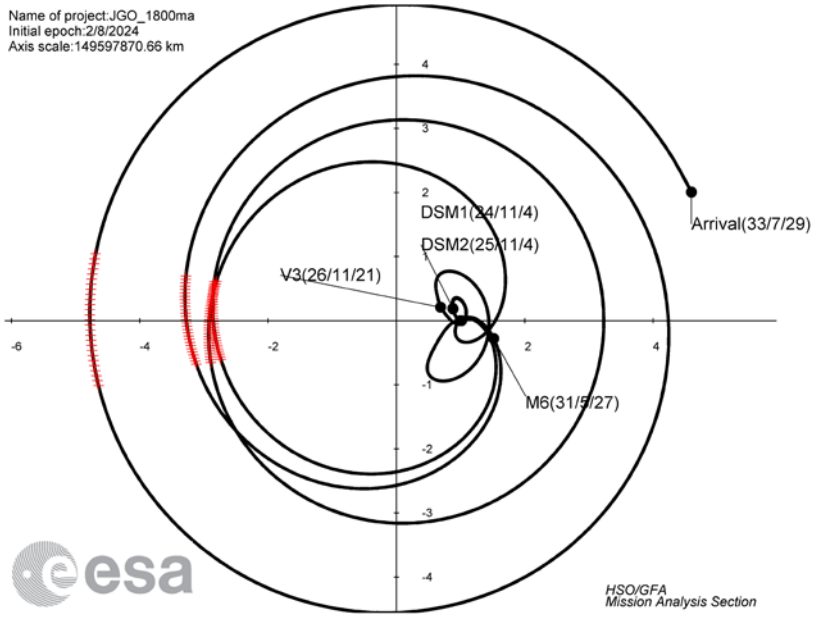

Figure 4-28: Interplanetary transfer in the Sun-Earth co-rotating frame. The superior conjunctions are shown with red '+' marker (option 1800ma)

It can be seen that the swing-bys and the DSM are far from a superior conjunction.

Figure 4-29 shows the evolution of the Sun-s/c-Earth angle and the Sun-Earth-s/c angle. When both angles are close to zero there is a superior conjunction.

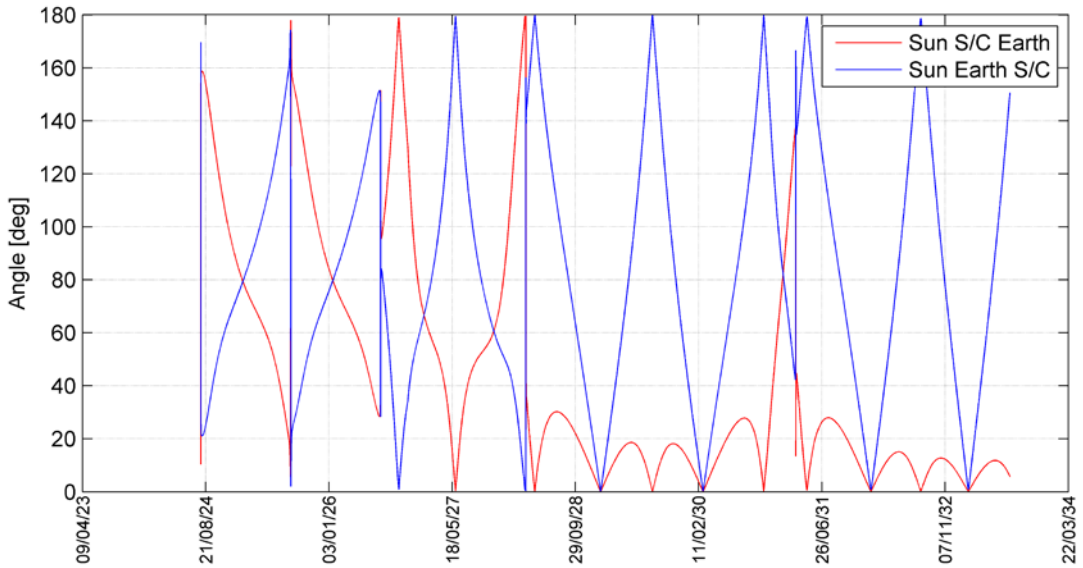

Figure 4-29: Evolution of Sun-S/C-Earth and Sun-Earth-S/C angles during the transfer (option 1800ma)

Figure 4-30 shows the evolution of the distance with respect to the Sun, Venus, Earth, Mars and Jupiter.

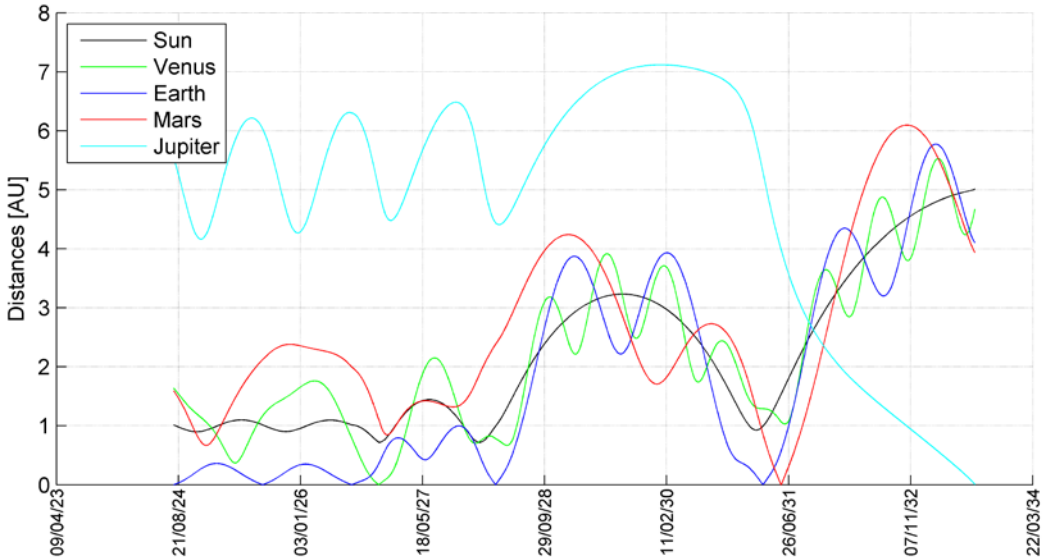

Figure 4-30: Evolution of distances during the interplanetary transfers (option 1800ma)

4.4.2 Option 180lolma

All features are roughly identical to those presented in Paragraph 4.4.1 for the option 1800ma, except for the first two EGA, which are replaced by LEGA. Therefore all figures are not repeated here.

From a geometrical point of view, the first LEGA is similar to the first LEGA of the option 150l0la, see Paragraph 4.2.3. The second LEGA is comparable to that of the option 230la (see Paragraph 4.3.2), except that the EGA perigee altitude is larger, 100,000 km instead of 40,000 km.

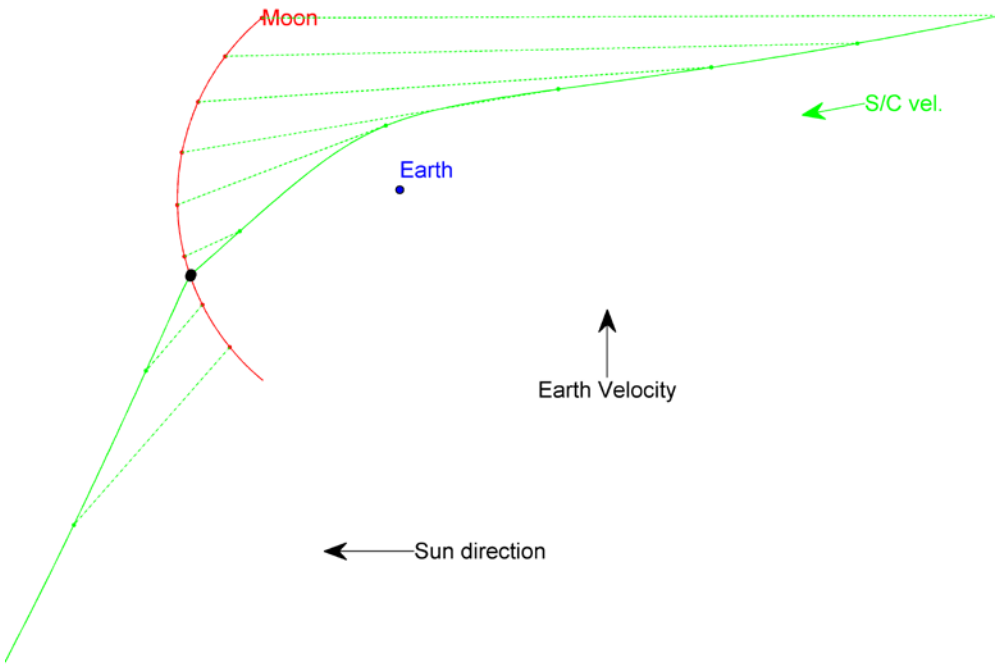

Figure 4-31: Ecliptic projection of the LEGA in the Sun-Earth co-rotating frame (second LEGA, option 180lolma)

The main features of the LEGA is summarized in Table 4-8. The leveraging of the LEGA is very good, about 500 m/s.

Table 4-8: LEGA main features (second LEGA, option 180lolma)

	Earth fly-by	Moon fly-by
Date	13/08/2026	14/08/2026
Vinf [km/s]	2.57	2.70
Pericentre radius [km]	106603	2037
Pericentre altitude [km]	99975	300
Transfer duration [hour]	33	
LEGA Vinf leveraging [km/s]	0.5	

4.4.3 Option 17ImeIem

The transfer follows an EEVEE-GA sequence. The inertial ecliptic projection is shown in Figure 4-32.

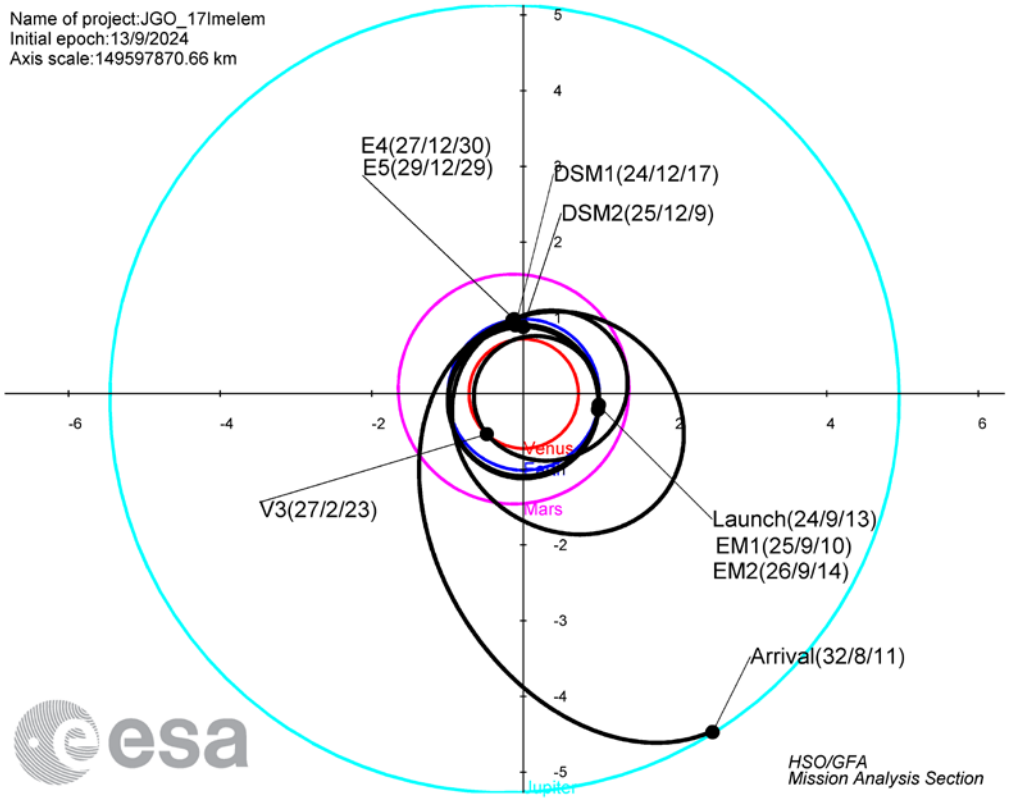

Figure 4-32: Interplanetary transfer in the ecliptic inertial frame (option 17ImeIem)

The projection in the Sun-Earth co-rotating frame is shown in Figure 4-33. It is visible that the Venus swing-by, the Jupiter arrival and the two DSM are far from the negative x-axis, meaning there is no risk of superior conjunction during or close to critical events of the interplanetary transfer.

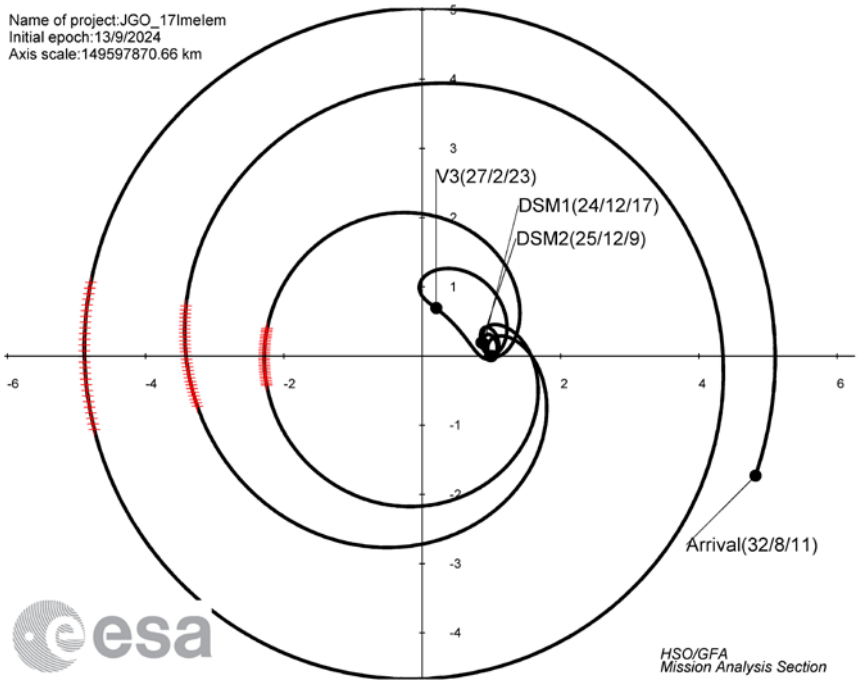

Figure 4-33: Interplanetary transfer in the Sun-Earth co-rotating frame. The superior conjunctions are shown with red '+' marker (Option 17ImeIem)

Figure 4-34 shows the evolution of the Sun-s/c-Earth angle and the Sun-Earth-s/c angle. When both angles are close to zero there is a superior conjunction.

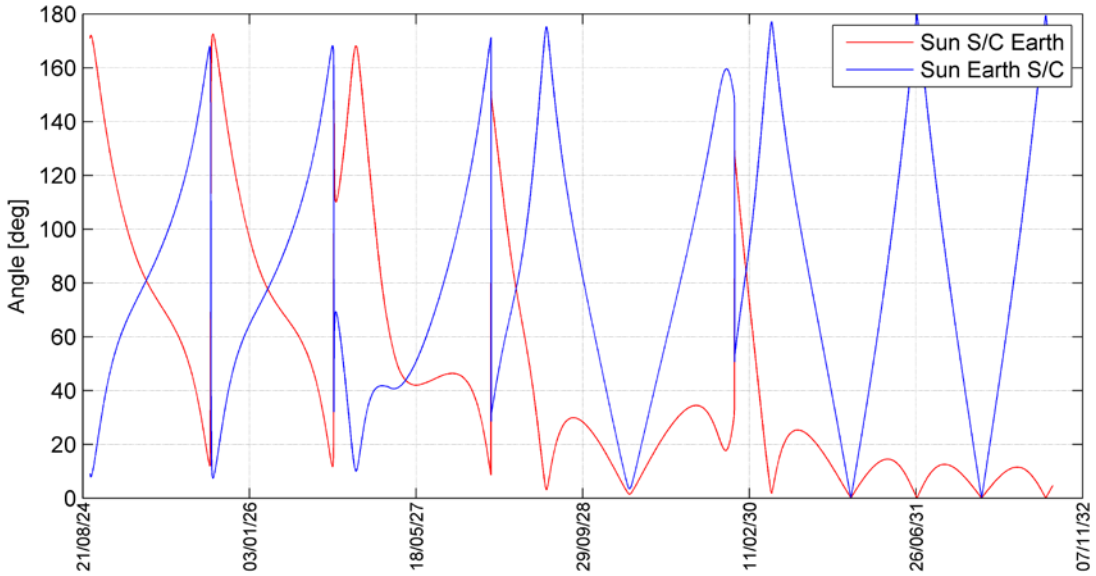

Figure 4-34: Evolution of Sun-S/C-Earth and Sun-Earth-S/C angles during the transfer (option 17 ImeIem)

Figure 4-35 shows the evolution of the distance with respect to the Sun, Venus, Earth, Mars and Jupiter.

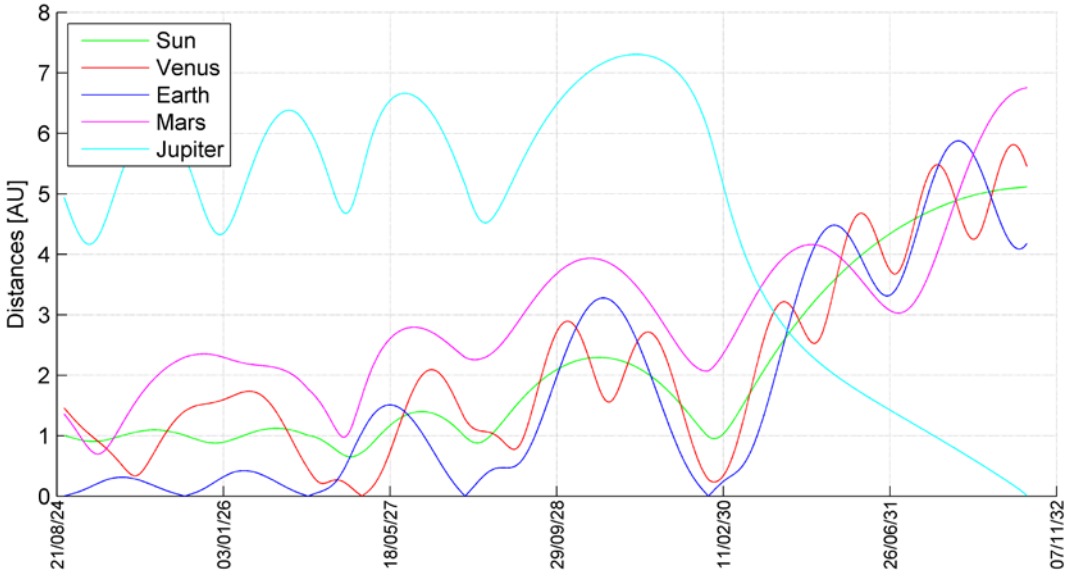

Figure 4-35: Evolution of distances during the interplanetary transfer (option 17ImeIem)

The first LEGA takes place in September 2025 is shown in Figure 4-36 in the Sun-Earth co-rotating frame. It is outbound radial /radial.

The first fly-by is performed with the Moon (periselenium altitude at 300 km) followed by a very high altitude EGA (~160000 km). The main features of the LEGA is summarized in Table 4-9. The leveraging effect of the LEGA is 360 m/s.

Table 4-9: LEGA main features (first LEGA, option 17ImeIem)

	Moon fly-by	Earth fly-by
Date	08/09/2025	25/08/2025
Vinf [km/s]	2.82	2.89
Pericentre radius [km]	2037	160876
Pericentre altitude [km]	300	93372
Transfer duration [hour]	28	
LEGA Vinf leveraging [km/s]	0.36	

The second LEGA takes place in September 2026 is shown in Figure 4-37 in the Sun-Earth co-rotating frame. It is outbound radial/tangential.

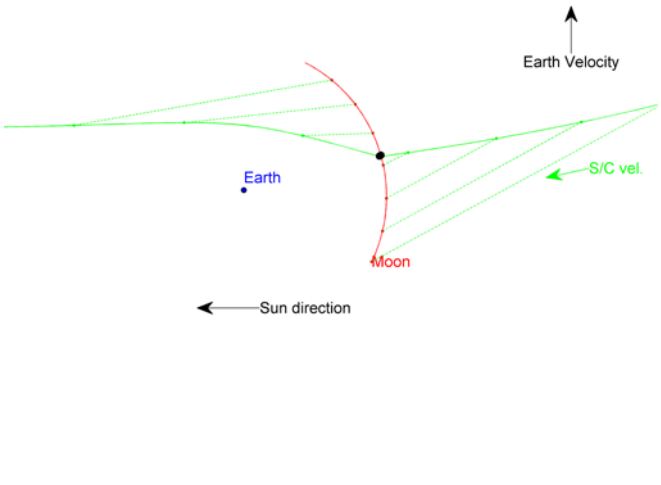

Figure 4-36: Ecliptic projection of the LEGA in the Sun-Earth co-rotating frame (first LEGA, option 17ImeIem)

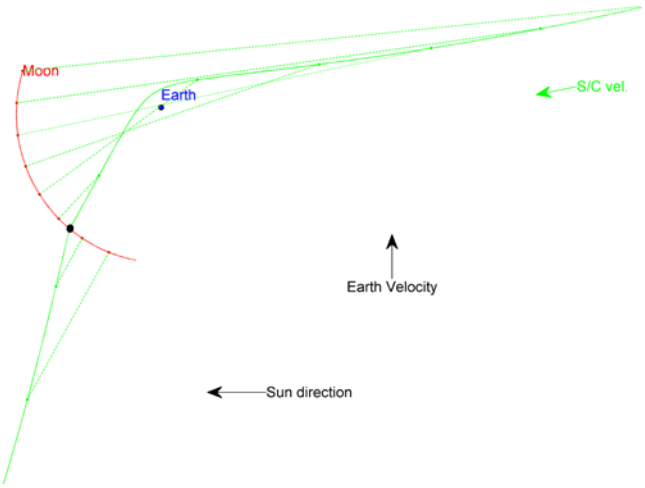

Figure 4-37: Ecliptic projection of the LEGA in the Sun-Earth co-rotating frame (second LEGA, option 17ImeIem

The first fly-by is performed with the Earth first (medium perigee altitude of 35000 km) followe by the Moon (periselenium at 300 km). The main features of the LEGA is summarized in Table 4-10. The leveraging of the LEGA is 400 m/s.

Table 4-10: LEGA main features (second LEGA, option 17ImeIem)

	Earth fly-by	Moon fly-by
Date	14/09/2026	15/09/2026
Vinf [km/s]	3.13	3.37
Pericentre radius [km]	41247	2037
Pericentre altitude [km]	34869	300
Transfer duration [hour]	29	
LEGA Vinf leveraging [km/s]	0.4	

4.5 Launch in 2025

The selection of options is presented in Table 4-11.

Table 4-11: Summary of transfer options for a launch in 2025

Case	180ma	200lma
Launch date	25/08/04	25/08/11
Launch V-infinity max [km/s]	2.80	2.00
Launch mass [kg]	5321	5925
Launch correction [m/s]	30	30
Launch window max [m/s]	75	43
DSM [m/s]	41	169
Swing-by date		
DSM [m/s]	0	0
Swing-by date	26/08/03	26/08/13
Swing-by date	26/11/21	26/11/29
Swing-by date	28/03/13	27/08/23
Swing-by date		29/02/16
DSM [m/s]	0	82
Swing-by date	31/03/13	31/02/21
Swing-by date	31/05/27	31/05/23
Transfer navigation (m/s)	135	160
Arrival date	33/07/29	33/08/05
Arrival V-infinity [km/s]	5.78	5.65
Arrival right ascension [deg]	254.6	254.9
Arrival declination [deg]	4.3	4.3
JOI [m/s]	928	885
Duration [year]	8.0	8.0
Closest distance to Sun [AU]	0.72	0.72
Closest DSM distance to Sun [AU]	0.90	0.91
Closest distance to Venus [km]	3420	6966

4.5.1 Option 180ma

The option 180ma follows an EVEE-GA sequence. The inertial ecliptic projection is shown in Figure 4-38.

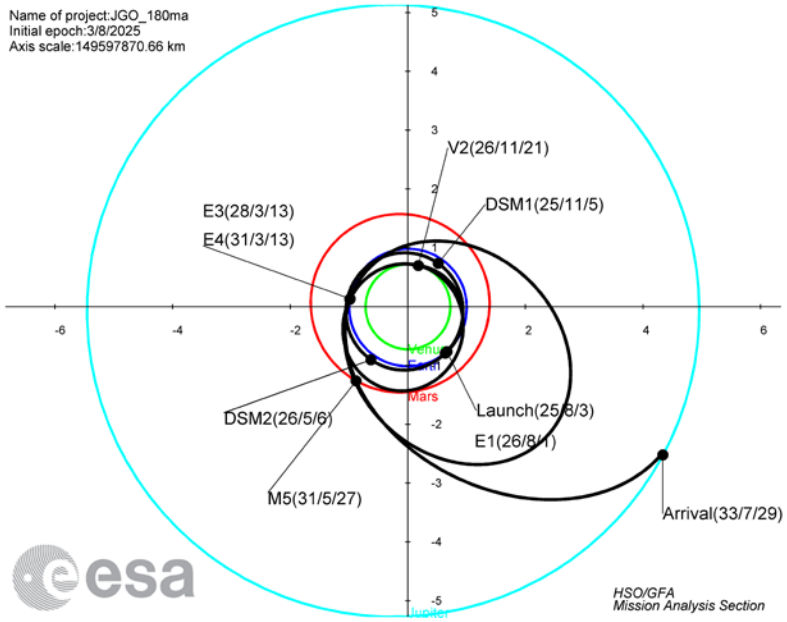

Figure 4-38: Interplanetary transfer in the ecliptic inertial frame (option 180ma)

The projection in the Sun-Earth co-rotating frame is shown in Figure 4-39.

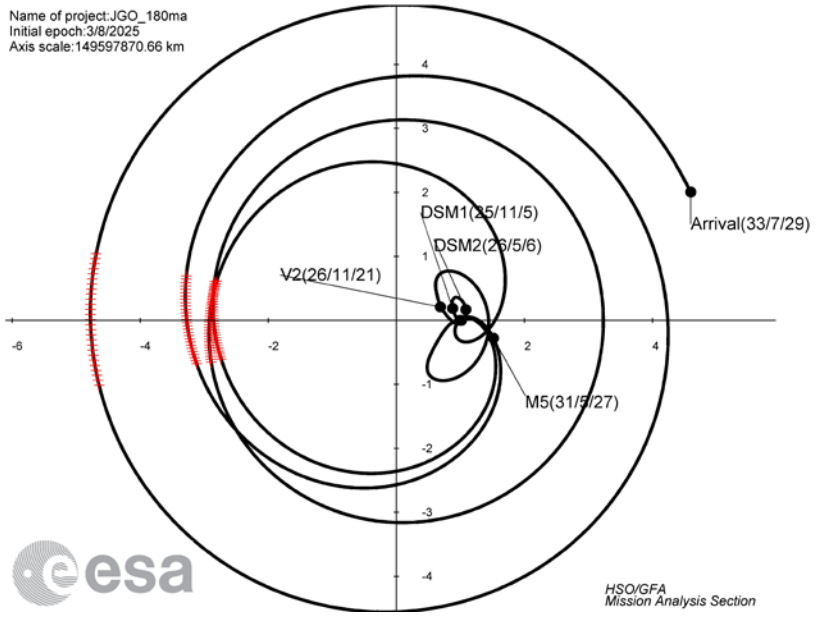

Figure 4-39: Interplanetary transfer in the Sun-Earth co-rotating frame. The superior conjunctions are shown with red '+' marker (option 180ma)

It can be seen that the swing-bys and the DSM are far from a superior conjunction.

Figure 4-40 shows the evolution of the Sun-s/c-Earth angle and the Sun-Earth-s/c angle. When both angles are close to zero there is a superior conjunction.

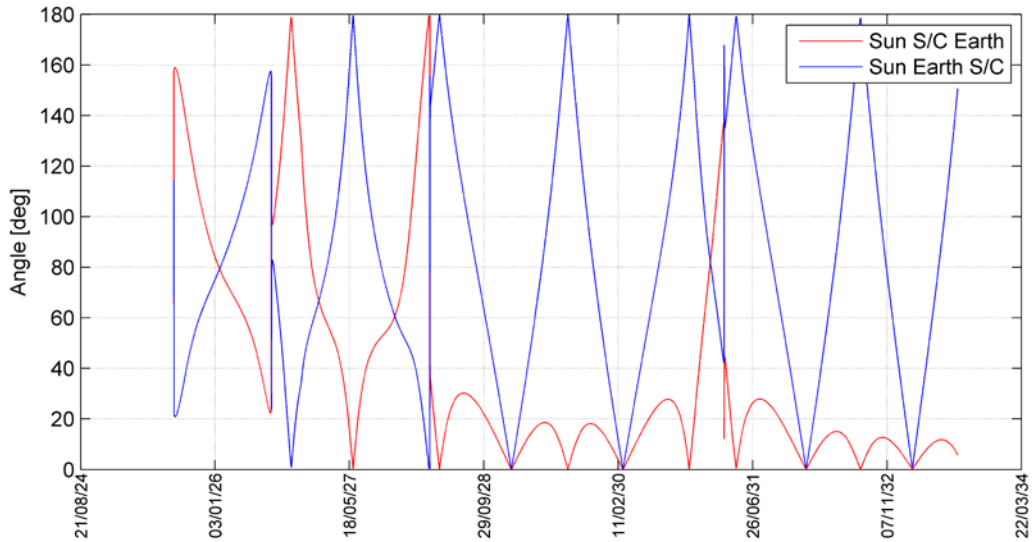

Figure 4-40: Evolution of Sun-S/C-Earth and Sun-Earth-S/C angles during the transfer (option 180ma)

Figure 4-41 shows the evolution of the distance with respect to the Sun, Venus, Earth, Mars and Jupiter.

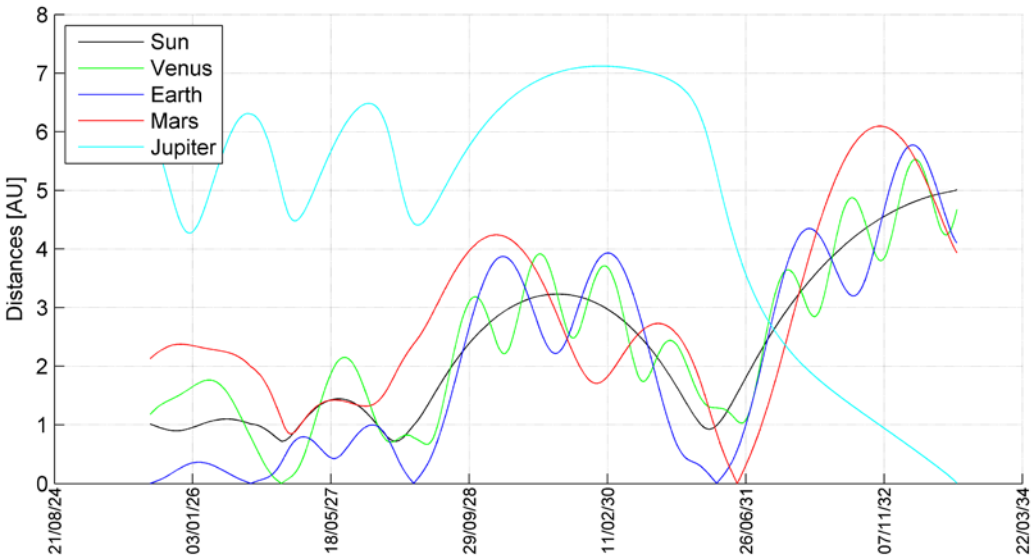

Figure 4-41: Evolution of distances during the interplanetary transfers (option 180ma)

4.5.2 Option 200lma

The transfer follows an EVEE-GA sequence. The inertial ecliptic projection is shown in Figure 4-42.

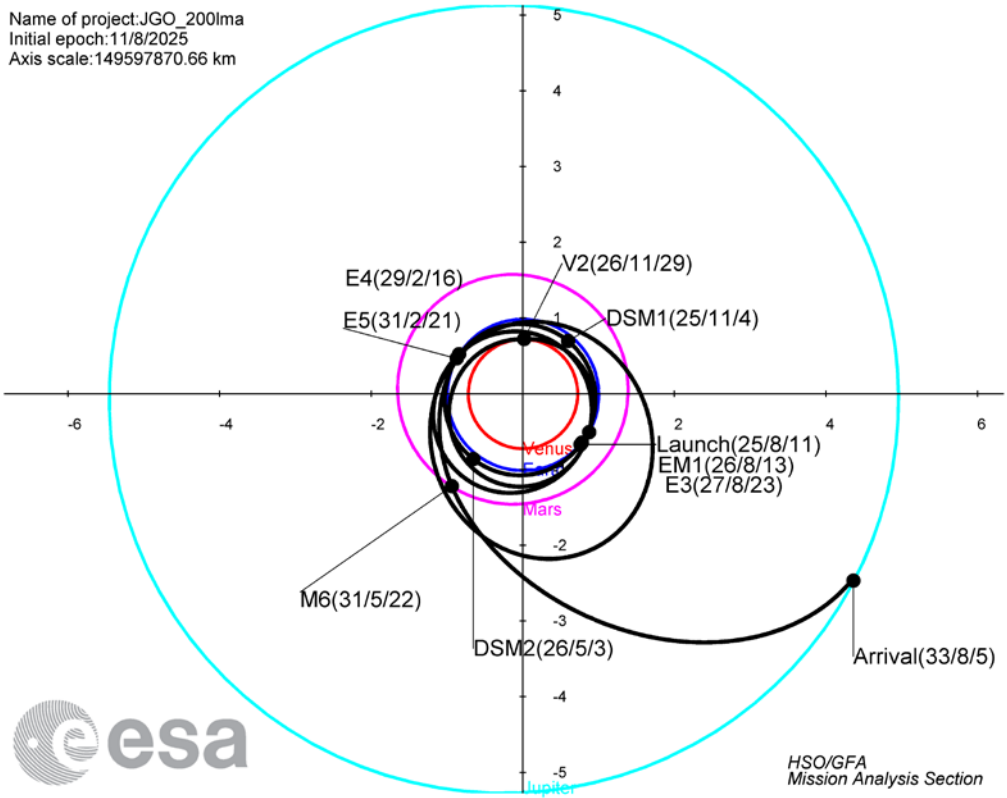

Figure 4-42: Interplanetary transfer in the ecliptic inertial frame (option 200lma)

The projection in the Sun-Earth co-rotating frame is shown in Figure 4-43 It is visible that the Venus swing-by, the Jupiter arrival and the two DSM are far from the negative x-axis, meaning there is no risk of superior conjunction during or close to critical events of the interplanetary transfer.

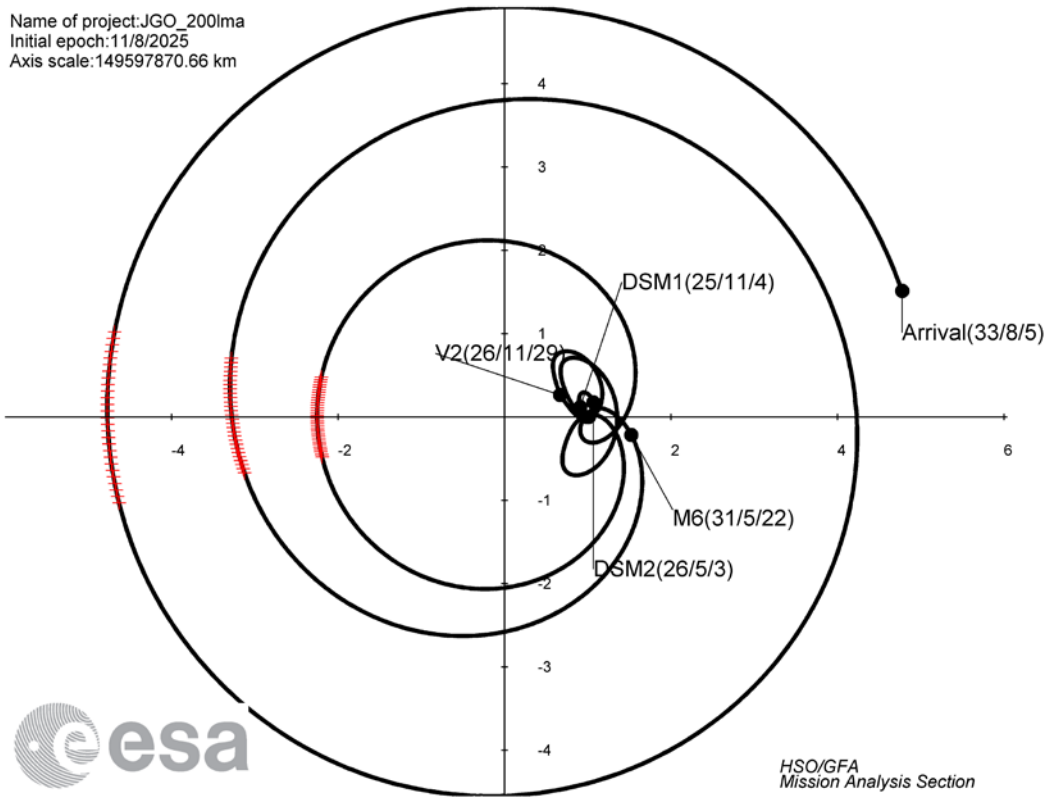

Figure 4-43: Interplanetary transfer in the Sun-Earth co-rotating frame. The superior conjunctions are shown with red '+' marker (Option 200lma)

Figure 4-44 shows the evolution of the Sun-s/c-Earth angle and the Sun-Earth-s/c angle. When both angles are close to zero there is a superior conjunction.

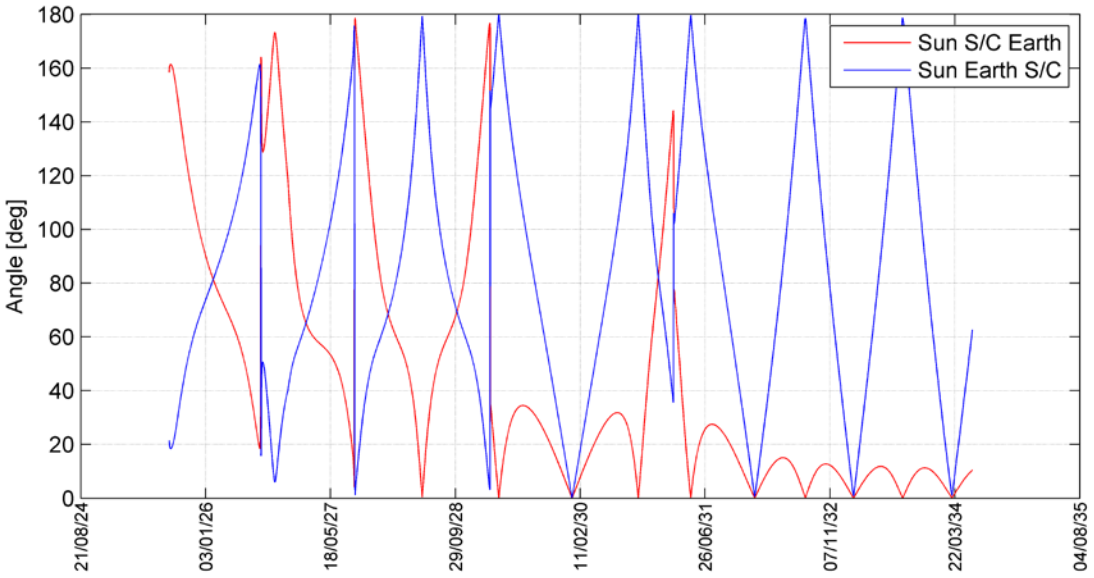

Figure 4-44: Evolution of Sun-S/C-Earth and Sun-Earth-S/C angles during the transfer (option 200lma)

Figure 4-45 shows the evolution of the distance with respect to the Sun, Venus, Earth, Mars and Jupiter.

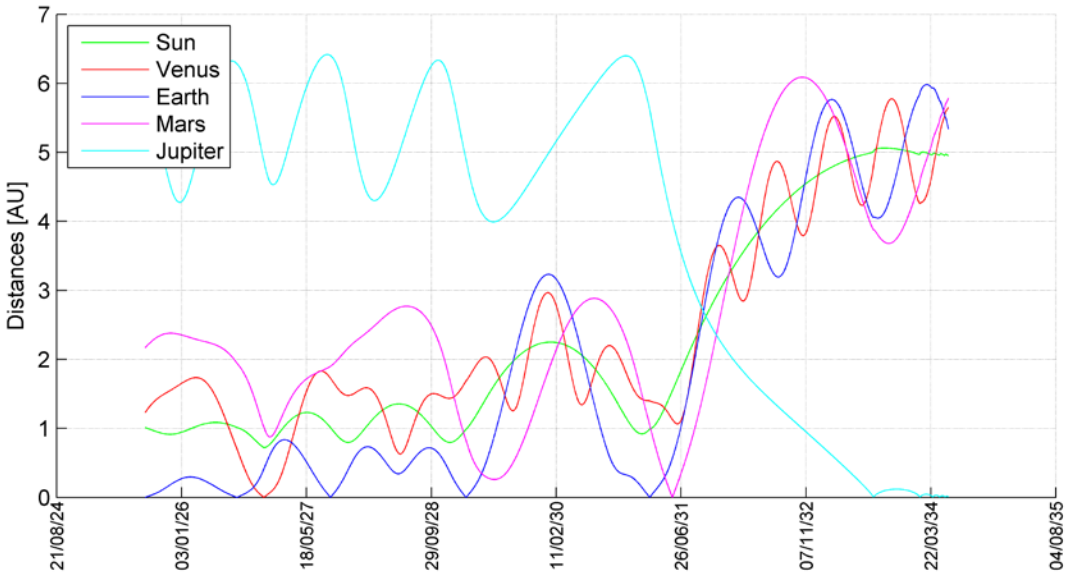

Figure 4-45: Evolution of distances during the interplanetary transfer (option 200lma)

From a geometrical point of view, the first LEGA is similar to the second LEGA of the option 180lolma, see Paragraph 4.4.2. Therefore it is not repeated here.

5 FROM JUPITER ARRIVAL TO EUROPA FLY-BYS

The Jupiter tour presented hereafter is an end-to-end consolidated trajectory. It was designed for the option 141a. Even if there are commonalities in the design of the Jupiter tour for all options, the superior solar conjunctions make each case specific. Therefore it was not possible to present generic results.

Upon arrival at Jupiter, the infinite velocity w.r.t. Jupiter is 5.5 km/s. In order to be captured in-orbit around the planet, the JOI is applied at perijove as shown in Figure 5-1.

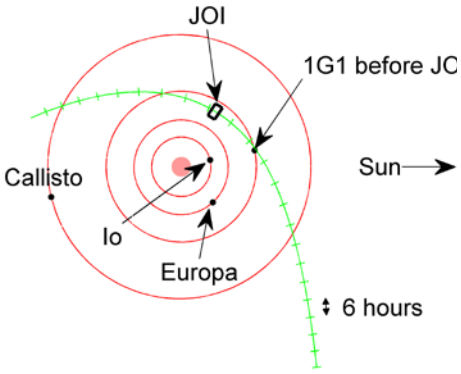

Figure 5-1: Spacecraft capture around Jupiter

The size of the JOI is 790 m/s (with ~1% gravity losses). A Ganymede gravity assist (1G1) is applied prior to the JOI to reduce the size of the capture manoeuvre. The altitude of the gravity assist is set to 400 km to guarantee a collision free fly-by in case of inaccurate orbit determination (see chapter on navigation). The time between G1 and the JOI is approximately 7.5 hours. This means that the JOI shall be implemented in open loop mode (timer for start and stop, spacecraft attitude) as there is not enough time to run an orbit determination.

After the JOI the spacecraft is injected into a 30:1 resonant orbit with Ganymede. At apojove the Perijove Raising Manoeuvre (PRM) is applied. This manoeuvre has a double purpose. On one side it is meant to raise the perijove in order to target the arrival velocity at the next Ganymede swingby necessary to initiate the Europa phase. On the other side it is used to stabilize the perijove of the orbit and compensate for the Sun perturbation. The size of the PRM is 91 m/s such as to reduce the infinite velocity at 2G2 down to 6.5 km/s . The trajectory between 1G1 and 2G2 is shown in Figure 5-2.

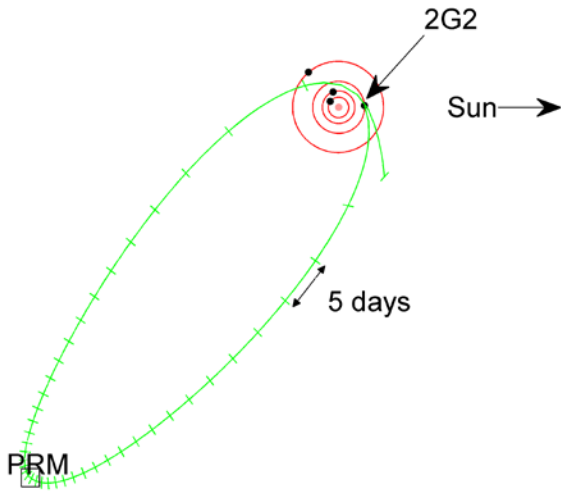

Figure 5-2: Trajectory from Jupiter arrival up to 2G2

The Europa phase is initiated by a near equatorial transfer from Ganymede: contrary to previous tours, Callisto is not used on the way to Europa. However the incoming asymptote of the hyperbola has a declination of -3.1 degrees w.r.t. Jupiter equatorial plane, which implies that it is not possible to achieve an orbit in the plane of the equator of Jupiter after the JOI (it could only be done at a prohibitive DeltaV cost). An inclination change manoeuvre could be performed at apojove, if the apojove were close to the line of nodes, but this is not the case

for the baseline scenario. The inclination shall be gradually reduced by repetitive Ganymede gravity assists.

Moreover the orbital period, initially equal to 30 times that of Ganymede, shall also be reduced before the transfer to Callisto prior to Europa science phase. This is also done with repetitive Ganymede gravity assists. The sequence that was chosen is 8:1 (between 2G2 and 3G3), 5:1+ (between 3G3 and 4G4) and 3:1 (between 4G4 and 5G5).

At 5G5 Ganymede is encountered outbound. The arrival date is September, 3 2030, it is the end of the so-called energy reduction phase. This part of the Jupiter tour is given in Figure 5-3 in the Jupiter Solar Orbital (JSO) frame (with positive x-axis pointing towards the Sun).

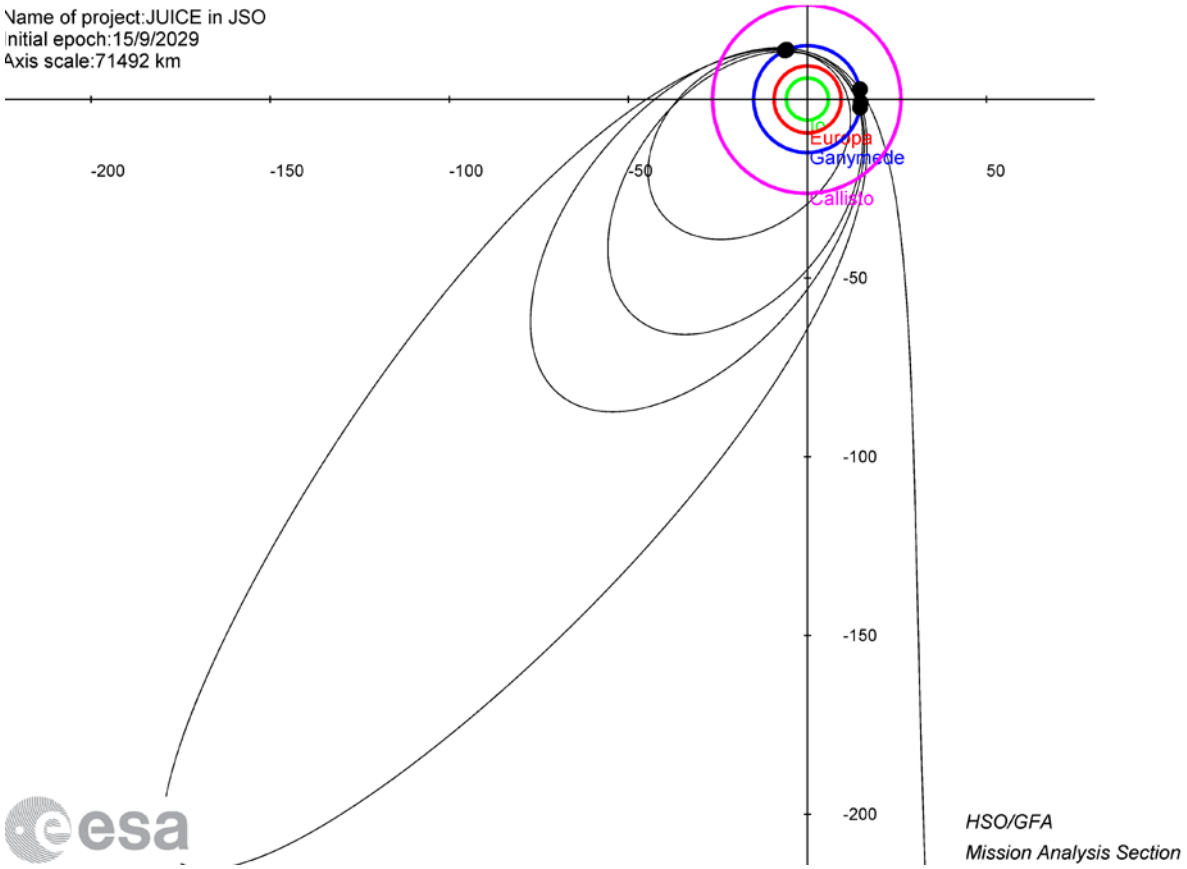

Figure 5-3: Trajectory from before 1G1 to 5G5 in the JSO

The evolution of the distance to Jupiter is shown in Figure 5-4.

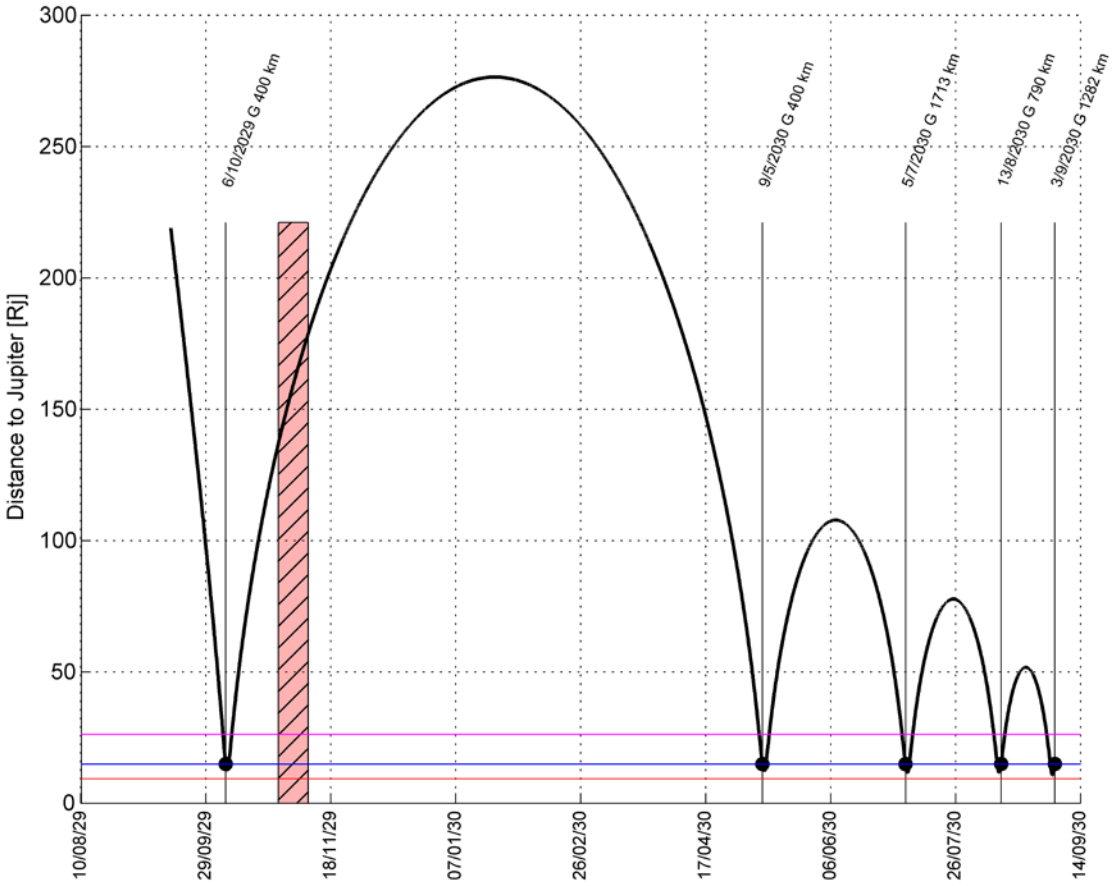

Figure 5-4: Evolution of the distance to Jupiter from 2G2 to 5G5. The orbital radii of the Galilean moons are represented as horizontal coloured lines. The fly-bys are represented as black dots. The presence of the first superior conjunction is visible weeks after the JOI (hatched area)

6 EUROPA FLY-BYS

The Europa phase is made of two fly-bys. The number of fly-bys was chosen such that the radiation dose is kept at a minimum level, while fulfilling the scientific objectives related to this moon.

The sequence is [Ganymede outbound]-[Europa fly-by at perijove]-E4:1-[Europa fly-by at perijove]-[Callisto inbound].

From a scientific point of view, a list of target areas was given as shown in Figure 6-1.

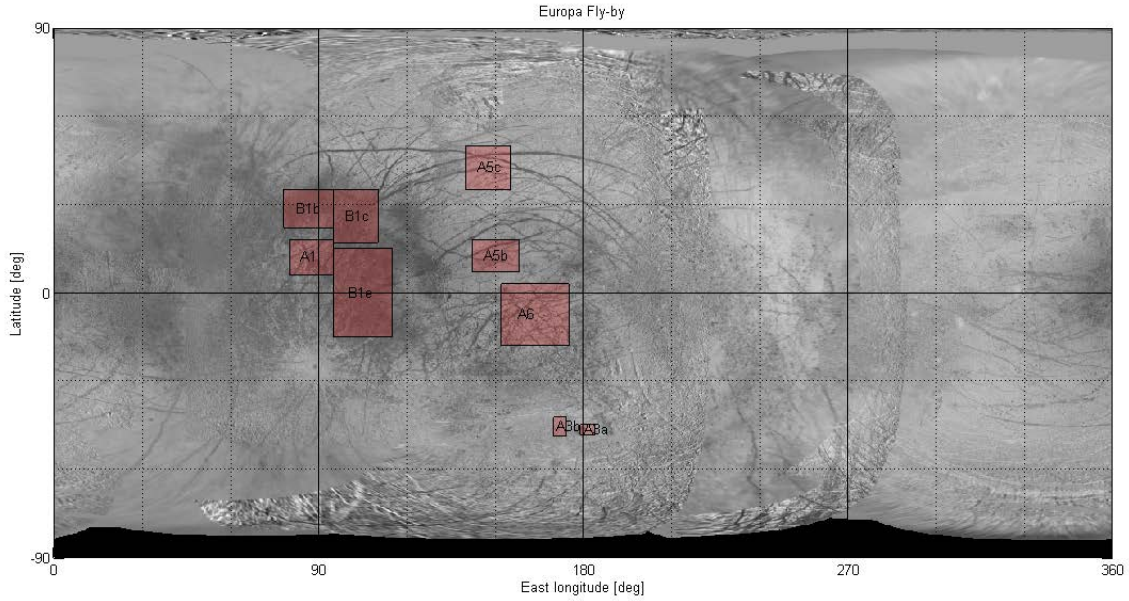

Figure 6-1: List of target areas as defined by the science team

From a dynamical point of view, it is impossible to obtain groundtrack with Closest Approach (C/A) over the trailing or leading side, i.e. with longitudes close to 90 deg or 270 deg. This automatically rules out the following sites: A1, B1b, B1c and B1e.

The structure of the solution space also leads to rather symmetrical solutions w.r.t. the equator: in other words the sequences are possible: either A5b and A6, or A3a, A3b and A5c. The best option (from a deltaV point of view) was A3a, A3b and A5c. The solution is given in Figure 6-2.

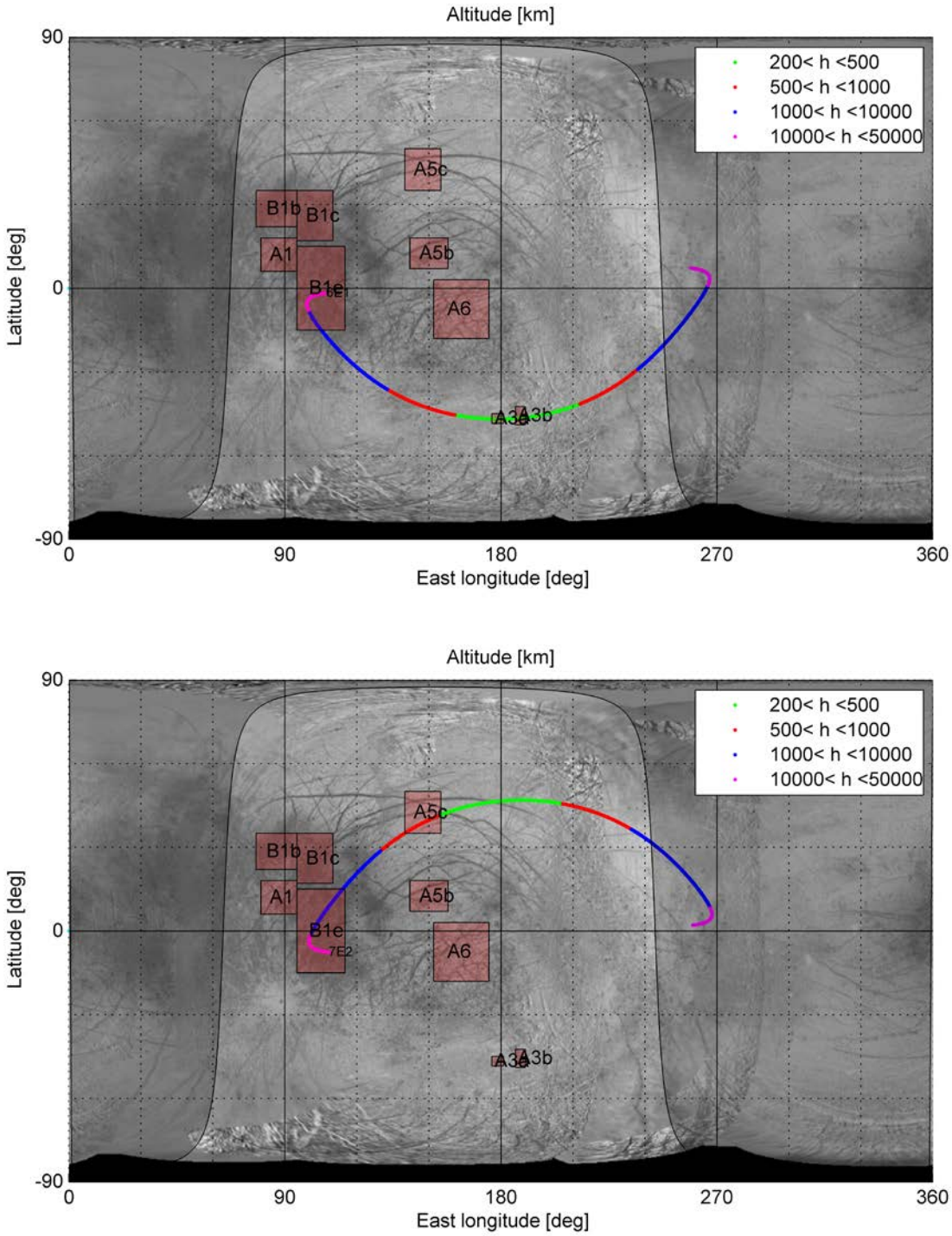

Figure 6-2: Groundtracks of 6E1 (top) and 7E2 (bottom). The Sun terminator at C/A is also indicated

The region A3a is called Thera Macula and the region A3b is called Thrace Macula (see Figure 6-3). These chaos fit all the evaluated criteria for the presence and preservation of biosignatures.

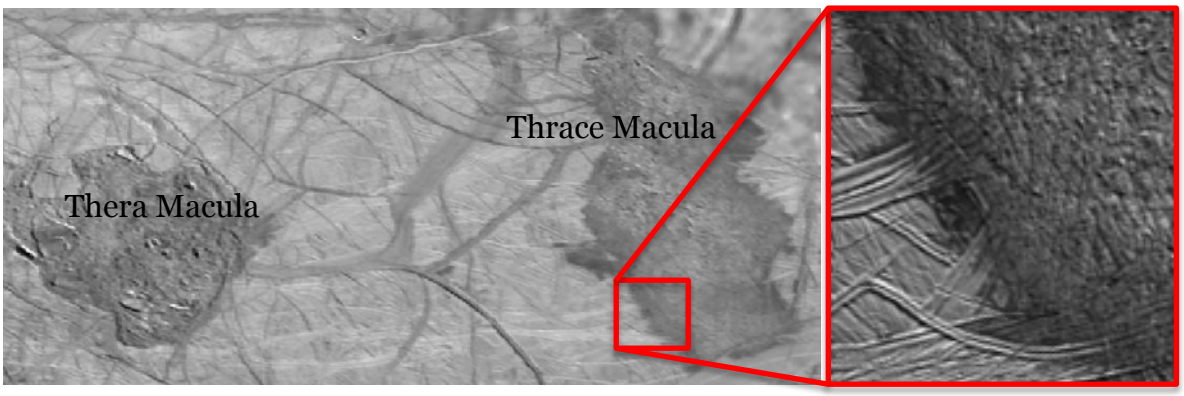

Figure 6-3: Thera Macula and Thrace Macula (left), zoom on Thrace Macula (right)

The region A5c is a lenticulae associated with prominent intersecting ridges of Minos with Udaeus lineae and Cadmus linea below (see Figure 6-4).

It can be observed that the C/A is over A3b while also flying nadir over A3a. The C/A of the other fly-by is roughly 30 deg East of A5c. However the altitude is lower than 600 km for the entire target area.

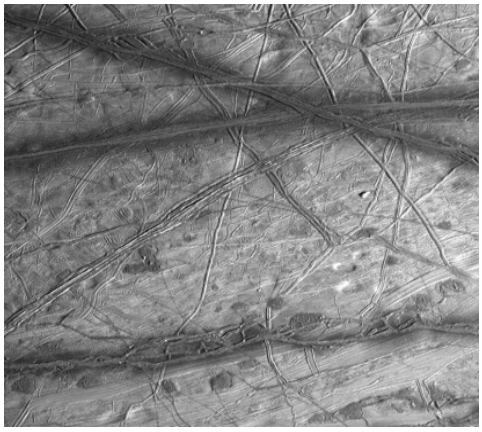

Figure 6-4: Intersection of Minos and Udaeus lineae with Cadmus linea below

For both fly-bys the approach hyperbola is over the trailing side of Europa; in other words the target areas A1, B1b, B1c and B1e can be observed on the incoming leg.

For both fly-bys the outgoing leg of the hyperbola is over the leading side. This means a comparative analysis of the trailing side vs leading side can done for altitudes greater than 5000-10000 km.

In CReMA 3.0, the Sun-Jupiter-Europa angle, also called solar longitude, was around 50 deg for both EGA (6E1 and 7E2), in-line with the range of illumination suggested by the science team from -15 deg to +60 deg (see RD21).

The first drawback of this value (50 deg) is that it induces a 4.8 hours eclipse 2 days after 6E1. The eclipse disappears when the solar longitude is smaller than ~30 deg.

The second drawback is related to the average solar power received by the solar arrays during 6E1 and 7E2. For stability reasons, the spacecraft is in push broom mode around closest approach. For the same reason, the SADM is in hold mode around closest approach. As a consequence there is an optimal cant angle of the arrays maximising the average power received around closest approach. This average power is shown in Figure 6-5.

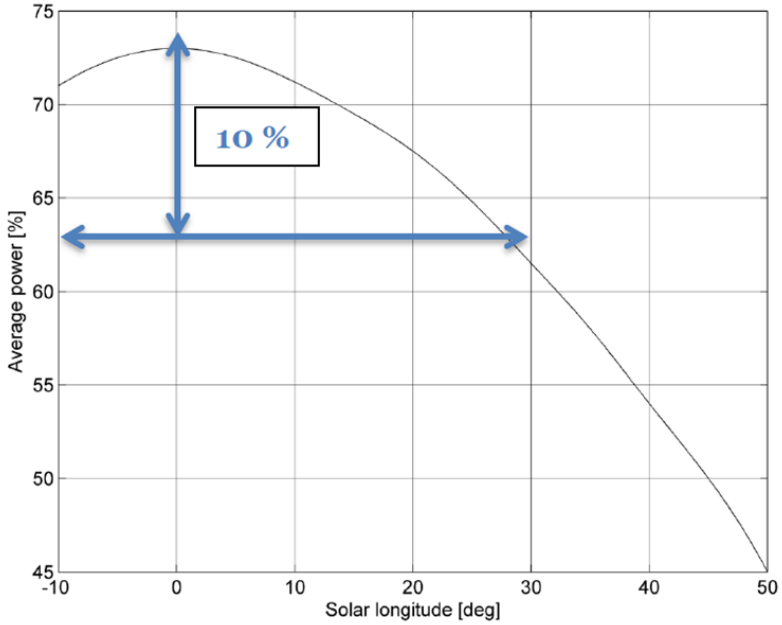

Figure 6-5: Average solar power received by the solar arrays around closest approach as a function of the solar longitude (6E1 and 7E2 being rather symmetric w.r.t the equator, only one plot is shown). A value of 100% corresponds to the case, where the solar arrays are always perpendicular to the Sun direction. The average solar power is maximised by the optimisation of the cant angle of the SADM

The optimal solar longitude is 0 deg (73%). For 15 deg, there is a reduction of 5% (68%), for 30 deg the reduction is 10% (see figure), while for 50 deg, the reduction is 28%.

The initial interval to find a solution (from -10 deg to 60 deg) was reduced to -10 deg to 30 deg, with the objective to find a solution below 15 deg if possible. In CReMA 3.1 the optimal solution had been chosen (solar longitude close to 15 deg). However this led to an accumulation of radiation in the 2:2- after the Europa science phase. The current solution permits a reduction of the radiation dose but at the cost of an increase in the solar longitude, which is close to 25 deg.

The trajectory corresponding to 5G5-6E1-7E2-8C1 is given in Figure 6-6. As written above, the solar longitude of 6E1 and 7E2 was around 15 deg before, while now it is 23 deg for 6E1 and 26 deg for 7E2. These values are consistent with the requirement to avoid an eclipse between 6E1 and 7E2. A feedback from industry has confirmed that such an illumination is also compatible with the power budget.

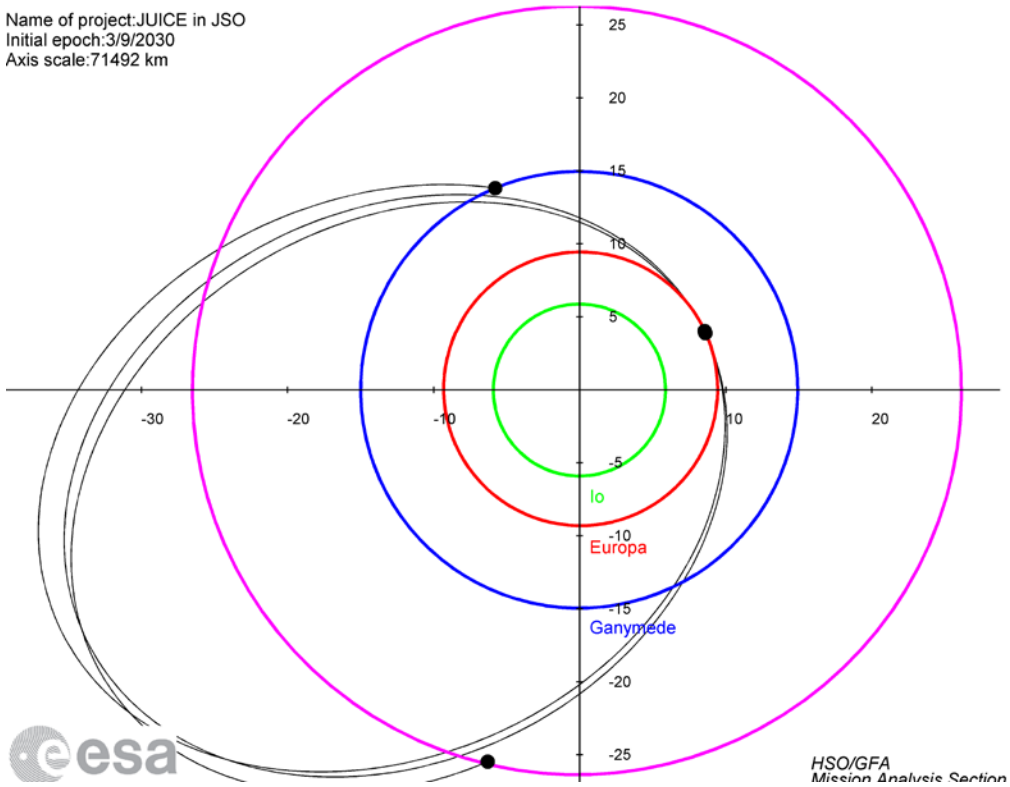

Figure 6-6: Trajectory from 5G5 to 8C1 in the JSO

The 3D view of both fly-bys is given in Figure 6-7 with shadow at the epoch of C/A.

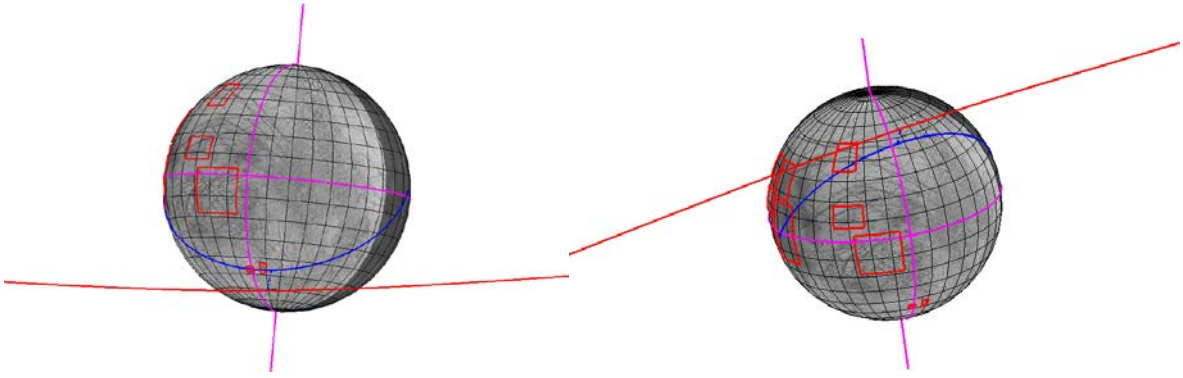

Figure 6-7: 3D representation of 6E1 (left) and 7E2 (right)

Both fly-bys are in daylight over the target areas. In order to show the illumination conditions, the evolution of the solar local time of the subsatellite point as a function of the longitude is given in Figure 6-8. The Sun tends to illuminate the trailing of Europa, where most of the target areas are located.

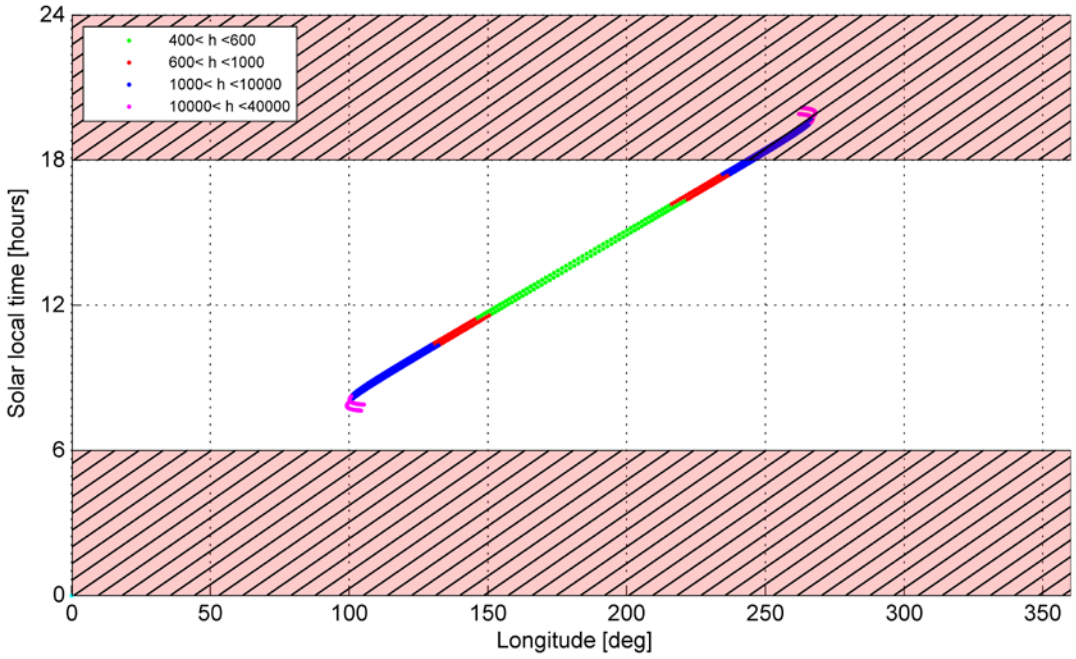

Figure 6-8: Solar local time of the subsatellite point as a function of the longitude during 6E1 and 7E2

All target areas on the incoming leg are in daylight. After the C/A the sun sets for a longitude of 245 deg: it corresponds to an altitude of 1500 km for 6E1 and 1400 km for 7E2. By using Figure 6-9, it corresponds to ~9.5 min after the C/A for both Europa fly-bys.

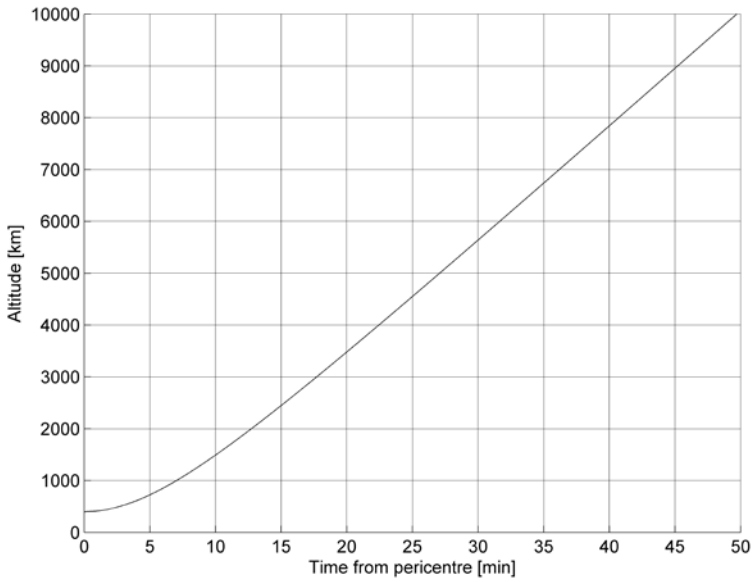

Figure 6-9: Altitude as a function of the time from C/A

It is also interesting to show the evolution of the subsatellite point velocity as a function of the longitude. It is given in Figure 6-10 together with the evolution of the altitude.

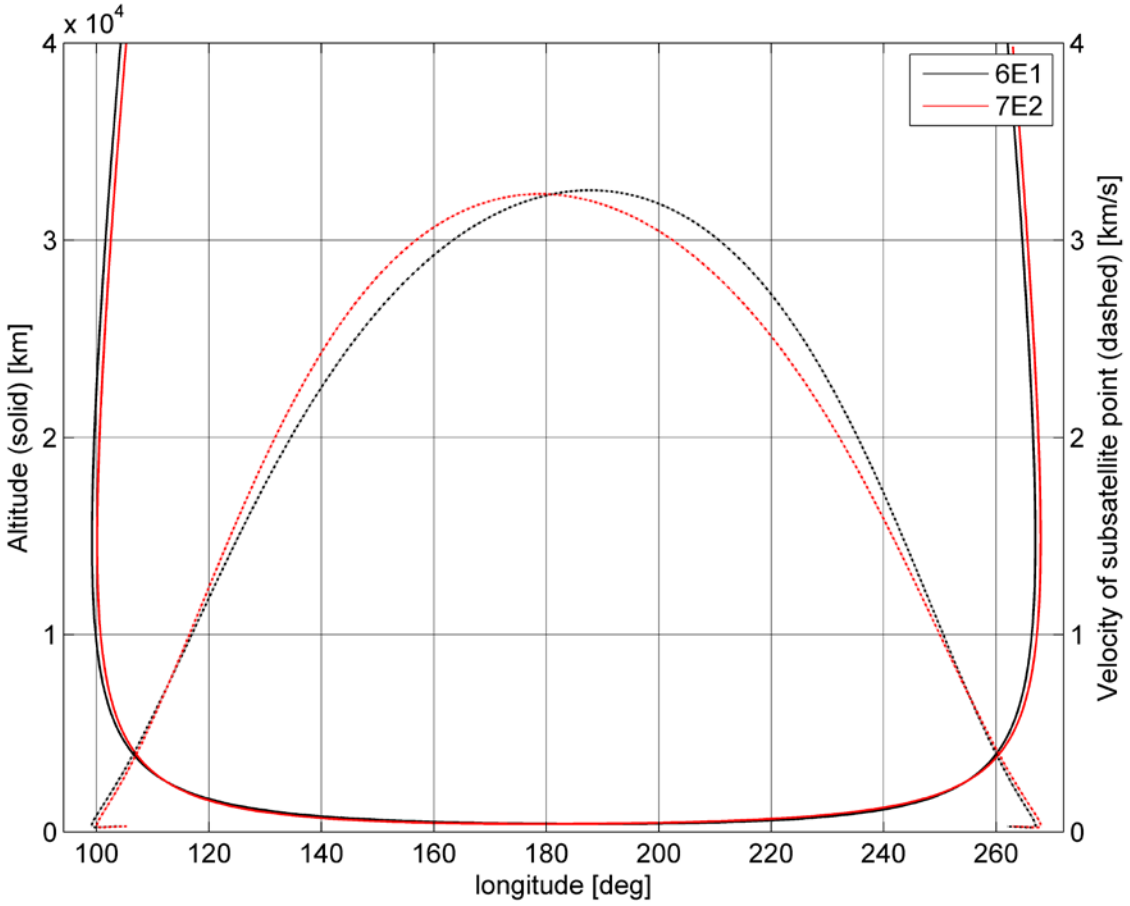

Figure 6-10: Evolution of the altitude and the ground velocity (i.e. subsatellite point velocity) as a function of the longitude

When the altitude is large, the spacecraft moves radially along the infinite velocity direction: the subsatellite point velocity is zero. It is actually not exactly zero because of the rotation of Europa.

At C/A the subsatellite point velocity is dominated by the spacecraft velocity and is just scaled down compared to the pericentre velocity: the inertial pericentre velocity is ~4.1 km/s at 400 km altitude and the subsatellite point velocity is ~3.2 km/s w.r.t. the surface.

From a scientific point of view (mainly for RIME), it is desirable to have Jupiter in shadow during the Europa fly-bys. This constraint cannot be taken into account a priori. However it is checked a posteriori. Figure 6-11 shows Jupiter's shadowing during the two fly-bys: it can be observed that only during 7E2 a full shadowing is obtained.

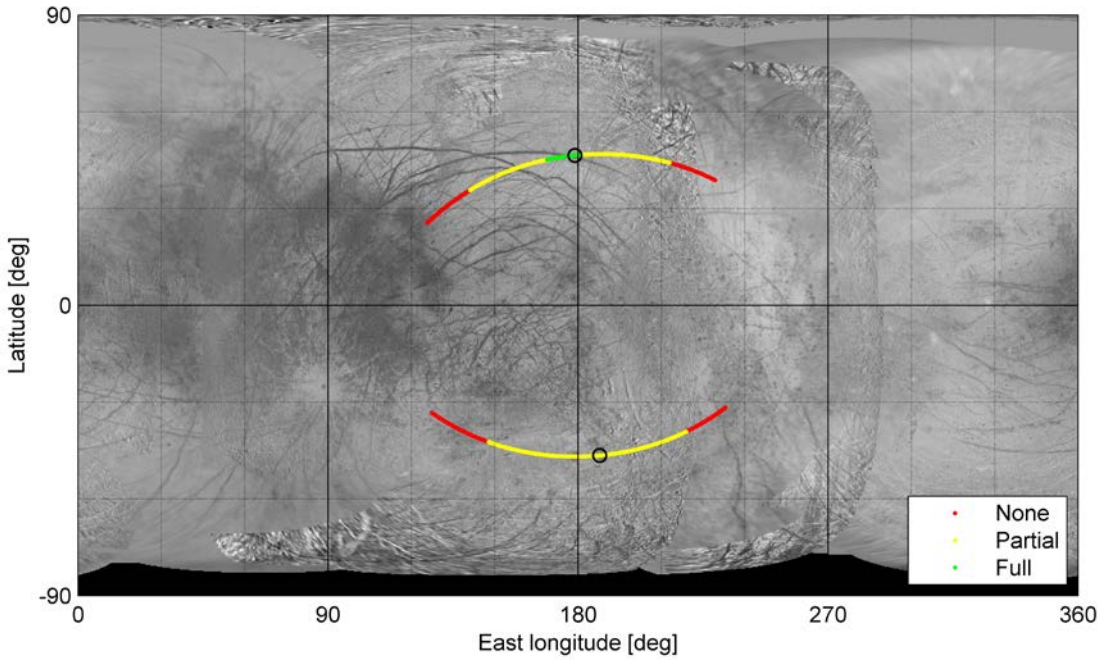

Figure 6-11: Jupiter's shadowing during the Europa fly-bys. A partial shadowing is observed during 6E1 (Southern fly-by). A full shadowing is obtained during 7E2 (Northern fly-by)

The main features of Jupiter's shadowing are summarized in Table 6-1. During 7E1 a full shadowing is obtained during 1.2 min, starting at 417 km and ending shortly after the pericentre passage at 404 km (for a pericentre altitude of 403 km).

Table 6-1: Summary of Jupiter's shadowing during the Europa fly-bys

			6E1	7E2
Partial	h_beg	[km]	649	679
	h_end	[km]	569	570
	duration	[min]	7.8	8.2
Full	h_beg	[km]	/	417
	h_end	[km]	/	404
	duration	[min]	/	1.2

7 JUPITER HIGH INCLINATION PHASE AND CALLISTO FLY-BYS

7.1 Baseline

The objective is to reach a minimum inclination of 22 deg w.r.t. Jupiter's equatorial plane. A series of resonant gravity assists is used to gradually raise the inclination before it is reduced back to the equatorial plane.

There are several free parameters that can be chosen: the moon to be used (Callisto or Ganymede), the infinite velocity and the resonance. The trade-off between duration, number of gravity assists and accumulated radiation dose is presented in Table 7-1.

Table 7-1: Options for the Jupiter high latitudes phase

Moon	Vinf [km/s]	Resonance	Nb GA	dt [day]	inc [deg]	rpmin [Rj]	rad [krad]
G	3	1:1	6	43	16	10.9	44
G	3	2:1	6	85	12	14	7
G	3	3:1	6	128	8	14.6	4
G	4	1:1	9	64	21	9.6	88
G	4	2:1	9	128	17	12.8	16
G	4	3:1	9	191	15	13.6	10
G	5	1:1	13	92	27	8.3	169
G	5	2:1	13	184	23	11.5	35
G	5	3:1	13	277	21	12.5	22
C	3	1:1	7	117	21	17	0
C	3	2:1	7	233	18	22.7	0
C	3	3:1	7	350	15	24.2	0
C	4	1:1	11	183	29	14	5
C	4	2:1	11	367	25	19.7	0
C	4	3:1	11	550	23	21.5	0
C	5	1:1	16	267	36	11.1	30
C	5	2:1	16	534	32	16.5	0
C	5	3:1	16	800	30	18.4	0

From this table using Callisto around 4 km/s with 1:1 resonance sounds like the best compromise. Initially the 11 fly-bys were used to reach the maximum inclination; it corresponds to a duration of 183 days. However the number of fly-bys is limited (for navigation DeltaV reasons), thus the theoretical maximum inclination cannot be reached anymore.

If the orbit cranking were initiated right after 8C1, the second superior conjunction would fall during the inclination raise. This issue was overcome by introducing an initial 3:3+ to jump over the conjunction. By doing so there a spurious encounter with Ganymede in between. This spurious encounter is transformed into a DVGA with Ganymede: the first advantage is to reduce the infinite velocity upon return at Callisto from 5 km/s to 4.8 km/s (useful to increase the maximum inclination); the other advantage is that the 9G6-10C2 transfer is a π-transfer, thus allowing for an initial cranking of the orbit up to an inclination of 3 deg. The superior solar conjunction is avoided in this leg.

After the ladder a series of three 1:1 is implemented. The next CGA (13C5) injects the spacecraft into a 5:6 resonant arc. The 5 Callisto revolutions permit to keep the overall duration of this phase roughly equal to 6 months, while the 6 spacecraft revolutions permit to reach a higher inclination that with a 5:4. The maximum inclination in the 5:6 is 29 deg.

After the 83 days of the 5:6, the orbit is cranked down via a series of four 1:1.

The evolution of the inclination during the Jupiter high latitudes phase is shown in Figure 7-1.

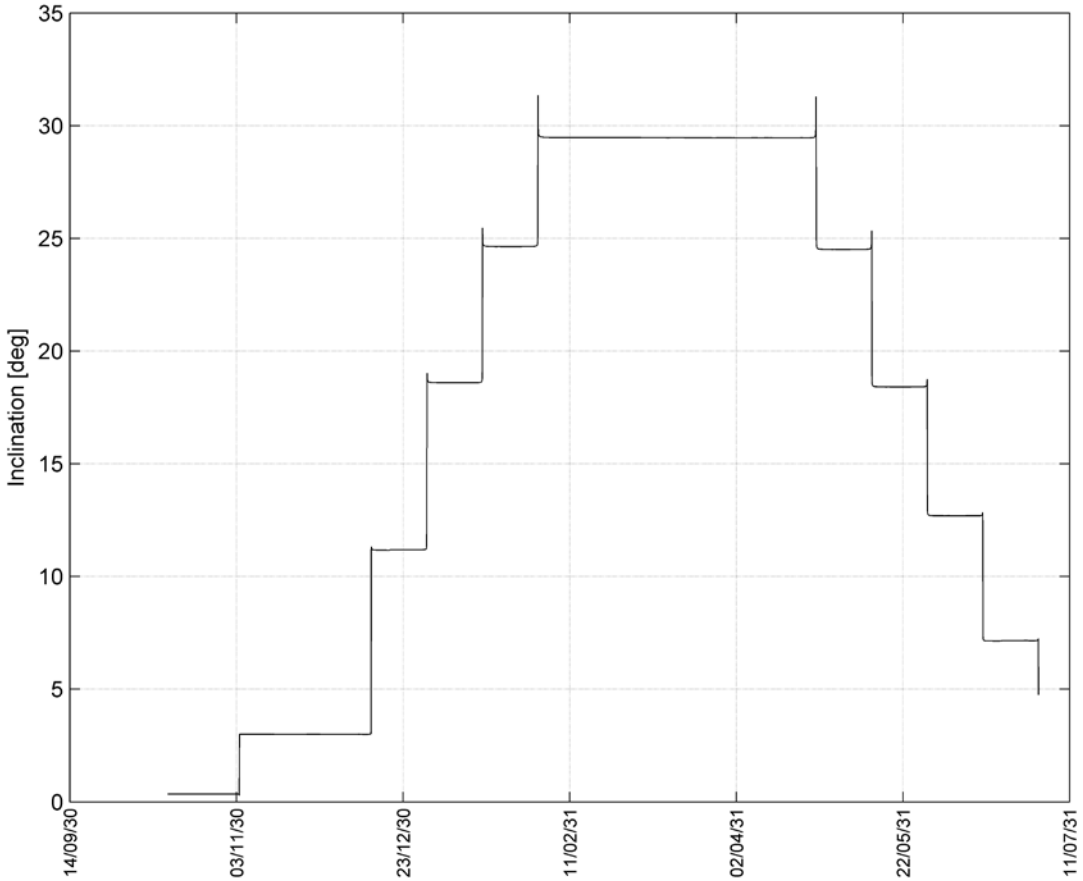

Figure 7-1: Evolution of the inclination during the Jupiter high latitudes phase

It remains close to zero degree at the beginning due to the two pseudo-resonance. Then it increases up to 29 deg (reached after 13C5), stays during nearly 3 months at its maximum before being reduced close to zero again for the transfer to Ganymede (18C10).

The evolution of the orbital radius during the Jupiter high latitudes phase is shown in Figure 7-2.

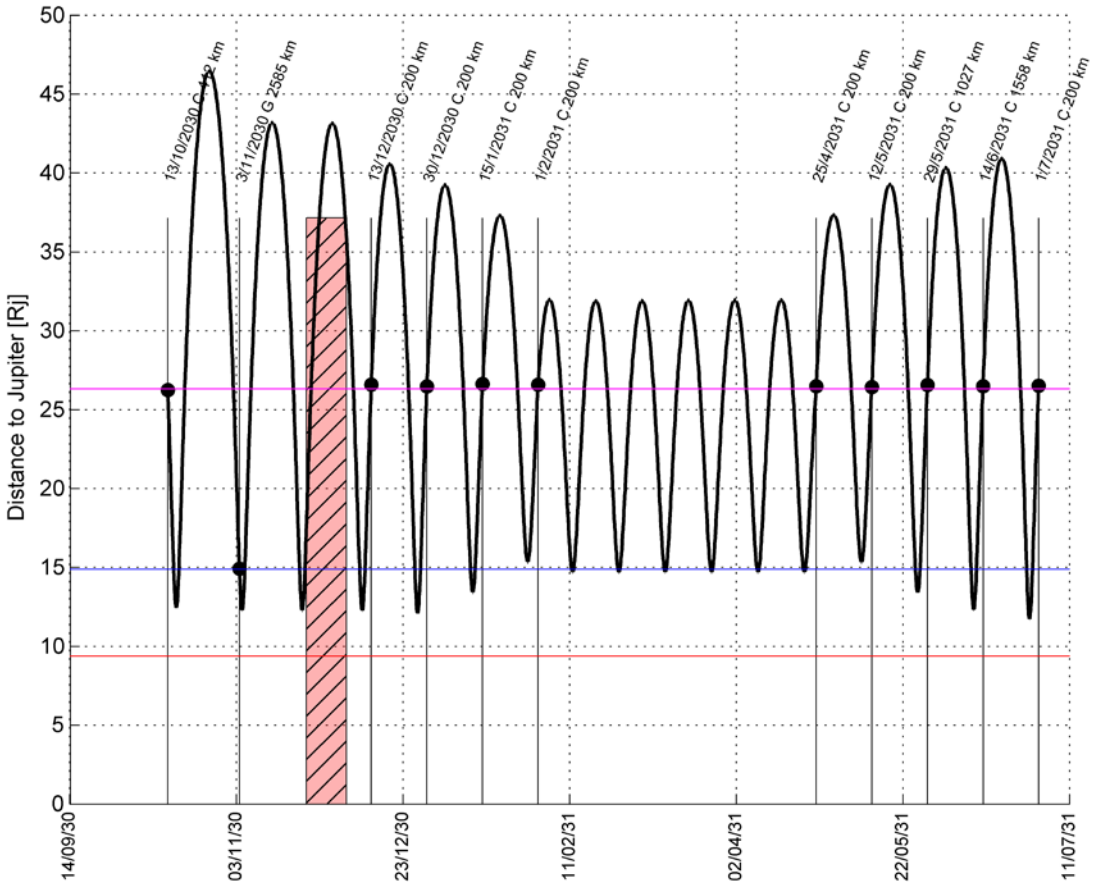

Figure 7-2: Evolution of the orbital radius during the Jupiter high latitudes phase

The orbit is elliptical at the beginning and at the end of this phase. This is where most of the 37 krad radiation dose of the inclined phase is accumulated.

The trajectory in the JSO is shown in Figure 7-3.

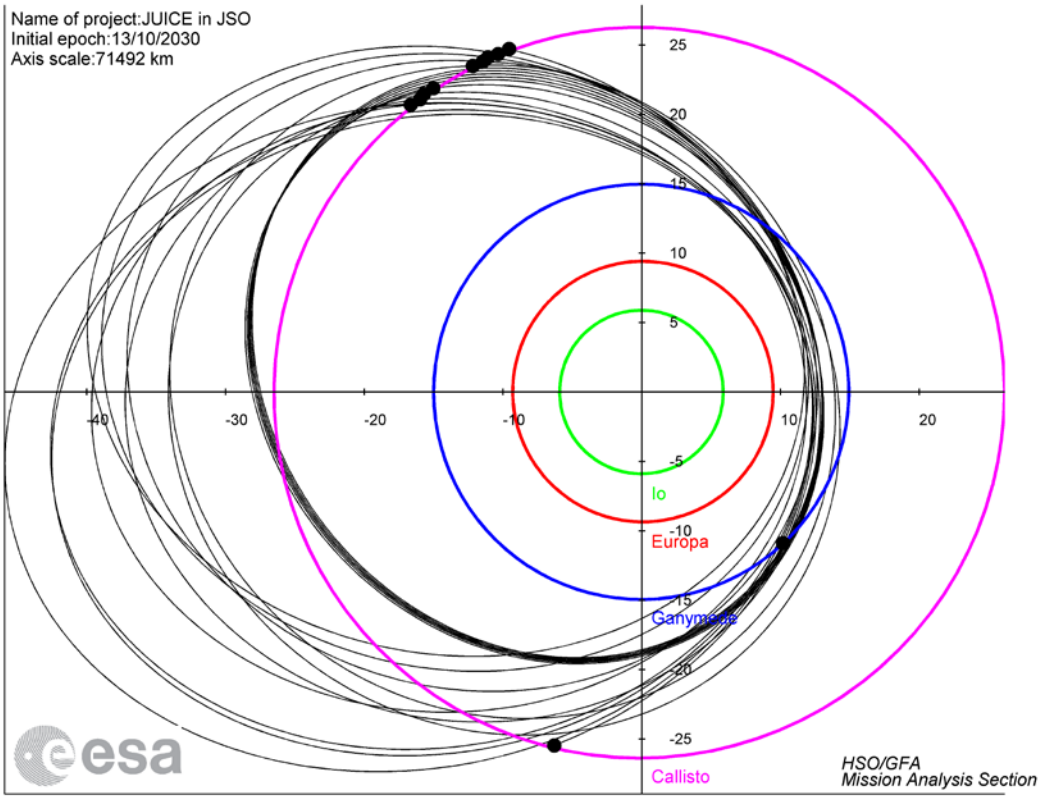

Figure 7-3: Projection of the trajectory in the JSO for the Jupiter high latitudes phase

The variation of the inclination is illustrated in Figure 7-4 by plotting the trajectory in 3D in the JSE frame. The 5:6 resonant orbit at maximum inclination is clearly visible.

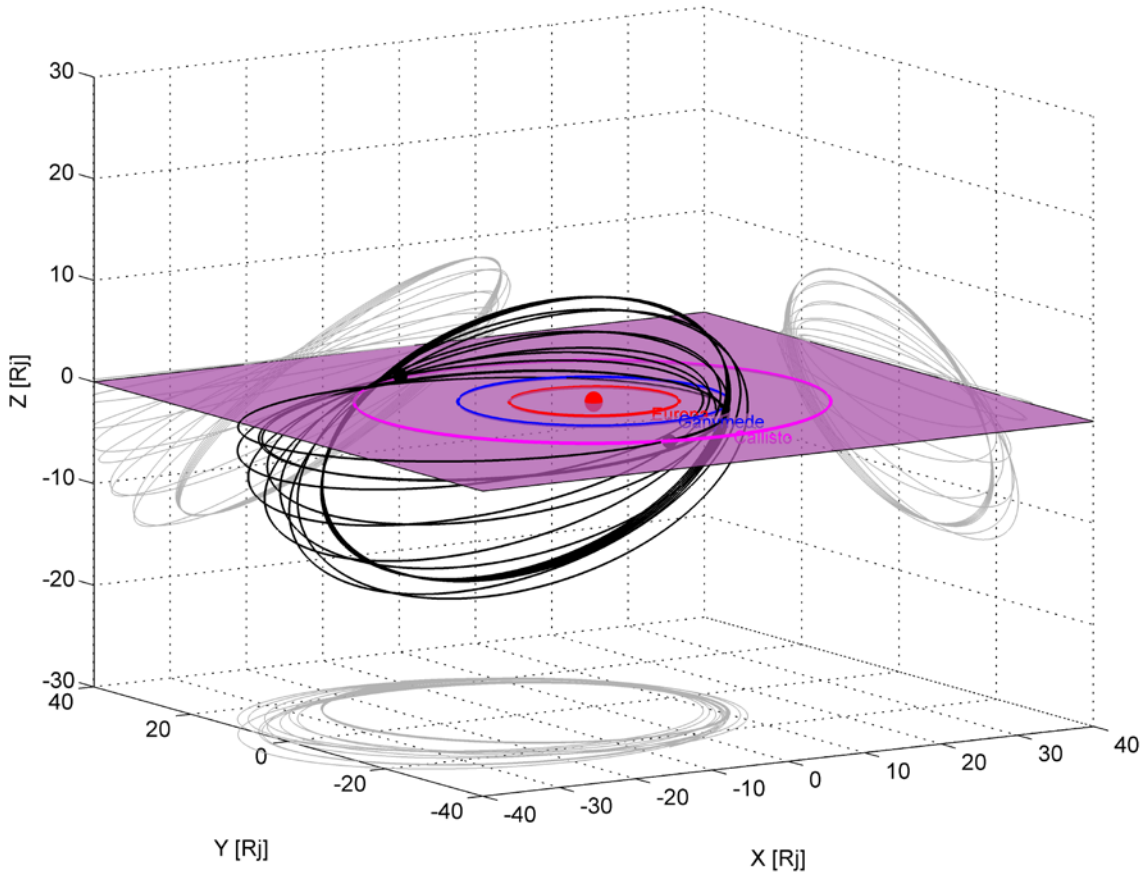

Figure 7-4: Three dimensions trajectory in the JSE for the Jupiter high latitudes phase

The series of Callisto fly-bys can also be used to fulfil the scientific requirements related to Callisto science. There is a list of primary target areas shown shaded in red Figure 7-5. Some areas, like the high latitudes, both North and South, are well covered.

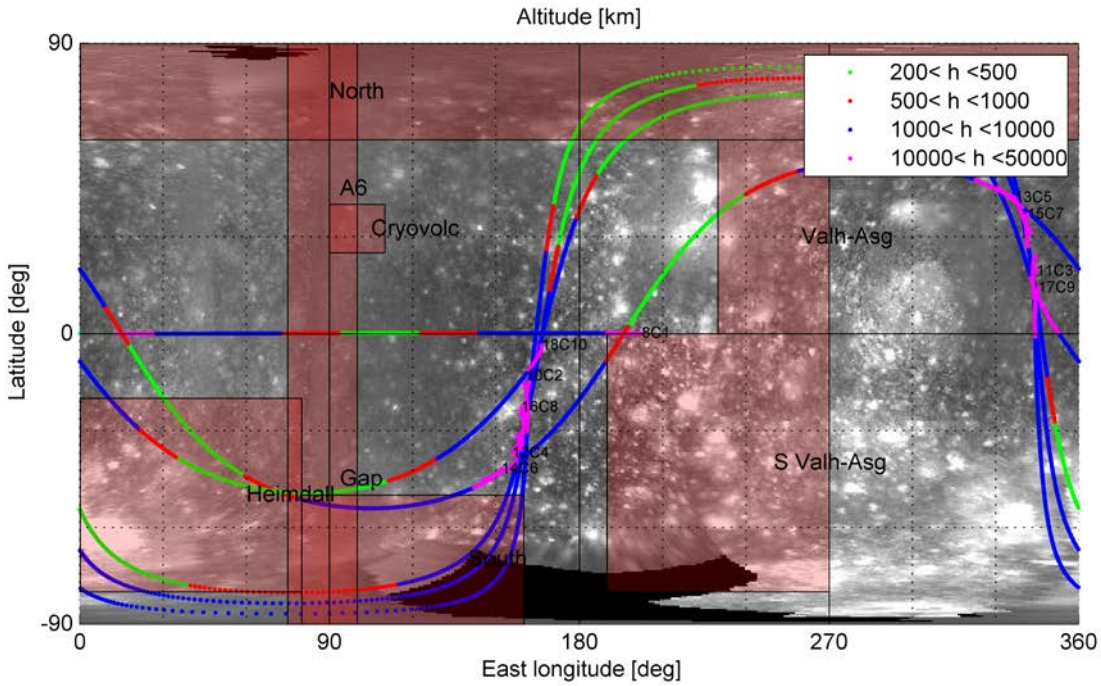

Figure 7-5: Callisto groundtraks of the fly-bys from 8C1 to 18C10

The evolution of the Z-distance as a function of the equatorial distance (i.e. norm of X-Y projection) is given in Figure 7-6.

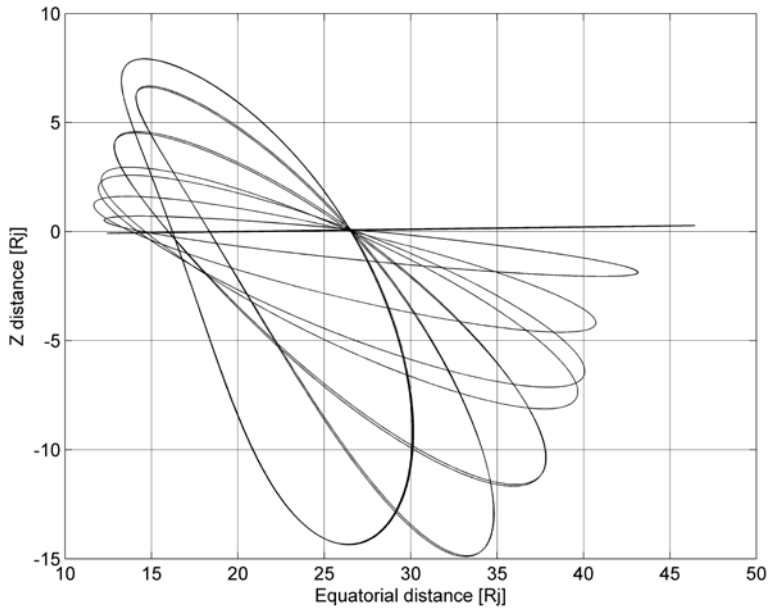

Figure 7-6: Z-distance as a function of the equatorial distance from 8C1 until 18C10

8 TRANSFER TO GANYMEDE

The final objective of the mission is to perform extensive science in-orbit around Ganymede. At the end of the Jupiter high latitudes phase, the infinite velocity w.r.t. Callisto is 4.8 km/s and the orbit is 1:1 resonant with that of Callisto. Assuming a single Callisto fly-by, the optimal strategy would increase the perijove up to Ganymede's orbital radius: the corresponding infinite velocity w.r.t. Ganymede would be 2.7 km/s.

The size of the Ganymede Orbit Insertion manoeuvre (GOI) is directly related to the infinite velocity magnitude. With 3.7 km/s its magnitude would be ~1400 m/s for a 200 x 10000 km capture elliptical orbit! It is therefore extremely important to reduce the infinite velocity w.r.t. Ganymede.

This reduction is performed in two steps: first via the standard Ganymede-Callisto ladder, then the low energy endgame with Ganymede. The standard Ganymede-Callisto ladder involves classical gravity assists of Ganymede and Callisto until the "gate" to the low energy endgame is reached. This gate is located around the point (in the Tisserand-Poincarré graph) which corresponds to a Hohmann transfer from Callisto to Ganymede. After this point, the low energy endgame with Ganymede involves distant fly-bys with Ganymede for which the orbit of the spacecraft does not intersect anymore that of Ganymede. In order to minimize the DeltaV expenditure, special attention is given to obtain a high entry (in terms of perijove radius), but also of beneficial spurious encounter(s) with Callisto.

8.1 Standard Ganymede-Callisto Ladder

The trajectory corresponding to this sequence is GGGCC, i.e. from 18C10 to 24G10, is given in Figure 8-1. The sequence is multi-purpose: as mentioned above, the objective is get close and high into the gate. A second objective is to prepare the targeting of the beta angle at Ganymede Orbit Insertion (GOI): the interval suggested by the science team (see RD21) is from 20 deg to 30 deg with increasing value after GOI. The knowledge of the baseline structure of the low energy endgame allows specifying a rough interval for the solar longitude at 24G10. Some tuning is possible by the modification of the resonance ratios and/or the number of resonant arcs. The objective of the Ganymede-Callisto ladder is therefore to also rotate the argument of perijove.

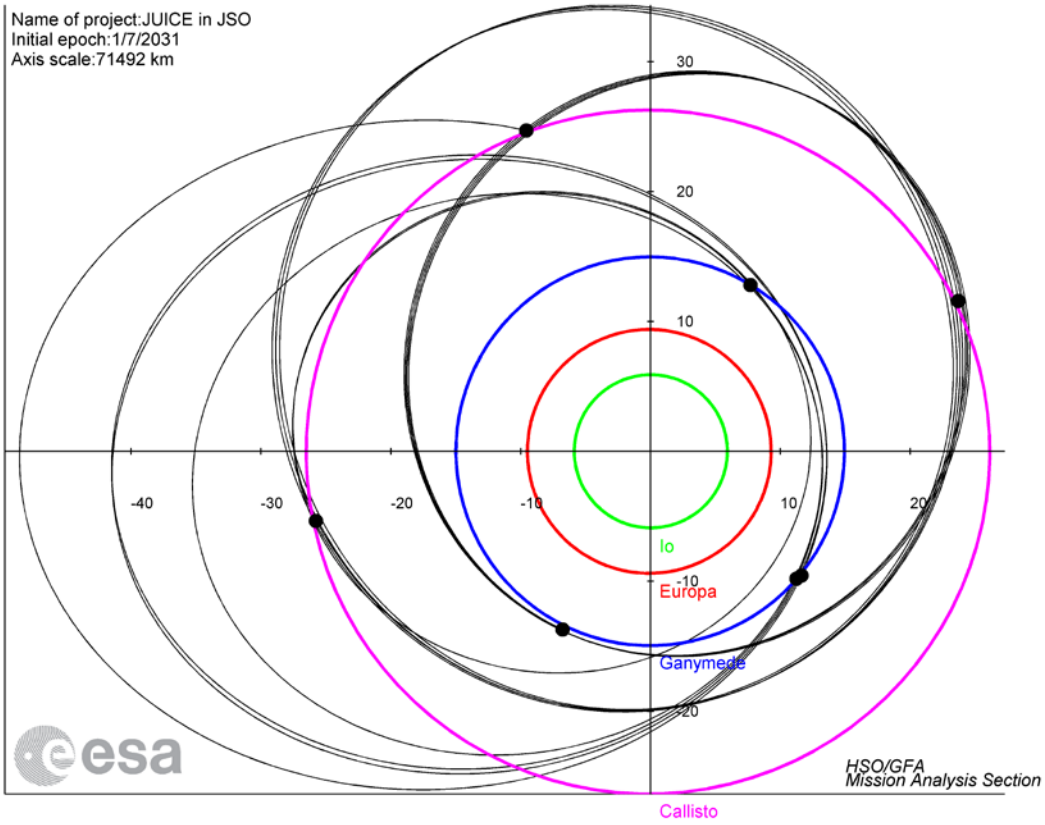

Figure 8-1: Trajectory from 18C10 to 24G10 in the JSO

The strategy is first to increase the orbital period with 18C10 (~22 days orbital period). Then the spacecraft is put in a kind of waiting orbit, 5:1 resonant with Ganymede (such as to recover the same sequencing as in the previous CReMA, i.e. having the superior solar conjunction in the Ganymede-Callisto ladder and not as an additional constraint during the low energy endgame). Then the orbital period is reduced with Ganymede down to 11.1 days. Ganymede is not massive enough to reduce in one go, therefore a $2{:}1^{+}$ is used as intermediate step.

The tuning of the line of apsides is finally obtained with a $3{:}3^{+}$ with Callisto. The $3{:}3^{+}$ is also used to avoid the third superior conjunction as can be seen in Figure 8-2 where the evolution of the distance to Jupiter is given.

Finally the low energy endgame is initiated at 24G10 by reaching Ganymede at the third perijove after 23C12.

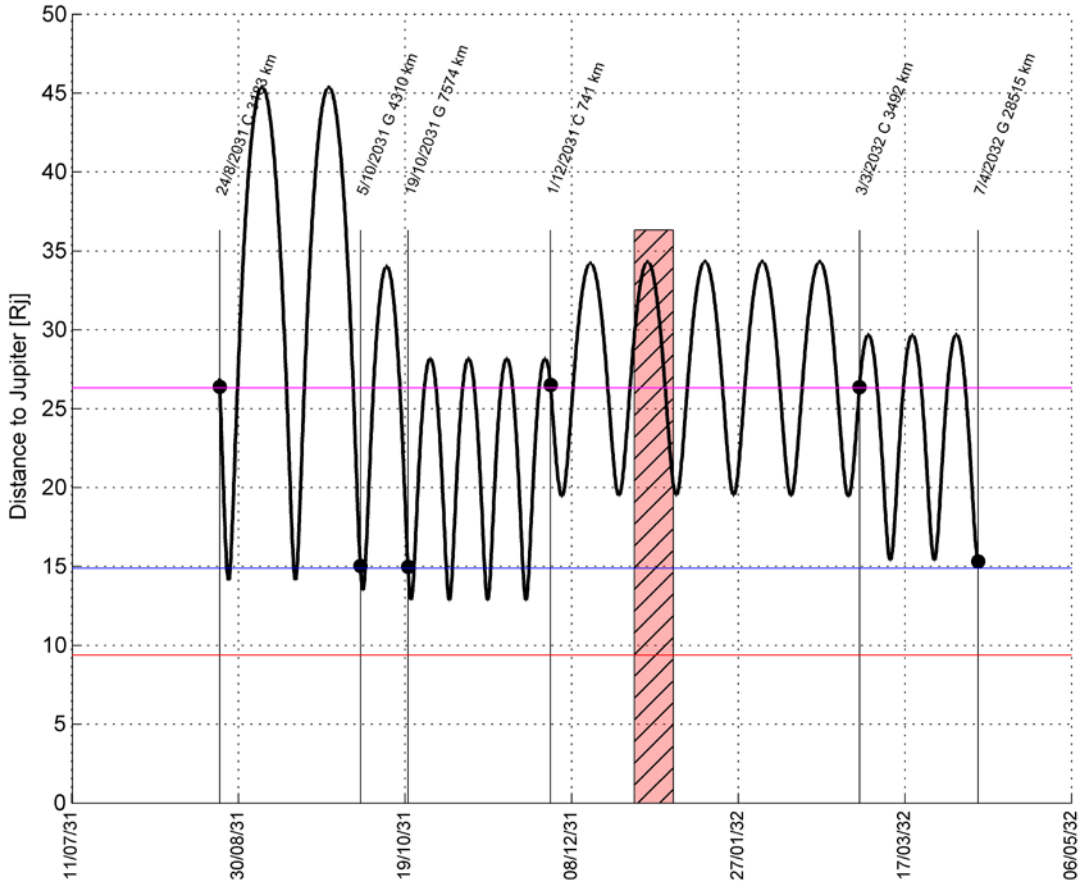

Figure 8-2: Evolution of the distance to Jupiter from 18C10 to 24G10

8.2 Low Energy Endgame (LEE)

From an orbital energy point of view, it is almost not possible anymore to use Callisto to further reduce the infinite velocity (at least with conventional methods). However there are still various ways to reduce this cost that involve only Ganymede: high energy endgame, high energy endgame together with a low energy capture (the boundary case being the gravitational capture) and finally full LEE.

In a high energy endgame, a series of DeltaV gravity assists are used. Between each consecutive gravity assist, there is a resonant transfer. The resonance is such that the orbital period decreases. After each gravity assist, the perijove also decreases. From a DeltaV point of view, it is beneficial to raise it back to the moon orbital radius. This approach requires less DeltaV than a direct capture.

The LEE is comparable to the high energy endgame, in the sense that it is based on moon fly-bys separated by resonant transfers. The difference is that the orbit of the spacecraft does not intersect that of the moon anymore. The main advantage of this approach is that

the perijove decreases much less after C/A (it is DeltaV optimal to keep the perijove as high as possible during the endgame). The drawback of a higher closest approach is that the orbital reduction capacity is lower. Depending on the case, additional resonant transfers are needed.

In order to save as much DeltaV as possible, a LEE to Ganymede is used. The sequence is different from that of the previous CReMA: 7:4, 5:3, 8:5, 3:2, 7:5 and 4:3. One reason is that it allows to fine tune the beta angle to lie between 20 deg and 30 deg. The other reason is related to Callisto: even if the LEE only involves Ganymede at first order, the influence of Callisto is still noticeable in the first resonant arcs when the apojove is above Ganymede's orbital radius. The proper selection of the resonance ratios permit to control the phasing with Callisto and hence to freely raise the perijove; its evolution is given in Figure 8-3.

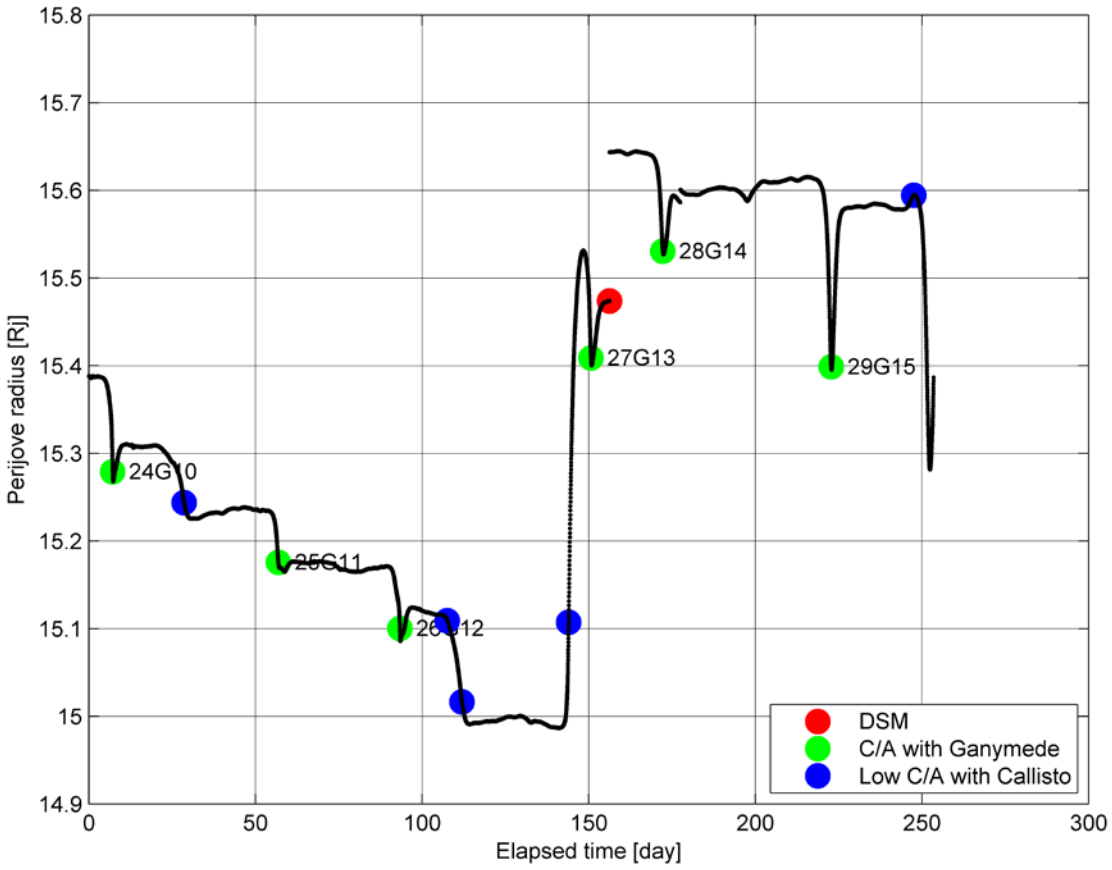

Figure 8-3: Evolution of the osculating perijove during the LEE. The initial time is taken short before 24G10. The green dots represent a distant fly-by of Ganymede. The blue dots represent a conjunction with Callisto (if the distance is lower than 500,000 km). The red dots represent DSM (mainly used to raise the perijove)

At about 50 days after 26G12 it can be seen that Callisto raises the perijove by 35,000 km (C/A at 190,000 km): the equivalent DSM would be 66 m/s; this is partially compensated by a detrimental reduction of about 7000 km one month before. This solution also benefit from a rather high entry perijove: 15.4 R_J, i.e. 35,000 km above Ganymede's orbital radius. Finally one DSM is needed in the 3:2 (25 m/s).

The LEE is 245 days long (34.5 Ganymede revolutions). The trajectory from 24G10 to GOI is given in Figure 8-4.

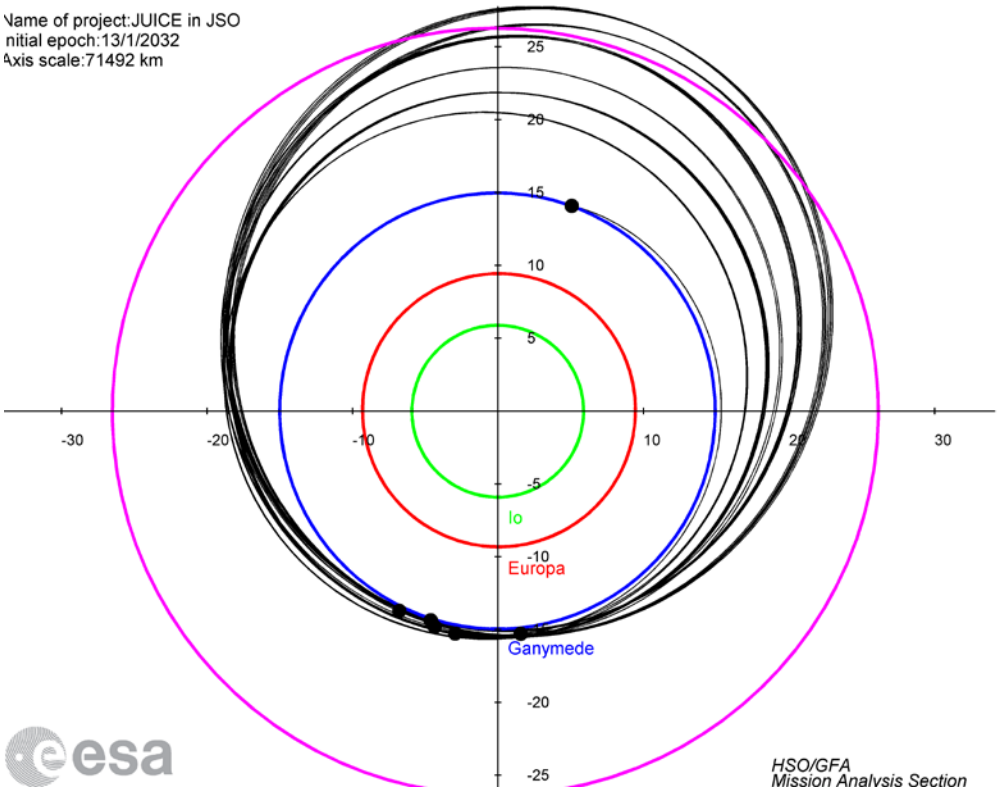

Figure 8-4: Trajectory 24G10 to the GOI in the JSO

The effect of each C/A is clearly visible through the reduction of the apojove radius. The benefit of the low energy endgame is also visible because the perijove radius is nearly constant. There is a slow prograde motion of the argument of perijove, which is taken into account for the proper targeting of the beta angle at GOI. Finally the gravitational capture is seen towards the end of the endgame when the spacecraft trajectory remains close to Ganymede's orbit for half a revolution. This part corresponds to the loop around the libration point L_2 of the Jupiter-Ganymede system. It can be visualized in Figure 8-5.

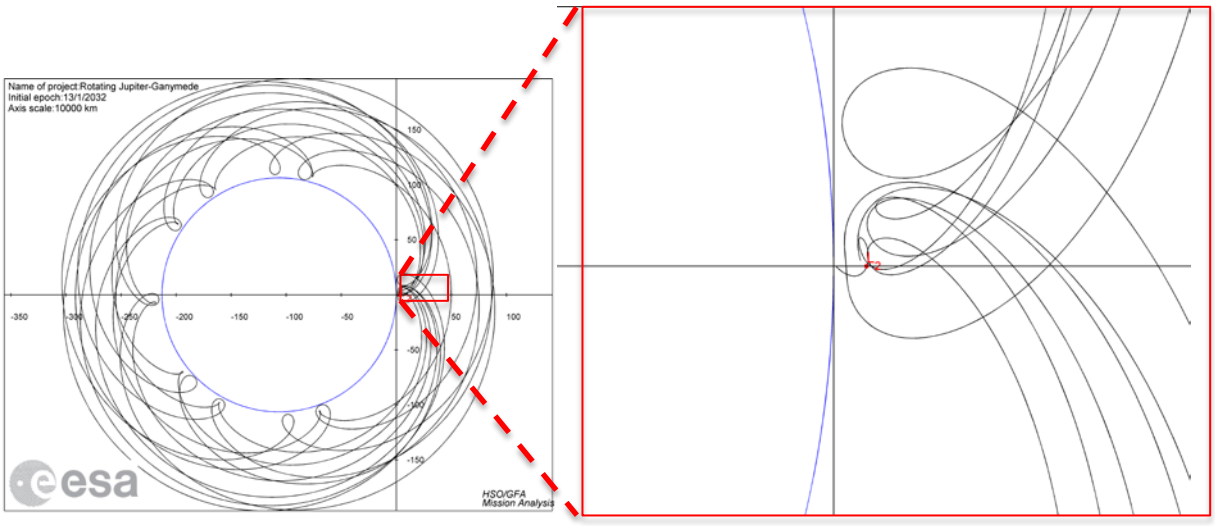

Figure 8-5: LEE in the Jupiter-Ganymede co-rotating frame (left) with a zoom on Ganymede (right), where the loop around L_2 is visible

At explained above, at the end of this phase, the spacecraft is captured in-orbit around Ganymede via the GOI. As will be shown in the summary Tisserand-Poincarré plot (and also in Table 11-1), the Jacobi constant prior to GOI is close to the level of the libration point L_2 of the Jupiter-Ganymede system. It means that this trajectory avoids the single point failure at GOI by being a gravitational capture. Figure 8-6 shows the trajectory in case the GOI is not applied: the spacecraft remains weakly captured. There are three pericentre passages before impact: there are less than 7 days to recover the missed GOI. Moreover the inclination, the RAAN and the argument of pericentre quickly vary during these seven days, thus impacting the science return and the orbit stability.

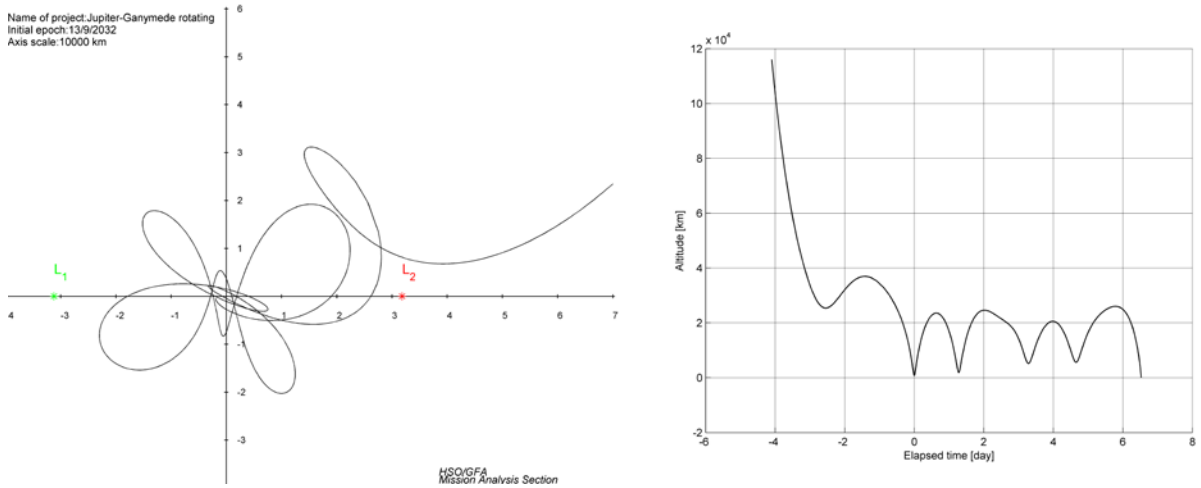

Figure 8-6: Gravitational capture in case the GOI is not applied. Trajectory in the Jupiter-Ganymede co-rotating frame (left) and evolution of the altitude (right). The missed GOI takes place at epoch 0 and the impact shortly before one week

The evolution of the distance to Jupiter is given in Figure 8-7.

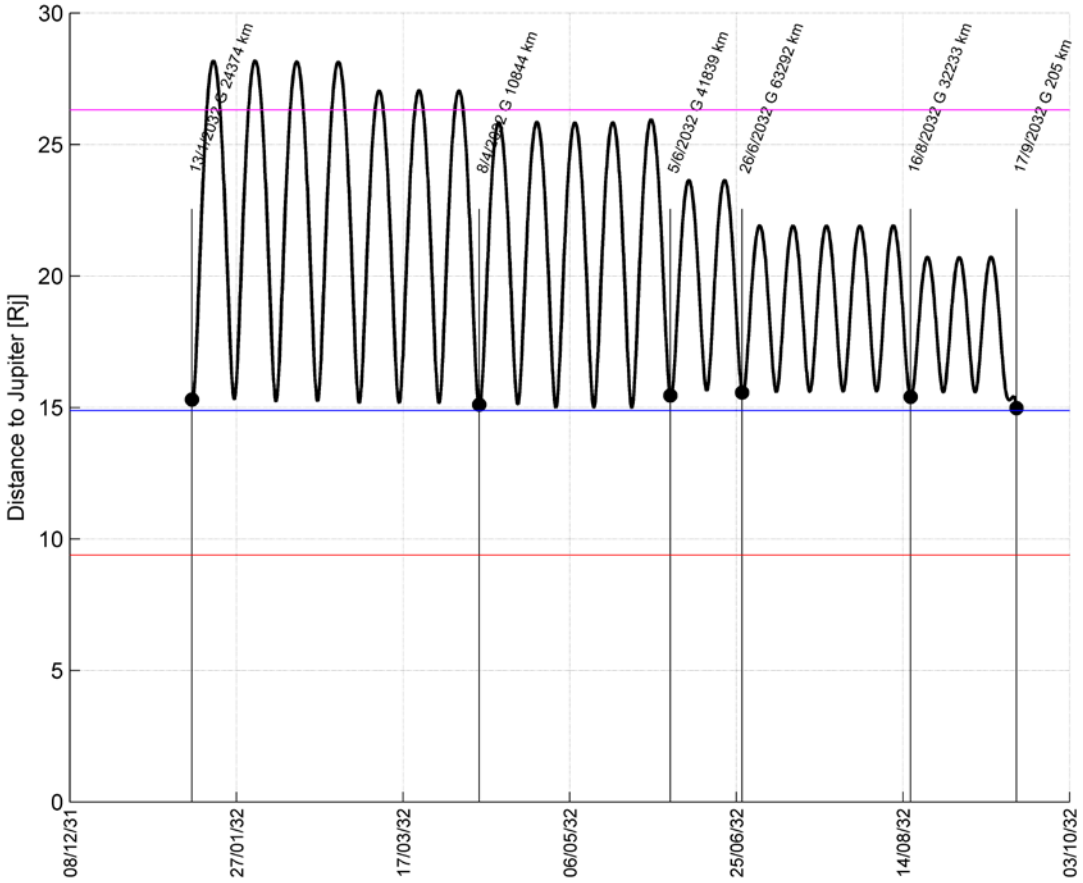

Figure 8-7: Distance to Jupiter during the LEE with Ganymede

9 SCIENCE PHASE AROUND GANYMEDE

9.1 Overview

Following the Ganymede Orbit Insertion (GOI), the Ganymede science phase consists of two distinct phases: an elliptic phase named Ganymede Elliptical Orbit (GEO) and a circular phase at 500 km altitude named Ganymede Circular Orbit (GCO-500).

During the elliptic phase the spacecraft performs the analysis of the magnetosphere of Ganymede together with a regional mapping, while the circular phase aims at obtaining a global mapping of the moon from a low altitude and the analysis of the interior of the moon. The two phases are summarised in Table 9-1.

Table 9-1: Phases during the science around Ganymede

Phase	hp [km]	ha [km]	Initial beta angle [deg]	duration [days]
GEO	200	10000	20-30	150
GCO-500	500	500	62	130
Mission Extension	500	500	free	free

The beta angle interval at the beginning of the GCO-500 guarantees short decreasing Ganymede eclipse (see Paragraph 15.1). For the GCO-500 the theoretical limit is 57.2 deg. A value of 62 deg gives some margin.

The initial argument of pericentre is theoretically free, but as will be seen later, it is constrained by orbital stability considerations.

For the GEO and the GCO, the following perturbations have been taken into account:

- Ganymede point mass attraction
- Ganymede 10x10 gravity model as per RD9: three models are available, the weak field, the strong field and the very strong field. In order to have a worst case, the very strong field was considered.
- Jupiter point mass
- Jupiter zonal coefficient J_2
- Other Galilean moons as point mass

9.2 GOI

This phase is illustrated in Figure 9-1.

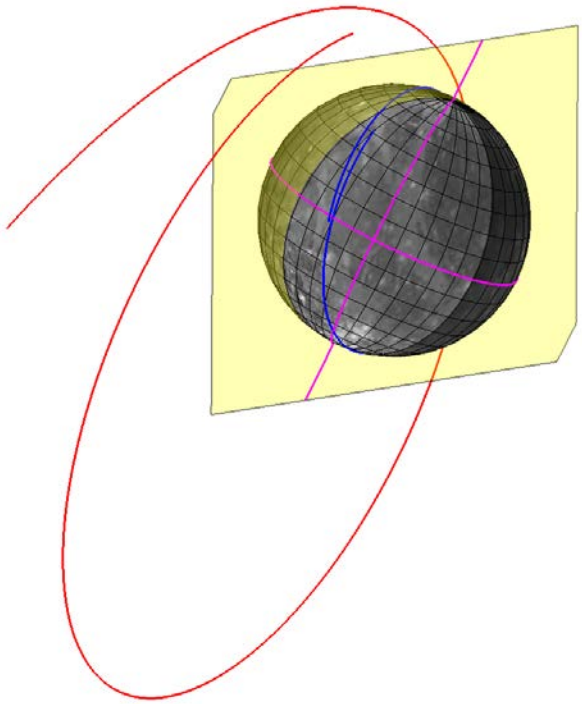

Figure 9-1: Representation of the GOI. The spacecraft trajectory is represented in red. Its groundtrack (subsatellite point) in blue. The yellow plane is the meridian containing the Sun direction (which is by definition perpendicular to the also shown terminator). The two magenta lines represent the equator and the outer meridian (180 deg longitude)

The initial beta angle of 20 deg can be observed as the angle (positive to the East) between the yellow plane and the groundtrack at equator (i.e. the ascending node). The cost of the GOI including gravity losses is 133 m/s. For this manoeuvre the gravity losses are very small (~0.5 %) thanks to the gravitational capture strategy.

As can be seen on the plot, the apocentre is over the day side of the moon (as a consequence of the capture via L_2 and not L_1).

9.3 GEO

Because of the high apocentre, the orbit is greatly perturbed by Jupiter. The main effect is a fast variation of the eccentricity: first the eccentricity decreases and then increases until impact. The lifetime of the orbit is directly a function of the eccentricity evolution. The eccentricity evolution is itself a function of the initial argument of pericentre. There are two stable values (~140 deg and ~320 deg) for which it is theoretically possible to find an infinite lifetime without Station Keeping manoeuvre (if only third body perturbation is

assumed). If a model with full perturbations is used, very small manoeuvres are still needed, but any lifetime requirement can easily be met.

The evolution of the pericentre and apocentre altitude is shown in Figure 9-2.

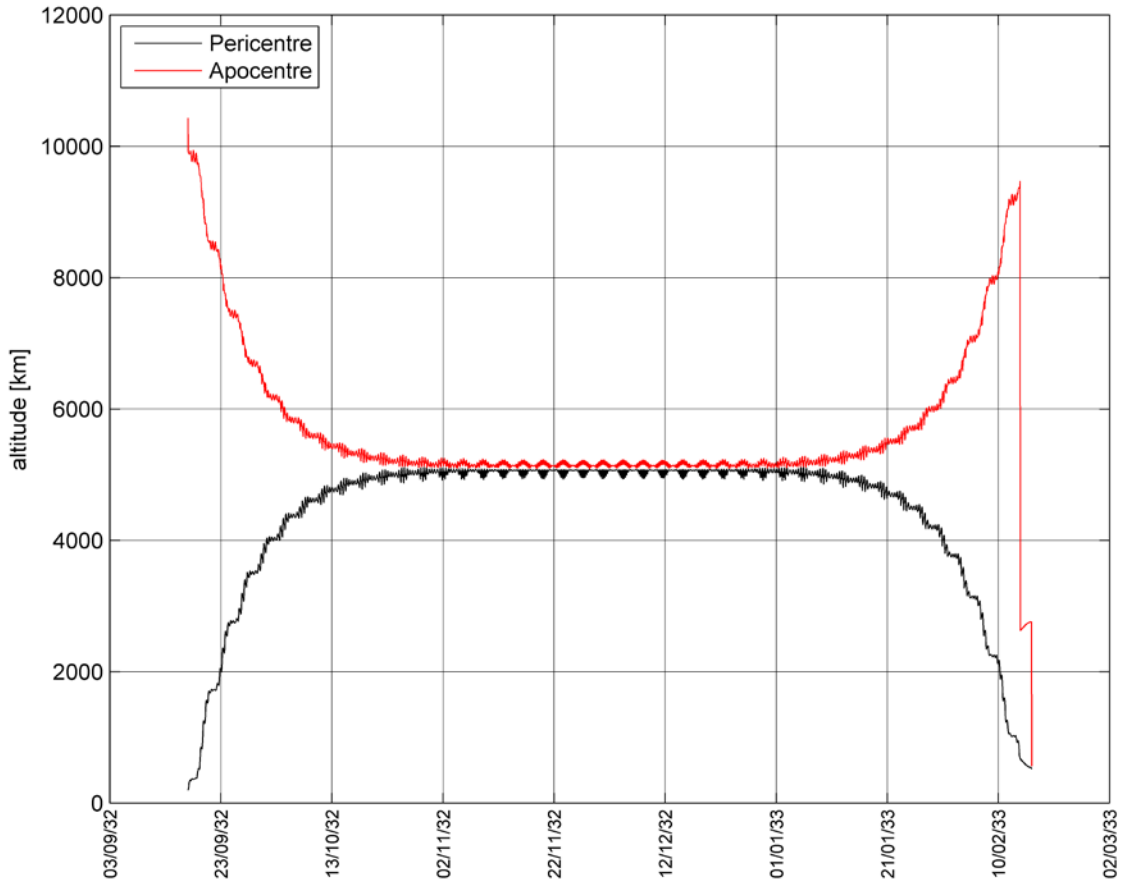

Figure 9-2: Evolution of the pericentre and apocente altitude during the GEO

As can be seen the GEO phase can be sub-divided into three sub-phases:

- An initial elliptic sub-phase, whose duration is roughly 3 weeks
- A near circular sub-phase, whose duration is roughly 15 weeks
- A final elliptic sub-phase, mirror of the initial sub-phase, whose duration is roughly 3 weeks. The end of this sub-phase is different because of the preparation of the GCO: as the altitude of the GCO is 500 km, the circularization must take place earlier. In order to keep low gravity losses, but also to be more robust from an operational point of view, a first manoeuvre is applied to reduce the apocentre altitude to 2500 km. Two days later a second manoeuvre is applied to circularize the orbit at 500 km. In case of a main engine malfunction at the epoch of application of

the first manoeuvre, the altitude at the epoch of the next pericentre passage (12 hours later) is 258 km: this critical phase is therefore not a single point failure case. Two pericentre passages later (i.e. 24 hours after the theoretical application of the first manoeuvre), the pericentre altitude is negative, which means that the S/C impacts the surface between the first and second pericentre passages. In order to have a margin greater than 12 hours, it is necessary to apply the first manoeuvre earlier. This means a higher pericentre and as a consequence a higher DeltaV cost. There is a trade-off between the DeltaV cost and the operations safety. This trade-off will be analysed in a later stage of the mission analysis.

The evolution of the inclination w.r.t. Ganymede's equatorial plane is shown in Figure 9-3.

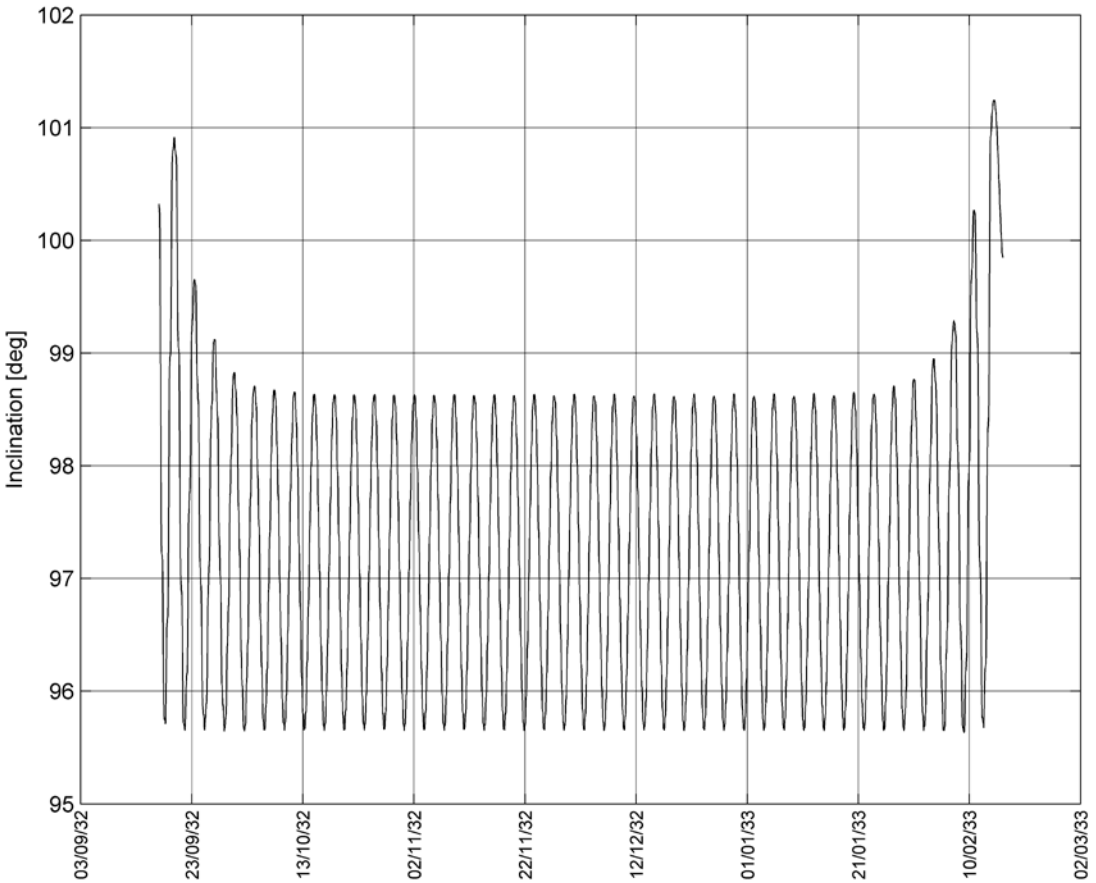

Figure 9-3: Evolution of the inclination during the GEO

The evolution is periodic during the circular sub-phase. The amplitude of the oscillation depends on the eccentricity. It explains the larger excursions during the elliptic sub-phases. The mean inclination is 97.1 deg: the orbit is retrograde. The amplitude of the oscillation is 1.5 deg during the circular sub-phase. The value of the mean inclination is given by the target beta angle rate (0.21 deg/day) and of the gravity potential model (its prograde

counterpart would have a mean inclination of ~86.5 deg). This mean inclination is smaller than for the previous CReMA (98.7 deg) due to a different initial beta angle (20 deg in the previous CReMA, 30 deg now).

The oscillation around the mean value is used to perform the circularization when the inclination has a specific value. This specific value at the beginning of the GCO-500 corresponds to what is needed to guarantee no eclipse. The amplitude of the oscillation defines in which interval can the inclination for the GCO be chosen.

A representation of the trajectory in three dimensions of the first revolutions is given in Figure 9-4.

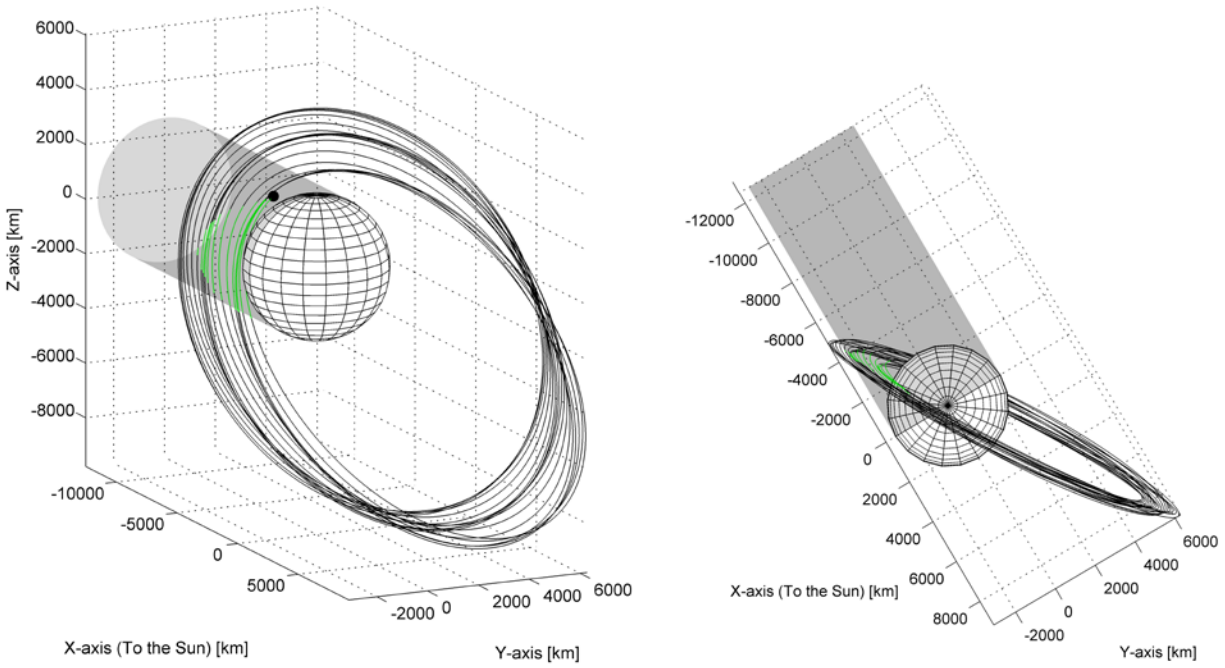

Figure 9-4: Representation in three dimensions of the GEO. The Sun shadow cone is also represented in light grey. The eclipses are shown in green close to the pericentre

The presence of eclipse is clearly visible. They get shorter and finally disappear. It is interesting to notice that the eclipse reduction is mainly due to the pericentre altitude raise rather than that of the beta angle increase. Still the period with eclipse is shorter than in the CReMA 3.1 (6 days now against 11 days before) because the initial beta angle is 30 deg vs 20 deg before. The duration of the longest eclipse has not changed: 40 min.

The evolution of the argument of pericentre is shown in Figure 9-5 in the Ganymede equatorial of date frame.

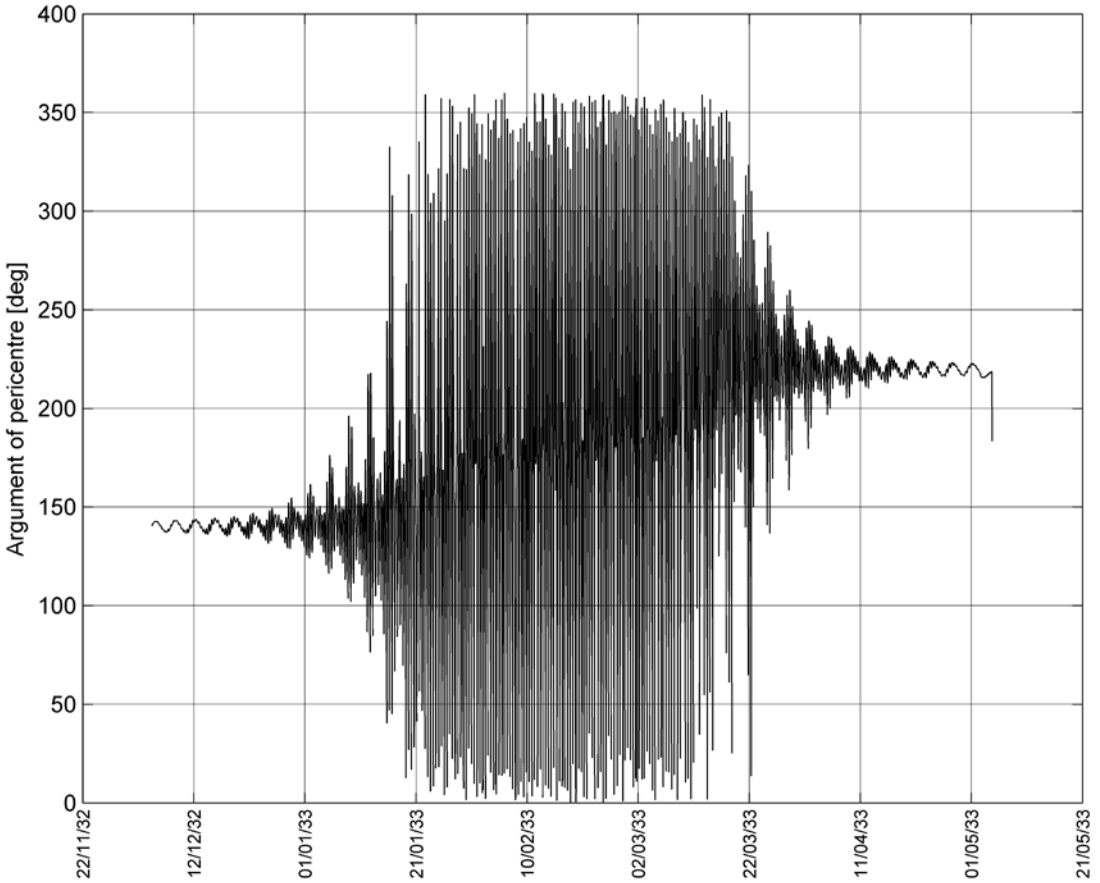

Figure 9-5: Evolution of the argument of pericentre during the GEO phase

It starts at the stable value (close to 140 deg) and ends at the unstable value (close to 220 deg). This value of 220 deg means that the apocentre is over the day side at the end of the GEO. If needed the final argument of the apocentre could be targeted towards the other unstable value (close to 40 deg): in this case, the apocentre would be on the night side.

The evolution of the beta angle is given in Figure 9-6.

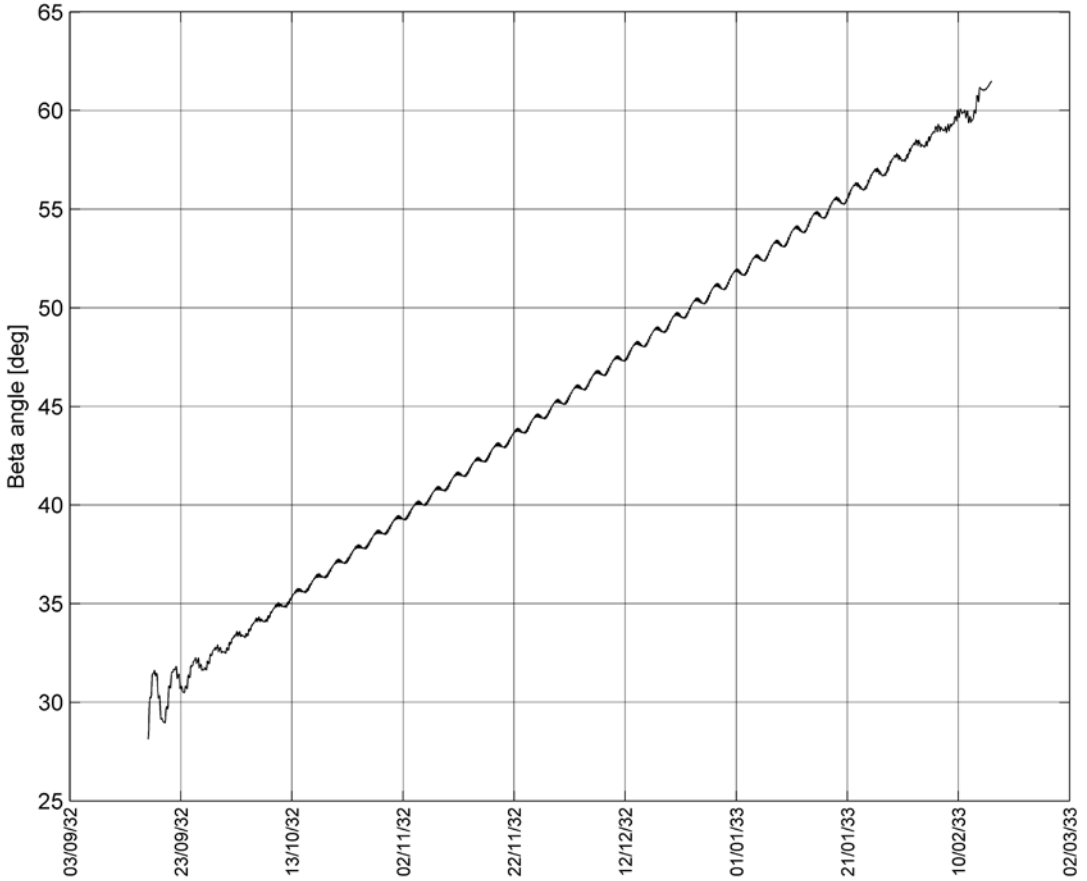

Figure 9-6: Evolution of the beta angle during the GEO

The initial beta angle is 30 deg. The final beta angle is 62 deg. As written above the variation is driven by a proper selection of the mean inclination.

The Earth beta angle is given in Figure 9-7. The range of variation is smaller: from 40 deg to 60 deg.

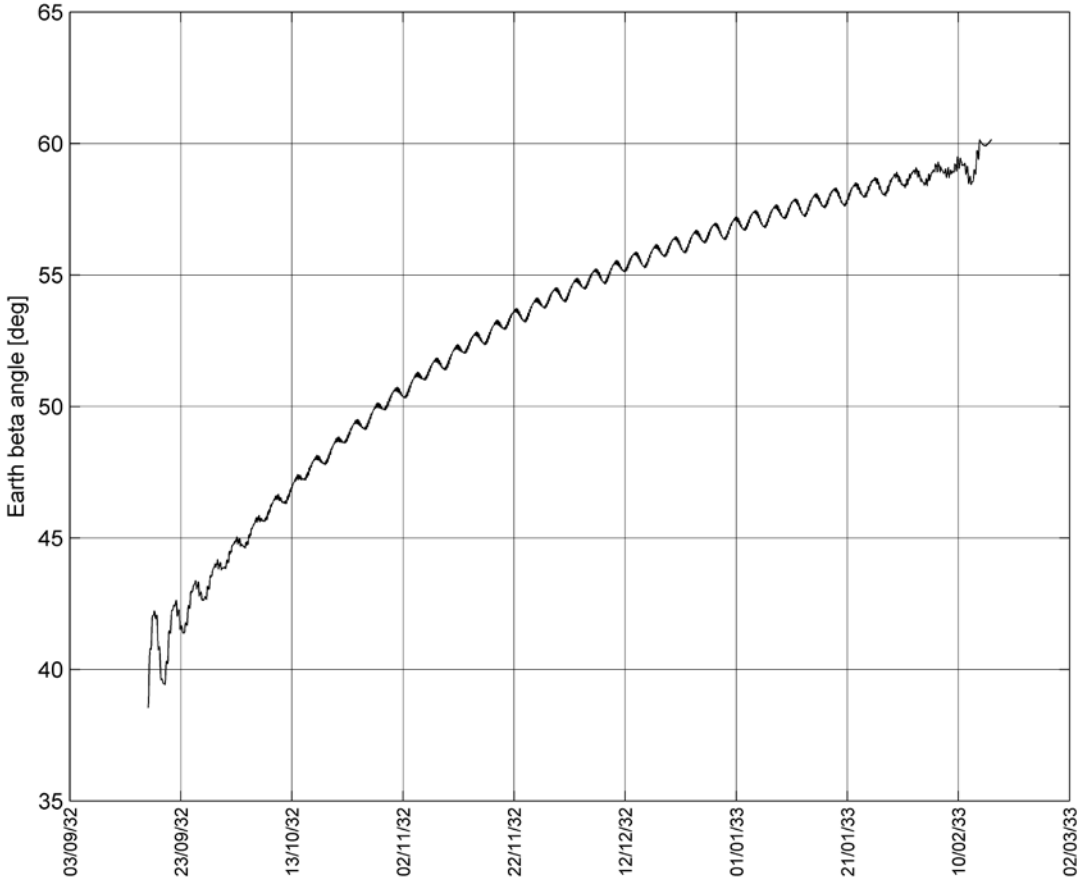

Figure 9-7: Evolution of the Earth beta angle during the GEO

At the end of the GEO a first manoeuvre is applied two days before the pericentre altitude is 500 km. At that time the pericentre altitude is 650 km and the apocentre altitude is 9600 km. The pericentre burn of 255 m/s with gravity losses reduces the apocentre down to 2650 km. For this burn the gravity losses are less than 1%.

Two days later the circularization burn of 227 m/s with gravity losses reduces the apocentre altitude down to 500 km. For this burn the gravity losses are again low, ~1%.

In case available propellant is lower than expected, the DeltaV savings resulting from a higher GCO altitude were assessed and are summarised in Table 9-2.

Table 9-2: Effect of a higher GCO altitude

GCO altitude [km]	1st Man. DeltaV [m/s]	1st Man. altitude [km]	2nd Man. DeltaV [m/s]	DeltaV saving [m/s]
500	254	924	227	0
700	241	1106	205	35
900	229	1290	185	67
1100	217	1476	168	96
1300	205	1663	152	124
1500	193	1850	139	150

In order to keep the balance between the two manoeuvres as for the baseline, the constraint on the intermediate semi-major axis was adapted accordingly. The DeltaV saving is given graphically in Figure 9-8.

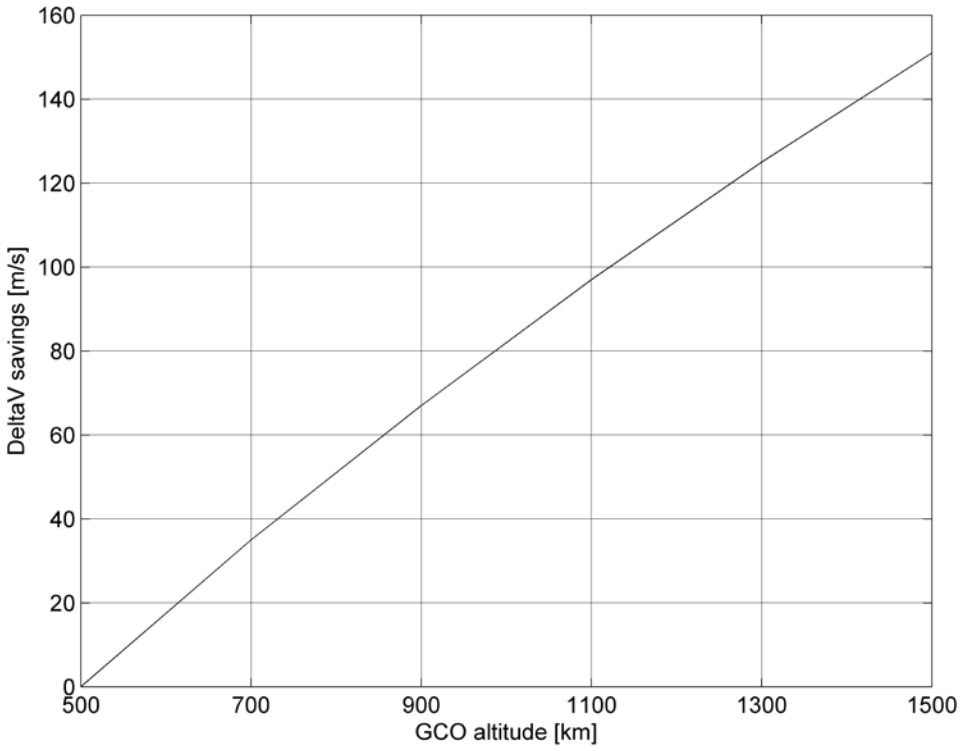

Figure 9-8: DeltaV savings as a function of the GCO altitude (the reference of no DeltaV saving is assumed for an altitude of 500 km)

9.4 GCO

When taking only J_2 term of Ganymede's gravity potential and Jupiter third body attraction, it is possible to shown that the zero eccentricity point is an unstable equilibrium point. It means that only small station keeping manoeuvres are needed.

When adding the entire gravity potential, this point is not an equilibrium point anymore, mainly because of the J_3 term of the potential. However for any field, it is possible to find a near circular orbit with argument of pericentre equal to 90 deg or 270 deg (see RD10), which is an unstable equilibrium point. This is what was done in this document for the very strong field case.

By using very small manoeuvres the altitude is kept very close to the required altitude as can be seen in Figure 9-9.

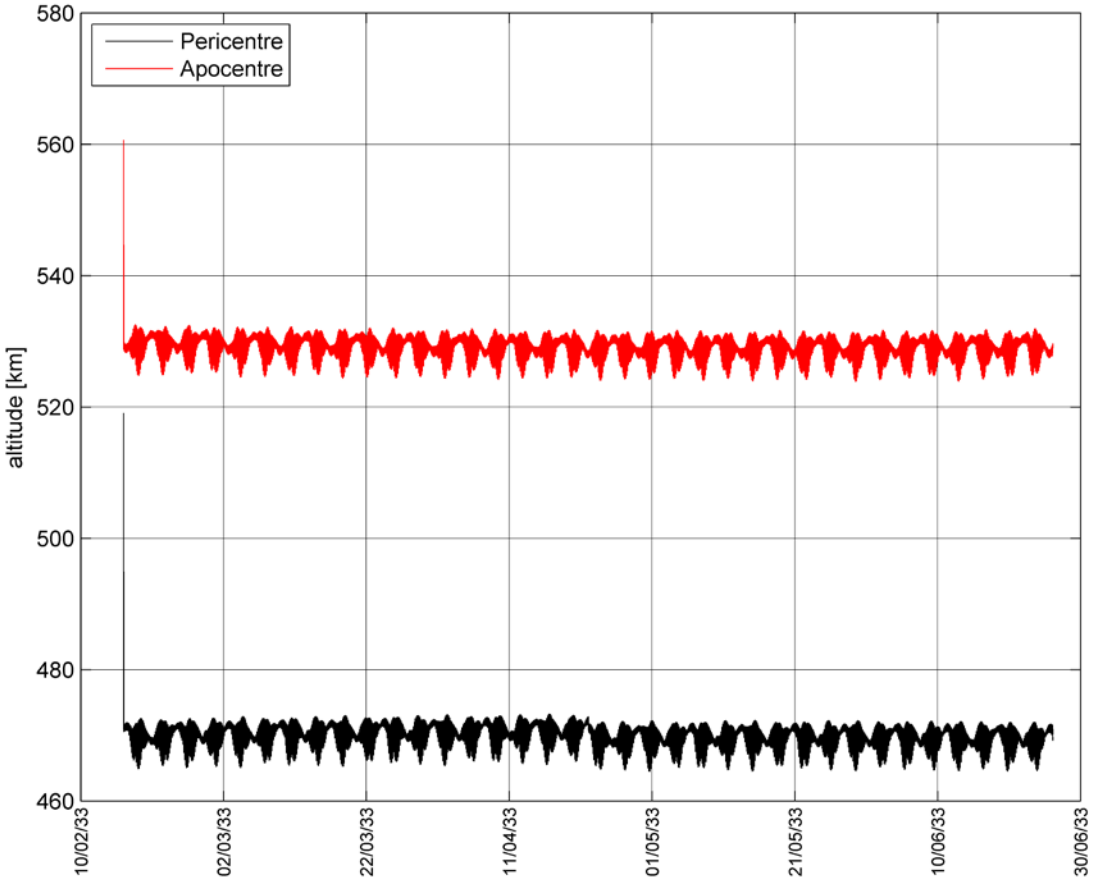

Figure 9-9: Evolution of the pericentre and apocentre altitude

For the GCO-500 the equilibrium point is found for an eccentricity of ~0.008. It corresponds to a variation of the altitude between 475 km and 525 km.

The evolution of the inclination is shown in Figure 9-10 in the Ganymede equatorial of date.

Because the eccentricity does not build up like for the GEO, the evolution stays purely periodic with the same amplitude. The mean inclination is 100.8 deg. The beta angle drift is slow: 0.07 deg/day. It has to be underlined that reaching a Sun-synchronous orbit is out of reach because the required inclination is 94.5 deg. The evolution of the beta angle is given in Figure 9-11: from 62 deg to 71 deg in 130 days.

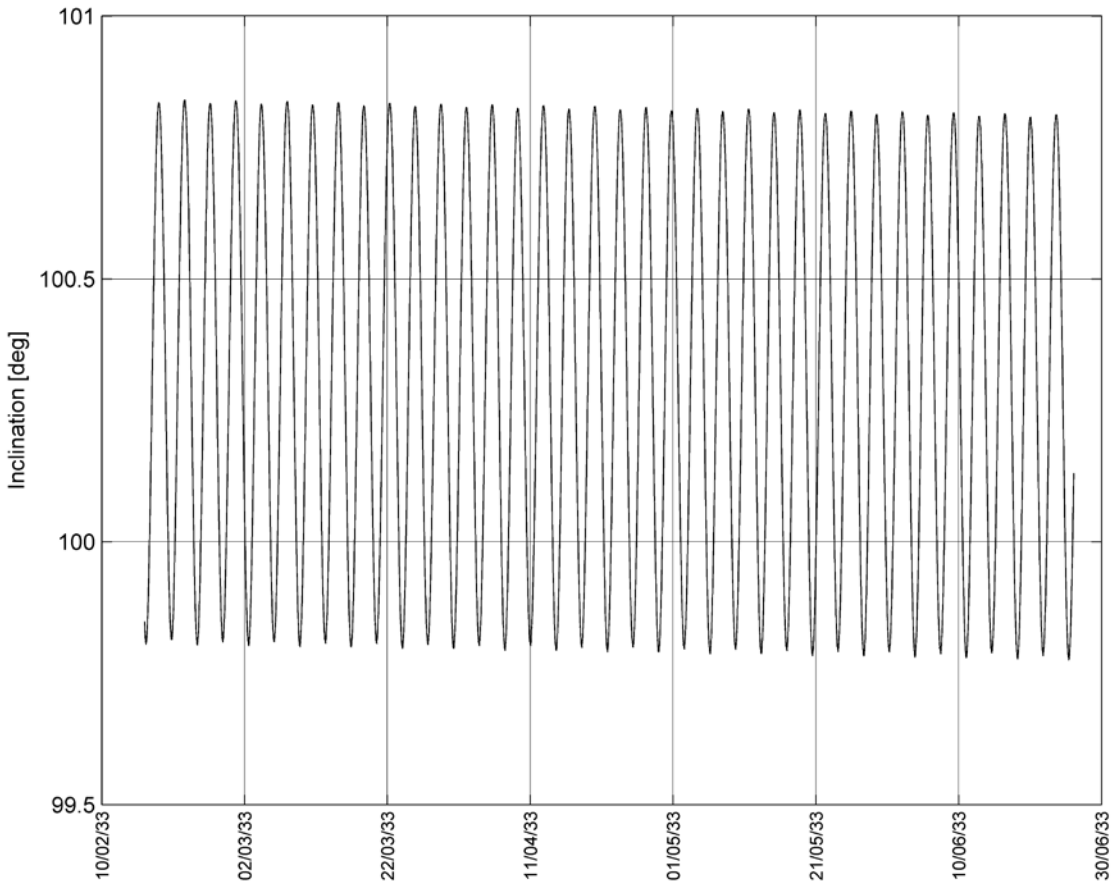

Figure 9-10: Evolution of the inclination during the GCO

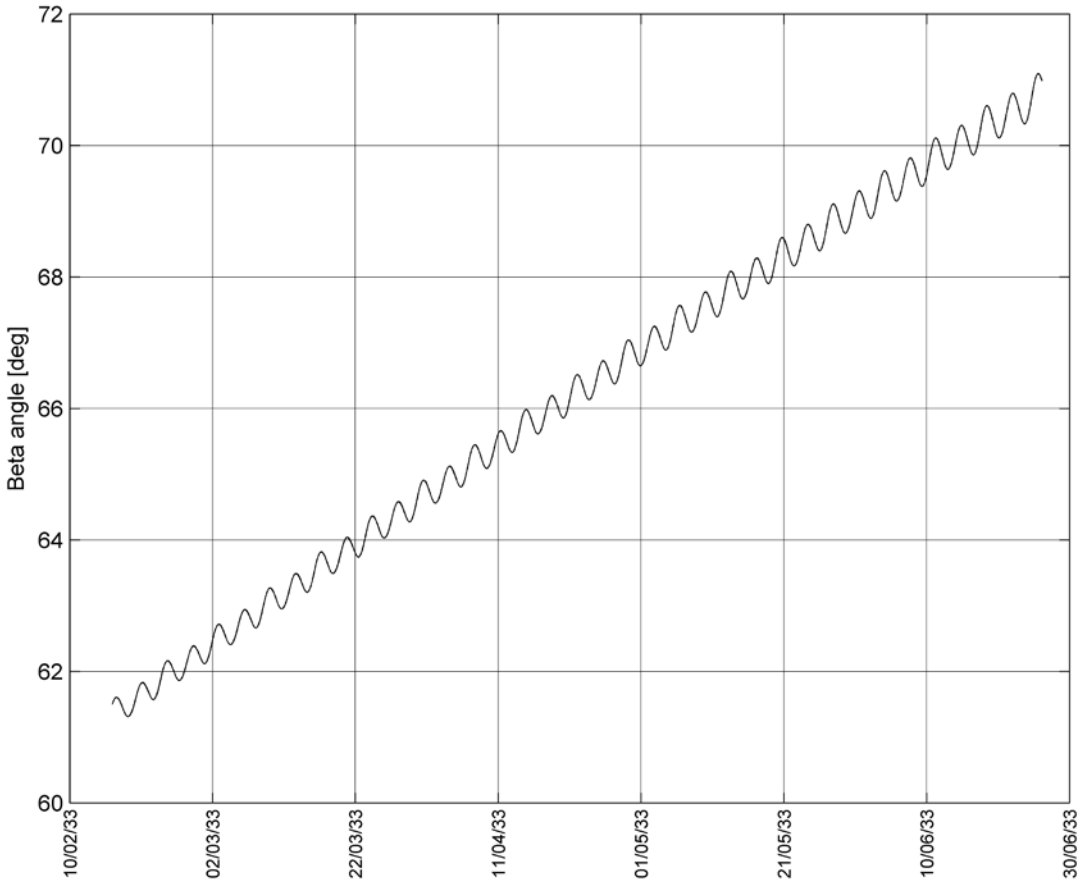

Figure 9-11: Evolution of the beta angle during the GCO

Unlike the GEO, the eccentricity does not strongly vary: therefore the evolution of the beta angle is roughly linear. The beta angle at the end of the nominal mission is 71 deg. A transfer to 200 km is then possible without having eclipse.

The Earth beta angle evolution is given in Figure 9-12. It is interesting to notice that the evolution is not linear; this is due to the evolution of the Sun-Ganymede-Earth angle, which is itself not linear during the GCO (whereas it is near linear during the GEO).

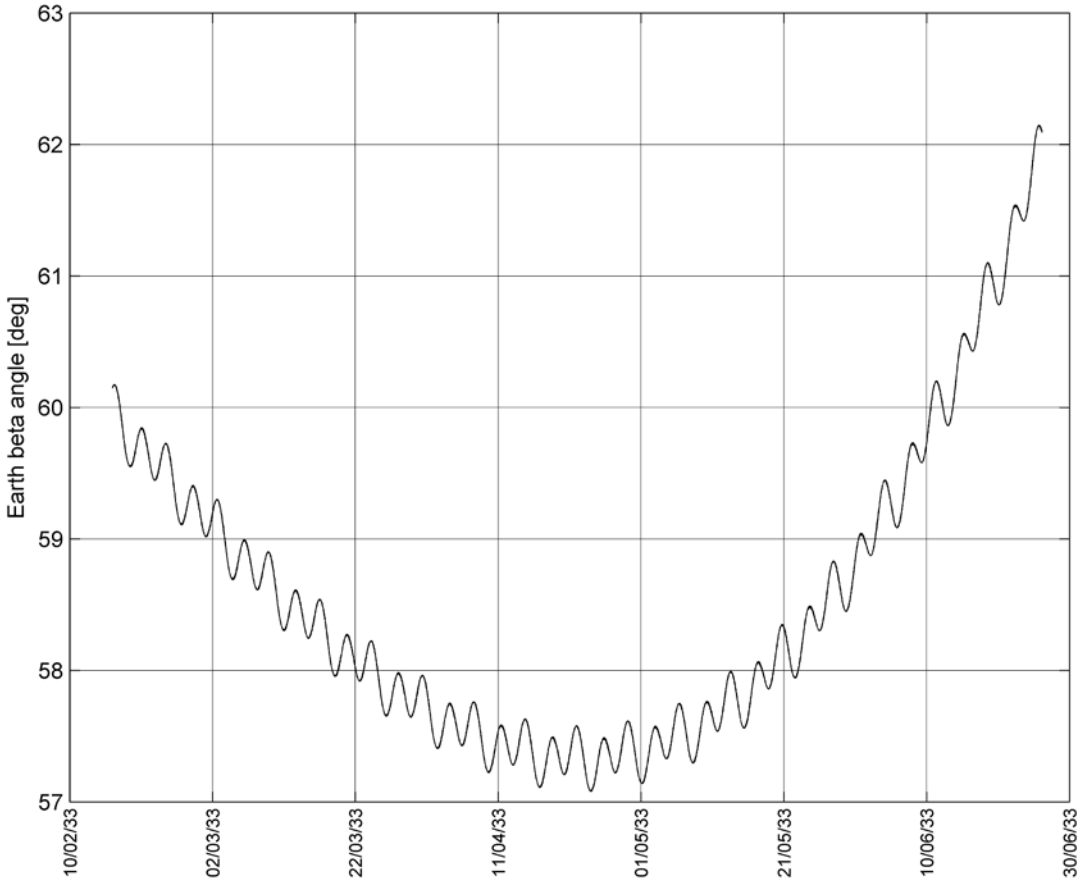

Figure 9-12: Evolution of the Earth beta angle during the GCO

If the mission is extended, the beta angle will grow further to ~80 deg before starting decreasing. Eventually eclipses will necessarily appear: if the spacecraft remains at 500 km, the eclipse will appear after ~1.3 years. If the spacecraft is transferred to e.g. 200 km, the eclipse will appear after ~11 months (assuming no inclination correction).

In terms of Earth beta angle, the evolution is shown in Figure 9-13 for two years. The complex profile is the outcome of the combination of the linear drift term (J_2 and Jupiter on the RAAN, rotation of Jupiter around the Sun) combined with the oscillating rotation of the Earth around the Sun.

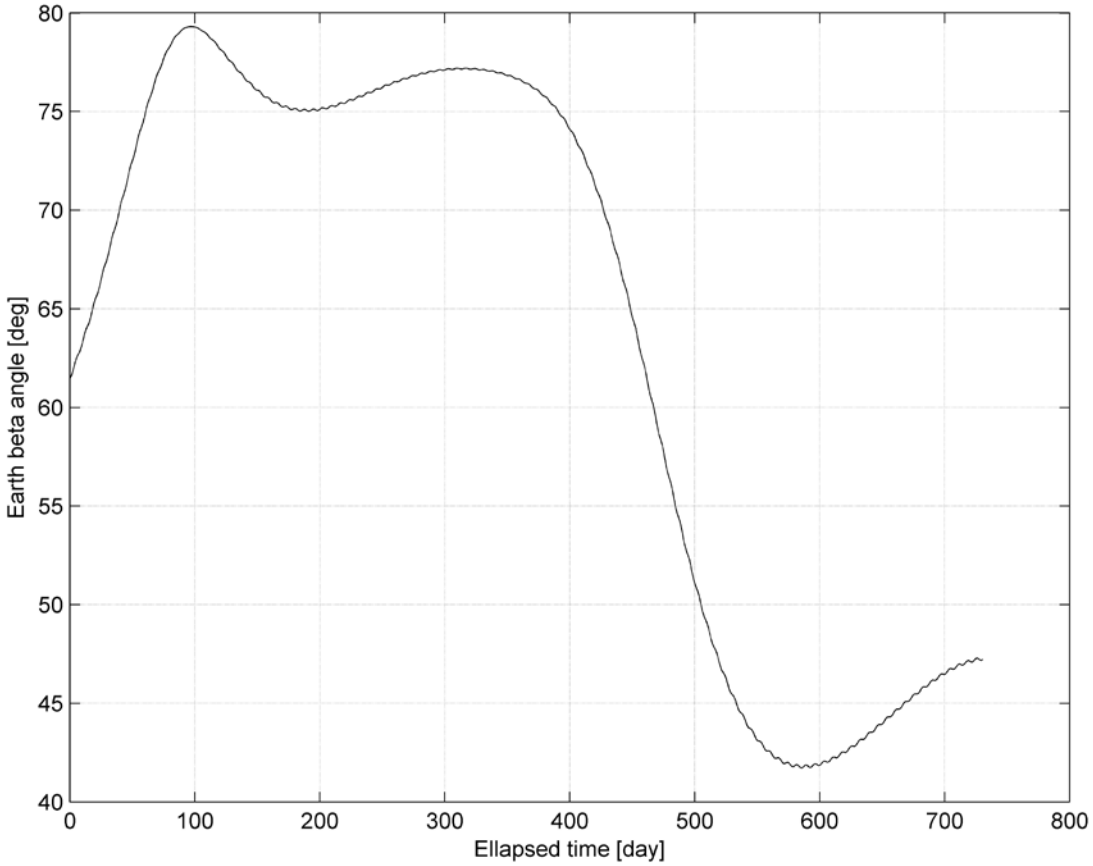

Figure 9-13: Evolution of the Earth beta angle in case of mission extension. It is assumed that the GCO is maintained as is. Reducing the altitude to 200 km only slightly affect the profile

10 EXTENDED SCIENCE PHASE

10.1 Trade-off

The science phase nominally ends after 280 days orbiting around Ganymede. If the orbiter is left on its orbit it will eventually crash onto Ganymede's surface within several weeks. Two strategies are possible: an uncontrolled impact or a controlled impact.

Uncontrolled impact: The uncontrolled case consists of letting the spacecraft orbit naturally evolve until it impacts Ganymede. This strategy does not guarantee flexibility in the selection of the impact latitude: as the orbit evolves under the perturbation of the third body, the argument of pericenter will naturally drift towards one of the two unstable values (i.e. 40 or 220 deg) and consequently the impact point will be close to this latitude (40 North or South). The longitude is also fixed by the initial conditions. However by extending the GCO-200 up to 7.15 days, it is possible to cover all longitudes. The main constraint remains therefore the latitude.

The impact may occur before or after pericentre passage because of the fast variation of the pericentre altitude from one orbit to the next. Hence the impact point might not be exactly at the reference latitude (40 North or South). If the targeted pericentre is missed and the impact takes place one revolution before or after, the longitude of the impact point is roughly rotated by 5.5 deg.

Controlled impact: If the re-entry has to occur at any latitude specified a posteriori after the science phase, (necessarily below the nominal inclination) and/or longitude a controlled de-orbit manoeuvre has to be performed It is here assumed that this is done while still flying on the circular orbit. This allows choosing any impact coordinate on Ganymede.

The nominal cost of deorbiting is 40.3 m/s. This DeltaV corresponds to a flight path angle at the surface of Ganymede equal to -2 deg. This is a safe value in order to ensure that the pericentre is below the Ganymede surface (i.e. -45 km) and the impact is achieved.

In order to assess the error on the impact point there are some operational and spacecraft related issues that need to be addressed. The s/c is at the end of life and probably not in its healthiest state. Even more important is the performance that can be expected from the thrusters at this point. The tank is almost empty and its performance can be well below expectations. At the same time besides the 40 m/s of DeltaV available for the deorbit burn, there will be additional residual propellant thanks to margins. This allows taking into consideration two different options:

- If the 40 m/s nominal burn is performed, with the cut-off of the engine stopped by a time condition, it could happen that the thrusters severely underperform and deliver a change in velocity which is not enough to crash onto Ganymede and which would result in a low pericentre grazing the surface and the crashing in an uncontrolled way.
- Otherwise the orbiter may blow down the tank residuals and thrust until the tanks is empty. In actual terms this will deliver a DeltaV which is larger than the 40m/s

required to deorbit and would ensure an impact with the moon on a steeper trajectory.

From an impact point of view the second option is extremely safe, but is not very accurate in terms of prediction of the impact point. For example if thanks to the residuals in propellant a total 50 m/s of de-orbit burn is imparted, the s/c could have a maximum error in the along-track impact point of 850 km, with respect to the nominal impact point. The problem is that an exact amount of the residuals in the tanks is not completely known until the burn is over.

If the impact point has to be precisely controlled and the dispersion reduced below a given threshold, it is needed to execute the nominal de-orbit burn in a more precise way, and this requires the availability of an accelerometer, which cuts off the thrust once the nominal deorbit DeltaV is achieved. If the DeltaV imparted for deorbiting can be controlled with an accelerometer, the propulsion system will be able to deliver a DeltaV of 40 m/s + error. Now assuming a 3sigma 1.5 % error in the nominal DeltaV the entry would occur within the following dispersion (along the direction of flight) of the actual impact point equal to [-80 km, +84 km] with respect to the nominal impact point.

Summarizing, the uncontrolled decay does not allow selecting the desired latitude. The accuracy of the impact point is mainly related to the knowledge of the orbit and that of the orbital perturbations.

Conversely in the case of the controlled entry there is a trade-off to be performed between the dispersion error of the impact point and the implementation of the manoeuvre. If the propulsion system over-burns until the tanks are empty the s/c will surely crash on Ganymede but with a large dispersion. (850 km for a 20% of over-burn). If a precise impact is sought, trying to minimize the impact error (i.e. less than +/- 90 km) an accelerometer is needed to cut-off the thrust when 40 m/s is reached.

There is actually a mixed strategy where the orbit naturally drifts. When the pericentre altitude has reached a threshold, e.g. 50 km, a de-orbit manoeuvre is applied. Therefore the manoeuvre cost is lower than for the controlled case and the accuracy of the impact point better, i.e. closer to 40 North or South: if the manoeuvre is performed when the pericentre altitude is e.g. 50 km, the cost becomes ~17 m/s.

In accordance with AD4, an uncontrolled impact is assumed, thus incurring no DeltaV.

10.2 Time to Impact

If the perturbations model and the orbit are perfectly known, it is possible to put the spacecraft on the unstable frozen eccentricity point. It means that the spacecraft could theoretically never impact the Moon.

A parametric analysis was run to simulate the finite accuracy of the orbit determination. It is not surprising that the eccentricity vector was found to be the driving parameter. In order to be conservative, an OD error of 500 m in the radial direction was assumed such that the eccentricity vector norm decreases (case (a)) or increases (case (b)) compared to

the stable case. The evolution of the pericentre and apocentre altitude is given in Figure 10-1.

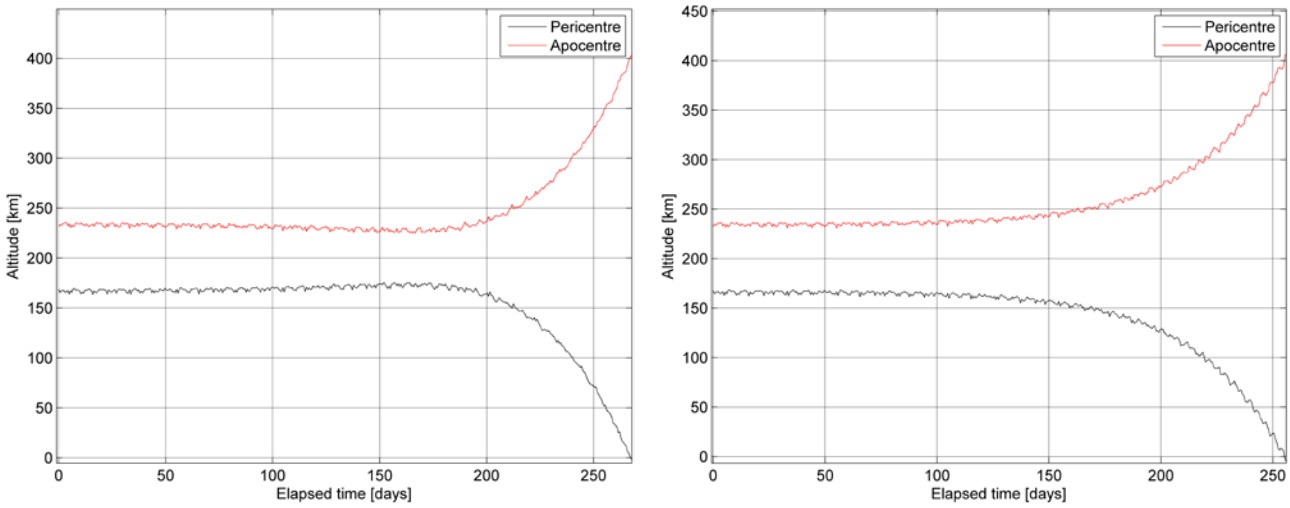

(a) (b)

Figure 10-1: Evolution of the pericentre and apocentre altitude if no S/K manoeuvre is performed. At initial time it assumes that the orbit lies on the unstable equilibrium point, only affected by an OD error in the radial direction (which directly affects the eccentricity vector)

The profile is slightly different (in case 'a' the eccentricity vector drifts towards the 40 deg unstable direction while in case 'b' it drifts towards the 220 deg unstable direction), but the lifetime is roughly equivalent: 250 days.

A more detailed analysis on the remaining uncertainty on the gravity potential at the end of the nominal mission together with the outcome of the navigation analysis would permit to refine this value, but at this stage it can be concluded that a lifetime of at least 6 months before impact is conservative.

The time to impact from 500 km is likely to be comparable.

11 JOVIAN TOUR OVERVIEW

The entire phase Jupiter is summarised in Table 11-1.

Phase	Label	Date yy/mm/dd	I/O	Acc. time [day]	Δt since last evt [days]	Acc. ΔV [m/s]	C/A [km]	v_∞ [km/s]	rp Long. [deg]	rp Lat. [deg]	Beta angle [deg]	Jup. solar L [deg]	Post Fly-by Period [days]	Post Fly-by n:m	Post Fly-by rp [Rj]	Post Fly-by Inc. [deg]	Post Fly-by Jac. Cst	Acc. Rad. [krad]
Energy red.	1G1	29/10/06	I	0	0	0	400	7.7	239	3	10	10	213.2	30:1	11.5	4	-1	0
	2G2	30/05/09	I	215	215	878	400	6.5	241	-23	2	356	57.2	8:1	12	2	2.66	3
	3G3	30/07/05	I	272	57	884	1720	6.5	249	-45	14	351	36.8	5:1$^+$	11.4	0	2.65	6
	4G4	30/08/13	O	310	38	884	791	6.5	279	-4	6	114	21.5	3:1	10.5	0	2.65	15
Europa Science	5G5	30/09/03	O	332	21	884	1282	6.5	273	-3	6	113	14.8	/	9.5	1	2.64	22
	6E1	30/09/17	I	345	14	884	403	3.7	188	-47	40	23	14.2	4:1	9.4	2	2.93	28
	7E2	30/10/01	I	360	14	903	403	3.7	179	47	39	26	14.3	/	9.4	0	2.93	41
	8C1	30/10/13	I	371	12	903	412	5	108	0	3	256	19.7	/	12.4	0	2.62	48
Jupiter High Latitudes	9G6	30/11/03	I	393	21	903	2544	4.9	269	-79	62	313	18	/	12.3	3	2.8	51
	10C2	30/12/13	O	433	40	903	200	4.8	222	71	59	129	16.7	1:1	12.1	11	2.65	62
	11C3	30/12/30	O	449	17	906	200	4.8	182	67	66	127	16.7	1:1	13.4	19	2.65	66
	12C4	31/01/15	O	466	17	907	200	4.8	182	53	64	126	16.7	1:1	15.3	25	2.65	68
	13C5	31/02/01	O	483	17	910	200	4.8	216	25	29	124	13.9	5:6	14.7	29	2.65	69
	14C6	31/04/25	O	566	83	917	200	4.8	35	-25	35	118	16.7	1:1	15.3	25	2.65	77
	15C7	31/05/12	O	583	17	920	200	4.8	360	-54	73	116	16.7	1:1	13.4	18	2.65	78
	16C8	31/05/29	O	599	17	921	1020	4.8	359	-65	78	115	16.7	1:1	12.3	13	2.65	80
	17C9	31/06/14	O	616	17	921	1547	4.8	356	-75	82	113	16.7	1:1	11.7	7	2.65	83
	18C10	31/07/01	O	633	17	923	200	4.8	71	-49	46	111	21.6	/	13.8	1	2.65	88
Transfer to Ganymede	19G7	31/07/20	I	651	18	930	10920	3.9	239	9	10	320	17.9	5:1	13.6	0	2.89	88
	20G8	31/08/24	I	687	36	930	9838	3.9	244	9	11	317	14.8	2:1$^+$	13.2	0	2.88	92
	21G9	31/09/10	O	703	16	930	3169	3.7	286	-8	10	59	11.1	/	12.3	0	2.88	97
	22C11	31/09/27	I	720	17	930	200	2.2	116	0	2	192	17.6	3:3$^+$	19.7	0	2.92	102
	23C12	31/11/25	O	779	59	964	3414	2.2	256	-3	3	26	13.3	/	15.4	1	2.92	103
	24G10	32/01/13	I	829	49	964	24364	/	191	-9	0	243	12.5	7:4	15.3	0	2.99	107
	25G11	32/03/03	I	878	50	964	97807	/	244	-2	1	219	12.0	5:3	15.2	1	2.99	112
	26G12	32/04/08	I	915	36	964	10840	/	185	-24	11	253	11.4	8:5	15.0	1	2.99	116
	27G13	32/06/05	I	972	57	964	41755	/	212	-1	14	252	10.8	3:2	15.6	1	3	123
	28G14	32/06/26	I	994	22	989	63356	/	227	4	14	257	10	7:5	15.6	1	3.01	125
	29G15	32/08/16	I	1044	51	992	32234	/	187	22	17	275	9.5	4:3	15.6	1	3.01	132
In-orbit around Gan.	GOI	32/09/17	/	1076	32	1125	313	/	318	12	29	71	/	/	/	/	/	138
	Man1	33/02/13	/	1226	150	1379	680	/	14	-40	62	38	/	/	/	/	/	220
	Man2	33/02/15	/	1228	2	1606	570	/	277	-20	62	141	/	/	/	/	/	220
	END	33/06/26	/	1358	130	1606	483	/	52	35	71	193	/	/	/	/	/	235

Table 11-1: Summary of the phase around Jupiter

A total of 29 fly-bys are used. The total radiation dose during the mission is 235 krad under 10 mm aluminium spheres shielding. As explained in Paragraph 3.7.5, this figure is only an estimation. The Europa phase represents ~10% of the total. Around 40 % of the dose is accumulated during the Ganymede in-orbit phase. In general the perijove radius is always greater than 10 Rj, except during the Europa phase (mandatory because of Europa's orbital radius of 9.4 Rj).

The first Ganymede swing-by (1G1) is performed with a safe pericentre altitude of 400 km. This minimum altitude constraint is then relaxed to 300 km, except for 2G2 to cope with the clean-up strategy of the JOI. The first Callisto swing-by (8C1) is performed at an altitude of 410 km (the minimum altitude constraint is active). This minimum altitude constraint is then reduced to 200 km (10C2). Both Europa fly-bys are performed with a pericentre altitude of 400 km.

The infinite velocity at Europa is lower than 4 km/s as required (3.7 km/s for 6E1 and 7E2). The Sun-Jupiter-Moon angle, or solar longitude, is 23 deg for 6E1 and 26 deg for 7E2.

The infinite velocity at 8C1 of 5 km/s is reduced by 0.2 km/s via a GC ladder. This GC transfer is a π-transfer, thus allowing for preliminary crank-up of the orbit (3 deg inclination after 9G5). The infinite velocity is then constant and equal to 4.8 km/s during the Jupiter high latitudes phase: because only Callisto resonant fly-bys are used, the infinite velocity does not vary significantly. The resonance ratio at maximum inclination (29 deg) is a 5:6 because it permits a slight increase of the inclination (0.5 deg) compared to the 5:4.

From 24G10 onwards, the infinite velocity is not given anymore because a low energy endgame is used and the infinite velocity concept is not valid anymore. However the Jacobi constant gives useful information: the (adimensioned) energy level increases under the effect of the perijove raise manoeuvres until the energy level of the L_2 point of the Jupiter-Ganymede is reached, showing the optimality of the solution.

At GOI the beta angle is 30 deg, i.e. between 20 deg and 30 deg as required. The inclination (w.r.t. Ganymede equatorial plane) is larger than 90 deg: the orbit is now retrograde. The drift in the GCO-500 is 0.07 deg/day, much slower than for the prograde option of the previous CReMA (0.15 deg/day).

The list of deterministic manoeuvres is detailed in Table 11-2. It has to be underlined some manoeuvres are essentially fixed in direction (in the local orbital frame), e.g. JOI, GOI or GEO-GCO transfer which are tangential: this would not change with a new tour or a new interplanetary option. Moreover the magnitude of these manoeuvres is also not subject to dramatic change. On the other hand, retargeting manoeuvres (out-of-plane, phasing) are not fixed in direction and magnitude: it shall be assumed that they can be anywhere, anytime in any direction.

Table 11-2: List of deterministic manoeuvres. The most relevant ones are the 1:1 EDVGA (#1 and 2), the JOI (#3), the PRM (#4), the Europa retargeting (#6), a fly-by pericentre altitude constraint assistance (#16), the LEE PRM (#17), the GOI (#19) and the GEO-GCO transfer (#20 and 21). The azimuth and declination are given in EME2000

Manoeuvre #	Epoch (UTC) [mjd2000]	Delta-V [m/s]	Azimuth [deg]	Declination [deg]
1	8283.66	44.369	85	28
2	8466.26	59.315	85	20
3	10872.53	787.390	3	5
4	10979.53	90.550	4	2
5	11115.95	5.702	64	-61
6	11219.43	18.901	124	-65
7	11310.03	2.980	95	-54
8	11333.25	1.048	108	43
9	11349.37	2.908	110	49
10	11362.99	7.658	262	-53
11	11449.51	2.934	110	49
12	11466.74	0.435	107	43
13	11476.86	0.008	95	-52
14	11493.60	2.299	92	-58
15	11512.83	7.059	358	-2
16	11598.33	33.720	188	-4
17	11849.74	25.324	292	-26
18	11870.99	2.214	299	-25
19	11948.06	133.116	188	64
20	12097.91	254.283	167	55
21	12099.96	226.854	166	54
22	12165.10	0.161	27	13

The evolution of the distance to Jupiter and of the Sun-Jupiter-Spacecraft angle is shown in Figure 11-1 from JOI to GOI.

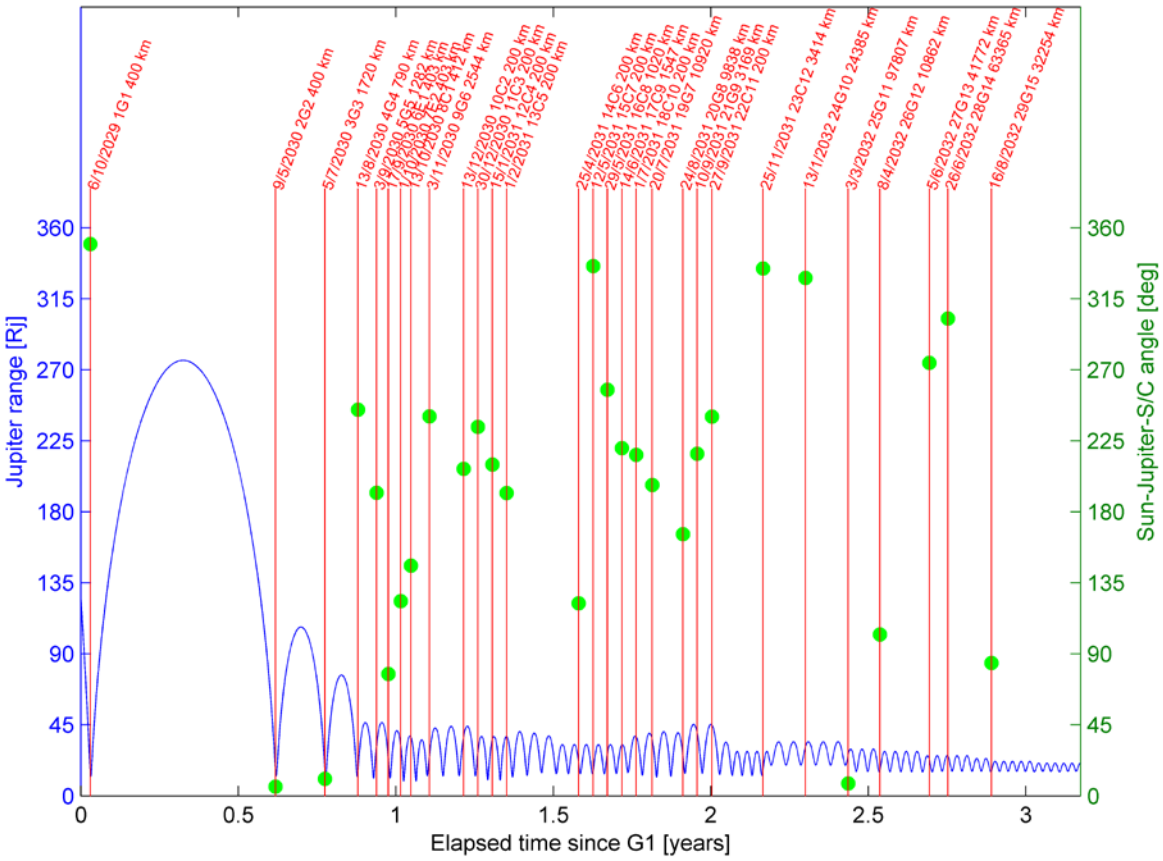

Figure 11-1: Evolution of the distance to Jupiter and of the Sun-Jupiter-Spacecraft angle during the phase around Jupiter

All Ganymede and Callisto swing-bys are also labelled with the date and the pericentre altitude. A similar plot showing the Sun Aspect Angle (SAA) at C/A is given in Figure 11-2. The SAA is defined as the angle between the zenith and the Sun directions: for instance, if the angle is 0 deg, the Sun is behind the S/C and the subsatellite point is in daylight. If the angle is 90 deg, the Sun is on the horizon of the subsatellite point. If the angle is larger than 90 deg, the subsatellite point is in the night.

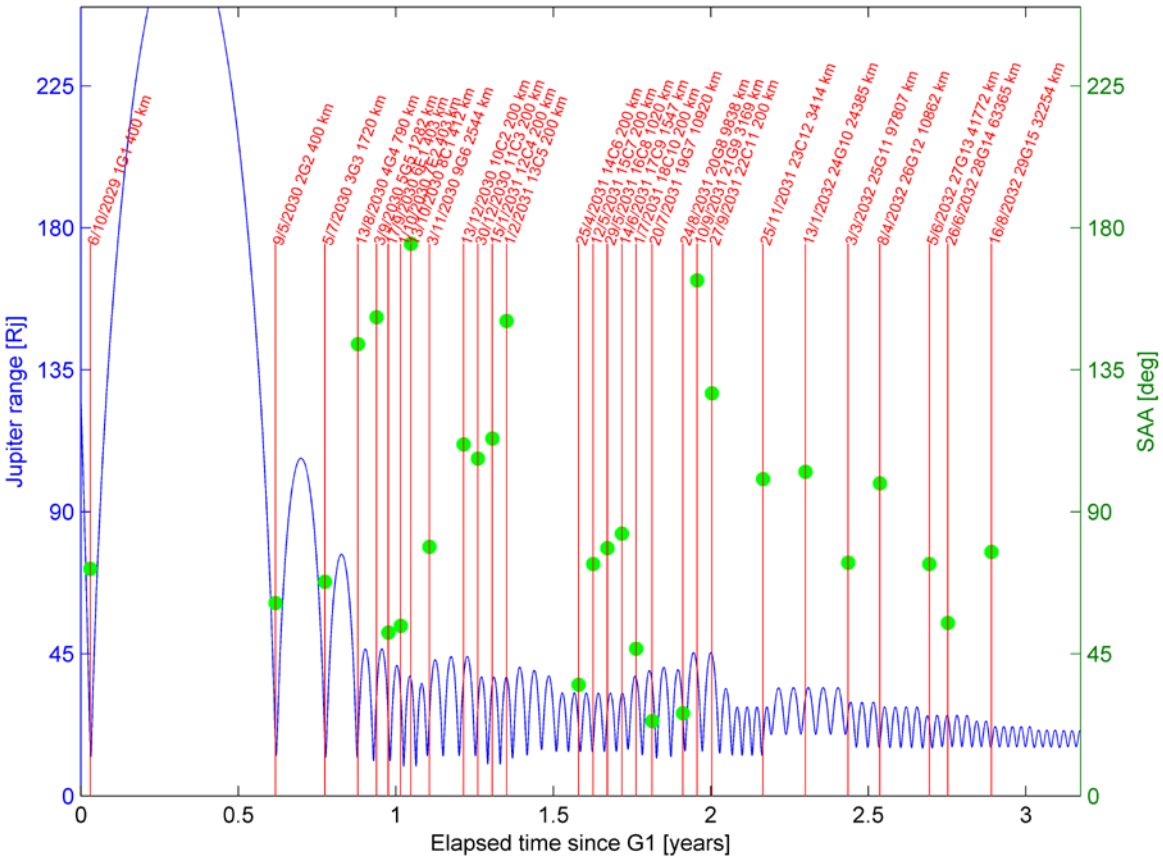

Figure 11-2: Evolution of the distance to Jupiter and of the SAA at C/A during the phase around

In terms of illumination, the inner-trailing side of Callisto will be in daylight for all fly-bys except 8C1 (inner-leading). Imaging the outer side is more difficult but with one good option 23C12. The first Ganymede swing-bys at the beginning of the tour have also a C/A in daylight (as a result of the energy reduction phase), before switching from inbound to outbound for 4G4 and 5G5, leading to the inner-trailing side in daylight. The Ganymede fly-bys during the low energy endgame allow imaging the leading side on the outbound leg.

The altitude during the fly-bys is given on a Mercator projection for Europa (Figure 11-3), Ganymede (Figure 11-4) and Callisto (Figure 11-5).

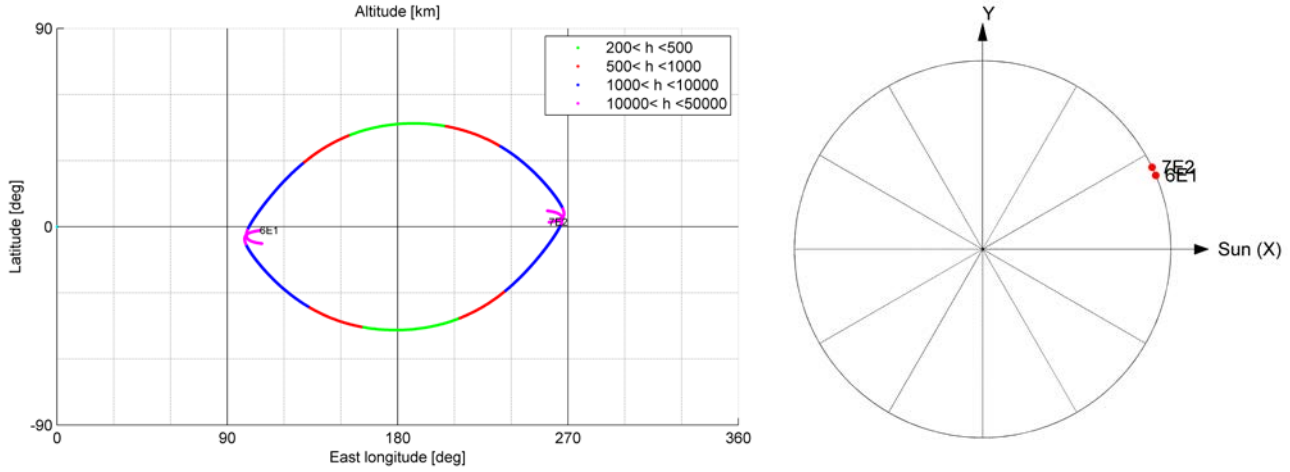

Figure 11-3: Altitude of Europa fly-bys (left) with their solar longitude (right)

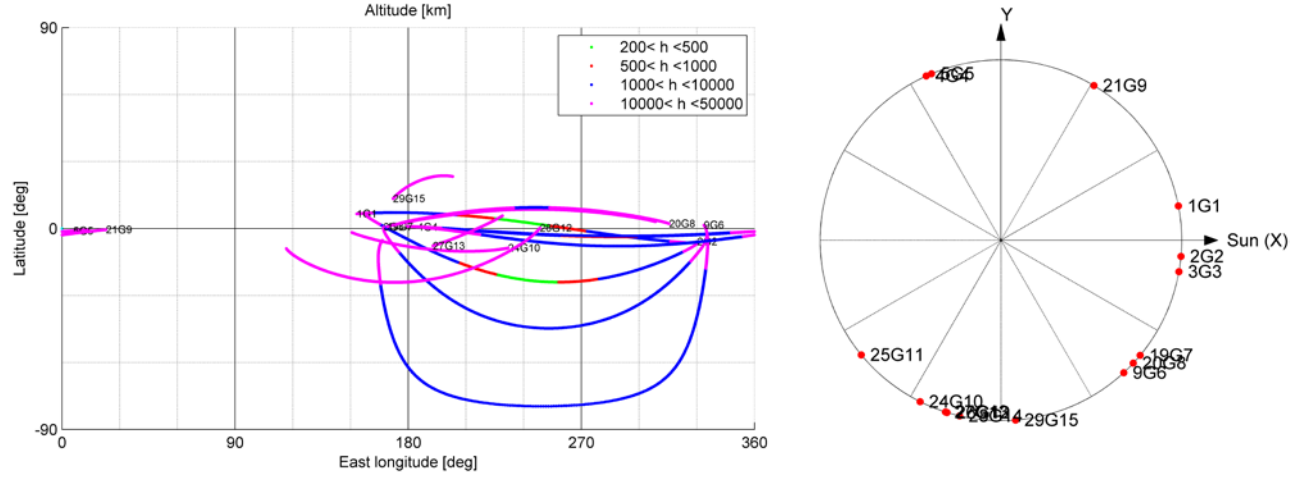

Figure 11-4: Altitude of Ganymede fly-bys (left) with their solar longitude (right)

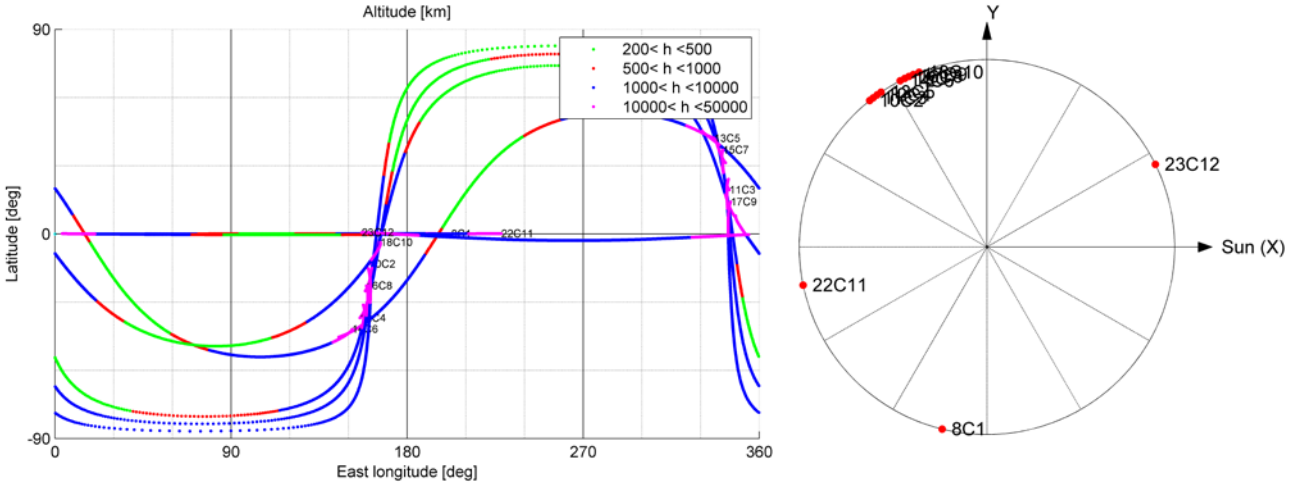

Figure 11-5: Altitude of Callisto fly-bys (left) with their solar longitude (right)

The ground velocity during the fly-bys is given on a Mercator projection for Europa (Figure 11-6), Ganymede (Figure 11-7) and Callisto (Figure 11-8). The plots are given for +/-6 hours w.r.t. C/A.

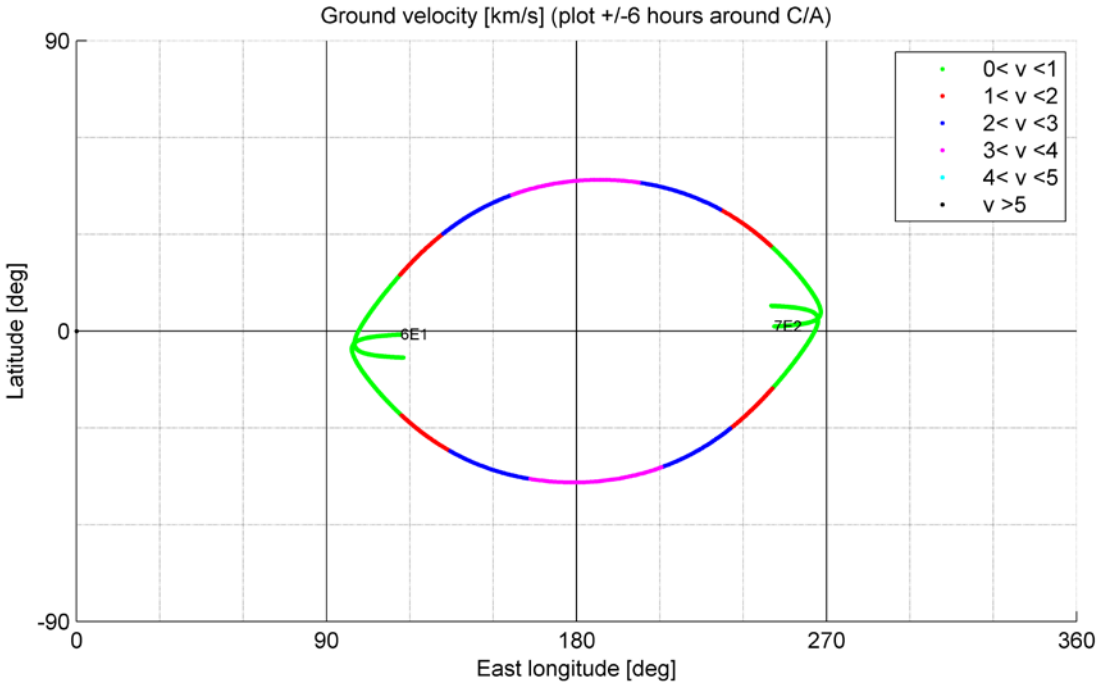

Figure 11-6: Ground velocity of the Europa fly-bys

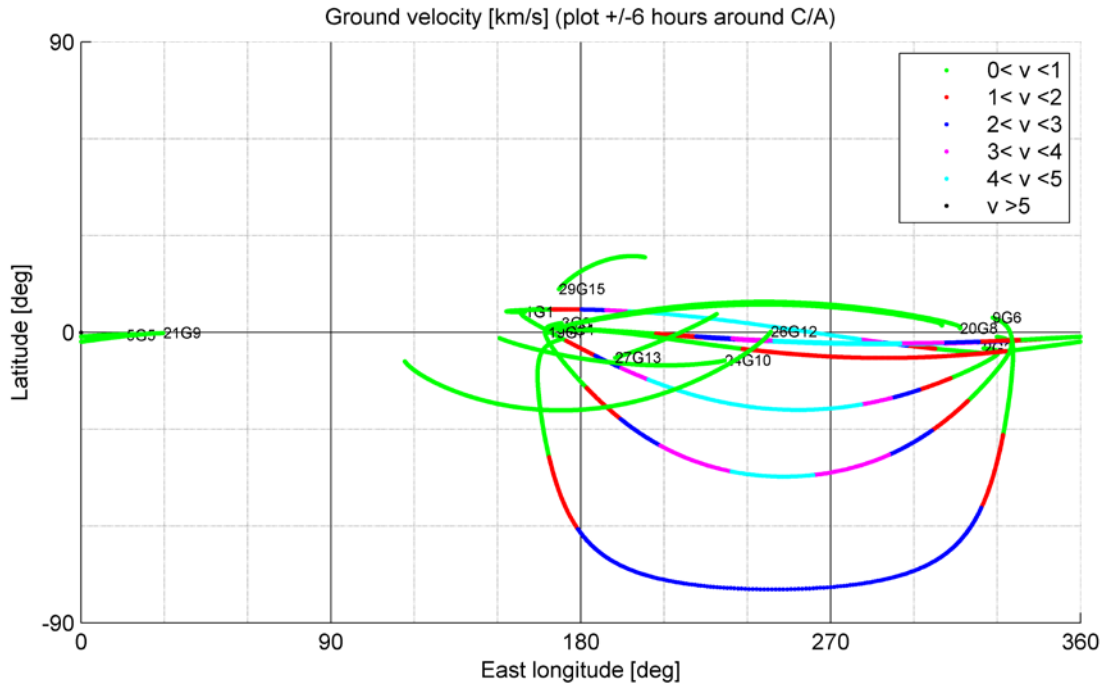

Figure 11-7: Ground velocity of the Ganymede fly-bys

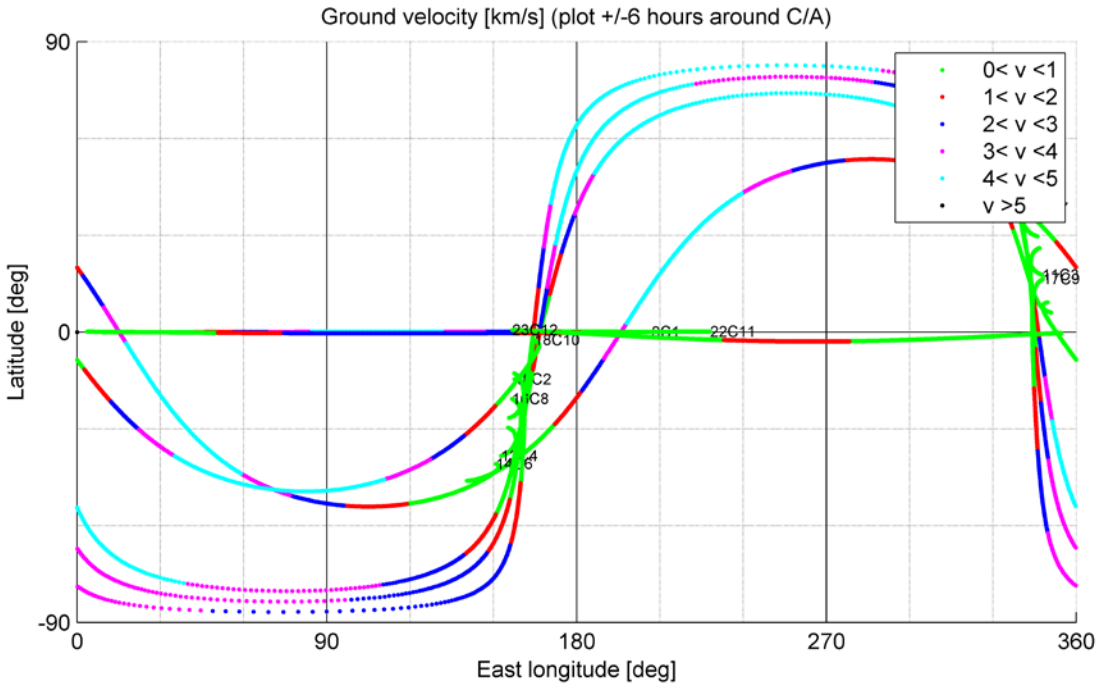

Figure 11-8: Ground velocity of the Callisto fly-bys

The entire trajectory can be represented in the Tisserand-Poincaré graph: each orbit between two gravity assists is represented in the perijove vs apojove plot. After each swing-by the perijove and the apojove are modified and are represented as a '+' on the graph. By

connecting all markers, it is possible to get a 'trajectory' in the perijove-apojove graph. This graph is given in Figure 11-9.

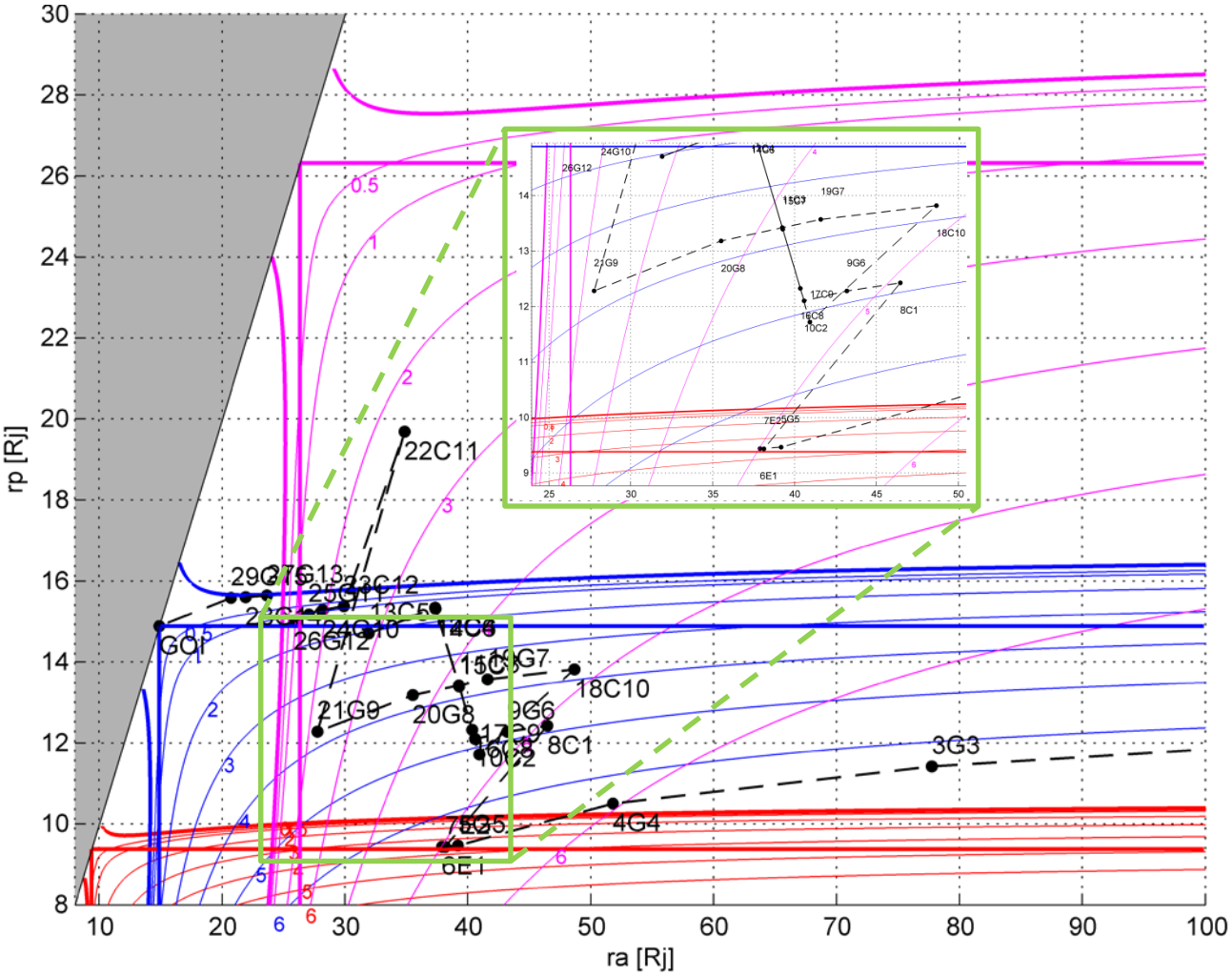

Figure 11-9: Perijove-apojove graph of the trajectory around Jupiter. The zoom is centred on the Europa science phase (perijove on Europa's orbital radius line), the Jupiter high latitudes phase (constant infinite velocity curve (with 3D artefacts)) and the Callisto-Ganymede ladder (reduction of the infinite velocity w.r.t. Callisto between 18C10 and 23C12)

All curves in red are related to Europa, all curves in blue are related to Ganymede and all curves in pink are related to Callisto. All curves correspond to energy levels (different values of the Jacobi constant). Let assume that the spacecraft starts with a given energy level, that of '3G3' for instance. It means that any further gravity assist with Ganymede will make the spacecraft move parallel to the surrounding blue lines. This is what happens when '4G4' is performed. The maximum move is bounded by the fly-by closest approach.

As mentioned above all lines are constant energy levels; they can also be seen as constant infinite velocity levels. By definition the concept of infinite velocity is connected to the intersection of the spacecraft orbit with that of the moon. The horizontal and vertical thick lines show the limit of intersection. Beyond these lines (left of the vertical or above the horizontal), the infinite velocity does not exist anymore: it is the region of low energy transfer. Hence it is more meaningful to refer to general energy level rather than infinite velocity.

The curved thick lines correspond to the libration point L_2 energy level.

The trajectory phases can be seen on this graph:

- The first horizontal part where the apojove is reduced while having a slowly decreasing perijove (3G3 to 5G5, 1G1 and 2G2 are out of the plot)
- The Europa science phase (5G5 to 8C1): the orbit is tangent to Europa's orbit.
- The Jupiter high latitudes phase (9G6 to 18C10). The infinite velocity is constant for this phase. But this is true in 3D, whereas the Tp-plot is only valid for planar motion. Therefore a variation of the in-plane infinite velocity is observed.
- The transfer to Ganymede (19G7 to 29G15). The first part shows the Ganymede infinite velocity reduction with the help of Callisto. The second part shows the effect of the Ganymede low energy endgame with the help of Callisto (26G12) and DSM (27G13). A zoom of the low energy endgame is given in Figure 11-10.

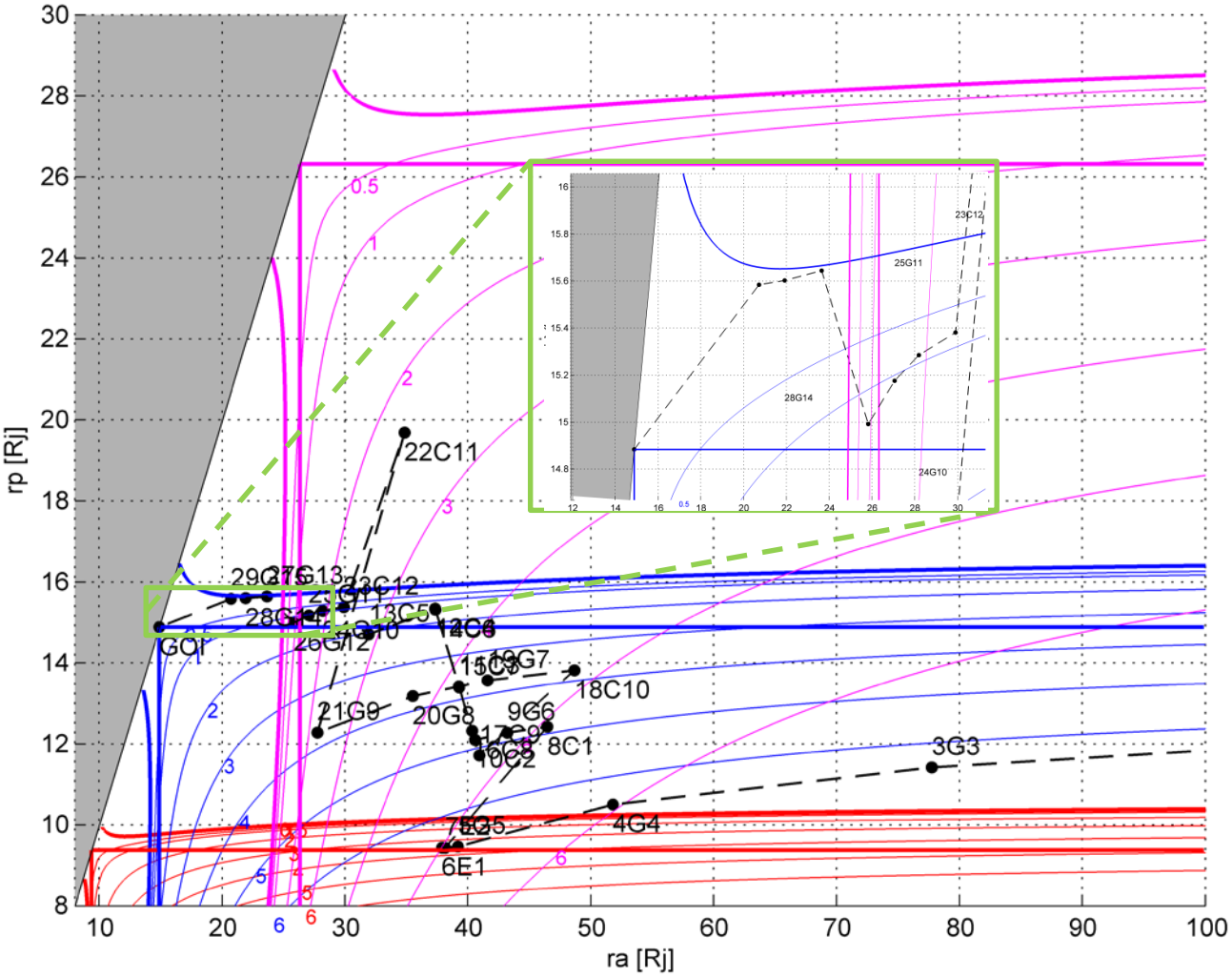

Figure 11-10: Perijove-apojove graph of the low energy endgame. The positive gravity pull of Callisto is visible after 26G12 with the increase of the perijove by 0.4 R_J

All swing-bys are above the horizontal thick line. Hence the term 'swing-by' is improper and shall be replaced by 'close approach'. The advantage of the low vs high energy is obvious: in that region the energy level curves are more horizontal than in the swing-by regime. It means that little DeltaV is needed to reach the capture orbit.

The evolution of the pericentre and the apocentre radii is shown in Figure 11-11.

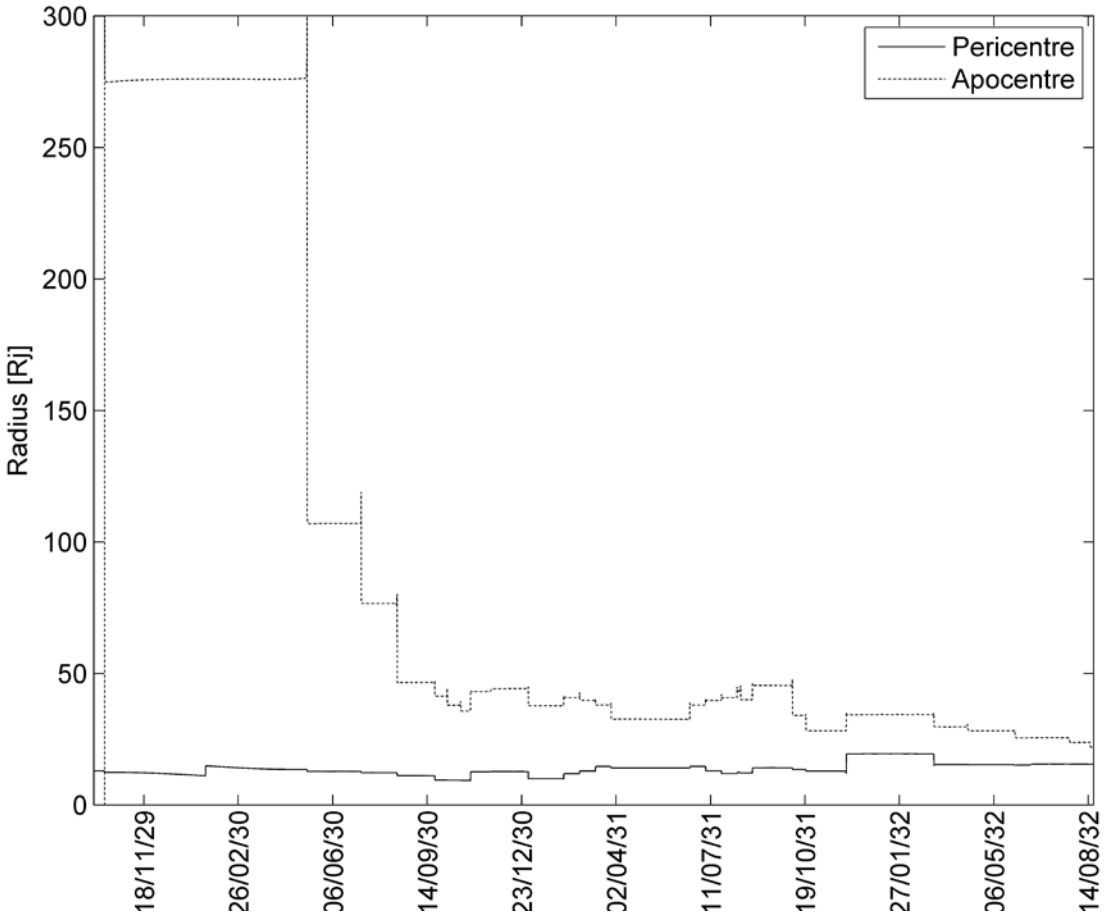

Figure 11-11: Evolution of the pericentre and apocentre radii from JOI to GOI

11.1 Equatorial

The entire trajectory around Jupiter is given in Figure 11-12.

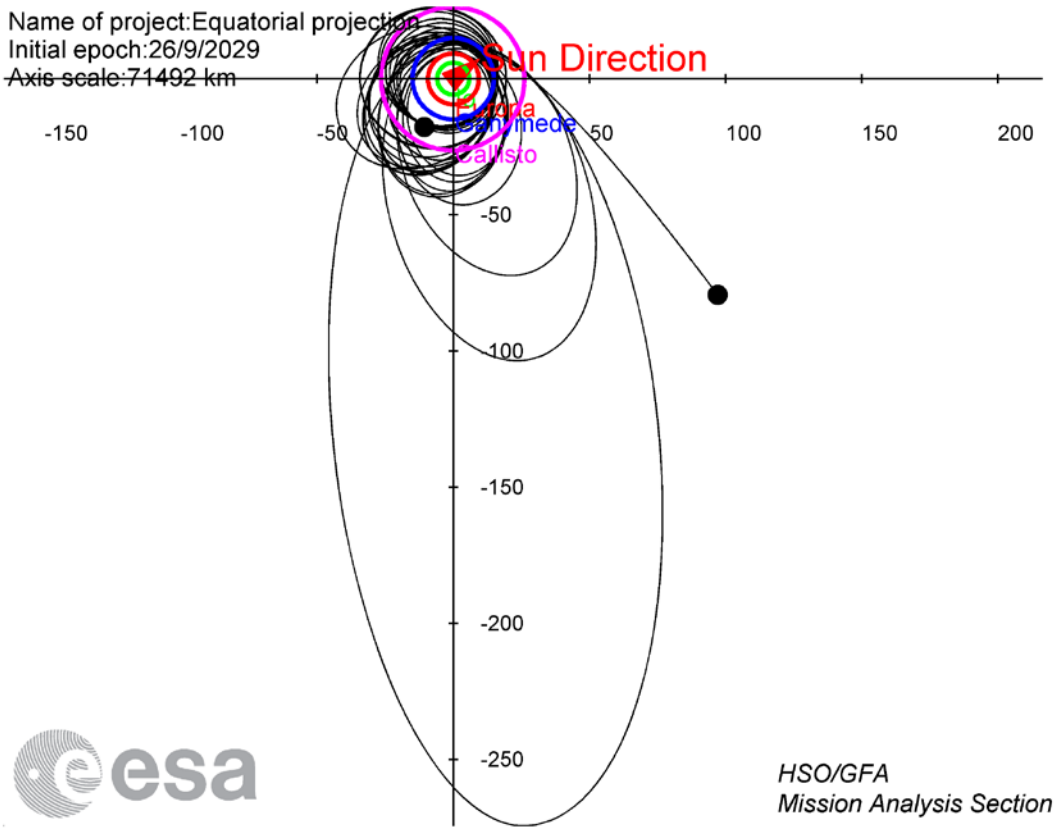

Figure 11-12: Trajectory in the Jupiter equatorial of date

The evolution of the inclination is shown in Figure 11-13.

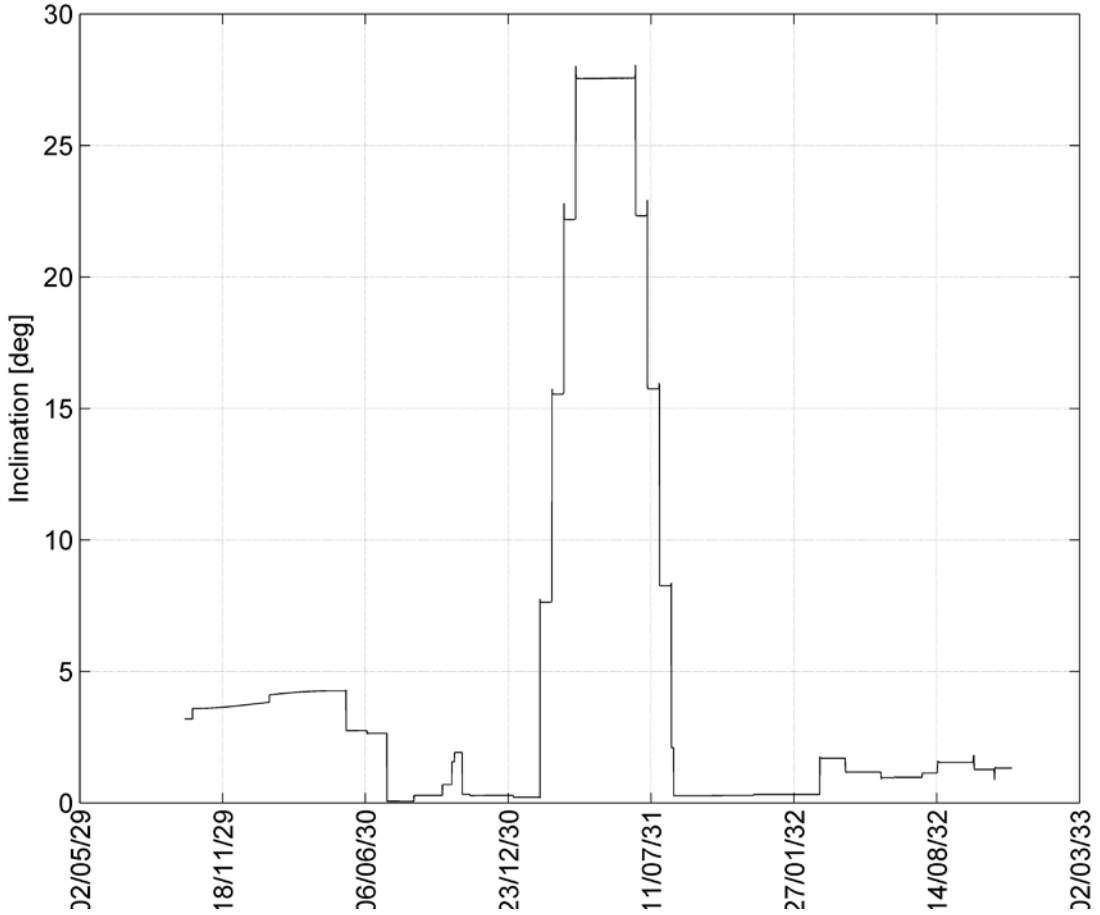

Figure 11-13: Evolution of the inclination in the Jupiter equatorial of date from JOI to GOI

The fast variation of the inclination at the end of the mission corresponds to the science phase around Ganymede where the orbit is near polar: the fast variation of the Z-component of the velocity incurs a fast variation of the instantaneous inclination w.r.t. Jupiter.

11.2 JSO

The trajectory is shown in Figure 11-14.

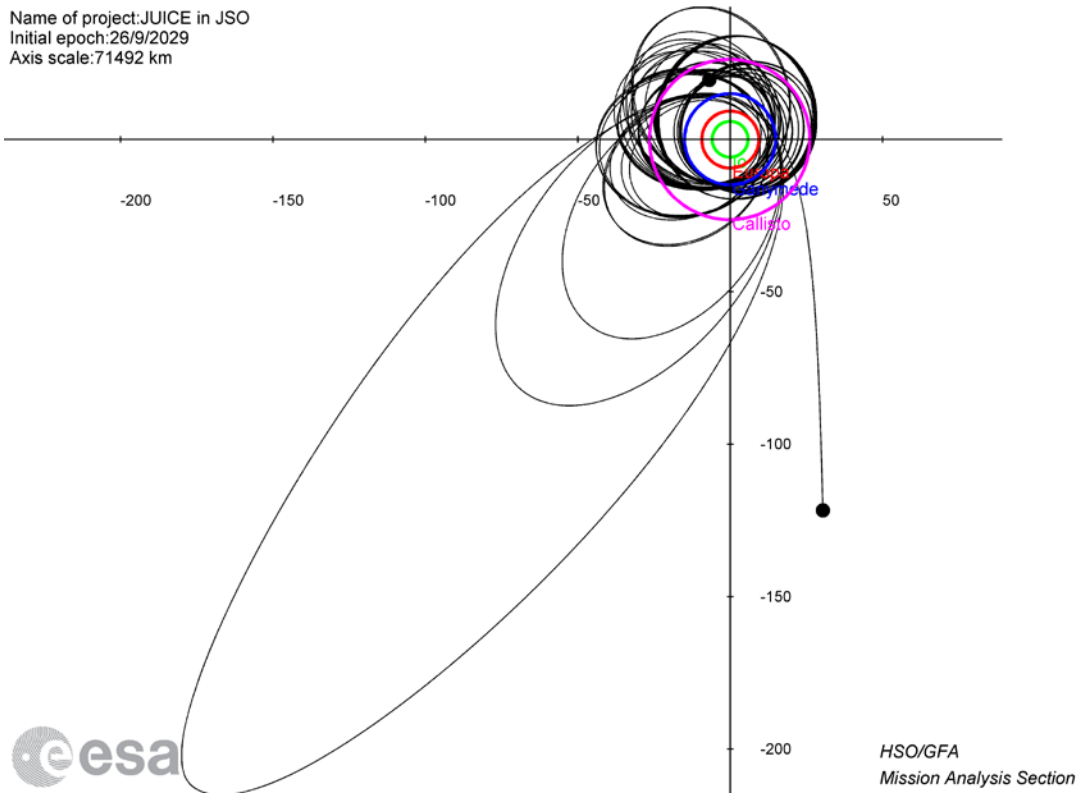

Figure 11-14: Trajectory in the JSO frame

11.3 Jovimagnetic System III

The evolution of the declination is shown in Figure 11-15.

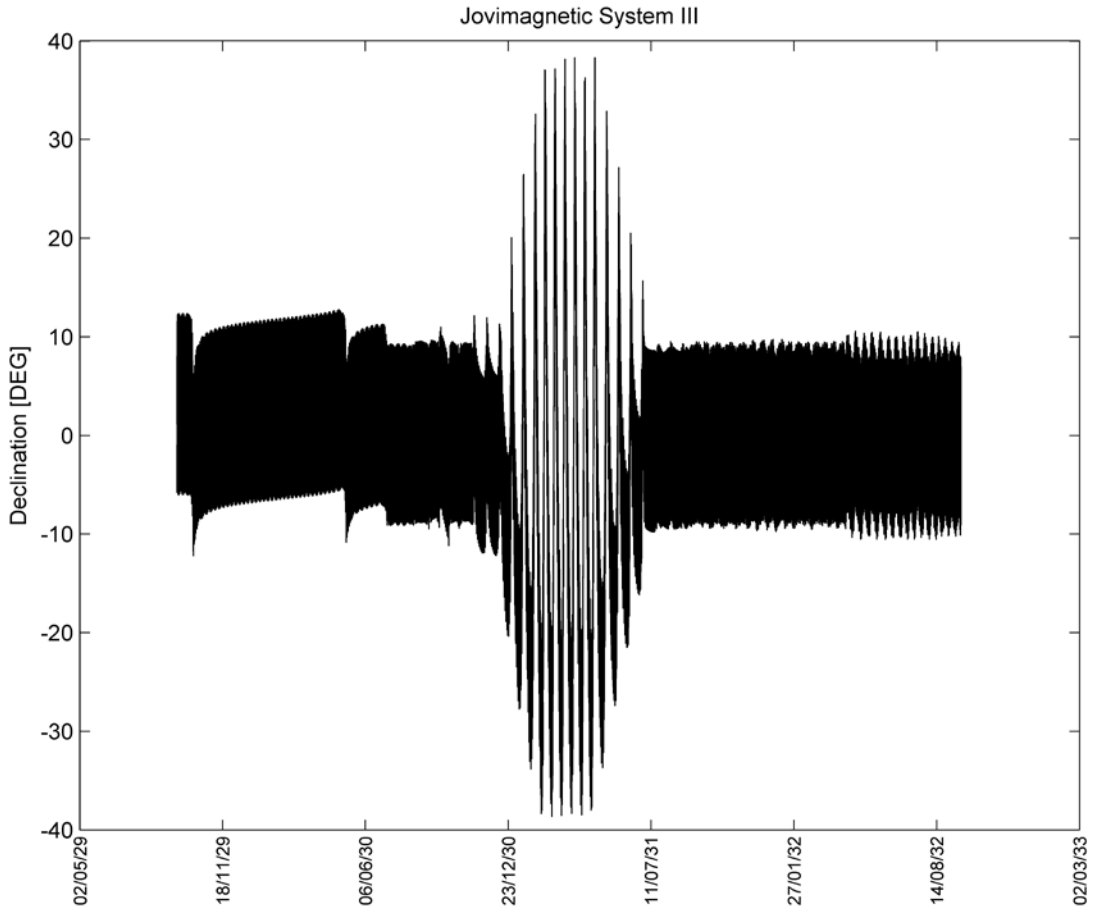

Figure 11-15: Evolution of the declination in the Jovimagnetic system III from JOI to GOI

For each orbit the fast variation due to Jupiter rotation can be observed: the magnitude of the fast variation is equal to twice the magnetic North pole tilt, i.e. 9.22 deg.

11.4 Fly-bys Rates

From an AOCS point of view, it is necessary to know the maximum angular velocity and acceleration encountered during a fly-by. In the analysis it is assumed that the spacecraft is Nadir pointing in push broom mode. The maximum angular rate is encountered at pericentre, while the maximum acceleration is encountered at a higher altitude. This altitude, together with the maximum rates, are given in Table 11-3.

.

Table 11-3: Maximum rates during flybys

F/B	hp [km]	Vinf [km/s]	ang vel [deg/s]	ang acc [mdeg/s^2]	h ang acc [km]
1G1	400	7.7	0.15	0.26	869
2G2	400	6.5	0.13	0.19	866
3G3	1720	6.5	0.09	0.09	2394
4G4	791	6.5	0.12	0.15	1320
5G5	1282	6.5	0.10	0.11	1887
6E1	403	3.7	0.12	0.16	705
7E1	403	3.7	0.12	0.15	705
8C1	412	5	0.11	0.13	847
9G6	2544	4.9	0.06	0.04	3337
10C2	200	4.8	0.12	0.15	600
11C3	200	4.8	0.12	0.15	600
12C4	200	4.8	0.12	0.15	600
13C5	200	4.8	0.12	0.15	600
14C6	200	4.8	0.12	0.15	600
15C7	200	4.8	0.12	0.15	600
16C8	1020	4.8	0.09	0.08	1545
17C9	1547	4.8	0.08	0.06	2157
18C10	200	4.8	0.12	0.15	600
19G7	10920	3.9	0.02	0.00	13000
20G8	9838	3.9	0.02	0.00	11764
21G9	3169	3.7	0.04	0.02	4061
22C11	200	2.2	0.07	0.05	591
23C12	3414	2.2	0.03	0.01	4297

The results are given until the beginning of the low energy endgame only: first the rates are slower in the low energy endgame due to the high C/A, but also formulas specific to two-body motion were used for the computation (19G7 and 20G8 around 10000 km are the illustration of low rates).

For Europa the rates are similar for 6E1 and 7E2. For Ganymede the highest rates are observed at the beginning of the tour: the overall maximum is 1G1 but as this fly-by is not used for science, 2G2 is the worst case. For Callisto the highest rates are observed during the high latitudes phase (low altitude, high infinite velocity).

12 NAVIGATION

This chapter is identical to the previous version of the CReMA

12.1 Interplanetary Transfer

12.1.1 Standard Fly-by

For the interplanetary navigation, no dedicated analysis was performed because of lack of time. However this phase of the mission is similar to other ESA missions with planetary fly-bys: Rosetta and Solar Orbiter (Bepi Colombo is excluded because it is a special case with low thrust). The analysis of the respective CReMA shows that an average value of 15 m/s/GA is a good estimate of the 99% stochastic DeltaV cost: it covers the Targeting Correction Manoeuvres (TCM) and the Clean-Up manoeuvres (CU). The standard ESOC approach to aggregate the individual cost is to linearly sum them.

The cost of the Jupiter approach is estimated to be 10 m/s as it only corresponds to TCM.

12.1.2 The Special Case of the LEGA

12.1.2.1 Introduction

Recently new interplanetary options have been identified: they rely on LEGA, see Chapter 4. The targeting cost of such fly-bys is identical to a standard EGA. However the clean-up cost is much larger: the reason is the short time between the LGA and the EGA, which is usually of the order of 1 to 1.2 day. This prevent any intermediate manoeuvre from an operational point of view; the dispersions of the first fly-by increase until the second fly-by, which finally amplifies them before the CU.

There are two categories of LEGA:

- The LGA is followed by the EGA (150l0la, 150la, 17OlOl, 150l0a, 150l0la, 180l0ma, 180l0lma, 200l0ma, 200l0lma, 17OlOl, 20OlUlm)
- The EGA is followed by the LGA (230la, 20OlUlm, 180l0lma, 200l0lma, 180lma, 200lma)

In order to maximise the effect of the LGA, its pericentre altitude is usually equal to 300 km (minimum altitude for safety reasons). The EGA pericentre altitude is free (above 300 km for safety reasons) and is optimised w.r.t. each specific interplanetary transfer; it can range from several thousands of km to several hundreds of thousands of km.

The analysis below groups the options according to the EGA pericentre altitude. This led to define 5 groups:

1. LGA first, then EGA (h_p~8000 km)

2. LGA first, then EGA (h_p~20000 km)
3. LGA first, then EGA (h_p>10000 km)
4. EGA first (~25000 km), then LGA
5. EGA first (~80000 km), then LGA

A detailed navigation analysis of each case has not been performed yet. However a preliminary analysis was conducted. It is assumed that the initial error in the B-plane of the first fly-by is dominated by the position error coming from OD and the position error due to a safe mode that would take place shortly before the LEGA. Based on experience it was decided to assume 15 km error in the B-plane to size the CU.

12.1.2.2 Group 1

As an example for this group, the case 150la was analysed. First the safety of the EGA was analysed. The reference pericentre altitude being 8000 km, level lines of pericentre altitudes are shown in the Moon B-plane in Figure 12-1 (left). It can be seen for 100 km dispersions, the pericentre altitude is 5000 km. For 15 km dispersions, the EGA pericentre altitude is above 7500 km: it is safe.

The CU DeltaV cost is shown in Figure 12-1 (right): for 15 km dispersions, it is 75 m/s. This value large enough to consider it covers as well the TCM cost.

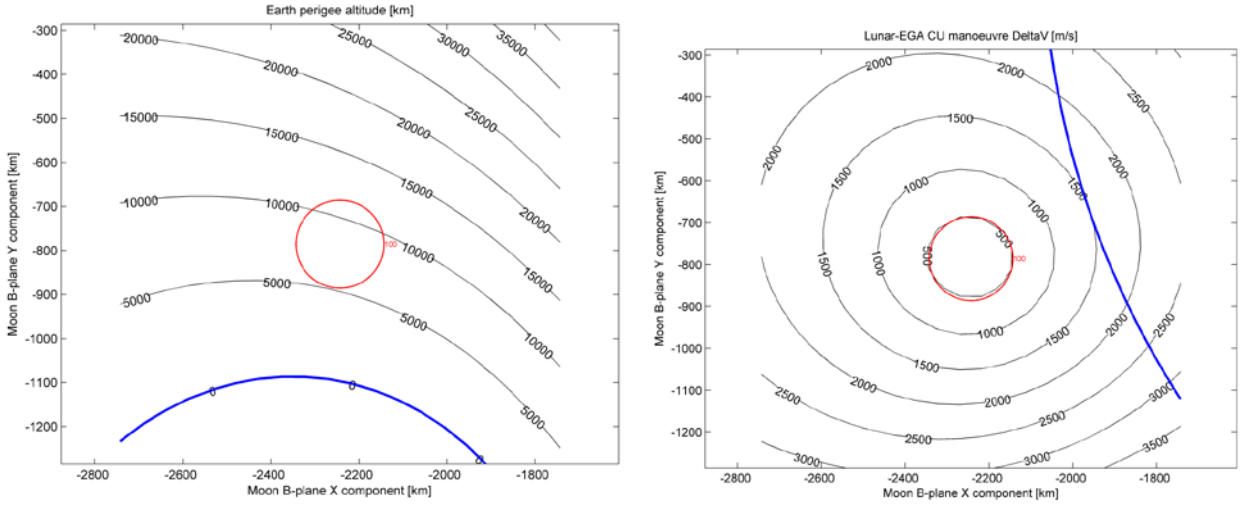

Figure 12-1: EGA pericentre altitude (left) and CU DeltaV cost (right) for Group1. The red level line shows an initial dispersion of 100 km in the Moon B-plane. The blue line represents the Earth surface (left) and the Moon surface (right)

12.1.2.3 Group 2

As an example for this group, the case 17OlOl was analysed. First the safety of the EGA was analysed. The reference pericentre altitude being 20000 km, level lines of pericentre altitudes are shown in the Moon B-plane in Figure 12-2 (left). It is obvious it is safe.

The CU DeltaV cost is shown in Figure 12-2 (right): for 15 km dispersions, it is 50 m/s. This value large enough to consider it covers as well the TCM cost. Without any surprise, the cost is lower than Group 1 due to a higher EGA pericentre altitude.

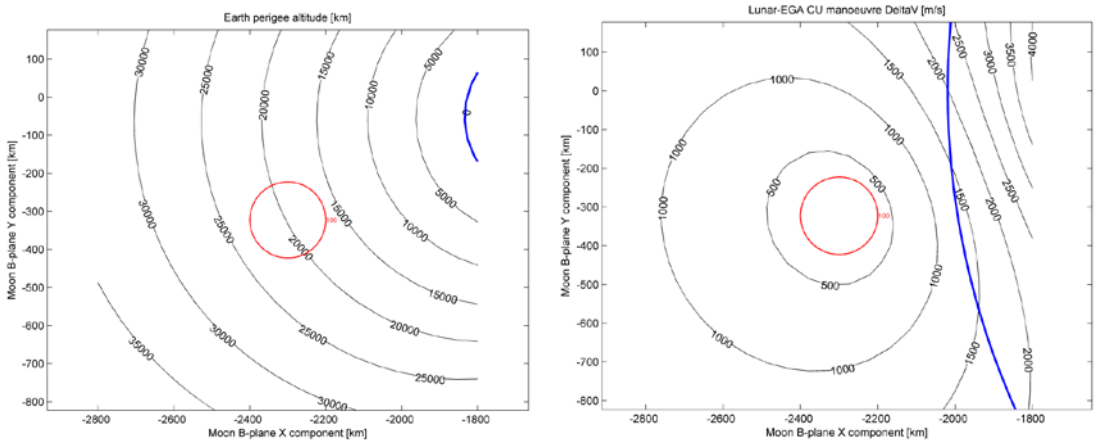

Figure 12-2: EGA pericentre altitude (left) and CU DeltaV cost (right) for Group2. The red level line shows an initial dispersion of 100 km in the Moon B-plane. The blue line represents the Earth surface (left) and the Moon surface (right)

12.1.2.4 Group 3

As an example for this group, the case 150l0a was analysed. First the safety of the EGA was analysed. The reference pericentre altitude being 175000 km, level lines of pericentre altitudes are shown in the Moon B-plane in Figure 12-3 (left). It is obvious it is safe.

The CU DeltaV cost is shown in Figure 12-3 (right): for 15 km dispersions, it is roughly 15 m/s. This value is comparable to a standard GA (see Paragraph 12.1.1). In order to cover the uncertainties due to the simplified model used here but also to cover the TCM, 10 m/s are added, thus leading to a cost of 25 m/s.

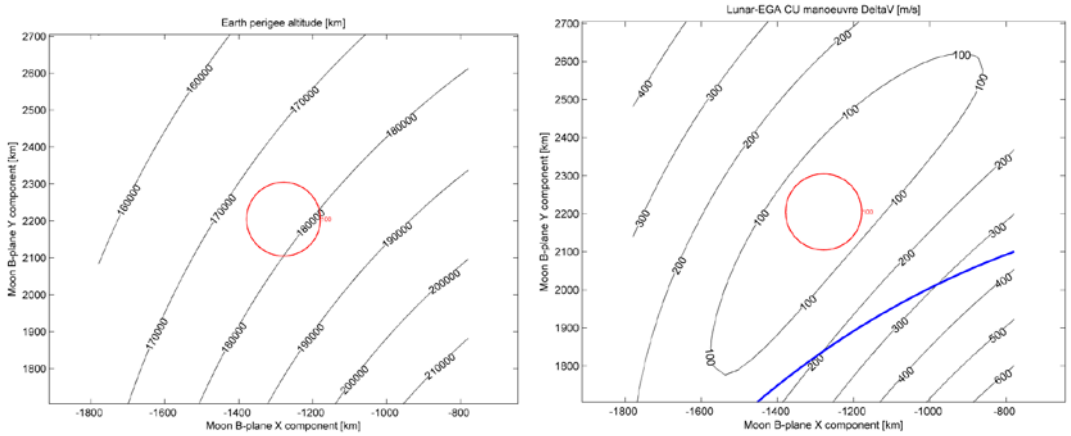

Figure 12-3: EGA pericentre altitude (left) and CU DeltaV cost (right) for Group3. The red level line shows an initial dispersion of 100 km in the Moon B-plane. The blue line represents the Moon surface (right)

12.1.2.5 Group 4

As an example for this group, the case 20OlUlm was analysed. First the safety of the LGA was analysed. The reference pericentre altitude being 300 km, level lines of pericentre altitudes are shown in the Earth B-plane in Figure 12-4 (left). It can be seen for 100 km dispersions, the pericentre altitude is below the surface. For 15 km dispersions, the minimum pericentre altitude is 225 km: it is safe.

The CU DeltaV cost is shown in Figure 12-4 (right): for 15 km dispersions, it is roughly 50 m/s.

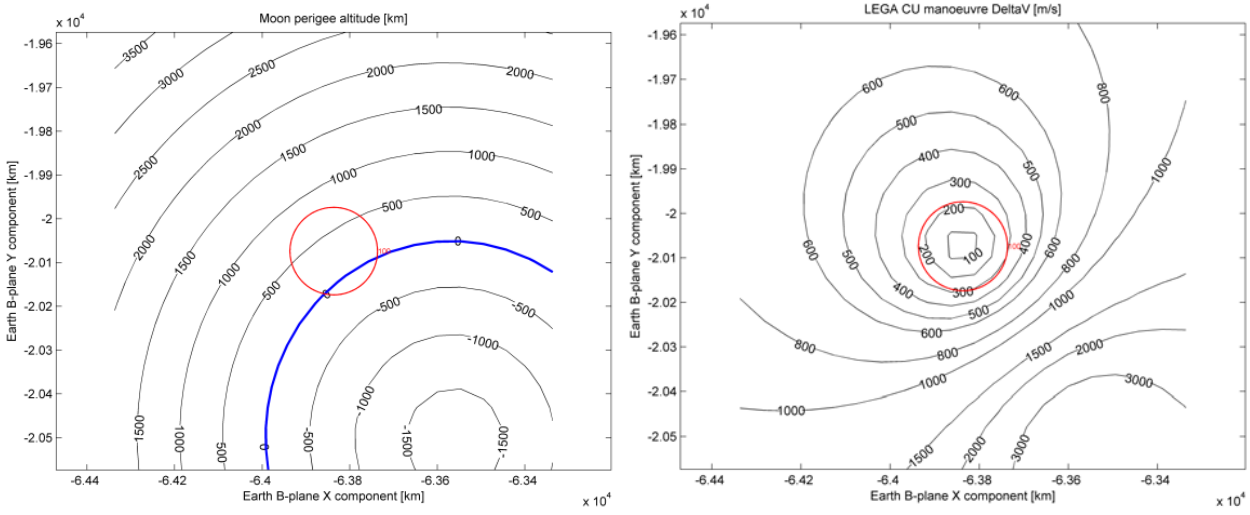

Figure 12-4: LGA pericentre altitude (left) and CU DeltaV cost (right) for Group4. The red level line shows an initial dispersion of 100 km in the Earth B-plane. The blue line represents the Moon surface

12.1.2.6 Group 5

As an example for this group, the case 180lma was analysed. First the safety of the LGA was analysed. The reference pericentre altitude being 300 km, level lines of pericentre altitudes are shown in the Earth B-plane in Figure 12-4 (left). It is obvious it is safe.

The CU DeltaV cost is shown in Figure 12-4 (right): for 15 km dispersions, it is 15 m/s. Following the rationale given in Paragraph 12.1.2.4, the navigation cost (TCM+CU) is taken equal to 25 m/s.

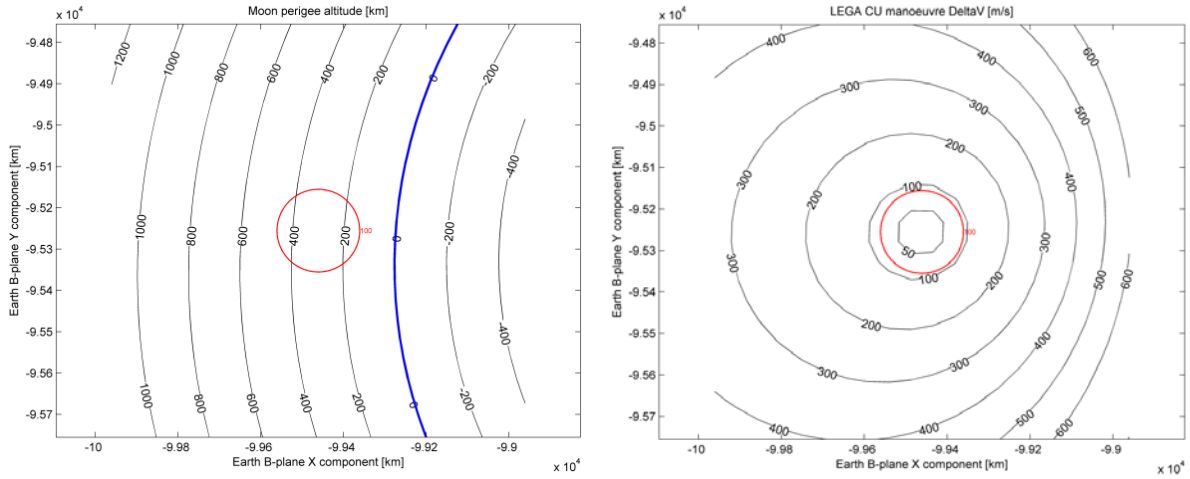

Figure 12-5: LGA pericentre altitude (left) and CU DeltaV cost (right) for Group5. The red level line shows an initial dispersion of 100 km in the Earth B-plane. The blue line represents the Moon surface

12.1.2.7 Summary

The main features of the LEGA applied to the different groups are summarised in Table 12-1. The last column represents the total navigation DeltaV allocation per fly-by (TCM+CU). A consolidated navigation analysis will be performed at a later stage.

Table 12-1: LEGA summary

Group	Options	Body 1	Body 2	Target hp1 [km]	Target hp2 [km]	Dispersed hp1 [km]	Dispersed hp2 [km]	Nav. DeltaV [m/s]
1	150lola, 150la*	Moon	Earth	300	8100	285	7700	75
2	17OlOl	Moon	Earth	300	~20000	285	19300	50
3	150loa*, 150lola, 180loma, 180lolma, 200loma, 200lolma,	Moon	Earth	300	~180000	285	~180000	25
4	230la, 20OlUlm*	Earth	Moon	~25000	300	225	~25000	50
5	180lolma, 200lolma, 180lma*, 200lma	Earth	Moon	~83400	300	275	~83400	25

* Tested cases

12.2 Jupiter Tour

The navigation analyses presented here are based on RD7 and RD19.

12.2.1 Introduction

Paragraph 12.2.2 gives the assumptions used to perform the analysis of the baseline scenario.

Paragraph 12.2.3 presents the navigation analysis assuming covariance matrix propagation. Two important features are related to this approach:

- Knowledge and dispersion are linearized w.r.t. the reference trajectory
- The DeltaV statistics can only be compiled for each manoeuvres separately. For instance the DeltaV @99% will be computed for each manoeuvre. There are two standard approaches to aggregate the individual DeltaV: Linear Sum (LS) (pessimistic, assumes full dependence of the manoeuvres) or Root Sum Square (RSS) (optimistic, assumes independence of the manoeuvres)

Parametric results then show the influence of key parameters on the DeltaV cost.

Paragraph 12.2.4 presents the navigation analysis assuming Monte Carlo (MC) approach. Non-linear targeting and propagation is used leading to a more realistic modelling. But the main advantage of this approach is to compute the DeltaV cost for each end-to-end sample, thus offering the capability to compute percentiles in a more realistic way than the LS or the RSS of the covariance approach.

12.2.2 Assumptions

12.2.2.1.1 Measurements

Three measurements types are considered: range, Doppler and optical.

Range and Doppler are performed using one ESA deep space network groundstation (CEB : Cebreros). The minimum elevation for ground station visibility is 10 degrees. The real operations will likely implement three stations at the same time (therefore also including New Norcia and Malargue) for the first fly-bys in order to have continuous coverage; it is also likely that only one station will be used (the one centred on the fly-by C/A) when the ephemeris steady state error is reached. This level of detail in the analysis was not possible at this stage of the study.

The range and Doppler data are collected every 60 min and 10 min, respectively. The noise standard deviation of the two-way range and two-way Doppler are 20 m and 0.2 mm/s, respectively. A range bias of 4 m is used. It is implemented as a consider parameter in the OD process, i.e. it is not estimated. It is assumed that range and Doppler are available during the fly-bys via the steerable MGA in case the spacecraft is in nadir pointing mode.

The optical data are acquired with the on-board camera and provide information on moons direction as seen from the spacecraft. The navigation camera is assumed to be able to process an image per day[1] with a noise of 8 μrad (1σ). The bias is considered to deal the uncertainties on the alignment of the navigation camera, moon limb measurement errors and spacecraft attitude determination. It is taken equal to 8 μrad (1σ).

All measurements taken two days before a manoeuvre are not used because of ground operations: this is the data cut-off[2]. Table 12-2 summarises the measurement assumption.

Table 12-2: Measurements assumptions

Measurement	Error (1 sigma)	Bias (1 sigma)	Frequency
Range	20 m	4 m (consider)	60 min
Doppler	0.2 mm/s	-	10 min
Optical	8 *m* rad	8 *m* rad (consider)	1 day

REM: the errors on the optical measurements are rather optimistic, even with an optical bench.

12.2.2.1.2 Uncertain Parameters

The initial spacecraft 1σ position and velocity error is assumed to be 1000 km and 1 m/s in all three components, respectively, considering about 1 % error of the PRM.

[1] In real operations the optical measurements will be taken by batches, at a distance given by the FOV. Example with Galileo: FOV = 0.5 deg, 800x800 pixels, moon occupies 150 pixels, moon radius of 2500 km, infinite velocity 5 km/s, perijove of one million km. This gives an average distance of 4.6 million kilometres and 10 days before the fly-by; at that distance several images are taken in a couple of hours

[2] In general the TCM data cut-off duration is the duration before a TCM, where no measurement are used. During this time, the OD process is performed on ground, the TCM is computed and finally uploaded on-board

The consider bias parameters are listed in Table 12-3. The ground station location error is a bias with respect to the inertial frame (ICRF). The Jupiter moon ephemeris errors for Europa, Ganymede and Callisto are also considered as biases.

Table 12-3: Consider biases

Contents	Error (1 sigma)
Ground station location w.r.t. ICRF (RARR, 3 axis)	33 cm
Jupiter moon ephemeris (3 axis)	1 km

The error on the solar radiation pressure model and Wheel-Off-Loading (WOL) during the Jupiter moon tour are considered in the non-gravitational acceleration error as exponentially correlated process noise. The error is given in Table 12-4.

Table 12-4: Exponentially correlated process noise

Contents	Error (1 sigma)	Corrected time
Non-gravitational acceleration	1.0e-11 km/s2	1 day

Such a value typically corresponds to a 3-axis stabilised spacecraft with pure torque capability.

TCM are performed in order to meet the flyby conditions. The manoeuvre execution errors are assumed to have a magnitude and direction components. The mechanization error is defined in Table 12-5. Deterministic manoeuvres also assumes the same execution errors.

Table 12-5: TCM mechanization error

Manoeuvre uncertainty	Error (1 sigma)
Delta-V magnitude error	1.00%
Delta-V direction error	0.50 deg
Minimum magnitude error	1 cm/s

12.2.2.1.3 Manoeuvre Strategy

Several manoeuvres are implemented in order to keep the trajectory close to the reference trajectory. The baseline manoeuvre sequence consists of TCM and CU. CU manoeuvres are defined to be at 3 and 7 days after the flybys (e.g. G3+3d). TCM manoeuvres are defined to be at 5 and 1 days prior to flybys (e.g. G3-1d). Time permitting, extra targeting manoeuvres are performed, e.g. apojove manoeuvres during the low energy endgame. The last TCM manoeuvre prior to a flyby do not target the coming moon but the next one; this strategy allows a significant reduction of the size of the CU manoeuvre.

Two guidance laws are used in this study.

- Fixed Time of Arrival (FTA) : Correcting the B-plane parameters and LTOF.
- Variable Time of Arrival (VTA) : Correcting the B-plane parameters but not LTOF.

FTA is applied throughout the trajectory as the preferred option. VTA is also used for most of last targeting manoeuvre before flybys.

12.2.3 Covariance Analysis

12.2.3.1 Baseline

The detailed manoeuvre history is given in Table 12-6 and Table 12-7.

Table 12-6: Jupiter tour navigation statistics (G2 to C17, covariance analysis)

Manoeuvre	det [m/s]	mean [m/s]	std [m/s]	90% [m/s]	95% [m/s]	99% [m/s]	SMAA- [km]	SMIA- [km]	LTOF- [sec]	SMAA+ [km]	SMIA+ [km]	LTOF+ [sec]
PRM+int	0	1.8	0.8	2.8	3.1	3.8	89804	3050	17796.4	8104	623	1686.6
G2-20d	0	0.9	0.6	1.8	2.1	2.8	8112	623	1688.4	597	47	134.9
G2-10d	0	0.2	0.1	0.4	0.4	0.6	597	47	135.0	243	43	58.0
G2-5d	0	0.2	0.2	0.5	0.5	0.7	243	43	58.0	162	37	39.6
G2-1d	0	0.6	0.4	1.0	1.2	1.6	1536589	117	233168.8	313462	47	47569.6
G2+3d	0	2.5	1.8	5.1	6.0	7.9	316085	47	47967.7	3435	5	600.0
G2+7d	0	0.8	0.6	1.7	2.0	2.6	3440	5	600.7	1096	4	171.5
G2+DSM	5.02	5.0	0.1	5.1	5.1	5.1	1114	6	174.3	641	61	118.0
G3-5d	0	0.4	0.3	0.8	1.0	1.3	643	62	118.3	98	28	19.9
G3-1d	0	0.4	0.3	0.8	1.0	1.2	290025	2565	42581.3	143863	495	21214.8
G3+3d	0	2.9	1.7	5.2	6.1	7.9	144907	499	21368.6	2220	18	606.6
G3+7d	0	1.7	1.3	3.5	4.2	5.5	2221	18	606.7	616	30	90.0
G3+apo	0	0.1	0.0	0.1	0.2	0.2	619	30	90.4	179	27	24.3
G4-5d	0	0.2	0.1	0.3	0.4	0.5	181	27	24.5	80	23	9.4
G4-1d	0	0.3	0.2	0.5	0.6	0.8	131718	106	16017.9	6497	77	1281.5
G4+3d	0	0.4	0.3	0.8	0.9	1.2	7467	82	1350.7	145	3	1032.9
G4+apo	0	3.0	2.2	6.1	7.3	9.6	147	4	1032.9	123	20	21.2
G5-1d	0	0.5	0.3	0.9	1.1	1.4	95080	462	3537.6	8349	434	959.0
G5+3d	0	3.5	2.3	6.8	8.0	10.5	8571	439	962.3	230	23	21.4
G5+apo	0	0.2	0.1	0.3	0.3	0.4	230	23	21.4	24	18	3.1
C6-1d	0	0.3	0.2	0.5	0.6	0.7	1023446	984	89103.6	76764	916	6758.3
C6+3d	0	2.4	1.8	4.9	5.9	7.7	85817	953	7513.8	7722	353	1703.9
C6+7d	0	0.9	0.7	1.9	2.2	2.9	7734	353	1704.3	966	12	1581.0
C6+apo	0	6.2	4.7	12.8	15.2	20.0	995	12	1581.2	3866	54	335.0
C6+DSM	21.5	21.5	0.2	21.8	21.9	22.0	3878	54	335.9	32289	48	2711.8
C7-apo	0	0.8	0.6	1.5	1.8	2.4	32290	48	2711.9	420	24	164.3
C7-apo	0	0.6	0.4	1.1	1.3	1.8	430	24	164.5	43	11	3.4
C7-5d	0	0.0	0.0	0.1	0.1	0.1	47	11	3.5	28	16	1.0
C7-1d	0	0.2	0.1	0.4	0.5	0.6	21983	153	1457.1	8879	11	587.1
C7+3d	0	1.0	0.7	2.0	2.4	3.2	9013	14	595.9	209	7	134.5
C8-1d	0	0.6	0.5	1.3	1.5	2.0	5060	2250	6461.1	2033	75	5234.8
C8+3d	0	5.2	3.5	10.2	12.1	15.8	2157	93	5365.0	85	5	105.1
E9-1d	0	0.5	0.3	0.9	1.1	1.4	21260	30	35668.9	694	3	1184.2
E9+DSM	30.6	30.6	0.8	31.6	31.9	32.4	822	5	1393.3	482	92	610.0
E10-5d	0	0.8	0.4	1.3	1.5	2.0	482	92	610.0	76	11	66.4
E10-1d	0	7.3	5.5	15.1	18.0	23.6	78777	1633	2312.7	1563	333	149.9
E10+3d	0	0.9	0.5	1.5	1.8	2.3	1649	362	157.8	69	61	5.9
E10+apo	0	0.1	0.1	0.2	0.2	0.2	70	62	6.0	66	9	2.2
C11-1d	0	0.6	0.3	1.1	1.3	1.6	27060	1486	3628.1	14797	257	1941.0
C11+3d	0	6.5	4.9	13.4	16.0	21.0	15532	598	2040.6	1974	19	260.3
C11+7d	0	0.2	0.1	0.3	0.4	0.5	1974	19	260.4	132	13	17.5
C11+apo	0	0.0	0.0	0.1	0.1	0.1	134	13	17.9	32	17	4.9
G12-5d	0	0.0	0.0	0.1	0.1	0.1	33	17	5.1	20	13	3.5
G12-1d	0	0.1	0.1	0.2	0.3	0.3	12767	535	252.1	2231	422	207.2
G12+3d	0	0.7	0.4	1.2	1.4	1.7	2962	431	213.7	166	33	276.2
C13-1d	0	0.5	0.3	1.0	1.2	1.5	67039	503	3756.0	10031	9	614.1
C13+DSM	2.67	3.0	0.7	3.9	4.4	5.2	10995	14	661.4	383	9	373.3
C14-apo	0	1.0	0.7	2.0	2.3	3.1	383	10	373.3	17	9	5.0
C14-1d	0	0.2	0.1	0.3	0.4	0.5	57524	73	3222.0	7042	19	393.5
C14+DSM	0.4	1.3	0.8	2.5	2.9	3.8	8378	21	468.0	149	9	67.9
C15-apo	0	0.2	0.1	0.4	0.5	0.6	150	10	67.9	13	4	3.1
C15-1d	0	0.2	0.1	0.3	0.4	0.5	42588	108	2441.8	4005	10	229.5
C15+DSM	1.26	1.7	0.5	2.4	2.7	3.4	5719	13	327.3	170	13	25.2
C16-apo	0	0.1	0.1	0.2	0.2	0.3	171	13	25.2	18	5	3.0
C16-1d	0	0.2	0.1	0.3	0.4	0.5	37229	68	2199.6	3052	7	180.2
C16+3d	0	0.4	0.3	0.8	1.0	1.3	4523	9	266.6	178	4	27.6
C16+7d	0	0.2	0.1	0.3	0.4	0.5	179	6	27.7	38	4	3.2
C16+apo	0	0.0	0.0	0.1	0.1	0.1	40	5	3.4	18	6	2.3
C17-1d	0	0.2	0.1	0.3	0.3	0.4	50188	121	3067.7	4903	16	300.0

Table 12-7: Jupiter tour navigation statistics (C17 to G34, covariance analysis)

Manoeuvre	det [m/s]	mean [m/s]	std [m/s]	90% [m/s]	95% [m/s]	99% [m/s]	SMAA- [km]	SMIA- [km]	LTOF- [sec]	SMAA+ [km]	SMIA+ [km]	LTOF+ [sec]
C17+3d	0	0.6	0.5	1.3	1.6	2.0	6686	21	408.4	149	6	23.5
C17+DSM	2.8	2.9	0.2	3.1	3.3	3.6	151	7	23.6	242	21	18.8
C18-apo	0	0.1	0.1	0.3	0.3	0.4	242	21	18.8	42	7	3.8
C18-1d	0	0.2	0.1	0.3	0.4	0.5	46840	3513	2806.0	2421	768	146.5
C18+3d	0	1.8	1.1	3.4	4.0	5.2	3516	859	210.6	52	16	39.8
C19-1d	0	0.2	0.1	0.4	0.5	0.6	81951	136	4921.4	4442	28	269.9
C19+3d	0	0.6	0.5	1.3	1.5	2.0	6311	30	381.1	147	6	48.3
C19+DSM	2.61	2.9	0.4	3.4	3.7	4.3	149	7	48.3	220	21	17.2
C20-apo	0	0.1	0.1	0.3	0.3	0.4	220	22	17.2	45	8	4.3
C20-1d	0	0.2	0.1	0.4	0.5	0.6	72498	145	4188.7	4564	15	263.3
C20+3d	0	0.6	0.4	1.2	1.4	1.9	6396	18	368.9	116	5	37.9
C20+DSM	1.98	2.1	0.1	2.2	2.3	2.6	118	6	38.0	196	15	17.4
C21-apo	0	0.1	0.1	0.2	0.3	0.3	196	16	17.5	21	6	2.9
C21-1d	0	0.2	0.1	0.4	0.5	0.7	23271	47	1331.1	2238	4	127.1
C21+DSM	0.74	1.0	0.3	1.4	1.6	2.0	3295	6	187.4	107	10	15.4
C22-apo	0	0.1	0.0	0.1	0.2	0.2	108	10	15.5	15	6	2.6
C22-1d	0	0.2	0.2	0.5	0.5	0.7	39989	158	2220.0	4244	11	234.9
C22+DSM	0.18	0.9	0.7	1.9	2.2	2.9	6176	16	341.9	113	8	53.1
C23-apo	0	0.2	0.1	0.3	0.4	0.5	114	9	53.1	11	4	3.0
C23-1d	0	0.2	0.1	0.3	0.3	0.5	38167	91	2095.4	3664	11	200.3
C23+3d	0	0.4	0.3	0.8	0.9	1.2	5801	14	317.3	153	4	84.9
C23+7d	0	0.2	0.2	0.4	0.5	0.7	155	4	85.0	40	4	5.0
C23+apo	0	0.0	0.0	0.0	0.1	0.1	41	4	5.2	15	5	2.7
C24-1d	0	2.8	2.1	5.7	6.8	8.9	72942	841	52115.3	16055	229	11126.5
C24+7d	0	1.0	0.5	1.7	2.0	2.6	17372	249	12040.1	207	4	143.7
C24+apo	0	0.1	0.0	0.1	0.1	0.2	210	4	145.4	40	5	25.4
C24+apo	0	0.0	0.0	0.1	0.1	0.1	68	5	44.8	23	3	14.2
G25-5d	0	0.0	0.0	0.1	0.1	0.1	25	3	14.8	18	3	7.6
G25-1d	0	0.2	0.1	0.4	0.5	0.6	33796	540	859.4	3071	75	803.5
G25+3d	0	2.0	1.5	4.0	4.8	6.3	3290	95	803.7	49	13	882.0
C26-1d	0	0.3	0.2	0.6	0.7	0.9	267080	227	27223.3	12647	138	1594.4
C26+3d	0	0.7	0.4	1.3	1.5	1.9	14428	143	1752.3	202	7	1083.0
C26+7d	0	0.0	0.0	0.1	0.1	0.1	205	7	1083.0	89	6	1081.5
C26+apo	0	1.8	1.3	3.6	4.3	5.7	95	6	1081.5	148	14	17.6
C27-5d	0	0.1	0.1	0.2	0.2	0.3	150	14	17.7	16	14	2.6
C27-1d	0	0.2	0.1	0.4	0.5	0.6	86220	2580	34000.8	10288	609	4077.2
C27+3d	0	1.1	0.7	2.1	2.5	3.2	11916	624	4701.2	287	8	810.8
C27+apo	0	0.4	0.3	0.9	1.1	1.4	294	8	811.3	112	13	53.6
C28-5d	0	0.1	0.1	0.2	0.2	0.3	112	13	54.3	21	13	5.0
C28-1d	0	0.3	0.1	0.5	0.5	0.7	89630	378	2280.7	9258	119	240.5
C28+3d	0	0.6	0.4	1.1	1.3	1.8	10150	123	263.5	244	9	369.0
C28+apo	0	0.6	0.4	1.2	1.4	1.9	245	9	369.0	11	6	5.6
C29-1d	0	2.5	1.8	5.1	6.0	8.0	6177	370	1898.3	1220	50	428.4
C29+3d	0	0.5	0.4	1.0	1.2	1.5	1322	53	464.5	162	53	93.4
C29+apo	0	1.5	1.1	3.0	3.5	4.7	163	56	93.8	29	2	6.2
G30-1d	0	0.5	0.3	1.0	1.1	1.5	2546	16	2123.2	383	24	112.8
G30+apo	0	0.7	0.5	1.4	1.7	2.2	393	32	156.0	441	9	50.1
G30+DSM	0.07	0.1	0.1	0.3	0.3	0.4	441	9	50.7	441	8	56.8
G31-apo	0	0.1	0.1	0.2	0.2	0.3	441	8	57.8	441	3	50.5
G31-apo	0	0.0	0.0	0.1	0.1	0.1	441	3	51.9	441	3	50.1
G31-apo	0	1.5	1.2	3.2	3.8	5.0	441	3	50.8	17	3	14.0
G31-apo	0	0.1	0.0	0.1	0.1	0.1	18	3	14.6	5	2	2.5
G31-1d	0	0.9	0.6	1.8	2.1	2.8	925	163	1127.3	215	13	51.6
G31+apo	0	0.4	0.3	0.8	0.9	1.2	222	23	85.6	215	12	34.4
G31+apo	0	0.1	0.0	0.1	0.2	0.2	215	13	35.0	214	5	34.0
G31+apo	0	0.0	0.0	0.0	0.0	0.1	214	6	34.1	214	5	33.8
G32-1d	0	1.3	0.9	2.6	3.0	4.0	651	168	713.2	546	13	114.5
G32+DSM	46.2	46.2	0.5	46.8	47.0	47.3	547	18	135.4	1067	237	470.6
G33-6d	0	1.8	1.0	3.2	3.6	4.6	1067	237	470.6	25	11	7.5
G33-1d	0	1.2	0.9	2.4	2.9	3.8	4222	126	3639.6	237	13	184.7
G33+DSM	14.4	14.4	0.3	14.8	14.9	15.1	282	13	226.1	1127	22	561.2
G34-apo	0	0.8	0.5	1.4	1.7	2.2	1127	22	561.3	26	10	13.2
G34-apo	0	0.1	0.1	0.2	0.3	0.4	28	10	14.7	8	7	3.8
G34-apo	0	0.1	0.1	0.2	0.2	0.3	11	8	5.8	7	6	2.4
G34-apo	0	0.1	0.1	0.2	0.2	0.3	9	6	3.3	7	5	1.3
G34-1d	0	0.3	0.2	0.6	0.7	0.9	8082	8	124565.7	869	2	13421.1
G34+apo	0	1.0	0.6	1.7	2.0	2.6	1037	2	15988.7	147	2	2290.6
G34+DSM	43.7	43.7	0.4	44.3	44.4	44.7	151	2	2358.5	4829	6	74305.6
GOI-10d	0	1.7	1.2	3.4	4.0	5.2	4829	6	74308.7	153	2	2384.2
GOI-5d	0	0.1	0.1	0.2	0.3	0.3	156	2	2420.0	63	0	928.5

In most of the cases, the first CU manoeuvre is the largest manoeuvre for each flyby. The large increase in delivery errors between TCM-5d and TCM-1d comes from the targeted moon: for TCM-5d it is the upcoming moon, while for TCM-1d it is the next moon. This approach permits to save a lot of DeltaV as explained in Paragraph 12.2.2.1.3.

These results can then be aggregated either with the LS approach or with the RSS approach. The outcome is presented in Table 12-8 and Table 12-9.

Table 12-8: Summary of the Jupiter tour navigation statistics (covariance analysis, LS)

Phase		Nb of F/B	LS				
			Mean	90%	95%	97%	99%
Energy reduction	G2 - C11	9	5.0	10.1	12.0	13.3	15.8
High latitudes	C11 - C24	13	1.7	3.6	4.4	4.8	5.8
Ganymede transfer	C24 - G30	6	2.4	4.8	5.6	6.2	7.4
Low-energy endgame	G30-GOI	5	2.5	5.1	6.1	6.7	7.9
Total	G2 - GOI	33	95	192	229	254	301

Table 12-9: Summary of the Jupiter tour navigation statistics (covariance analysis, RSS)

Phase		Nb of F/B	RSS				
			Mean	90%	95%	97%	99%
Energy reduction	G2 - C11	9	5.0	6.5	7.1	7.4	8.1
High latitudes	C11 - C24	13	1.7	2.4	2.6	2.8	3.1
Ganymede transfer	C24 - G30	6	2.4	3.2	3.4	3.6	4.0
Low-energy endgame	G30-GOI	5	2.5	3.2	3.5	3.7	4.0
Total	G2 - GOI	33	95	124	135	143	157

First it can be observed that the cost varies from one phase to another: it is maximum during the energy reduction phase and minimum during the high latitudes phase. The input for the navigation budget is @99%: it means that the real cost lies between 157 m/s and 301 m/s for the baseline case. On average per fly-by, it lies between 4.8 m/s and 9.1 m/s.

12.2.3.2 Parametric Analysis

The parametric studies of the Jupiter moon tour navigation is summarised in Table 12-10. They are taken from RD7: when this document was written, the assumptions were slightly different from the baseline described in the previous section; moreover the analysis was

only performed for the phase from G2 to C11. However the objective here being to compare w.r.t. a baseline, it is considered acceptable.

Different options in the measurements (with and without optical measurements), moon ephemeris error assumption (none, 1 km, 2 km, variable), and TCM data cut-off duration (0, 1 or 2 days) are presented.

Table 12-10: Summary of the parametric studies for navigation

Case		2p0	2p1	2p2	2p3	2p4	3p0	2p9
Optical meas.		YES	YES	YES	YES	YES	NO	YES
Moon eph. error [km]		1	NO	2	1	1	1	Var.
Data cut-off [day]		1	1	1	0	2	1	1
Delta-V [m/s]								
Mean		4.0	3.8	4.4	3.6	5.4	5.2	4.4
LS	@91%	8.1	7.6	8.7	7.3	10.8	10.5	8.7
	@95%	9.4	8.8	10.1	8.4	12.5	12.2	10.1
	@99%	12.1	11.4	12.9	10.8	16.2	15.9	13.0
RMS	@91%	5.3	5.0	5.8	4.8	7.0	6.9	5.7
	@95%	5.7	5.4	6.2	5.2	7.5	7.4	6.2
	@99%	6.6	6.3	7.1	6.0	8.6	8.7	7.1

The case 2p4 is the closest to the baseline presented in the previous paragraph; as explained before the figures are slightly different because of slightly different assumptions: for LS @99%, it is 16.2 m/s/GA in Table 12-10 and 15.8 m/s/GA in Table 12-8; for RSS @99%, it is 8.6 m/s/GA in Table 12-10 and 8.1 m/s/GA in Table 12-9.

However when the study was performed, the baseline was 2p0 (1 day data cut-off instead of 2 days for 2p4). All other cases are identical to 2p0, except for one parameter. This makes the comparison easier with 2p0 rather than 2p4 for which more than one parameter changes. The analysis shows that:

- 2p0 vs 2p1 and 2p2: the steady state moon ephemeris errors have an impact on the average DeltaV cost: ~7%/km @99%
- 2p0 vs 2p3 and 2p4: the TCM data-cut-off plays an important role. The increase from 24 hours to 48 hours translates into an increase of 35 % of the average DeltaV cost @99%
- 2p0 vs 3p0: the optical navigation reduces about 30 % the average DeltaV cost @99%; the optical navigation is useful beyond the ability to reduce moon ephemeris errors (which are the same for both cases)

The case 2p9 includes variable moon ephemeris uncertainties. This case intends to simulate the progressive improvement in the moon ephemeris estimation. The first flyby with Ganymede or Callisto is assumed to be affected by 10 km error (1σ) on each axis, the second encounter by 5 km (thanks to the reconstruction of the first fly-by), all others by 1 km, i.e. the steady state value. For Europa encounter, the transverse component of the ephemeris error is assumed to be 1 km, because of the Laplace resonance with Ganymede (and Io). The other directions follows the same evolution as for Ganymede and Callisto. The assumptions for the moon ephemeris errors are summarised in Table 12-11.

Table 12-11: Moon position error considering the large uncertainty of the first encounters

Target flyby	Consider moon position error [km] (radial, transverse, normal)
G2	5, 5, 5
G3	1, 1, 1
G4	1, 1, 1
G5	1, 1, 1
C6	10, 10, 10
C7	5, 5, 5
C8	1, 1, 1
E9	10, 1, 10
E10	5, 1, 5
C11	1, 1, 1

In order to make a fair comparison between 2p0 and 2p9, it is important to smooth the results over the entire mission: indeed the difference between the two cases is strong for the first-bys, then decreases and finally becomes zero once the steady-state values are reached. This smoothing is obtained by assuming that the average cost for the part from G12 to G34 is the same for 2p0 and 2p9 and equal to that of 2p0 for the part from G2 to C11. It leads to a slight increase of 7 % between 2p0 and 2p9. The conclusion is that modelling all fly-bys with a steady-state bias is accurate enough.

From this parametric analysis, it is concluded that:

- The optical measurements are useful beyond the reduction of the moon ephemeris error
- The data cut-off greatly affects the DeltaV cost

12.2.4 Monte Carlo Analysis

In Paragraph 12.2.3 a covariance analysis was performed. Such an analysis allows to calculate statistics for each manoeuvre independently. The overall DeltaV cost depends how the individual costs are aggregated. The two extreme cases are the LS and the RSS, the real cost falling in-between.

The only way to answer where the real cost is to perform a Monte Carlo (MC) analysis: each sample is propagated over the entire phase considered in the analysis. It is then very easy to calculate percentiles on the individual samples with all manoeuvres each (as opposed to the individual manoeuvres covariance).

12.2.4.1 Non-linear Targeting and Propagation

In the covariance matrix approach, the manoeuvre covariance matrix is calculated based on the knowledge and dispersion matrices on one hand and on the guidance matrix on the other hand. The underlying assumption is a linearization of the dynamics from the epoch of the manoeuvre until the target epoch, that of the position in the B-plane. The propagation is then done with the help of the state transition matrix. Again the underlying assumption is a linearization of the dynamics.

When the MC was implemented into the in-house navigation S/W, it was decided to numerically propagate each sample for a higher fidelity. A first guess of the DeltaV is computed based on the linearized solution. It is then tuned to correct the target position deviation. Consequently, for the same deviation, the DeltaV from the MC analysis will differ from that of the covariance analysis.

12.2.4.2 From G2 to C11

Because of lack of time, the MC analysis was only performed from G2 to C11 with the same assumptions as for the case 2p0 presented in paragraph 12.2.3.2. It was decided that it would then be acceptable to extrapolate the result to the end-to-end trajectory. The comparison of the results of the MC analysis are summarised in Table 12-12.

The results of the covariance analysis are those of the case 2p0 in Table 12-10. The MC analysis results were analyzed in three ways: LS, RSS and so-called ‘Real’. The latter case corresponds to the computation of the percentiles based on the individual samples, not on the individual manoeuvres (as for LS and RSS).

The first observation is that the LS and RSS costs are different from the MC to the COV analyses: the main reason is the detrimental, although more realistic, effect of the non-linear targeting and propagation.

As explained before, the LS and the RSS being extremes cases, the Real case shall fall in-between. It is exactly what is observed: it is at 79% between RSS and LS @90%, at 79% between RSS and LS @95% and at 74% between RSS and LS @99%. In the next paragraph, it is considered that the Real case is on average at 75% between the RSS and the LS costs.

The real cost is closer to the LS cost: the first reason is the effect of all consider biases. The other effect of the chain effect of a large error: it affects several consecutive manoeuvres before the guidance gets back to the nominal case[3].

Table 12-12: Covariance analysis vs Monte Carlo analysis

Case		MC	Cov
DeltaV / FB [m/s]			
Mean		4.8	4.0
LS	@90%	9.8	8.1
	@95%	12.0	9.4
	@99%	16.4	12.1
RSS	@90%	6.5	5.3
	@95%	7.2	5.7
	@99%	8.7	6.6
Real	@90%	9.1	N/A
	@95%	11.0	N/A
	@99%	14.4	N/A

12.3 Summary

The average stochastic cost per F/B used in the DeltaV budget is calculated in two steps:

1. The reference average cost is taken from Table 12-8 and Table 12-9@99% for LS and RSS: 4.8 m/s/GA for RSS and 9.1 m/s/GA for LS
2. The final average cost is taken at 75% between RSS and LS: 4.8+(9.1-4.8)*0.75

➔ 8 m/s/GA

[3] There is on-going work on the improvement of the guidance strategy

13 PLANETARY PROTECTION

This chapter is identical to the previous version of the CReMA

Following AD2 and AD4, there are Planetary Protection (PP) requirements related to Mars (category III), Europa (category III) and Ganymede (category II). For Mars and Europa, these requirements necessitate the assessment of the impact probability.

13.1 Europa

13.1.1 Introduction

A preliminary analysis for Europa is presented in and RD16. The requirement states that it shall be shown that the probability of inadvertent contamination of a subsurface ocean by viable terrestrial microorganisms is lower than 1.10^{-4} for the mission.

The abovementioned probability P_{cont} follows from the Coleman-Sagan formula, which is the product of several factors:

$$P_{cont} = F_1F_2F_3F_4F_5F_6F_7$$

Where F_1 is the total number of cells relative to cultured cells, F_2 is the bioburden reduction treatment fraction, F_3 is the cruise survival fraction, F_4 is the radiation survival fraction, F_5 is the probability of landing at an active site, F_6 is the burial fraction and F_7 is the probability that an organism survives and proliferates.

The first approach consists in trying to assess each factor. However most of them are hard to accurately compute. Therefore the second approach is to consider that all factors are equal to 1, except that related to impact with Europa: F_5. This factor is actually the product of the collision probability with Europa, denoted P_{PP} in the following, with the probability of having this collision at an active site, which is also supposed to be equal to 1. This approach puts a lot of pressure on mission design; on the other hand, if the 1.10^{-4} requirement is satisfied under these conditions, no further discussion is needed for the other factors.

The collision probability with Europa P_{PP} is the sum of two terms: the probability of a loss of the spacecraft followed by an impact with Europa (named $P_{(E,long)}$) + the probability to enter a safe mode followed by an impact with Europa (named $P_{(E,short)}$).

13.1.2 Long Term Failure

The first term of the overall probability corresponds to the loss of the spacecraft: the objective is to assess the collision risk with Europa at any stage of the Jupiter tour (the spacecraft loss can be due to H/W failure, radiation or micro-meteoroids damage, in one event or after the loss of a critical equipment and its redundancy). Based on the reference trajectory, the Tisserand-Poincare graph of the Jupiter tour is given in Figure 11-9.

Europa orbital radius is 9.4~Rj. Taking a maximum radius of 11~Rj allows concluding that the interval from G3 to C11 shall be analysed. Outside this interval the collision probability will be extremely small in comparison. At this stage, the analysis is not run over the end-to-end trajectory because of over-lengthy computational time.

The collision probability is assessed via MC analysis. A (much faster) covariance analysis cannot be used instead, because the propagation time can extend over years with potentially many close approaches in between. It makes the problem highly non-linear and not suitable for this approach.

One MC simulation is run for each TCM or CU manoeuvre of the trajectory; the underlying assumption is a loss of the spacecraft between the application of the TCM and the next one. The concept of the sampling is shown in Figure 13-1.

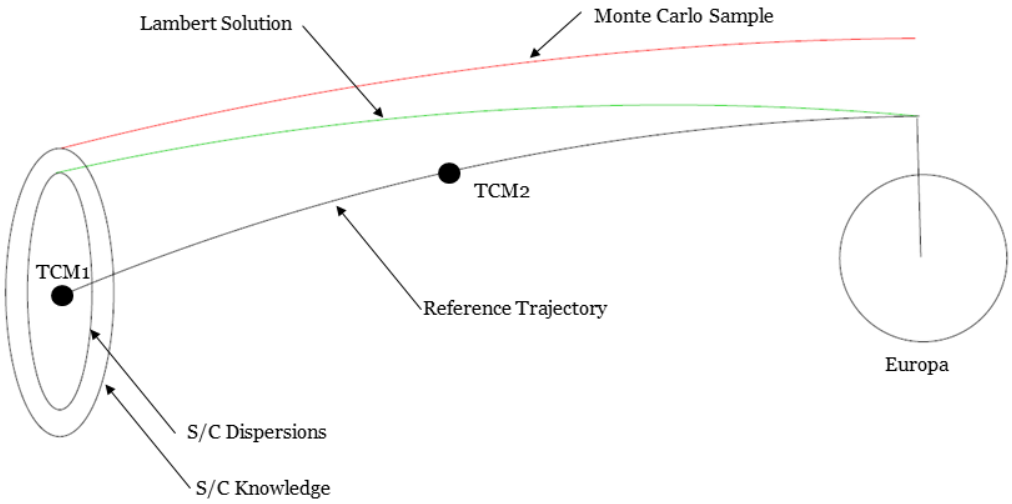

Figure 13-1: Overview of the MC sampling

As a reference for navigation, three manoeuvres are assumed in every arc: one CU manoeuvre after a fly-by, one TCM at apojove and another TCM shortly before the next fly-by. The assumptions are summarized in Table 13-1.

Table 13-1: Initial state dispersions for the long term analysis. Only the diagonal terms are given. They are based on the navigation analysis for G2 and are assumed equal for all other arcs. Knowledge errors are much smaller

Axis	CU	TCM 1	TCM 2
Pos. R-axis [km]	720	390	380
Pos. S-axis [km]	1150	6450	300
Pos. T-axis [km]	220	1280	300
Vel. R-axis [m/s]	10.6	1.8	1.2
Vel. S-axis [m/s]	7.6	0.5	0.5
Vel. T-axis [m/s]	0.5	0.3	1

For the moons, it is assumed that the driver is the phasing, i.e. a common angular shift. For each run one sample of standard deviation 0.0043 deg is taken. The true anomaly of all moons is shifted by this amount[4].

For each run, the number of samples is chosen equal to 10000. It is justified by the fact that probability collisions already stabilize after 1000 samples (see Figure 13-2 as illustration for the TCM at apojove between E9 and E10).

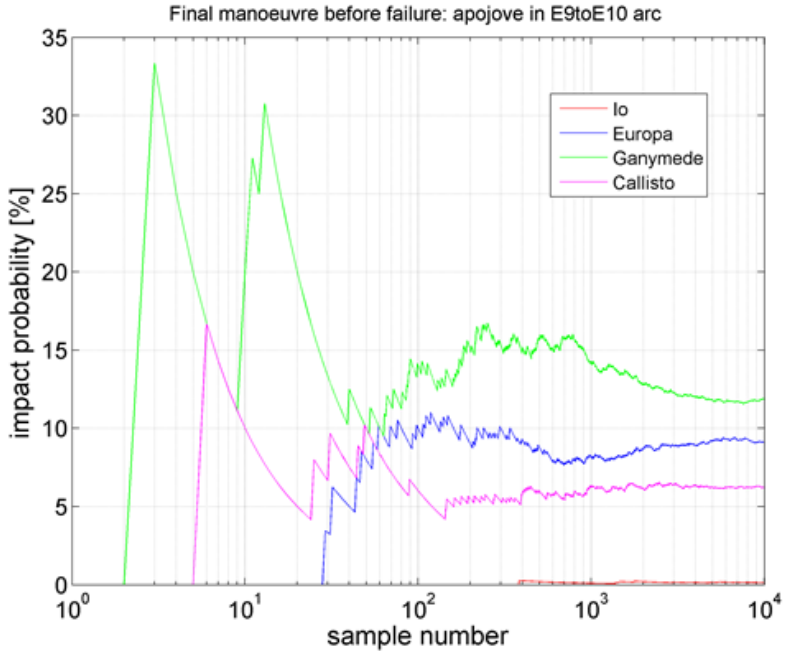

Figure 13-2: Collision probability as a function of the samples number. It is assessed over 50 years. There are 24 similar intervals considered in the analysis

[4] 0.0043 deg corresponds to an along-track shift of 50 km for Europa, 80 km for Ganymede and 141 km for Callisto

The collision is assessed over 50 years. The 200 years value was linearly extrapolated from the 50 years value to reduce the (very heavy) computational burden. Beyond 200 years it was agreed that the spacecraft is sterilized by the radiations trapped in the Jupiter environment.

As an output the collision probability with Europa can be assessed for each phase of the Jupiter tour between G3 and C11 (see Figure 13-3).

At the edges of this interval, the probability is small, about 4% at the beginning and 3% at the end. Outside this interval, the perijove radius rapidly increases, therefore the probability is considered to become very small: from JOI to G3 first, then from C11 to GOI, the collision probability is kept constant and equal to 1%. This figure is considered conservative.

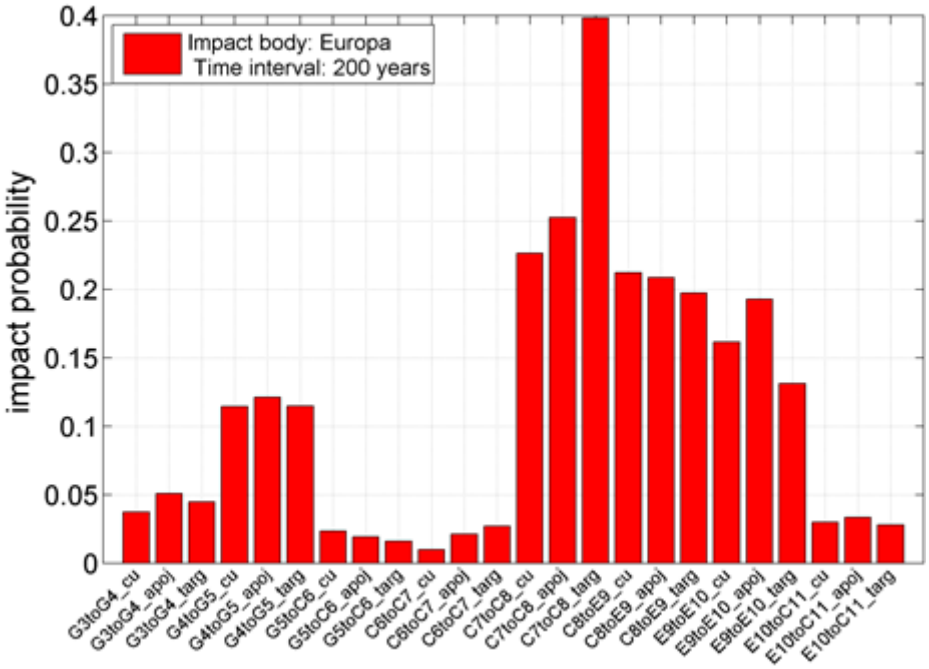

Figure 13-3: Collision probability with Europa for each manoeuvre of the Jupiter tour between G3 and C11. The probability is assessed over 200 years

On each time interval Δt_n between two consecutive manoeuvres n and $(n+1)$, a probability rate of spacecraft loss, $p_{(L,n)}$, can be defined (in units per 1/day). This probability rate is the sum of the spacecraft reliability given by the manufacturer with the loss probability due to radiation or micrometeoroid impact. Moreover, there is a conditional probability of Europa collision, $P_{(C,n)}$, given the spacecraft fails in time interval Δt_n. The latter was already given in Figure 13-3. The probability P_n of impacting Europa is therefore:

$$P_n = \Delta t_n p_{(L,n)} P_{(C,n)}$$

The objective is to sum all these probabilities over all intervals, i.e. from 1 to $N = 24$. Each term of the sum shall be multiplied by the probability that the spacecraft was not lost before the current interval, $P_{(NoL,n)}$. This probability is defined as:

$$P_{(NoL,n)} = 1 - \sum_{i=1}^{n-1} \Delta t_i p_{(L,i)}$$

The overall probability to impact Europa $P_{(E,long)}$, given a successful launch of the mission, can be calculated as follows:

$$P_{(E,long)} = \sum_{i=1}^{N} P_i P_{(NoL,i)}$$

13.1.3 Short Term Failure

The short term failure corresponds to the impossibility to perform the Europa fly-bys targeting manoeuvres due to e.g. entering a safe mode. This may lead to an impact if the spacecraft state vector dispersions are large enough prior to the non-performed manoeuvre. This second kind of failure is handled by standard pericentre off-targeting of the Europa fly-bys as illustrated in Figure 13-4.

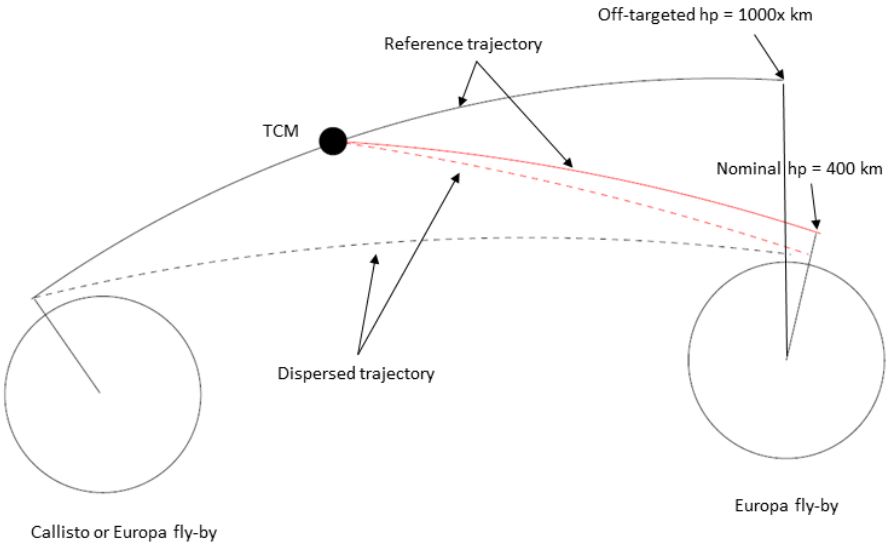

Figure 13-4: Off-targeting concept of the Europa fly-bys

The objective of the analysis is to find the required pericentre altitude offset that meets a given collision probability. The methodology to derive it is given in Figure 13-5: the a priori collision probability is a known input coming from the navigation analysis.

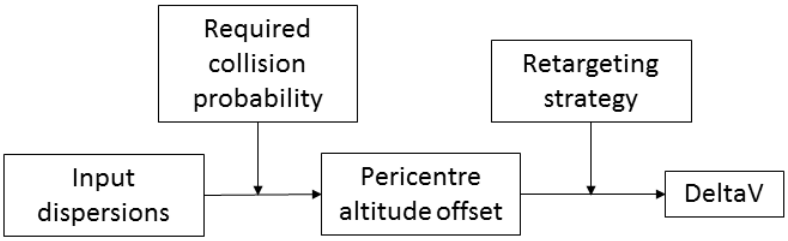

Figure 13-5: Off-targeting strategy outline

This probability is then combined with the required collision probability $P_{(E,short)}$, which is given by:

$$P_{(E,short)} = P_{PP} - P_{(E,long)}$$

where P_{PP} is the top requirement for PP, i.e. 1.10^{-4}; however the analysis is preliminary, therefore a lower value is considered in the following. For the general case the pericentre offset is given in Figure 13-6.

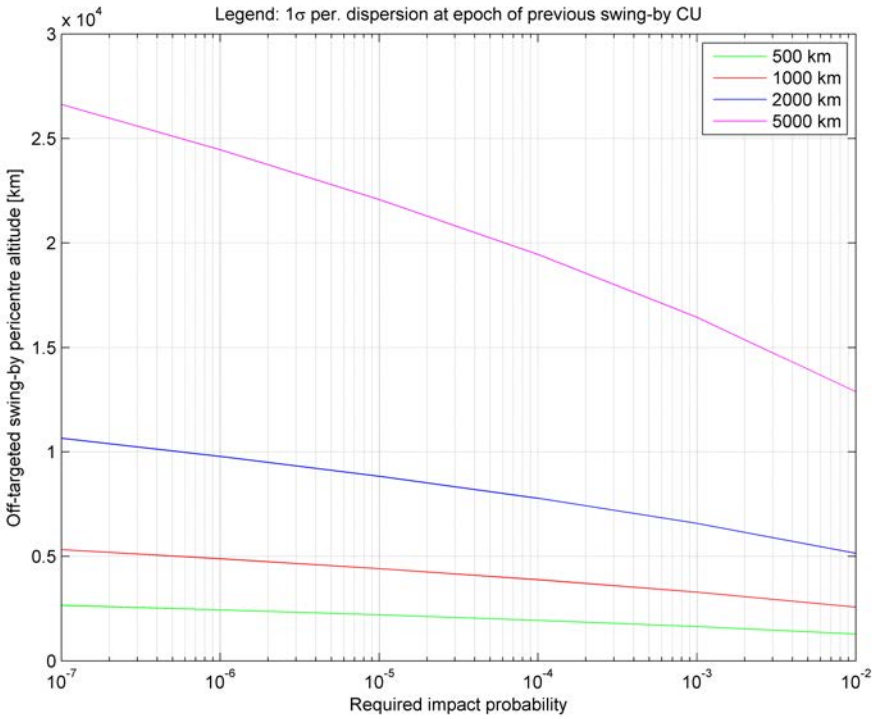

Figure 13-6: Off-targeted pericentre altitude as a function of the initial dispersions and the collision probability

The new pericentre altitude is targeted by the fly-by preceding the Europa encounter: C8 for E9 and E9 for E10. At some intermediate point between the fly-bys, the pericentre must be retargeted. The cost of this manoeuvre will be a function of the fly-by conditions (infinite velocity vector, reference pericentre altitude) and the time to pericentre. Both E9

and E10 are similar in terms of infinite velocity vector (Vinf=3.7 km/s aligned with Europa's velocity, h_p=400 km); therefore the cost of the retargeting manoeuvre is similar and is given in Figure 13-7 for various time to pericentre.

This closes the methodology presented in Figure 13-5 for short term failure.

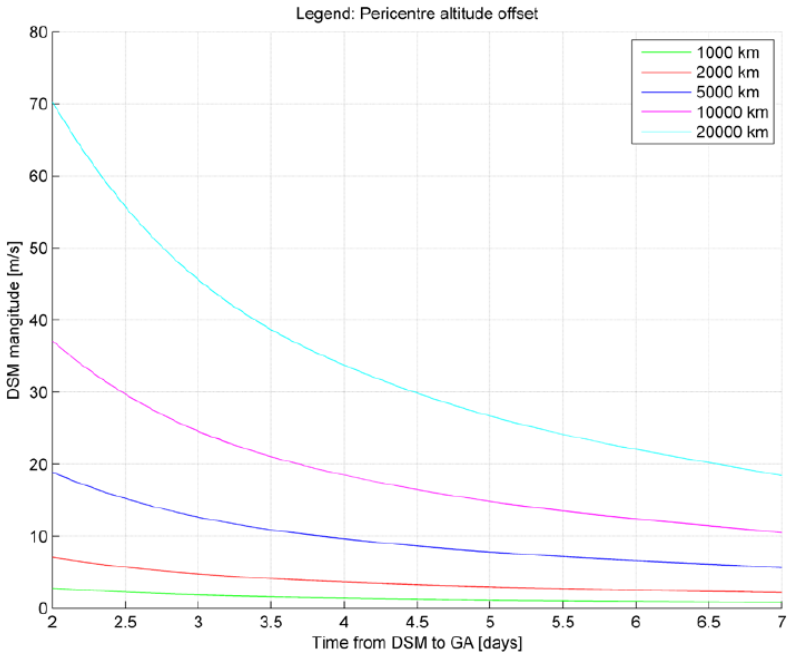

Figure 13-7: Retargeting manoeuvre DeltaV cost as a function of the time to pericentre. The cost is given for several pericentre altitude offset

13.1.4 Conclusion

In this analysis, the PP requirement for Europa is met via two different strategies, one for the long term failure and one for the short term failure. The details are summarized in Table 13-2.

Table 13-2: Synthesis of PP for Europa

Step	Value	Unit
P_{PP} requirement for Europa	1.10^{-4}	/
100% margin on P_{PP} requirement → New requirement	5.10^{-5}	/
$p_{(L,n)}$ (assumption)	1.10^{-6}	1/day
$P_{(E,long)}$	$2{,}4.10^{-5}$	/
$P_{(E,short)}$	$2{,}6.10^{-5}$	/
$P_{(E,short)}$ for each EGA	$1{,}3.10^{-5}$	/

Apriori standard deviation of EGA h_p	500	km
h_p offset	2000	km
DeltaV for retargeting 3 days prior to GA	4	m/s
DeltaV for both EGA	8	m/s

This preliminary analysis shows that the PP requirement for Europa can be fulfilled. The DeltaV cost is estimated to be 8 m/s. The cost of the retargeting will be refined in the future based on the real knowledge and dispersion covariance given by the navigation analysis.

13.2 Ganymede

Following the recommendation of AD4, no special measure is applied for Ganymede.

13.3 Mars

Planetary requirements applicable to Mars are recalled in AD2. One requirement is related to the inadvertent contamination of the planet by the launch vehicle. All the options implementing a MGA necessitate at least one EGA (160a) beforehand; for the other options necessitating a MGA, several VGA and/or EGA are needed beforehand (141a, 1800ma, 180l0lma, 180ma and 200lma). Excluding the option 160a, the impact probability of the launch vehicle upper is therefore negligible. At this stage it is considered that the probability is also very small for the case 160a; it will be analysed and hopefully confirmed at a later stage of the study.

Another requirement is related to the inadvertent contamination of Mars by the spacecraft itself. A preliminary analysis has been conducted (see RD17). The approach is comparable to that used for Mars missions, e.g. MEX or Exomars.

Three considered sources of errors are: the S/C knowledge and dispersion matrices after the EGA CU and the Solar Radiation Pressure (SRP).

The strategy consists in off-targeting the MGA pericentre and re-target it 2 weeks before the MGA (this number, 2 weeks, will be subject to optimisation at a later stage).

In AD2 it can be found that “the probability of impact on Mars by any element not assembled and maintained in ISO level 8 conditions shall be ≤ 1x10-4 for the first 50 years after launch”.

For JUICE it is assumed that the collision risk is concentrated over the time between the EGA and the MGA.

Assuming 80 km at 1σ in Mars B-plane for velocity knowledge and 40 km at 1σ for TCM dispersion, it gives a subtotal of 460 km at 3.8σ (the probability of 1.10^{-4} corresponds to 3.8σ). Adding 1100 km for the SRP (tumbling vs attitude controlled S/C), it gives a total of 1500 km in the B-plane.

The re-targeting manoeuvre to apply 2 weeks before the MGA is then 1.4 m/s. Putting margin on top of this number leads to recommend a cost of 3 m/s. Such a level is

compatible with the level of a TCM of the standard navigation. Therefore both manoeuvres can be combined to reduce the cost.

A detailed analysis will be performed at a later stage, but Mars PP is not considered as a critical issue.

14 DELTA-V BUDGET

The deterministic DeltaV budget is summarised in Table 14-1.

Table 14-1: Deterministic DeltaV budget

Launch year	2022			2023			2024			2025	
Option	141a	150l0a	150l0la	160a	230la	150l	1800ma	1801olma	17Imelem	180ma	200lma
DeltaV cost [m/s]											
Launch window	57	80	59	44	42	36	63	103	90	75	43
Interplanetary flight	104	214	283	126	183	232	49	101	149	41	251
JOI	792	903	903	946	927	903	928	928	923	928	885
JOI to Europa phase end	124	105	105	120	119	105	106	106	120	106	103
Jupiter high latitudes	30	30	30	30	30	30	30	30	30	30	30
Transfer to Ganymede	60	60	60	60	60	60	60	60	60	60	60
GOI	135	135	135	135	135	135	135	135	135	135	135
GEO to GCO-500	500	500	500	500	500	500	500	500	500	500	500
Total	1802	2027	2075	1961	1996	2001	1871	1963	2007	1875	2007

The JOI to Europa phase end includes a provision for the Planetary Protection (PP) via an off-targeting strategy (5 m/s). The GEO to GCO-500 phase includes a margin of 20 m/s for the necessary improvement of the robustness of the solution: currently only two days are assumed between the two transfer manoeuvres although four days are considered throughout the rest of the document; moreover the time to impact in case the first transfer manoeuvre is not implemented (because of e.g. safe mode) is just four days.

The stochastic DeltaV budget is summarised in Table 14-2. No provision is made for contingencies (e.g. missed fly-by, failed GOI, …).

Table 14-2: Stochastic DeltaV budget

Launch year	2022			2023			2024			2025	
Option	141a	150l0a	150l0la	160a	230la	150l	1800ma	1801olma	17Imelem	180ma	200lma
DeltaV cost [m/s]											
Launcher dispersions	30	30	30	30	30	30	30	30	30	30	30
Interplanetary GA	85	95	155	70	95	130	100	120	105	85	110
JOI CU	30	30	30	30	30	30	30	30	30	30	30
Jupiter tour GA	232	232	232	232	232	232	232	232	232	232	232
GOI approach	10	10	10	10	10	10	10	10	10	10	10
Station keeping	40	40	40	40	40	40	40	40	40	40	40
Total	427	437	497	412	437	472	442	462	447	427	452

The JOI CU is estimated to cost 30 m/s as detailed in RD24. This value is in-line with preliminary assumptions made in previous versions of the CReMA. On-going efforts are dedicated to GOI CU assessment (zero cost is assumed for the time being, which is optimistic).

15 ECLIPSES AND EARTH OCCULATIONS

15.1 Eclipses

15.1.1 Interplanetary Transfer

They are summarised in Table 15-1 for all options. There is always a short eclipse upon departure because the escape direction is always radially inwards, meaning that the launch is in the night (the eclipse time is computed starting at an altitude of 250 km).

During the cruise, the eclipses depend on the option and range from zero to 118 min (EGA4 in 150l0a). The longest eclipse is encountered a couple of days after JOI for options 150l0a, 150l0la, 230la, 150la and 17ImeIem; it is either 5.5 hours or 6.8 hours (230la and 17ImeIem).

Table 15-1 Eclipses during the interplanetary transfer [unit=minutes]. 'V'=Venus, 'E'=Earth, 'm'=Moon, 'M'=Mars, 'J'=Jupiter.

	Launch	GA1	GA2	GA3	GA4	GA5	GA6	JOI
141a	E: 6	E: 0	V: 0	E: 170	M: 0	E: 24		J: 0
150l0a	E: 6	m: 36 ; E: 0	E: 0	V: 0	E: 118	E: 24		J: 332
150l0la	E: 7	m: 37 ; E: 0	m: 33 ; E: 0	V: 0	E: 0	E: 25		J: 332
160a	E: 6	E: 0	M: 0	E: 0	E:0			J: 0
230la	E: 7	E: 0 ; m: 0	V: 0	V: 17	E: 49	E: 0		J: 408
150la	E: 6	m: 28 ; E: 0	V: 0	E: 179	E: 24			J: 332
1800ma	E: 6	E: 0	E: 0	V: 0	E: 32	E: 26	M: 58	J: 0
180l0lma	E: 8	m: 35 ; E: 0	m: 0 ; E: 0	V: 0	E: 32	E: 26	M: 58	J: 0
17ImeIem	E: 7	m: 40 ; E: 0	m: 0 ; E: 0	V: 0	E: 0	E: 0		J: 407
180ma	E: 6	E: 0	V: 0	E: 32	E: 26	M: 58		J: 0
200lma	E: 7	m: 0 ; E: 0	V: 0	E: 63	E: 42	E: 20	M: 49	J: 0

More analyses were performed in RD23: first over the energy reduction phase (JOI + subsequent GGA sequence), then by patching a generic (virtual) tour to all options. From these analyses, attempts to reduce/eliminate the long eclipses were tried.

From the energy reduction phase analysis, three groups of interplanetary transfers were identified:

- Group I (15X series): negative Sun declination at JOI, positive incoming infinite velocity declination
- Group II (230la, 17ImeIem): Sun close to the equator at JOI (close to Spring equinox)
- Group III (141a, 160a, 1800ma, 18l0lma, 180ma, 200lma):
    - 141, 160a: negative Sun declination at JOI, negative incoming infinite velocity declination

- 18X series, 200lma: positive Sun declination at JOI, positive incoming infinite velocity declination

It is shown in the memo that long eclipses appear in the geometrical configuration of Group I and II. For Group I, there are long eclipse that can be reduced to the battery upper limit for less than 15 m/s (TBC). For the time being no easy solution was found for group II. If this confirmed for group II, there is obviously an issue with these options as long as the longest eclipse is constrained to 4.8 hours. For Group III, there is no eclipse.

Reducing/removing the long eclipses during the rest of the tour will be possible in specific cases (full resonance) w/o redesigning the tour. For the other cases, this new constraint will add up to the existing ones in the design of the tour. It is impossible to give a consolidated answer w/o a case by case analysis, but it will translate into the introduction of additional fly-bys; thus time, DeltaV and radiation dose.

On-going analysis is conducted on the backup launch in 2023. Results should be available in the course of 2017.

15.1.2 Jupiter Tour

The eclipses during the Jupiter tour are presented in Figure 15-1 for the option 141a.

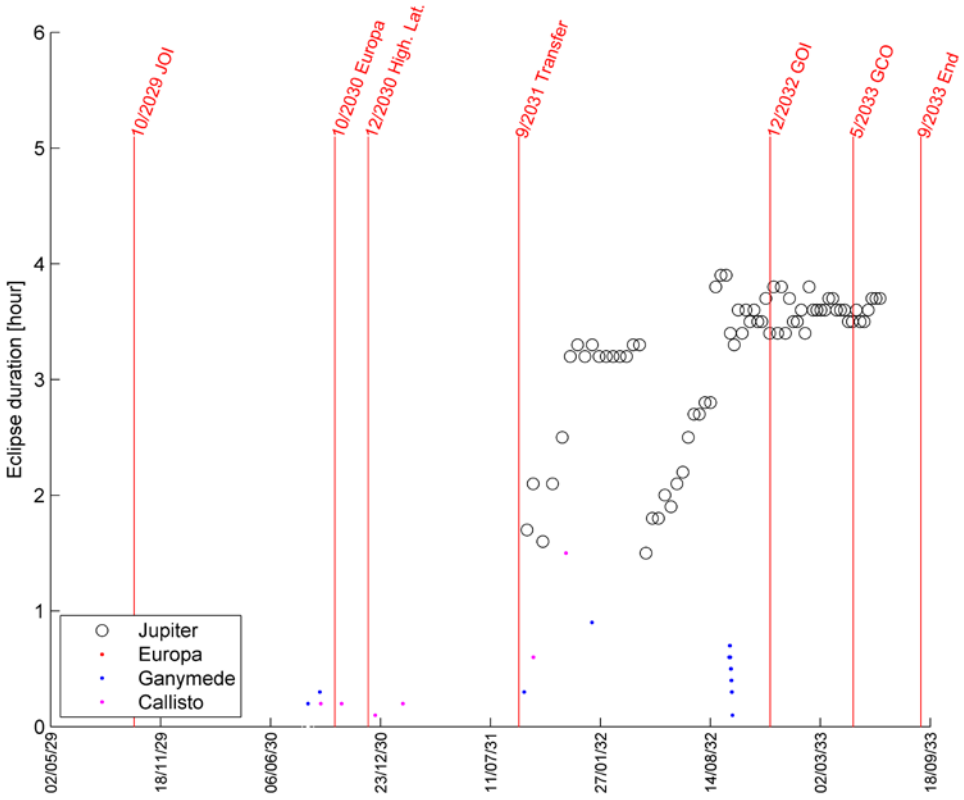

Figure 15-1: Eclipses during the Jupiter tour

They are also summarised in a tabular form in Table 15-2.

Table 15-2: Summary of the eclipses during the Jupiter tour

#	Year	Month	Day	Duration [hour]	Body
1	2030	AUG	13	0.2	Ganymede
2	2030	SEP	3	0.3	Ganymede
3	2030	SEP	5	0.2	Callisto
4	2030	OCT	13	0.2	Callisto
5	2030	DEC	13	0.1	Callisto
6	2031	FEB	1	0.2	Callisto
7	2031	SEP	10	0.3	Ganymede
8	2031	SEP	15	1.7	Jupiter
9	2031	SEP	26	2.1	Jupiter
10	2031	SEP	27	0.6	Callisto
11	2031	OCT	14	1.6	Jupiter
12	2031	OCT	31	2.1	Jupiter
13	2031	NOV	18	2.5	Jupiter
14	2031	NOV	25	1.5	Callisto
15	2031	DEC	3	3.2	Jupiter
16	2031	DEC	16	3.3	Jupiter
17	2031	DEC	29	3.2	Jupiter
18	2032	JAN	11	0.9	Ganymede
19	2032	JAN	12	3.3	Jupiter
20	2032	JAN	24	3.2	Jupiter
21	2032	FEB	6	3.2	Jupiter
22	2032	FEB	18	3.2	Jupiter
23	2032	MAR	2	3.2	Jupiter
24	2032	MAR	14	3.2	Jupiter
25	2032	MAR	26	3.3	Jupiter
26	2032	APR	7	3.3	Jupiter
27	2032	APR	18	1.5	Jupiter
28	2032	APR	30	1.8	Jupiter
29	2032	MAY	11	1.8	Jupiter
30	2032	MAY	23	2	Jupiter
31	2032	JUN	3	1.9	Jupiter
32	2032	JUN	14	2.1	Jupiter
33	2032	JUN	24	2.2	Jupiter
34	2032	JUL	4	2.5	Jupiter
35	2032	JUL	15	2.7	Jupiter
36	2032	JUL	25	2.7	Jupiter
37	2032	AUG	4	2.8	Jupiter
38	2032	AUG	14	2.8	Jupiter
39	2032	AUG	23	3.8	Jupiter
40	2032	SEP	2	3.9	Jupiter
41	2032	SEP	11	3.9	Jupiter
42	2032	SEP	17	0.6	Ganymede
43	2032	SEP	17	0.6	Ganymede
44	2032	SEP	18	0.7	Ganymede
45	2032	SEP	18	0.6	Ganymede
46	2032	SEP	19	0.7	Ganymede
47	2032	SEP	19	3.4	Jupiter
48	2032	SEP	19	0.6	Ganymede
49	2032	SEP	20	0.5	Ganymede
50	2032	SEP	20	0.5	Ganymede
51	2032	SEP	21	0.4	Ganymede
52	2032	SEP	21	0.4	Ganymede
53	2032	SEP	22	0.3	Ganymede
54	2032	SEP	22	0.3	Ganymede
55	2032	SEP	23	0.1	Ganymede
56	2032	SEP	26	3.3	Jupiter
57	2032	OCT	3	3.6	Jupiter
58	2032	OCT	10	3.4	Jupiter
59	2032	OCT	17	3.6	Jupiter
60	2032	OCT	25	3.5	Jupiter
61	2032	NOV	1	3.6	Jupiter
62	2032	NOV	8	3.5	Jupiter
63	2032	NOV	15	3.5	Jupiter
64	2032	NOV	22	3.7	Jupiter
65	2032	NOV	29	3.4	Jupiter
66	2032	DEC	6	3.8	Jupiter
67	2032	DEC	14	3.4	Jupiter
68	2032	DEC	21	3.8	Jupiter
69	2032	DEC	28	3.4	Jupiter
70	2033	JAN	4	3.7	Jupiter
71	2033	JAN	11	3.5	Jupiter
72	2033	JAN	18	3.5	Jupiter
73	2033	JAN	26	3.6	Jupiter
74	2033	FEB	2	3.4	Jupiter
75	2033	FEB	9	3.8	Jupiter
76	2033	FEB	16	3.6	Jupiter
77	2033	FEB	23	3.6	Jupiter
78	2033	MAR	3	3.6	Jupiter
79	2033	MAR	10	3.6	Jupiter
80	2033	MAR	17	3.7	Jupiter
81	2033	MAR	24	3.7	Jupiter
82	2033	MAR	31	3.6	Jupiter
83	2033	APR	7	3.6	Jupiter
84	2033	APR	15	3.6	Jupiter
85	2033	APR	22	3.5	Jupiter
86	2033	APR	29	3.5	Jupiter
87	2033	MAY	6	3.6	Jupiter
88	2033	MAY	13	3.5	Jupiter
89	2033	MAY	20	3.5	Jupiter
90	2033	MAY	28	3.6	Jupiter
91	2033	JUN	4	3.7	Jupiter
92	2033	JUN	11	3.7	Jupiter
93	2033	JUN	18	3.7	Jupiter

The eclipses occur when the spacecraft flies in the shadow of Jupiter. The longest eclipse takes place in the weeks before the GOI (3.9 hour).

Finally it was shown in Paragraph 9.3 that short eclipses will take place at the beginning of the GEO because of the combination between low pericentre altitude and low beta angle. They are clearly visible on the figure at the epoch of the JOI: the initial duration is 0.7 hour and they disappear in 6 days; this is 5 days shorter than for the previous CReMA and is due to the beta angle at GOI of 30 deg instead of 20 deg. They take place twice per day, roughly every 12 hours (i.e. the orbital period of the GEO. On September, 19 there is also a 3.4 hour eclipse by Jupiter (eclipse by Jupiter have a frequency equal to the orbital period of Ganymede, i.e. 7.1 days). The orbital period of the GEO can be tuned such that the eclipse by Ganymede is included into the eclipse by Jupiter.

15.2 Occultations

The Earth can be occulted by:

- The Sun: roughly every synodic period between the Earth and Jupiter (~399 days)
- Jupiter: when the S/C is in-orbit around the planet
- Ganymede: during swing-bys and during the GEO/GCO phase
- Europa and Callisto: they take place only during swing-bys.

15.2.1 Occultations by the Sun

An occultation by the Sun, or superior conjunction, is of first importance because the data link between the Earth and the S/C is progressively degraded and then interrupted. From RD4 it is assumed that a minimum Sun-Earth-Spacecraft (SES) angle of **5 deg** is necessary to upload a TCM or download navigation measurements. The inferior conjunction together with the occultations are shown in Figure 15-2.

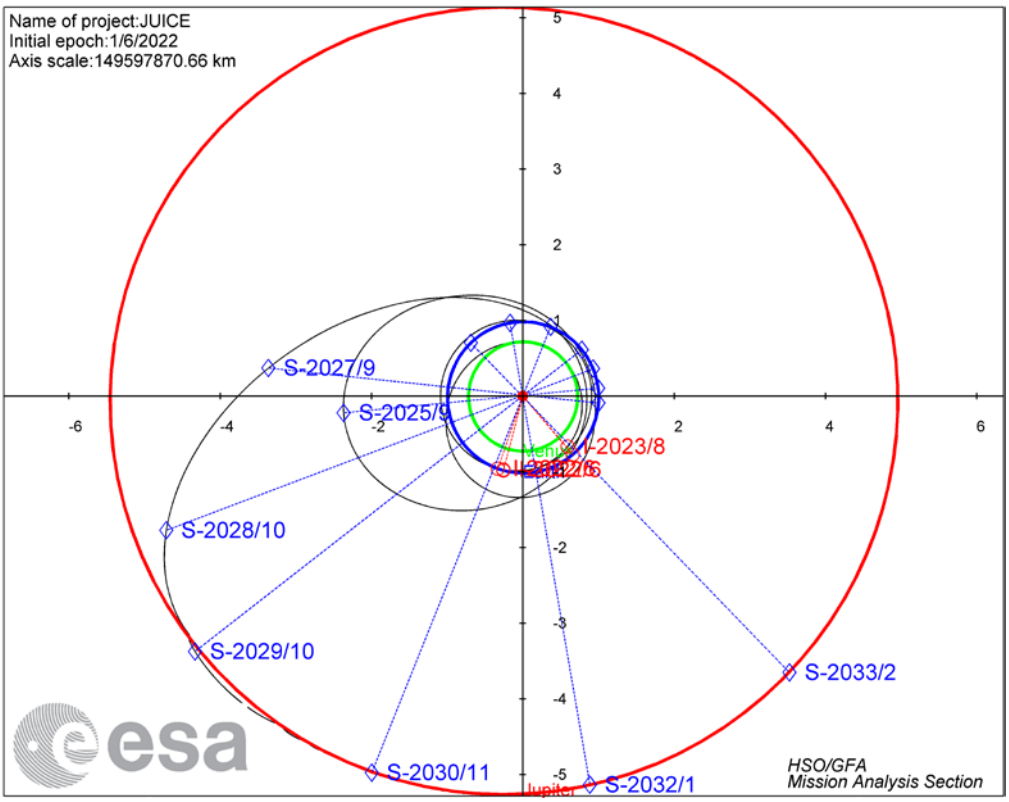

Figure 15-2: Inferior conjunctions (in red) and occultations (in blue) during the interplanetary transfer

The occultations are summarised in Table 15-3 for the interplanetary flight.

Table 15-3: Earth occultations by the Sun during the mission

#	Beginning	End	Duration [days]
1	19/09/2025	09/10/2025	19.5
2	10/09/2027	26/09/2027	16.5
3	07/10/2028	21/10/2028	13.5
4	25/10/2029	07/11/2029	13.5
5	24/11/2030	06/12/2030	12.0
6	26/12/2031	07/01/2032	12.0
7	27/01/2033	09/02/2033	13.0

- Occultation #1 to #3: they take place during the interplanetary flight. No GAM or DSM is located inside or close to the occultation.
- Occultation #4: it takes place 18 days after JOI. Taking into account the one-week margin, it leaves 11 days to perform the CU of the JOI.

- Occultation #5: it falls between 9G6 and 10C2. With the one-week margin on both sides, it leaves 14 days after 9G6 and less than a day before 10C2.
- Occultation #6: it falls between 23C12 and 24G10. With the one-week margin on both sides, it leaves 24 days after 23C12 and a negative margin of one day with 24G10: this fly-by will be tight.
- Occultation #7: it takes place during the GEO. There is only 4 days to the first manoeuvre of the GEO/GCO transfer: it would be beneficial to extend the GEO by e.g. 3-4 days.

The detailed analysis of the backup launch in 2023 has not been performed: there is no reason for the Earth occultations to take place at the same epoch in the timeline.

15.2.2 Occultations by Jupiter and the Galilean Moons

They are given in Figure 15-3.

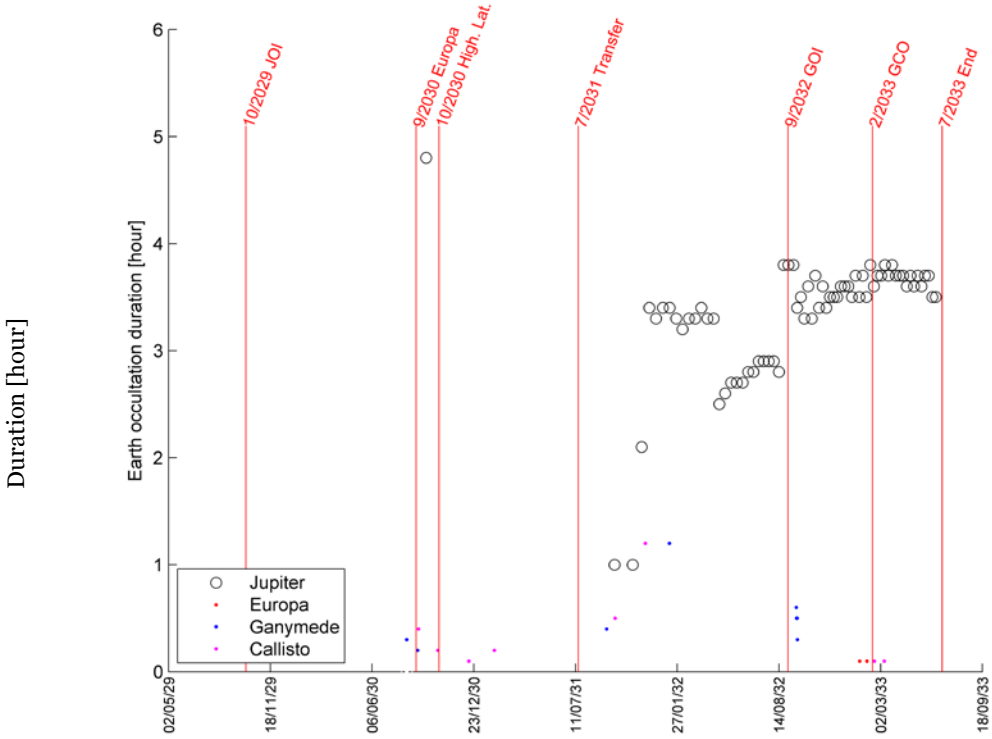

Figure 15-3: Earth occultation by Jupiter assuming the spacecraft is in-orbit around Ganymede

This figure is course very comparable to Figure 15-1.

16 COMMUNICATIONS

The ground stations considered are Cebreros, New Norcia and Malargue (see Section 3.7.4 for stations coordinates).

16.1 Launch in 2022 (Option 141a)

The evolution of the range between the Earth and the Sun on one side, Jupiter and the spacecraft on the other, during the Jupiter tour are given in Figure 16-1.

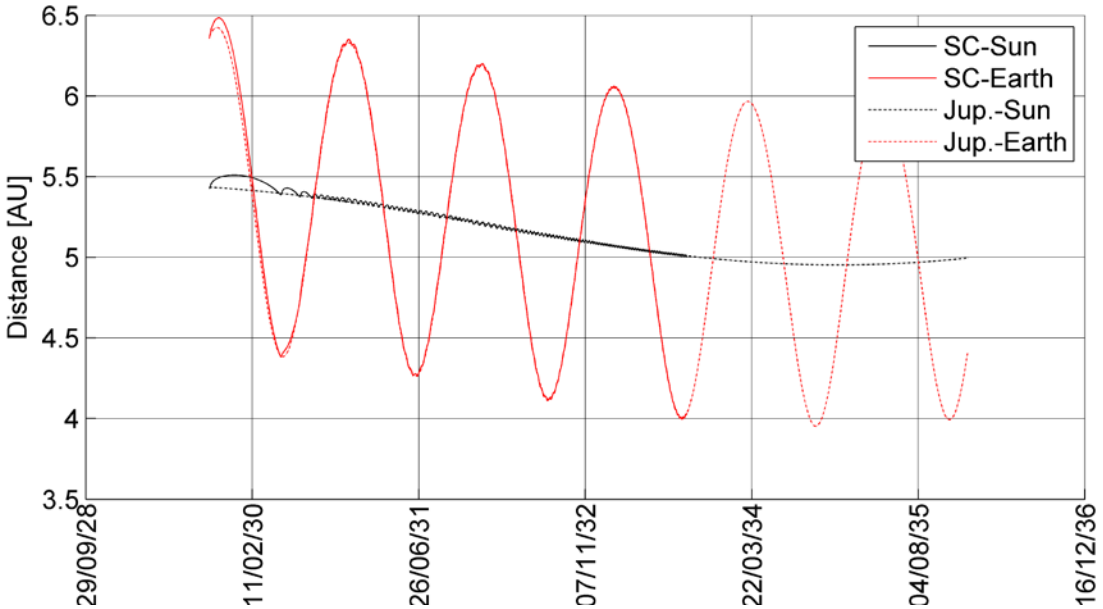

Figure 16-1: Earth to Jupiter range for the 2022 launch

Except for the small deviation during the first highly eccentric orbit, the evolution of the spacecraft distance (to the Sun and the Earth) is the same as Jupiter itself. The maximum Earth to spacecraft distance is about 6.5 AU.

The evolution of the maximum elevation is given in Figure 16-2.

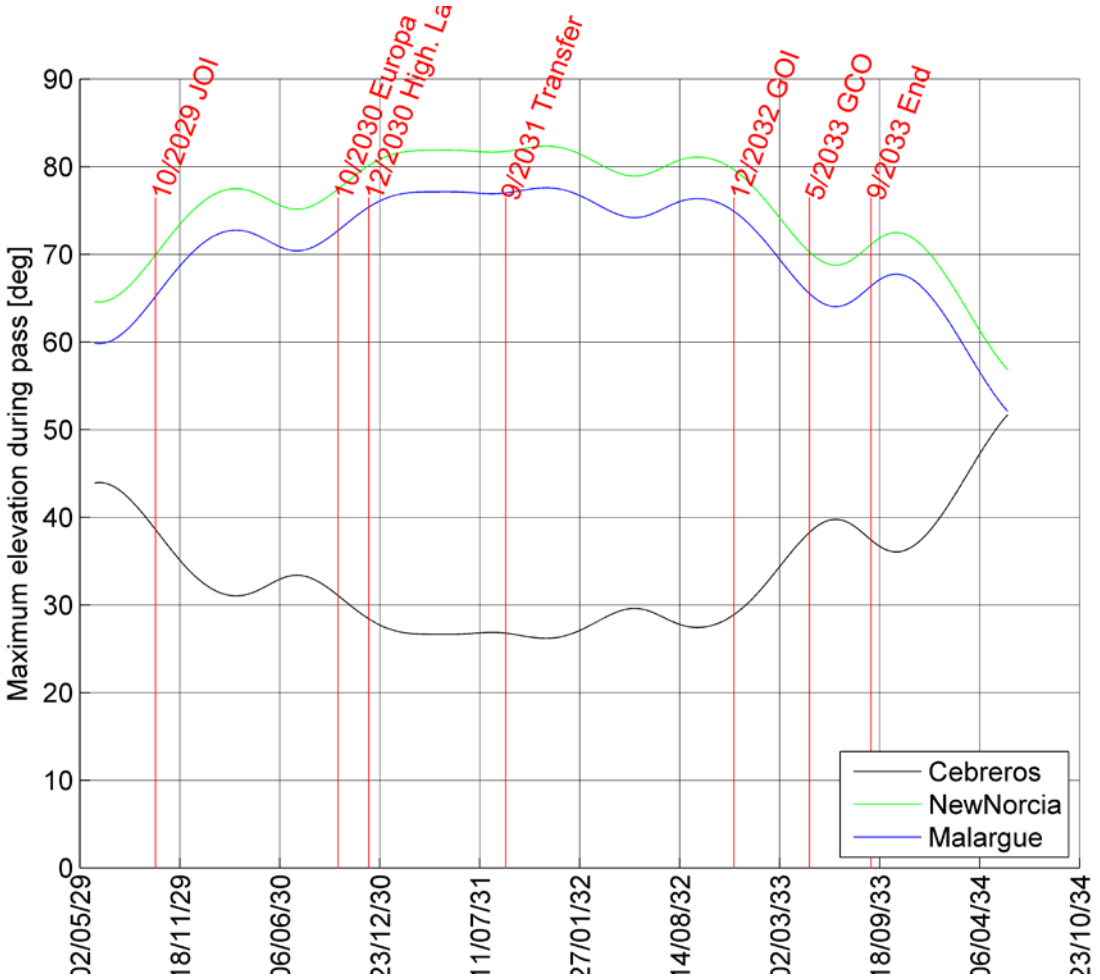

Figure 16-2: Evolution of the maximum elevation for the Jupiter tour timeframe of the option 141a

The first general remark that applies to all figures is that the evolution is always comparable for New Norcia and Malargue: the reason is that both groundstations have comparable latitude (31 deg South for New Norcia and 36 deg South for Malargue). The difference in longitude does not produce any difference because of the Earth rotation.

During the entire mission, it is beneficial to use either Malargue or New Norcia: until the beginning of the Ganymede science phase, the maximum elevation is always greater than 70 deg for Malargue and 75 deg for New Norcia. During the Ganymede phase, the maximum elevation is reduced by 5 deg.

The duration of the daily passes is given for a minimum elevation of 10 deg in Figure 16-3.

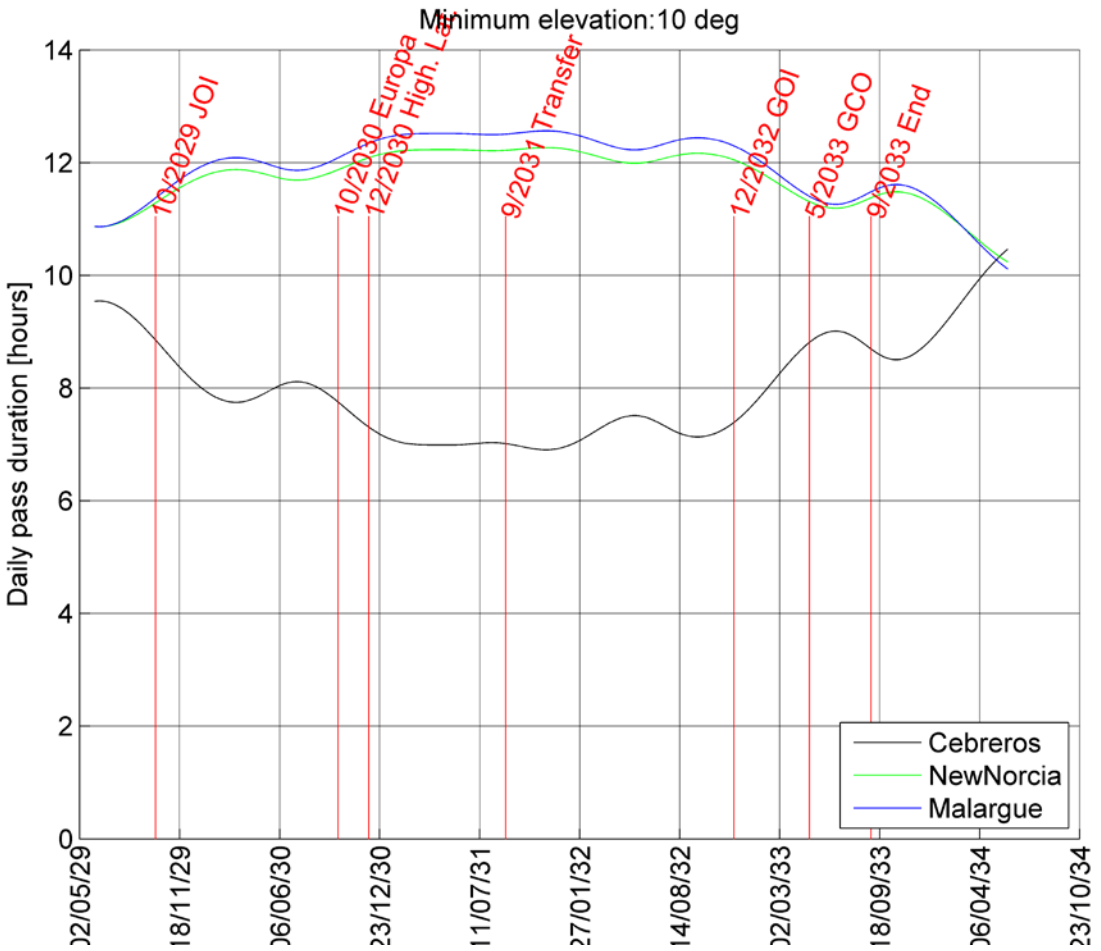

Figure 16-3: Duration of the ground stations passes for the launch in 2022

This plot follows the conclusions obtained for the plot showing the maximum elevation: the optimum scheme consists in using either Malargue or New Norcia. The average daily visibility is 12.2 hours and the minimum daily visibility is 11.3 hours (during the Ganymede science phase).

The effect of S/C occultation by Jupiter and the Galilean moons is excluded. This effect is assessed in section 16.2.

16.2 Parametric Analysis

In order to cover any launch date and interplanetary transfer duration, parametric analyses have been conducted by varying the epoch between 2032/01/01 and 2040/12/31. The evolution of the distance between the Earth and Jupiter is given in Figure 16-4. Two movements affect the results: the rotation period of the Earth around the Sun and that of Jupiter.

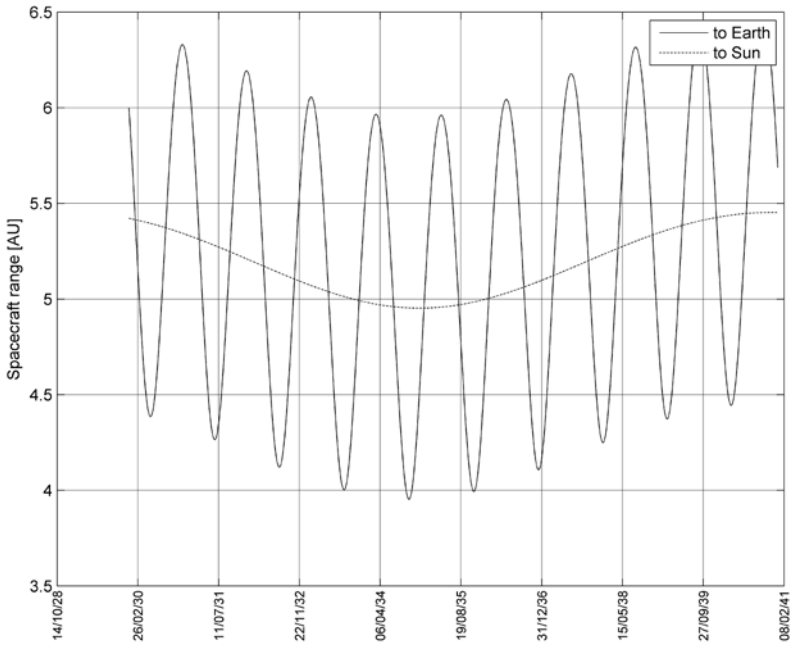

Figure 16-4: Evolution of the distance between the Earth and Jupiter for the timeframe 2032/01/01 to 2040/12/31

The evolution of the maximum elevation for all ground stations is given in Figure 16-5.

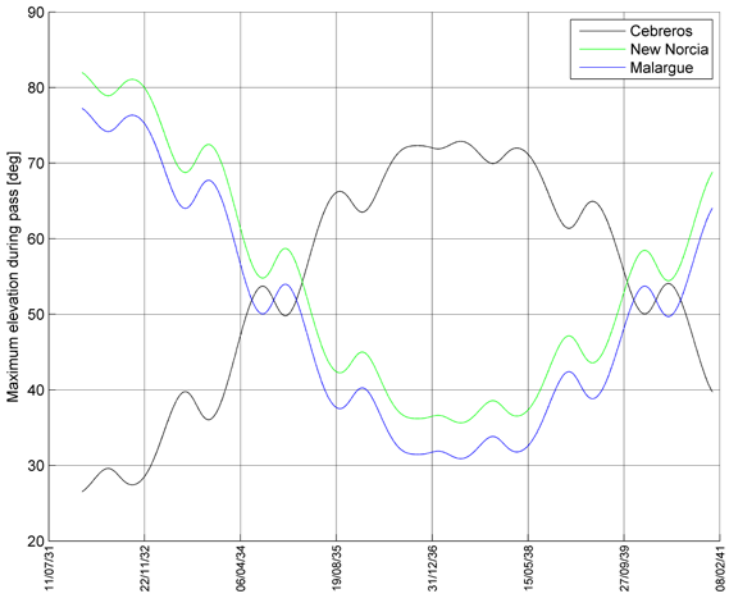

Figure 16-5: Evolution of the maximum elevation for the timeframe 2032/01/01 to 2040/12/31

It shows that if the arrival date takes place two years after the 141a, it will then be beneficial to use Cebreros instead of New Norcia or Malargue. The reason for that is that 2034, the declination of Jupiter is positive as can be seen in Figure 16-6.

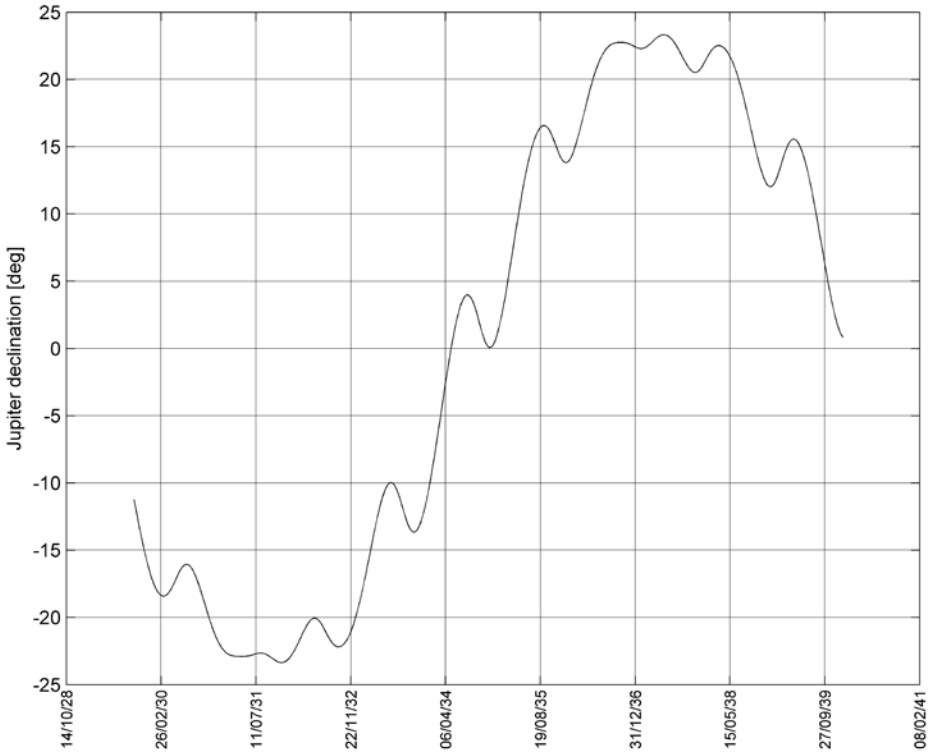

Figure 16-6: Jupiter's declination from 2029 to 2040

The duration of the daily pass excluding the effect of occultations is given in Figure 16-7.

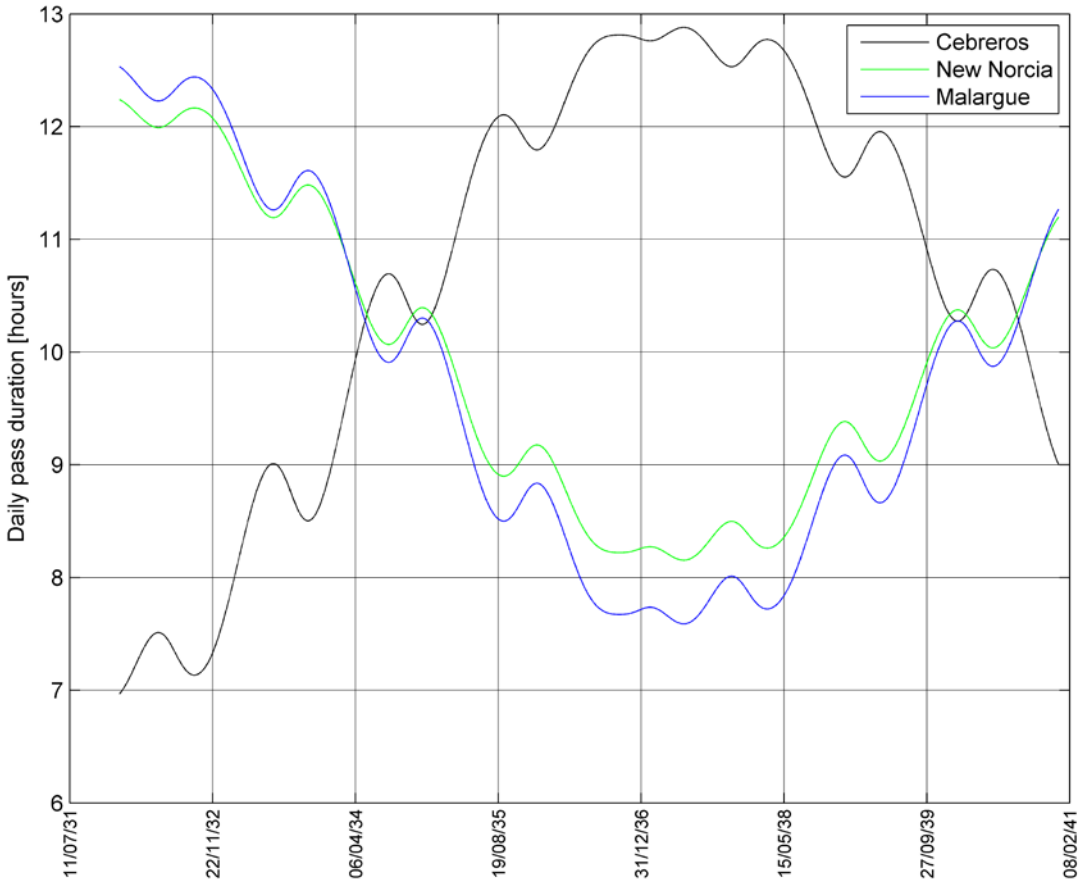

Figure 16-7: Daily pass duration excluding the occultations for the timeframe 2032/01/01 to 2040/12/31

16.3 Effect of Earth Occultations

This section was tested on the previous baseline (case 140a). However the results and conclusions should only slightly differ for the current baseline and the other options.

As shown in Figure 15-3 the visibility from Earth during the Jupiter tour is affected by occultations by Jupiter and the fours Galilean moons. From the figure it is clear that occultations by Io, Europa and Callisto are negligible; therefore they are not analysed in greater details.

16.3.1 Occultation by Ganymede

The occultations by Ganymede are not negligible around GOI. The reason is easily understood: at GOI the beta angle is 20 deg. It means that part of the orbit around Ganymede is in eclipse. The Earth direction being close to the Sun direction, it follows

Earth occultations by Ganymede. As the eclipses quickly reduce and finally disappear, the same applies to the occultations.

Around this period the pattern of overlap is given in Figure 16-8.

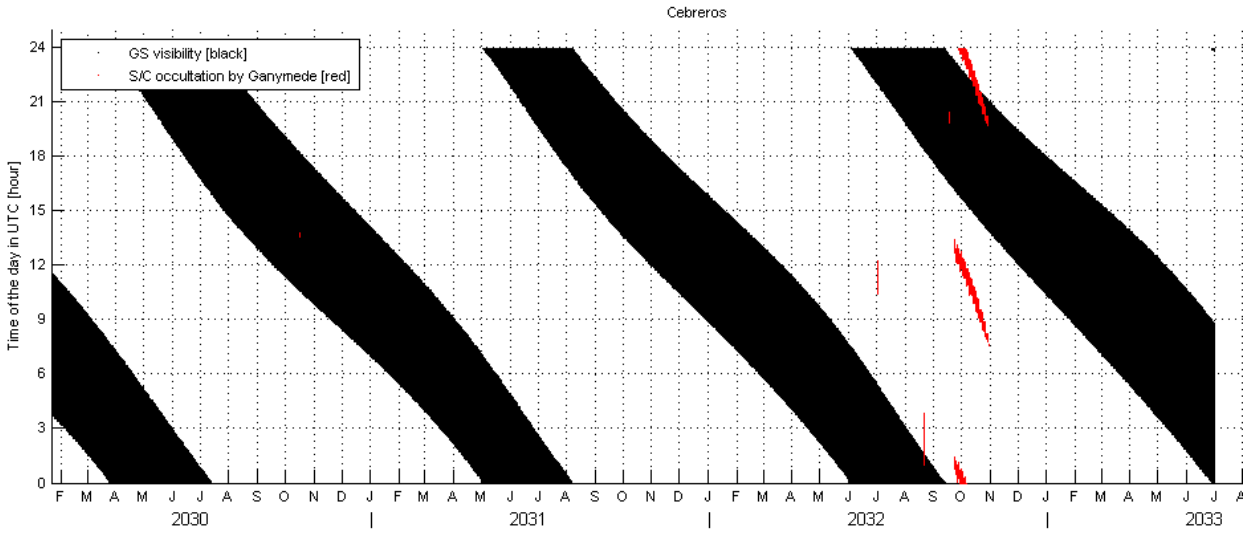

Figure 16-8: Cebreros visibility and Earth occultation by Ganymede around the GOI

It can be seen that there is an overlap after GOI. However by changing the epoch of the GOI (at nearly no DeltaV cost), it is possible to shift the daily visibility w.r.t. the occultations. From the figure a shift of the GOI epoch by 3 hours would be sufficient. Such a strategy can be applied to any ground station. Therefore the overlap can be cancelled.

16.3.2 Occultations by Jupiter

The occultations by Jupiter can be split into two groups: the first group before the GOI, the second group after GOI. Before the GOI the overlap between the ground station visibility and the occultation is a function of the S/C trajectory. After the GOI it is essentially fixed and given by Ganymede's orbit around Jupiter, i.e. a modification of the trajectory will not affect the occultations profile.

Before the GOI the profile of the occultations is linked to the S/C trajectory. In Figure 16-9 it is given for Cebreros.

Most of the overlapping occultations take place during the transfer to Ganymede, i.e. in a part of the mission, where the science might be less demanding. There are 11 overlaps ranging from ~1h up to ~3h: this effect can be neglected. As an illustration the same plot is given for New Norcia in Figure 16-10.

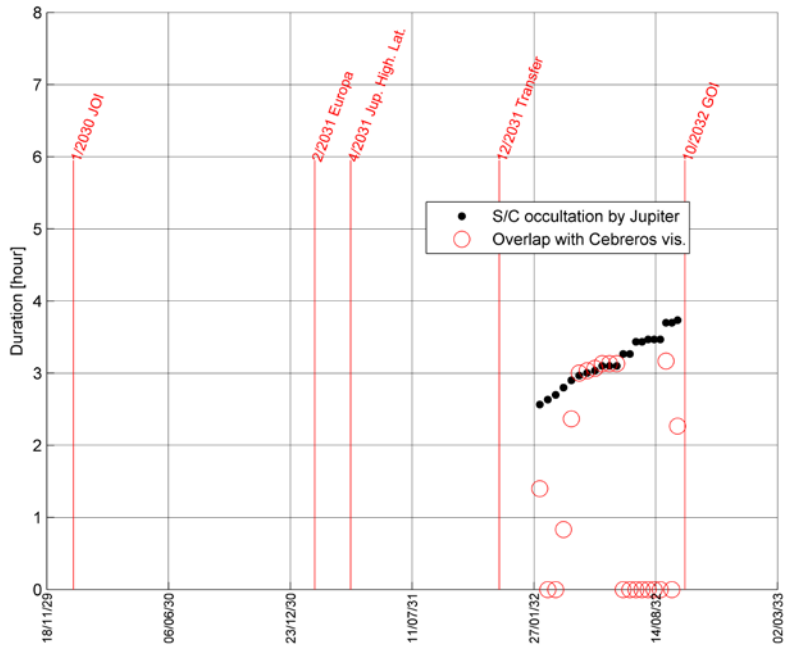

Figure 16-9: Cebreros visibility and Earth occultation by Jupiter before the GOI

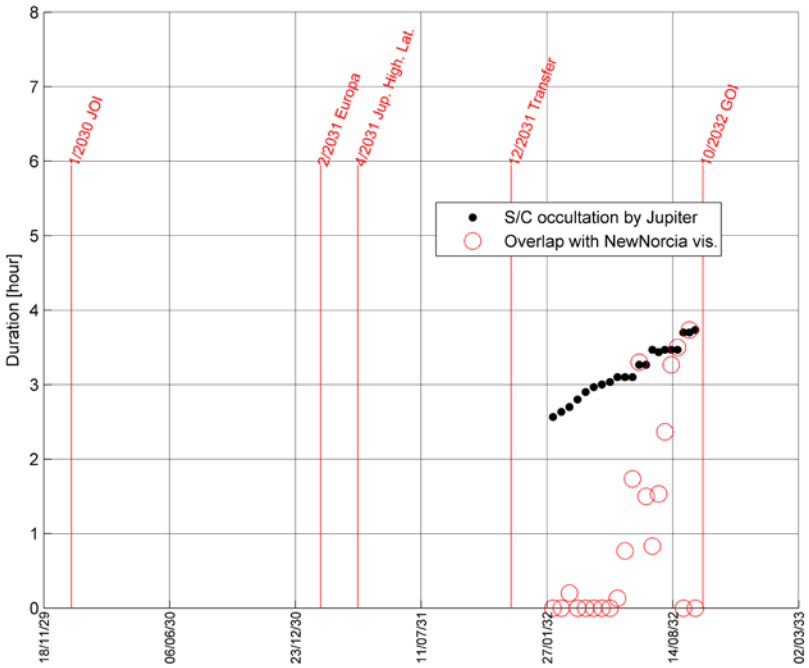

Figure 16-10: New Norcia visibility and Earth occultation by Jupiter before the GOI

The overlapping profile is different, but the conclusion remains the same. It has to be understood that these figures are dependent on the S/C trajectory: any modification of the reference trajectory will automatically lead to a different occultation profile. However it is likely that the occultation before being in-orbit around Ganymede will always have a low impact on the communications.

The overlaps with the Galilean moons are by essence much more seldom and usually short before the GOI, see Figure 15-3. Therefore they were not analysed.

After the GOI the profile of the occultations is given by Ganymede's orbit. This profile is superimposed on the Cebreros visibility in Figure 16-11.

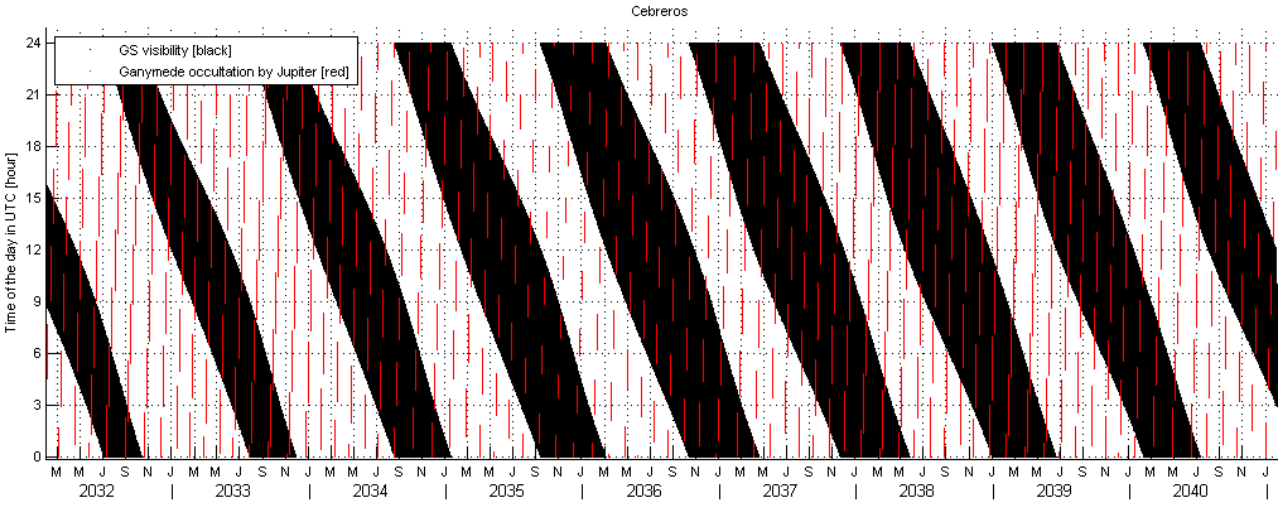

Figure 16-11: Cebreros visibility and Earth occultation by Jupiter after the GOI

It is clear that there is an overlap on a regular basis. In order to assess the impact of this overlap, the real groundstation visibility was computed by averaging technique with a window of 90 days. The reduction compared to the visibility case without occultation is shown in for Cebreros.

This value depends on when the Ganymede science phase takes place. To simplify a flat reduction of 0.3 h for any date can be kept for Cebreros. The same plot is given in Figure 16-13 for New Norcia and in Figure 16-14 for Malargue.

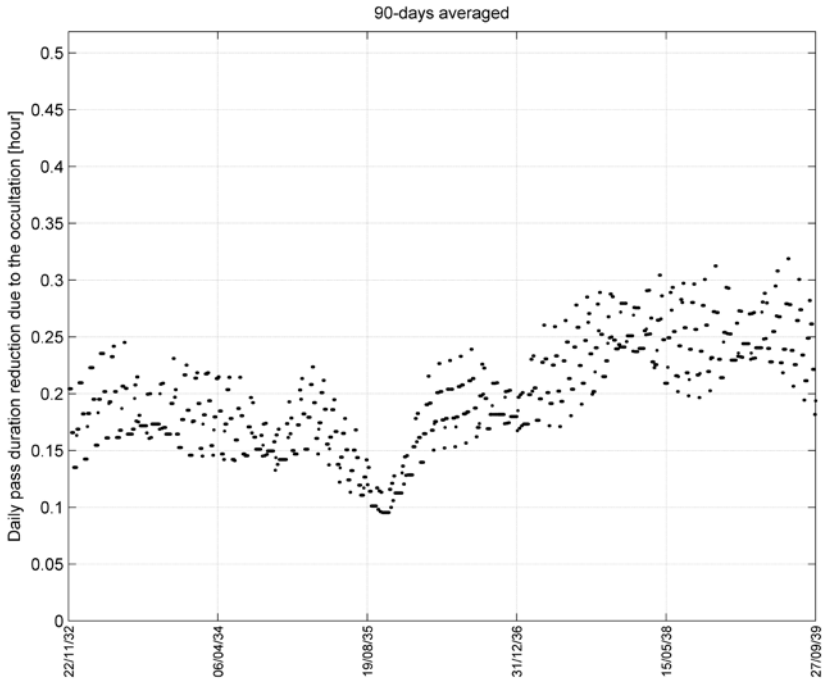

Figure 16-12: Daily pass reduction due to the overlap with occultations by Jupiter after the GOI (Cebreros)

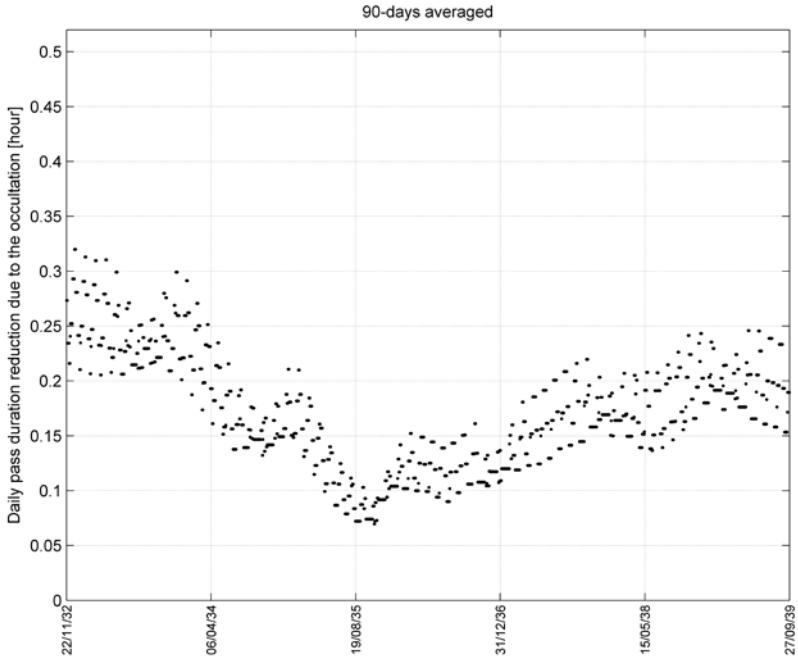

Figure 16-13: Daily pass reduction due to the overlap with occultations by Jupiter after the GOI (New Norcia)

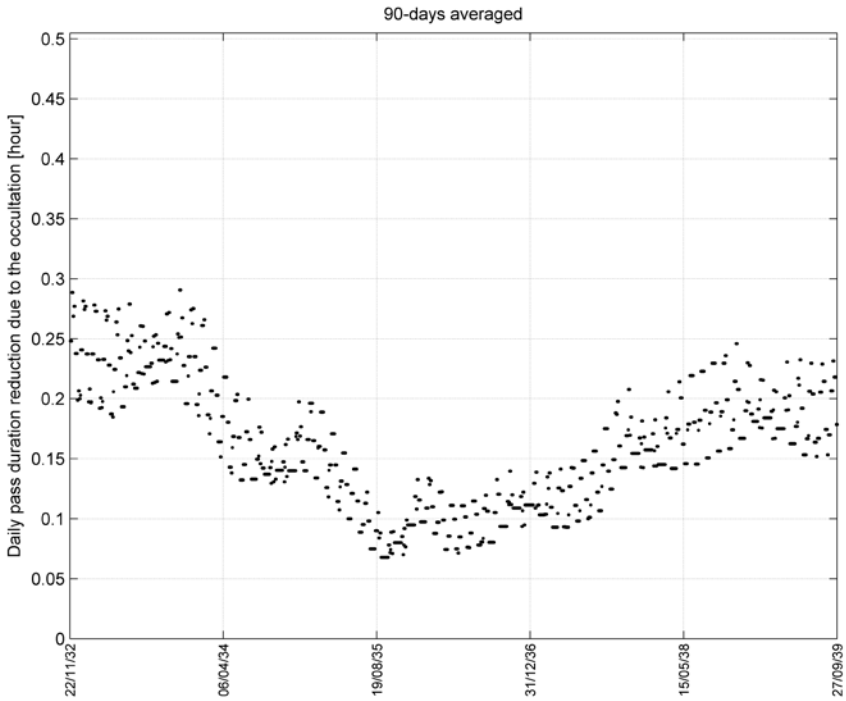

Figure 16-14: Daily pass reduction due to the overlap with occultations by Jupiter after the GOI (Malargue)

It can be observed that the profiles are different, but the maximum reduction remains essentially the same.

--- END OF DOCUMENT ---